The Role of Enterochromaffin Cells as Sensors in the Gastrointestinal Lumen

by

Alyce Maree Martin (BMS, BSc(Hons))

Thesis
Submitted to Flinders University
for the degree of

Doctor of Philosophy (PhD)

College of Medicine and Public Health

9th November, 2018

To Mum, the most inspirational person I know

and

In loving memory of Marion Ruth Sharman
"Nan"
(1942-2016)

Table of Contents

List of Figures

List of Tables

Nomenclature

5-HIAA	5-Hydroxyindole acetic acid
5-HT	5-Hydroxytryptamine, serotonin
5-HTP	5-Hydroxytryptophan
Abx	Antibiotics
AC	Adenylate cyclase
ADORA2B	Adenosine receptor 2B
α-MG	alpha-methylglucoside
ANOVA	Analysis of variance
ATP	Adenosine triphosphate
AUC	Area under the curve
BAT	Brown adipose tissue
BBM	Brush border membrane
BMI	Body mass index
cAMP	Cyclic adenosine monophosphate
CaSR	Calcium sensing receptor
CCK	Cholecystokinin
cDNA	Copy deoxyribose nucleic acid
CNS	Central nervous system
DAPI	4',6-diamidino-2-phenylindole
DCA	Deoxycholic acid
D-map	Dimensional map
DMSO	Dimethylsulphoxide
DP	Dark phase
DPP-IV	Dipeptidyl peptidase-4
EC cell	Enterochromaffin cell

EDTA	Ethylenediaminetetraacetic acid
ELISA	Enzyme-linked immunosorbent assay
ENS	Enteric nervous system
FBG	Fasting blood glucose
FFA	Free fatty acid
FFAR	Free fatty acid receptor
FSC-A	Forward scatter
g	Gravity
g	Grams
GABA	Gamma-Aminobutyric acid
GF	Germ free
GI	Gastrointestinal tract
GIP	Gastric inhibitory peptide
GLP-1	Glucagon-like peptide 1
GLP-2	Glucagon-like peptide 2
GLUT	Hexose transporter
GPCR	G protein-coupled receptor
GSIS	Glucose stimulated insulin secretion
GTT	Glucose tolerance test
HbA_{1c}	Glycated hemoglobin
HBSS	Hank's Balanced Salt Solution
HFD	High fat diet
HSL	Hormone sensitive lipase
iBAT	Interscapular brown adipose tissue
IBD	Inflammatory bowel disease
IBS	Irritable bowel syndrome

IL-13	Interleukin 13
IL-1β	Interleukin 1β
IP_3	Inositol triphosphate
ITT	Insulin tolerance test
L-AADC	L-amino acid decarboxylase
LCFA	Long chain fatty acid
LCN2	Lipocalin 2
LDL	Low-density lipoprotein
LFD	Low fat diet
LP	Light phase
LPS	Lipopolysaccharide
Lrp5	Lipoprotein receptor-related protein 5
MAO-A	Monoamine oxidase A
MCFA	Medium chain fatty acid
MNE	Mean normalised expression
MRI	Magnetic resonance imaging
mRNA	Messenger ribonucleic acid
n	Number of replicates
NMDS	Non-metric multidimensional scaling
OR1G1	Olfactory receptor 1G1
OTUs	Operational taxonomic units
PACAP	Pituitary adenylate cyclase-activating polypeptide
PBS	Phosphate buffered saline
PEG	Polyethylene glycol
PERMANOVA	Permutational analysis of variance
PGC1α	Peroxisome proliferator-activated receptor gamma coactivator 1-alpha

PYY	Peptide YY
rpm	Rotations per minute
RQ	Respiratory quotient
rRNA	Ribosomal ribonucleic acid
SCFA	Short chain fat acid
SEM	Standard error of the mean
SERT	Serotonin reuptake transporter
SGLT1	Sodium-glucose co-transporter 1
SGLT3	Sodium-glucose co-transporter 3
SSC-A	Side scatter
SSRI	Selective serotonin reuptake inhibitor
SST	Somatostatin
sWAT	Subcutaneous white adipose tissue
T1R2	Taste 1 receptor member 2
T1R3	Taste 1 receptor member 3
T2D	Type 2 diabetes
TG	Thapsigargin
TGR5	G protein-coupled bile acid receptor 1
TLR	Toll-like receptor
TNBS	Trinitrobenzenesulfonic acid
TPH	Tryptophan hydroxylase
TPH1/2	Tryptophan hydroxylase isoform 1/2
TRPA1	Transient receptor potential cation channel, subfamily A, member 1
UCP1	Uncoupling protein 1
VMAT1	Vesicle monoamine transporter 1
WAT	White adipose tissue

Thesis Summary

Enterochromaffin (EC) cells are a specialised type of enteroendocrine cell within the mucosal lining of the gastrointestinal tract that synthesise and secrete almost all serotonin (5-HT) in the body. EC cell-derived 5-HT is a pleiotropic bioamine, with a wide range of physiological roles, including platelet aggregation, GI motility, bone density regulation, liver regeneration and inflammation. A growing body of evidence also highlights the role of 5-HT in the regulation of glucose homeostasis and energy metabolism, via effects on hepatic gluconeogenesis, mobilization of hepatic free fatty acids and the browning of white adipose tissue. The broad physiological effects of EC cell-derived 5-HT have direct implications for metabolic disorders such as type 2 diabetes (T2D) and obesity, where energy homeostasis is significantly perturbed.

The gut microbiome has been demonstrated to regulate metabolism, and a dynamic relationship exists whereby microbial metabolites such as short chain fatty acids (SCFAs) can increase EC cell 5-HT synthesis. Evidence also suggests an increase in 5-HT following nutrient ingestion. Details related to how EC cells respond to ingested nutrients and the microbiome are scarce, however, and despite their role in regulating a number of important physiological functions, primary EC cell biology has been inadequately studied.

The aims of this work were, firstly, to isolate primary EC cells from the duodenum and colon of mice and interrogate their nutrient sensing capacity of primary EC cells under low- and high-fat diet conditions, and to evaluate whether this nutrient sensing capacity is region-dependent. This work then aimed to determine whether luminal nutrients, particularly sugars and SCFAs, acutely increase 5-HT release. Finally, this work aimed to develop a mouse model of microbial dysbiosis and depleted gut 5-HT, to determine whether the gut microbiome alters host metabolism through a gut 5-HT-dependent pathway.

This study has demonstrated the novel finding that regional subpopulations of EC cells exist, with respect to their size, nutrient sensing capacity and response to a number of nutrient stimuli. In particular, duodenal and colonic EC cells have the capacity to detect a number of sugars and sweet tastants, through hexose transporters and taste receptors, respectively, as well as free fatty acids within the GI lumen. In addition, the capacity of EC cells to detect these nutrients is dependent on the region of the gut they exist in, and can be influenced by dietary changes. In addition, this work has found that in an acute setting, sugars such as glucose, fructose and sucrose, differentially increase the release of 5-HT from duodenal and colonic EC cells, while SCFAs do not. Findings in this study also demonstrate that gut 5-HT acts as a signalling nexus between the gut microbiome and host metabolism, by affecting blood glucose control and adiposity. Finally, this work provides the first evidence of existence of a bi-directional relationship between the gut microbiome and gut 5-HT. This study has, therefore, demonstrated that EC cells are important, region-specific sensory cells that can detect and respond to changes in the luminal environment of the GI tract, and that this can have significant consequences for regulating host metabolism and potentially human health.

Publications during candidature

The following publications have arisen from work associated with this thesis:

Alyce M. Martin, Amanda L. Lumsden, Richard L. Young, Claire F Jessup, Nick J. Spencer and Damien J. Keating (2017), 'The nutrient-sensing repertoires of mouse enterochromaffin cells differ between duodenum and colon', *Neurogastroenterology and Motility*, e13046

Alyce M. Martin, Amanda L. Lumsden, Richard, L. Young, Claire F. Jessup, Nick J. Spencer and Damien J. Keating (2017), 'Regional differences in nutrient-induced secretion of gut serotonin', *Physiological Reports*, Vol. 5, Issue 6, e13199

Alyce M. Martin, Richard L. Young, Lex Leong, Geraint B. Rogers, Nick J. Spencer, Claire F. Jessup and Damien J. Keating (2017), 'The diverse metabolic roles of peripheral serotonin', *Endocrinology*, Vol. 158, Issue 5, pp. 1049-1063

The following publications have arisen from work unrelated to this thesis:

Heshan Peiris, Michael D. Duffield, Joao Fadista, Claire F. Jessup, Vinder Kashmir, Amanda J. Genders, Sean L. McGee, **Alyce M. Martin**… (+23), Damien J. Keating (2016), 'A Syntenic Cross Species Aneuploidy Genetic Screen Links RCAN1 Expression to β-cell Mitochondrial Dysfunction in Type 2 Diabetes', *PLoS Genetics*, Vol. 12, Issue 5, e1006033

Leah Zelkas, Ravi Raghupathi, Amanda, L. Lumsden, **Alyce M. Martin**, Emily Sun, Nick J. Spencer, Richard L. Young and Damien J. Keating (2015), 'Serotonin-secreting enteroendocrine cells respond via diverse mechanisms to acute and chronic changes in glucose metabolism', *Nutrition & Metabolism*, Vol. 12, p. 55

Declaration

I certify that this thesis does not incorporate without acknowledgment any material previously submitted for a degree or diploma in any university; and that to the best of my knowledge and belief it does not contain any material previously published or written by another person except where due reference is made in the text.

Alyce Maree Martin

19th December 2017.

Acknowledgements

I am greatly indebted to my Primary Supervisor, Prof. Damien Keating, to whom I express the utmost gratitude for his invaluable guidance, knowledge, mentorship and time-commitment throughout my candidature. Without his direction and contagious drive for success, this work would not have been possible. It has been a privilege to be part of the Molecular and Cellular Physiology Lab, and to work in such a cohesive team environment.

I am also extremely thankful to my Associate Supervisors, Dr. Claire Jessup, Prof. Nick Spencer and Prof. Rainer Haberberger, for the expertise, advice and time they have dedicated to me. I would particularly like to thank Claire; for all the chats over coffee, for letting me use her office when I needed a respite, and for always leaving her door open, and Nick; for being the most entertaining of travel companions and for his contagious enthusiasm - it has been extremely motivating.

I would like to acknowledge the support of all the people who have contributed to this work, through the provision of technical assistance and advice. I would especially like to thank my fellow lab member, Dr. Mandy Lumsden; my colleague and collaborator, A/Prof Richard Young; and past lab members, Dr. Michael Duffield and Dr. Heshan Peiris, for all their input and friendship. My thanks also go to Dr. Sheree Bailey and Ms. Jennifer Washington for their help with the flow cytometry, Melinda Kyloh for her expertise on the art of a good dissection, and Dr. Dusan Matusica for his, at times, colourful input and advice on a great deal of things – both science and life-related. This work would also not be possible without the assistance of all the staff at both the Flinders University College of Medicine and Public Health (CoMAPH) Animal Facility and SAHMRI Bioresources, and all the mice who were sacrificed in the name of research – I am eternally grateful.

I would also like to acknowledge the financial contributions made to me, through the Australian Government Research Training Program Scholarship, the Centre for Neuroscience, and various other small grants that have made much of this work possible.

I have been extremely privileged to make many friends throughout my candidature, all of whom have enriched my time as a PhD Candidate with much fun, love and laughter. I am especially grateful for the invaluable friendships of Emily Sun (my “Lab Wife”), Shee Chee Ong, Jastrow Canlas and Lauren Jones – my lunch-time, pub-time, coffee-time, focus group who I value immensely.

Of course, I must thank my fiancé Michael for his constant love, support and understanding – for sticking by me through good times and bad, for celebrating my achievements, and for tirelessly reminding me of how far I have come. He has been an integral part of this journey, and I could not have done it without him.

Finally, I must thank my wonderful Mum, Kristina, whose love, dedication and unwavering support has been behind every facet of this work. Words fail to express the magnitude of how grateful I am to her, for all that she has committed to helping me get to this point. This achievement is as much hers as it is mine.

CHAPTER 1: Literature Review

The majority of work presented in this chapter is comprised of published work, from the following publication: Alyce M Martin *et al.* (2017), 'The diverse metabolic roles of peripheral serotonin', *Endocrinology*, 158(5):1049-1063. The relative author contributions to this work are as follows: AM Martin, and DJ Keating were involved in planning the content of the manuscript. AM Martin reviewed the literature. CF Jessup, RL Young, L Leong, GB Rogers and NJ Spencer provided critical input and advice. AM Martin and DJ Keating wrote the paper and all authors were involved in drafting the manuscript. This work is supported by funding from the Australian Research Council and National Health and Medical Research Council (CI: DJ Keating). No competing interests are declared.

1.1 Introduction

Enteroendocrine cells collectively constitute the largest endocrine tissue in our body (nebigilAhlman and Nilsson, 2001). These cells are scattered amongst the gastrointestinal (GI) epithelium and make up about 1% of all cells lining the GI tract. They consist of an array of different cell types, each secreting a number of hormones in response to various physiological stimuli, including nutrient levels and gut distension. Enterochromaffin (EC) cells within the GI mucosa are a type of specialized enteroendocrine cell that synthesize and secrete between 90-95% of total body serotonin (5-hydroxytryptamine, 5-HT) (Erspamer, 1954). They are the most significant source of this important multi-functional bioamine and constitute about half of all enteroendocrine cells. The remaining systemic pool of 5-HT is synthesized predominantly by serotonergic neurons within the central nervous system (CNS) (Walther et al., 2003a, Haahr et al., 2015, Li et al., 2011, Pissios and Maratos-Flier, 2007, Simansky, 1996), with much smaller amounts produced by the enteric nervous system (ENS) (Gershon et al., 1965), pancreatic islets (Kim et al., 2010), mammary glands (Laporta et al., 2013, Marshall et al., 2014, Matsuda et al., 2004, Stull et al., 2007), immune cells (Ahern, 2011) and adipose tissue (Crane et al., 2015). Plasma 5-HT does not cross the blood-brain barrier (Nakatani et al., 2008) and indeed, central

and peripheral sources of 5-HT may have opposing roles in energy homeostasis (Namkung et al., 2015).

The synthesis of 5-HT requires the rate-limiting enzyme tryptophan hydroxylase (TPH) which exists as two isoforms. TPH1 is predominantly localized in gut EC cells as well as other non-neuronal sources, while TPH2 is largely restricted to neurons of the CNS (Walther et al., 2003a) and ENS (Li et al., 2011). A small proportion of enteric neurons (~1%) also contain 5-HT (Costa et al., 1996). EC cell-derived 5-HT is a pleiotropic bioamine, with wide-ranging actions including roles in platelet aggregation (Walther et al., 2003b), GI motility (Keating and Spencer, 2010), regulation of bone density (Yadav et al., 2009), liver regeneration (Lesurtel et al., 2006) and inflammation (Margolis et al., 2014). Recent studies demonstrate that 5-HT also regulates glucose homeostasis, hepatic gluconeogenesis, mobilization of hepatic free fatty acids and the browning of white adipose tissue (Crane et al., 2015, Watanabe et al., 2010, Sumara et al., 2012). The broad physiological effects of EC cell-derived 5-HT have direct implications for metabolic disorders such as type 2 diabetes (T2D) and obesity where energy homeostasis is significantly perturbed. One mechanism underlying this may involve EC cells acting as a signalling nexus between the gut microbiome and host, with gut dysbiosis and altered bacterial signalling in obese individuals identified as a pathway through which gut 5-HT may impact metabolic control (Le Chatelier et al., 2013, Reigstad et al., 2015).

1.2 Biosynthesis and secretion of EC-cell 5-HT

Enterochromaffin cells make up the single largest enteroendocrine cell population within the gastrointestinal tract (Nilsson et al., 1987) and are the major source of circulating 5-HT (Gershon and Tack, 2007, Bertrand, 2006). The life cycle of EC cells begins with LGR5-positive adult stem cells, located in the intestinal crypts. These stem cells differentiate into progenitor transit-amplifying cells, which proceed to differentiate further and commit to the EC cell lineage while migrating up the crypt axis. Once at the crypt/villus base, these cells

cease differentiation and, particularly in the small intestine, migrate up the villus axis as mature endocrine cells (Barker, 2014). While the precise turnover rates of EC cells are unknown, the turnover rate of the intestinal epithelium, in particular mucosal enterocytes, is approximately 3-5 days. As such, the presence of certain stimuli within the gut lumen, such as gut microbiota, has the potential to rapidly increase EC cell numbers (Yano et al., 2015).

The heterogeneity of EC cell shape, size, luminal contact sites and secretory granule contents suggests the existence of several subpopulations of these cells (Hansen and Witte, 2008, Diwakarla et al., 2017, Martins et al., 2017). In particular, subpopulations of EC cells have been identified based on the co-localisation pattern of 5-HT with secretin and substance P, with respect to their position along the GI tract and the crypt-to-villus axis (Roth and Gordon, 1990). These subpopulations of 5-HT-containing cells can be further defined by the varied combinations of other hormones, such as CCK, secretin, PYY and chromogranin A, found to be either co-stored within the same vesicle, or in distinct vesicles within the same cell (Fothergill et al., 2017b). The terms ‘open-type’, referring to EC cells which have luminal contact and ‘closed-type’ cells that appear clustered with no luminal contact, have been used to describe possible subpopulations of EC cells (Kusumoto et al., 1988). Although, the majority of EC cells are likely to be ‘open-type’ EC cells, as EC cells without distinct projections have been seen in less than 5% of all examined parts of the GI. These cells lacking projections may also represent naïve EC cells (Gustafsson et al., 2006). Cellular characteristics of these cells remain unknown. The presence of subpopulations of EC cells is further supported by distinct nutrient sensing abilities of some, but not all, 5-HT containing EC cells within the gut (Young, 2011).

EC cells are dispersed throughout the GI tract mucosa from the oesophagus to the rectum in varying densities in rodent (Fujimiya et al., 1991, Moore et al., 2005) and porcine (Raghupathi et al., 2013) models. Within the small intestine, most EC cells exist in mucosal

crypts, shown by 5-HT immunoreactivity in tissue segments (Fujimiya et al., 1991). Being a mechanosensitive cell (Bertrand, 2004), EC cells can be stimulated to release 5-HT by peristaltic contractions within the gut, a nutrient bolus or faecal deposition (Spencer et al., 2011, Bertrand, 2006). Other sensory capabilities of EC cells have been described within whole tissue preparations and *in vivo* animal models and will be discussed in more detail in section *1.5.3 Nutrient sensing*.

1.2.1 Synthesis of 5-HT by EC cells

EC cells are responsible for the release of the vast majority of total 5-HT into the GI lumen as well as into the portal circulation (Racké et al., 1995) (Figure 1.1). The synthesis of 5-HT begins with the essential dietary amino-acid, L-tryptophan, which is taken up into cells via a plasma membrane amino acid transporter and is subsequently converted to 5-hydroxytryptophan (5-HTP) by the rate-limiting enzyme, TPH1 (Walther et al., 2003a). The conversion of 5-HTP to 5-HT is mediated by L-amino acid decarboxylase (L-AADC) (Rahman et al., 1981). Vesicular monoamine transporter 1 (VMAT1) embedded within vesicular membranes allows the newly synthesised 5-HT to be packaged into large dense core vesicles, which migrate towards the plasma membrane to undergo exocytosis (Wu et al., 2011, Bertrand and Bertrand, 2010).

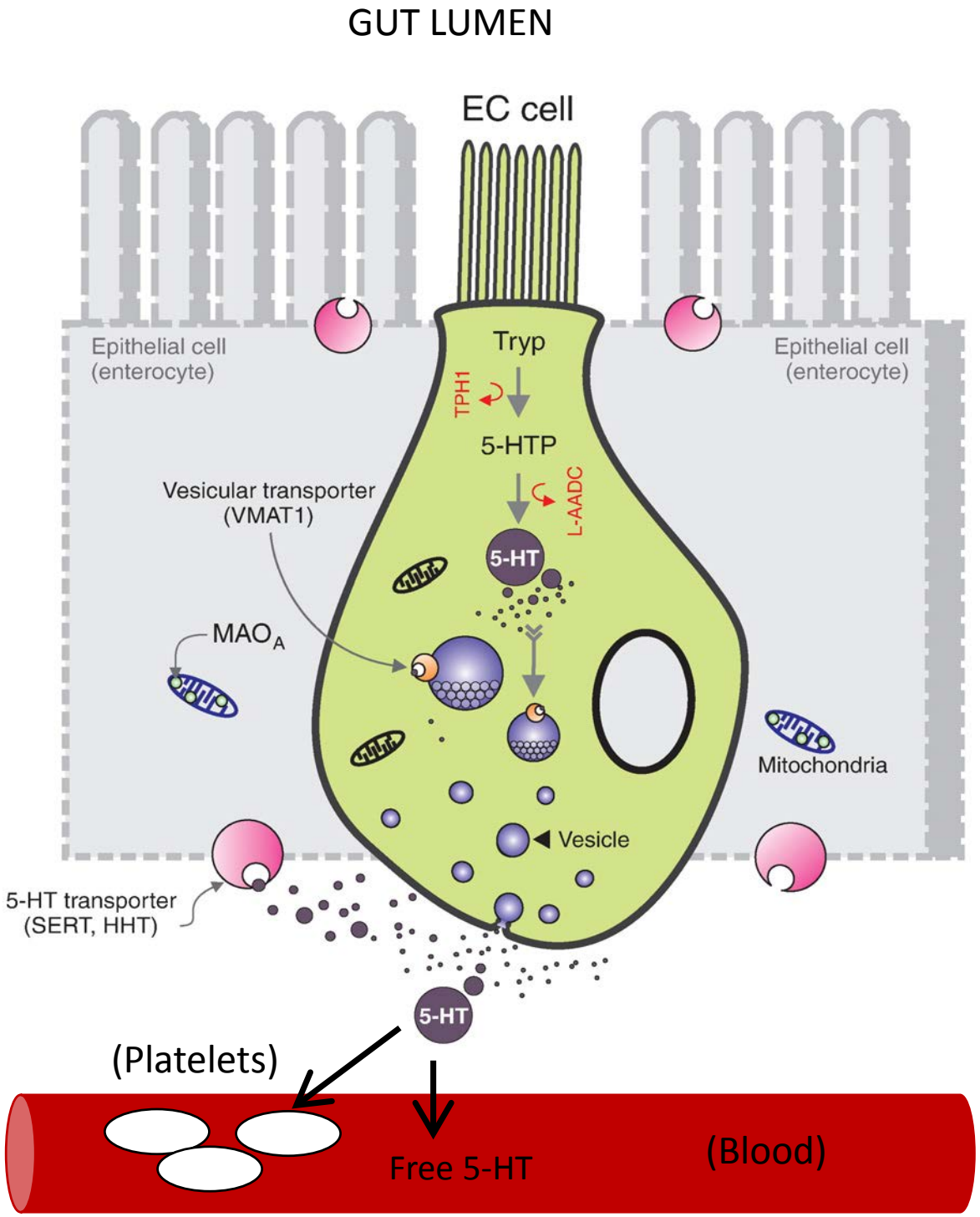
GUT LUMEN
EC cell
Epithelial cell
(enterocyte)
Epithelial cell
(enterocyte)
Tryp
TPH1
5-HTP
L-AADC
5-HT
Vesicular transporter
(VMAT1)
MAO$_A$
Mitochondria
Vesicle
5-HT transporter
(SERT, HHT)
5-HT
(Platelets)
Free 5-HT
(Blood)

Figure 1.1 – Synthesis and secretion of 5-HT from EC cells in the intestinal mucosa. Dietary L-tryptophan (Tryp) is converted to 5-hydroxytryptophan (5-HTP) via the rate-limiting enzyme, tryptophan hydroxylase 1 (TPH1). 5-HTP is then converted to 5-hydroxytryptamine (5-HT) by L-amino acid decarboxylase (L-AADC), and transported by VMAT1 into large dense core vesicles. Following release, 5-HT can be transported into neighbouring cells or circulating platelets though the serotonin reuptake transporter (SERT), with a small percentage existing as free circulating 5-HT. All free 5-HT is metabolised by the liver, with only platelet 5-HT entering the systemic circulation. Following uptake into cells, 5-HT can be metabolised by mitochondrial monoamine oxidase A (MAO_A). Adapted from Bertrand & Bertrand (2010).

1.2.2 Secretory mechanisms of EC cell 5-HT release

Following biosynthesis within EC cells, 5-HT is stored for release in acidified large dense core vesicles (Raghupathi et al., 2016). This process is dependent upon the presence of VMAT1 and acidification of the vesicles via the vacuole H^+-ATPase proton pump. Inhibition of either of these proteins significantly attenuates both basal and stimulus-induced 5-HT secretion (Raghupathi et al., 2016). While precise signalling pathways have not been elucidated in primary EC cells, 5-HT release in response to high potassium or acetylcholine is dependent on entry of extracellular calcium into the cell, largely through voltage-gated L-type calcium channels (Raghupathi et al., 2013). The influx of extracellular calcium is also an important mechanism by which EC cells respond to mechanical stimuli. Specifically, the mechanically sensitive Piezo2 channel rapidly induces an inward cation current, membrane depolarisation and L-type calcium channel activation following a local mechanical stress stimulus (Woo et al., 2014). The influx of calcium via these channels is then likely to trigger vesicle membrane fusion and 5-HT exocytosis. Vesicle size is a major determinant of vesicle release kinetics (Albillos et al., 1997, Zhang and Jackson, 2010), as stability of an initial fusion pore is influenced by size-related curvature of the vesicle membrane (Zhang and Jackson, 2010). The mechanisms of 5-HT exocytosis can be considered unique, as 5-HT is stored within large vesicles, but the amount of 5-HT released per exocytosis event is significantly lower in EC cells in comparison to hormone secretion from other endocrine cells, such as adrenaline release from chromaffin cells in the adrenal medulla. This is despite EC cells and chromaffin cells having comparative vesicle size (Raghupathi et al., 2013). Rather, the amount of 5-HT that is released per exocytosis fusion event in EC cells is similar to the release of dopamine from much smaller synaptic vesicles in neuronal cells (Staal et al., 2004). This indicates that release of 5-HT from EC cells may occur via synaptic-like kinetics, such as rapid opening and closing of the fusion pore, termed ‘kiss-and-run’. This results in low amounts of 5-HT released per fusion event, rather than the larger payload released with full vesicle fusion. Indeed, the fusion

pore size within EC cell secretory vesicles has been shown to be less than 9 nm, which is much smaller than that found in chromaffin cells, and acts to tightly control the amount of 5-HT released (Raghupathi et al., 2016). As such, increased stability of the fusion pore in response to certain stimuli, such as glucose, results in increased quantal release of 5-HT per fusion event (Raghupathi et al., 2013, Zelkas et al., 2015), while stimulants such as acetylcholine or high potassium increase the frequency of 5-HT exocytosis events (Raghupathi et al., 2013). The physiological relevance of this may relate to the close proximity between nerve endings and EC cells as these cells mature and migrate up the crypt/villus axis, such that the levels of 5-HT released with these kinetics are very close to the activation threshold of neighbouring 5-HT receptors on intestinal nerve endings (Raghupathi et al., 2013). Many 5-HT receptors are activated at 5-HT concentrations between 1-10 nM, while 5-HT_3 receptors are activated at 5-HT levels above 10 nM (Murray et al., 2011). Under acute stimulatory conditions, such as intestinal contraction or the presence of luminal nutrient stimuli, increased release of 5-HT per fusion event may exceed this activation threshold of 5-HT_3 receptors (Raghupathi et al., 2013). In addition, the comparatively small amount of 5-HT that is released per exocytosis fusion event may also minimise the desensitisation of local higher-affinity 5-HT receptors on adjacent nerve endings.

1.2.3 5-HT receptors

The family of 5-HT receptors is comprised of 13 distinct seven-transmembrane G protein-coupled receptors (GPCRs) and one ligand-gated ion channel which have been highly conserved throughout evolution (Nichols and Nichols, 2008, Hoyer et al., 2002). The existence of one or more of these receptors on respective target tissues facilitates 5-HT-mediated activity and associated physiological outcomes throughout the body. A multitude of serotonergic signalling pathways exists, with several potential pathways for each receptor subtype based on their respective GPCR coupling and signalling cascades (Figure 1.2): (1) $5\text{-HT}_{1(A,B,D\text{-}F)}$ and $5\text{-HT}_{5(A,B)}$ receptors coupled to Gαi/o inhibit adenylate cyclase (AC) activity, (2) $5\text{-HT}_{2(A\text{-}C)}$

receptors coupled to Gαq activate the phospholipase C cascade, (3) 5-$HT_{3(A-E)}$ receptor ion channels selectively allow the passage of cations, (4) 5-$HT_{4(S,L)}$, 5-HT_6 and 5-HT_7 receptors couple to $G\alpha_s$ and positively couple to AC (Masson et al., 2012, Hannon and Hoyer, 2008). Within these families, multiple 5-HT receptor subtypes have been identified, each of which has distinct ligand-binding domains and a multitude of different downstream signalling pathways and effectors (Noda et al., 2004, Hannon and Hoyer, 2008). Signalling pathways by individual 5-HT receptor subtypes may also be dependent upon the type of cell in which they are expressed. An example of this is the signalling through 5-HT_{1A} receptors occurring via inhibition of AC in transfected HeLa cells (Fargin et al., 1989), and via activation of AC in HEK-293 cells (Albert et al., 1999) and rat hippocampus (Markstein et al., 1999). Differential responses in various tissues expressing the same 5-HT receptor may also be due to the capacity of G protein-coupled receptors to undergo oligomerization to form homodimers and heterodimers (Nichols and Nichols, 2008), such as the 5-$HT_{1A,2A,2C}$ and 5-HT_4 homodimers and the 5-HT_{1A}-5HT_7 heterodimer (Herrick-Davis, 2013).

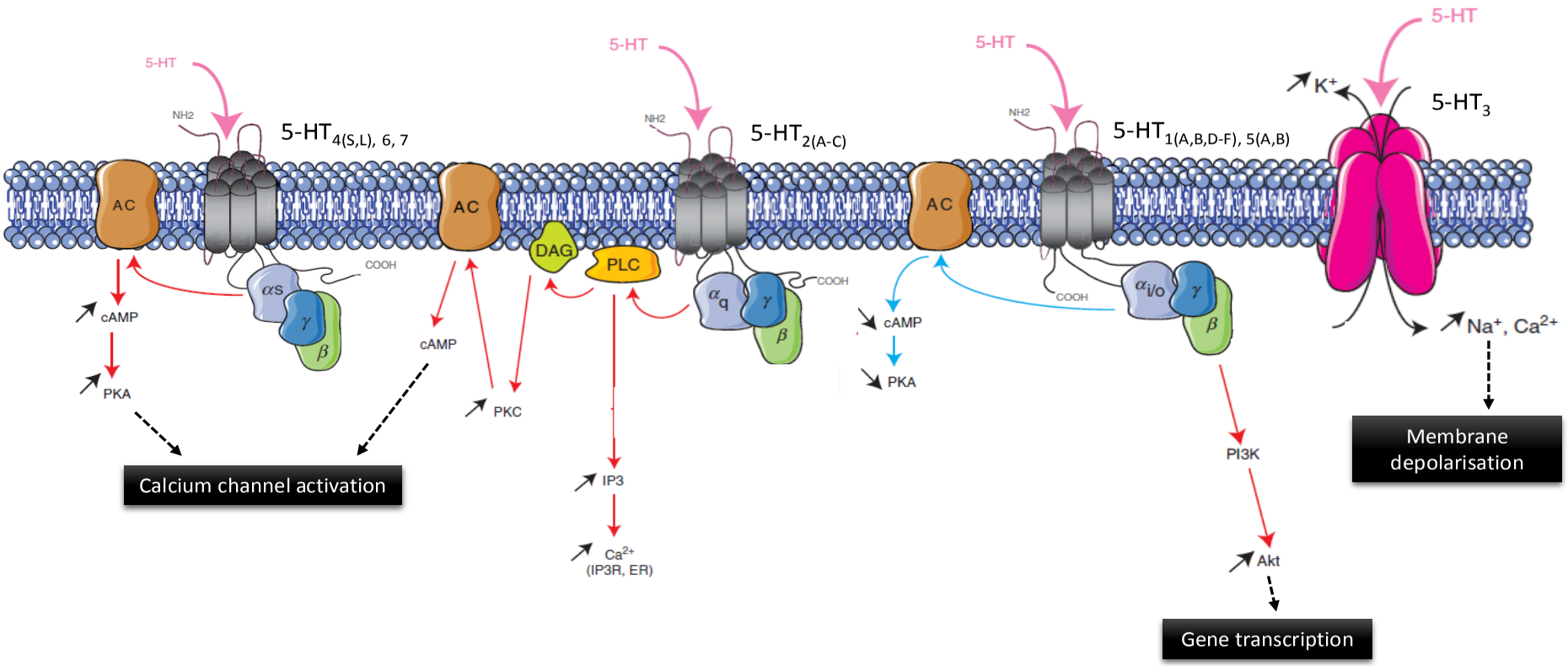

Figure 1.2 – Simplified schematic of selected 5-HT receptor subtype signalling pathways: (1) 5-HT_1 and 5-HT_5 receptors coupled to Gαi/o inhibit adenylate cyclase (AC) activity, leading to reduced cyclic-AMP (cAMP) and protein kinase a (PKA) activity. (2) 5-HT_2 receptors coupled to Gαq increase inositol triphosphate (IP3) and calcium channel activation and, thus, calcium release from endoplasmic reticulum (ER) stores. This receptor also activates a phospholipase C (PLC) cascade, whereby increasing diacylglycerol (DAG)-mediated protein kinase C (PKC) activity, and activation of AC. (3) 5-HT_3 receptor ion channels selectively transport cations, (4) 5-HT_4, 5-HT_6 and 5-HT_7 receptors couple to $G\alpha_s$ and positively couple to AC to increase cAMP and PKA, leading to calcium channel aviation (red arrows: activation, blue arrows: inhibition). Adapted from (Masson et al., 2012).

1.2.4 Serotonin reuptake transporter (SERT) function

5-HT is highly positively charged at physiological pH, thus preventing it from passing through lipid membranes (Hansen and Witte, 2008). Luminally secreted 5-HT can be taken up by epithelial cells within the gut lumen, while 5-HT released into the basolateral space can enter the portal circulation, primarily stored in platelets (Bertrand and Bertrand, 2010). The transport of 5-HT is dependent upon the presence of the serotonin reuptake transporter (SERT) on the plasma membrane of target cells, and is critical to terminate serotonergic signalling (Coleman et al., 2016). The binding of Na^+ and Cl^- ions to SERT is essential for 5-HT uptake, and changes to the structural conformation through genetic mutations or inhibitor binding can have significant effects on SERT activity (Coleman et al., 2016). Consequently, the physiological activity of 5-HT can be augmented by increasing the bioavailability of circulating 5-HT. Such is the action of selective serotonin-reuptake inhibitors (SSRIs) (Gershon and Tack, 2007, Takahashi et al., 2002, Thazhath et al., 2014), which bind to the SERT allosteric site to induce an outward-open conformational change. This increases exposure of the allosteric site to extracellular substrates, allowing them to reach a central binding site, but also inhibits the transition of SERT to the inward-facing conformation (Coleman et al., 2016). Feedback mechanisms regulating plasma membrane SERT expression have been demonstrated in HEK293 cells pre-treated with 5-HT, which dose-dependently decreased SERT expression (Jorgensen et al., 2014). This is indicative of a regulatory negative-feedback mechanism, possibly involving substrate translocation, whereby downstream intracellular activity of 5-HT is controlled. Increased SERT expression, on the other hand, is observed in cultured thalamocortical neurons following chronic exposure to 5-HT, an effect which is blocked by treatment with an SSRI (Whitworth et al., 2002). This suggests SERT may be regulated by different mechanisms during acute and chronic exposure to 5-HT; however, it may also be a reflection of different stages in cell development which require 5-HT for growth and

development, as with neuronal cell differentiation during embryonic development (Cote et al., 2007).

Once SERT has facilitated the uptake of 5-HT into target cells, 5-HT is rapidly degraded to either 5-hydroxyindoleacetic acid (5-HIAA), by monoamine oxidase A (MAO-A) (Weissbach et al., 1957), or to 5-HT-O-glucuronide (Korf and Sebens, 1970), both of which are excreted in urine. The liver is the major site of free 5-HT entering the circulation from the gut via the portal vein, leaving only platelet 5-HT. 5-HIAA is the primary metabolite from the catabolism of 5-HT, and excreted levels in urine are often used as an indicator of the amount of circulating 5-HT synthesised by EC cells. Urinary 5-HIAA therefore provides a useful tool for the analysis of the levels of either or both EC cell 5-HT synthesis and circulating 5-HT in various disease states (Cubeddu et al., 1992, Takahashi et al., 2002, Castejon et al., 1999, Sumara et al., 2012).

1.3 Diverse physiological roles of peripheral 5-HT

A diverse range of physiological processes are influenced by circulating 5-HT, via activation of 5-HT receptors and/or cellular uptake through SERT. Serotonin signalling is evident and necessary throughout development, and alterations to circulating 5-HT can have substantial physiological effects.

1.3.1 Cardiovascular function

A role of peripheral 5-HT in regulating cardiovascular function has been well-established, as platelet stores of 5-HT promote platelet aggregation and haemostasis, while affecting blood flow by modulating vasculature and cardiac muscle.

1.3.1.1 Platelet aggregation and haemostasis

Most circulating 5-HT is taken up by and stored within platelets via SERT. During platelet activation, stored 5-HT is released from dense granules and can trigger platelet aggregation via

a combination of intracellular and extracellular signalling pathways. 5-HT released from platelets can act in an autocrine manner on 5-HT_{2A} receptors, which results in an increase in intracellular calcium (Wolf et al., 2016) and downstream activation of transglutaminase. When activated, transglutaminase acts with intracellular 5-HT stores to serotonylate several small GTPase molecules involved in exocytosis of α-granules, thereby making them constitutively active and enhancing the release of factors involved in irreversible platelet aggregation (Walther et al., 2003b). In addition, 5-HT induces a switch in surface N-glycan components involved in cell-to-cell adhesion, also via a 5-HT_{2A}-dependent signalling pathway (Mercado et al., 2013). Further to enhancing platelet aggregation, 5-HT increases thrombin generation by covalently cross-linking to a variety of adhesion proteins and clotting factors on the cell surface of a subpopulation of platelets (Dale, 2005).

Circulating 5-HT protects red blood cells from degradation, however this is not mediated through 5-HT receptors (Amireault et al., 2013). Rather, the antioxidant properties of 5-HT act to preserve red blood cells from oxidative damage that contributes to haemolysis. Mice lacking 5-HT through genetic ablation of TPH1 exhibit anaemia due to reduced red blood cell counts and haemoglobin levels compared with wild type counterparts (Amireault et al., 2011). This is not only due to increased oxidation and haemolysis of red blood cells, but a defect in the differentiation of erythroid precursor cells to red blood cells, whereby reducing the number of circulating mature red blood cells (Amireault et al., 2011).

As such, EC-cell-derived 5-HT plays a substantial role in haemostasis, as mice lacking *Tph1* have increased blood clotting time and reduced red blood cell survival which can be rescued by administration of endogenous 5-HT. Decreased circulating 5-HT, therefore, conveys protection from diseases associated with enhanced blood clotting and thrombus formation and instability, such as thromboembolism (Walther et al., 2003b). While addition of

exogenous 5-HT has been shown to be a useful tool in prolonging shelf-life for blood transfusions and post-transfusion red blood cell survival (Amireault et al., 2013).

1.3.1.2 Cardiac and vascular function

Several 5-HT receptor subtypes are expressed in distinct regions within the human heart. For example, cardiac valves express 5-HT_{2B} receptors, arteries express 5-HT_{1B} and 5-HT_{2A}, and atrium and ventricles express 5-HT_4 receptors (Kaumann and Levy, 2006). This may relate to the functionality of each region of the heart, and the downstream mechanisms of each receptor subtype. Each receptor subtype plays an important role in overall cardiovascular function, expression of 5-HT_{2B} receptors, in particular, is required for the development of cardiac tissue (Nebigil et al., 2000).

Exogenous 5-HT administration has pharmacological effects on heart rate, force of heart contractions, and a diverse range of effects on the peripheral vasculature (Kaumann and Levy, 2006). Physiological regulation of splanchnic blood flow and blood pressure involves the activation of 5-HT receptors, to elicit coordinated changes in vascular diameter and cardiac smooth muscle contractions (Watts et al., 2012, Gentilcore et al., 2007). Activation of 5-HT_{2A} receptors increases vascular smooth muscle contractions via a p42/44 MAPK pathway (Bhaskaran et al., 2014), while activation of 5-HT_{1B} receptors has been demonstrated to result in vasodilation of cerebral blood vessels (Wolf et al., 2016). Altered circulating 5-HT has a number of downstream consequences for cardiovascular function. In particular, overexpression of SERT is responsible for pulmonary artery smooth muscle hyperplasia (Eddahibi et al., 2001), and may also contribute to post-prandial hypotension (Gentilcore et al., 2007). As such, pharmaco-therapeutics aimed at targeting 5-HT receptors and modifying circulating 5-HT levels convey significant risks, due to potential cardiovascular complications (Tack et al., 2012, Watts et al., 2012).

1.3.2 Liver regeneration

Following hepatic injury, such as hepatic ischemic reperfusion injury or partial hepatectomy, peripheral 5-HT has been demonstrated to play a key role in hepatic tissue regeneration through 5-HT_{2A} and 5-HT_{2B} receptors (Fausto et al., 2006, Lesurtel et al., 2006). A number of genes regulating cell proliferation and apoptosis pathways downstream of 5-HT receptor signalling are also upregulated in hepatocytes, sinusoidal epithelial cells and pit cells within regenerating hepatic liver (Chang et al., 2015). Under conditions of increased metabolic demand, in particular during pregnancy and the transition to lactation, 5-HT affects the expression of key metabolic enzymes in hepatocytes (Laporta et al., 2013). The role of peripheral 5-HT in hepatic influences on metabolism will be discussed in further detail in section *1.4.1.1*.

1.3.3 Genito-uterine function

Circulating 5-HT has a significant role in influencing sexual function, through vascular and non-vascular mechanisms, and modulating other endocrine functions (Frohlich and Meston, 2000). This is evidenced by increased circulating 5-HT following treatment with SSRIs being associated with sexual dysfunction in both men and women (Corona et al., 2009). In particular, regulation of appropriate vasodilation and vasoconstriction by 5-HT may play a key role in maintaining normal sexual function and arousal response, as hypertension has also been associated with sexual dysfunction in both men (Dusing, 2005, Bansal, 1988) and women (Nascimento et al., 2015, De Franciscis et al., 2013).

Smooth muscle activity, such as that in the bladder and uterus, is also affected by circulating 5-HT. Several 5-HT receptors are expressed throughout the urinary tract in rabbits and pharmacological blockade of these receptors demonstrates regional functionality of 5-HT at specific sites along the urinary tract (Lychkova and Pavone, 2013). In particular, contractions of the bladder are characterised by initial rapid contractions followed by tonic contractions,

however the specific 5-HT receptors mediating this vary between species (Frohlich and Meston, 2000). Uterine smooth muscle contractions in both rat (Wrigglesworth, 1983) and human tissue (Maigaard et al., 1986) are stimulated by 5-HT *in vitro*. Functionally, the activity of 5-HT on uterine contractions likely contributes to menstruation, during which females experience cyclical 5-HT levels over the course of the menstrual cycle (Blum et al., 1992). Midluteal, late luteal and premenstrual phases are associated with increased circulating 5-HT, while levels decline during menstruation, follicular and ovulation phases (Rapkin et al., 1987). Perturbed levels of serum 5-HT during these phases is associated with premenstrual syndrome, however this is largely associated with central serotonergic symptoms (Rapkin et al., 1987). The fluctuations in circulating 5-HT seen in females therefore makes it challenging to study physiological effects of 5-HT in both males and females and may underlie differences seen in physiological processes involving 5-HT signalling pathways.

1.3.4 Embryogenesis and mammary gland function

During pregnancy, circulating 5-HT contributes to a number of physiological processes. In particular, 5-HT plays a substantial role throughout embryonic development (Amireault and Dube, 2005), through regulation of embryonic neuronal, craniofacial and cardiac tissue development, via signalling to several 5-HT receptors (Cote et al., 2007, Nebigil et al., 2000, Lauder et al., 2000). Effects on maternal physiology during pregnancy and lactation are also mediated by 5-HT, which principally include mammary gland development and function, in addition to increased metabolic enzyme function within the liver. Administration of 5-HT precursors to pregnant mice, to increase circulating 5-HT, has been demonstrated to increase glucose transport into the mammary gland via upregulation of GLUT1 and GLUT8 transporter expression (Laporta et al., 2013). While EC cell 5-HT may contribute to this in an endocrine manner, mammary tissue also expresses TPH1 and can synthesise 5-HT (Matsuda et al., 2004), indicating possible autocrine and paracrine activity of 5-HT in mammary tissue. The relative

contributions of EC cell and mammary gland 5-HT have yet not been established, however a 5-HT autocrine-paracrine loop has been established in mice, contributing to overall mammary gland development and lactation (Matsuda et al., 2004)

1.3.5 Immunity and inflammation

A role of peripheral 5-HT and 5-HT receptors as activators of immune responses and inflammation is well characterised. A number of cell types involved in the immune response; namely natural killer cells, macrophages, dendritic cells, T cells and B cells, express an array of 5-HT receptors and have the capacity to take up 5-HT via SERT, while some also appear to be able to synthesise 5-HT (Ahern, 2011). As such, 5-HT has been implicated in a number of diseases associated with inflammation, particularly asthma and pulmonary inflammation, gastrointestinal inflammation resulting in irritable bowel syndrome (IBS), inflammatory bowel disease (IBD), ulcerative colitis and Crohn's disease (Wheatcroft et al., 2005, El-Salhy et al., 1997, Linden et al., 2003, Kidd et al., 2009, Haub et al., 2010, Bischoff et al., 2009). Notable increases in EC cell numbers and inflammatory mediators, including T-cells, have been observed following C*ampylobacter* (Spiller et al., 2000) and *T. spiralis* (Wheatcroft et al., 2005) infection, however it is unknown if inflammation precedes the increase in EC cell numbers and accompanying increase in total 5-HT release. Patients with IBS demonstrate impaired platelet 5-HT uptake due to decreased SERT expression, whereby increasing the levels of circulating free 5-HT, which correlates with duodenal immune activation (Foley et al., 2011). In addition, increased 5-HT bioavailability in mice lacking SERT exacerbates intestinal inflammation in a TNBS-induced model of colitis in mice (Bischoff et al., 2009). The relationship between 5-HT and inflammation is complex, as several pro-inflammatory cytokines and immune mediators are also stimulators of 5-HT release.

1.3.5.1 Innate immunity

The innate immune system is considered the first line of defence for the non-specific targeting of invading foreign organisms and pathogens (Shajib and Khan, 2015). Cells involved in the innate immune response to pathogens or infection are primarily eosinophils, mast cells, natural killer cells, monocytes, macrophages and dendritic cells (Ahern, 2011). These cell types have the capacity to respond to circulating 5-HT through 5-HT receptors, while monocytes, macrophages, mast cells and dendritic cells can uptake and store 5-HT via SERT (Baganz and Blakely, 2013). Despite the ability of mast cells to also synthesise 5-HT in mice, exogenous 5-HT increases mast cell accumulation via 5-HT_{1A} receptors and uptake through SERT (Kushnir-Sukhov et al., 2006). Mast cell activation plays a key role in the innate immune response, through the release of one or a combination of inflammatory mediators such as histamine, proteases, cytokines and chemokines (Urb and Sheppard, 2012). Mast cells can also act to recruit other innate immune defence cells, such as eosinophils, natural killer cells, neutrophils and adaptive immune cells (dendritic cells and T-cells) which are also modulated by 5-HT (Urb and Sheppard, 2012). Circulating 5-HT is thought to contribute significantly to eosinophil infiltration, mediated via 5-HT_{2A} receptors (Boehme et al., 2004).

Natural killer cells respond acutely to pathogens and are among the first responders in the innate immune pathway. The cytotoxic activity of natural killer cells is increased *in vitro* with SSRI treatment, suggesting their activity may be mediated via SERT expression and 5-HT uptake (Evans et al., 2008). In addition, proliferation of natural killer cells in humans is increased with long-term SSRI treatment (Hernandez et al., 2010). In addition, the increased cytotoxic activity of human natural killer cells *in vitro* in response to 5-HT was mimicked by 5-HT_{1A} receptor agonists, suggesting this may also be a potential pathway for cell activation (Hellstrand and Hermodsson, 1990).

Dendritic cells are involved in antigen presentation to T-cells following pathogen exposure. Dendritic cells contain a variety of 5-HT receptors, the expression of which is dependent upon the stage of maturity (Ahern, 2011). As such, the functional consequences of 5-HT signalling may vary depending on the life cycle of the cell. Chemotaxis, or the ability of cells to detect and respond to the chemical environment, is increased in immature human dendritic cells in response to 5-HT acting on 5-HT_1 and 5-HT_2 receptors (Muller et al., 2009). In mature dendritic cells, however, release of several pro-inflammatory cytokines was enhanced in the presence of 5-HT, through activation of 5-HT_4 and 5-HT_7 receptors (Muller et al., 2009). Signalling of 5-HT to dendritic cells, therefore, leads to the accumulation of immature cells at the site of inflammation and the secretion of inflammatory cytokines which influence T-cell signalling. As such, 5-HT signalling to dendritic cells can have longer-term consequences for immune function and inflammation, due to their ability to signal cells in the adaptive immune response and as such has implications of pathogenesis of allergic diseases such as asthma.

1.3.5.2 Adaptive immunity

Adaptive immunity involves the destruction of invading pathogens through recognition of specific antigens by T and B-cells (Shajib and Khan, 2015). Immunological staining of primate intestinal mucosa shows that as 5-HT-containing cells migrate up the crypt/villus axis, they are at times in very close proximity to, and in some cases in direct contact with both T-cell and B-cells (Yang and Lackner, 2004), suggesting a close relationship between these cell types may exist. A number of 5-HT receptors are expressed on T-cells, which like dendritic cells vary with maturity. Naïve T-cells selectively express 5-HT_7 receptors, which contributes to early T-cell activation and cell proliferation, while expression of 5-HT_{1A} and 5-HT_{2A} receptors is enhanced following T-cell activation (Leon-Ponte et al., 2007, Abdouh et al., 2001). Considering evidence that T-cells themselves can synthesise 5-HT through expression

of TPH1, which is upregulated following T-cell activation (Leon-Ponte et al., 2007, Chen et al., 2015), activity of 5-HT on T-cells may be through either autocrine or paracrine signalling. Similar to T-cells, adaptive immune B-cells responsible for antigen presentation and antibody production also contain 5-HT_{1A} receptors, which are upregulated following cell activation (Abdouh et al., 2001). Expression of SERT has also been found on B-cells, indicating uptake and potential storage of 5-HT may play a role in modulating B-cell activity (Gordon and Barnes, 2003).

While 5-HT plays an important role in promoting immunity and inflammation, certain inflammatory mediators, including interleukins 1β (IL-1β) and 13 (IL-13) also appear to increase the release of 5-HT from EC cells (Manocha et al., 2013, Shajib et al., 2013, Kidd et al., 2009). This is also demonstrated in mouse models of colitis and intestinal inflammation, with IL-13 mediating an increase in EC cell number and mucosal 5-HT content, which is prevented in mice lacking IL-13 cytokine production and increased with exogenous IL-13 administration (Shajib et al., 2013, Manocha et al., 2013). This was also associated with an increase in infiltrating macrophages, consistent with the activity of 5-HT on immune cells. In addition to increasing EC cell numbers (Manocha et al., 2013, Shajib et al., 2013), chronic exposure to IL-13 acts at a transcriptional level to increase biosynthesis of 5-HT in BON cells, a human carcinoid EC cell line, through augmented TPH1 expression (Manocha et al., 2013). The role of EC cell 5-HT in modulating the immune system and peripheral inflammation is evidently complex, with 5-HT both contributing to the immune defence system while also being increased by inflammatory cytokines. The latter may be a positive driver to further increase the activity of several immune cells as a means of overcoming infection, however, this may also contribute significantly to diseases associated with increased inflammation, as a heightened response to IL-1β is seen in EC cells derived from patients with Crohn's disease (Kidd et al., 2009).

1.4 Metabolic roles of peripheral 5-HT

Gut-derived 5-HT is a regulator of metabolism (Young et al., 2015) through interactions with key metabolic target tissues (Table 1.1) and altered gut-derived 5-HT is related to both T2D and obesity. Platelet-free plasma 5-HT and blood glucose levels are positively correlated in humans (Takahashi et al., 2002), fish (Tubio et al., 2010), sheep (Watanabe et al., 2014) and rodents (Watanabe et al., 2010). Circulating plasma 5-HT is increased in individuals with T2D (Young et al., 2018), as further evidenced through the measurement of urinary levels of the major 5-HT metabolite, 5-HIAA (Takahashi et al., 2002), and positively correlate to glycated haemoglobin (HbA_{1c}) (Young et al., 2018). Gain-of-function polymorphisms in *TPH1* are associated with body mass index (BMI) and waist circumference, both being measures of obesity, in a genome-wide association study of 8,842 non-diabetic individuals (Kwak et al., 2012). Increased intestinal and plasma 5-HT levels are also observed in mice with diet-induced obesity (Kim et al., 2011, Bertrand et al., 2011). However, the absence of 5-HT, through genetic or pharmacological blockade of peripheral TPH, protects against the development of metabolic syndrome in mice on a high fat diet (Crane et al., 2015, Sumara et al., 2012).

Table 1.1 – Effects of 5-HT on metabolically active target tissues.

Tissue	Effect of 5-HT on target tissue
GI tract	Modulation of intestinal motility via 5-HT_3 and 5-HT_4 receptors Increased luminal bicarbonate and electrolyte secretion Increased fat absorption by increasing bile acid turnover
Pancreas	Serotonylation of exocytosis proteins Inhibition of insulin secretion via 5-HT_{1D} receptors Increased GSIS insulin secretion via 5-HT_2 and 5-HT_3 receptors Increased β-cell mass during pregnancy via 5-HT_{2B} and 5-HT_3 receptors
Liver	Increased bile acid synthesis and secretion Increased gluconeogenesis via 5-HT_{2B} and 5-HT_{2C} receptors Decreased glycogen synthesis Decreased glucose uptake
White adipose (WAT)	Increased lipolysis via 5-HT_{2B} receptors Decreased adiponectin secretion via 5-HT_{2A} Inhibition of WAT "browning"
Brown adipose (BAT)	Decreased thermogenesis via 5-HT_{3A} receptors
Bone	Decreased bone turnover and renewal via 5-HT_{1B} and 5-HT_{2A} receptors and uptake via SERT Decreased osteocalcin synthesis and secretion

1.4.1 5-HT regulates blood glucose and obesity through effects on hepatocyte and adipocyte function

1.4.1.1 Hepatocyte function

One of the major regulators of plasma glucose is the liver, with hepatic glycogenolysis being the main contributor to plasma glucose levels during fasting, followed by gluconeogenesis as the predominant contributor during periods of extreme fasting or starvation (DeFronzo et al., 1989, Rui, 2014). Fasting-induced increases in blood glucose are mediated, in part, by the activation of hepatocyte 5-HT_{2B} receptors. Binding of plasma 5-HT to 5-HT_{2B} receptors enhances the activity of two key rate-limiting enzymes in gluconeogenesis, glucose-6-phosphatase and fructose 1,6-bisphosphatase (Sumara et al., 2012). Enhanced activity of these key enzymes occurs at a transcriptional level, through increased cAMP downstream of 5-HT_{2B} receptor stimulation, subsequent activation of cAMP-dependent protein kinase A (PKA), and increased activity of the transcription factor, cAMP-response element binding (CREB) factor (Lin et al., 1997). While 5-HT increases glucose production by hepatocytes, this is limited by the presence of endogenous substrates; particularly glycerol generated from lipolysis, and glycogen stored within hepatocytes. Exaggerated hepatic glucose production is the major determinant of glycaemic control, with its contribution to plasma glucose levels significantly augmented in T2D (DeFronzo et al., 1989). As such, augmented gut 5-HT may contribute to the development and progression of metabolic diseases through increased hepatic glucose output.

Simultaneous to increases in hepatic gluconeogenesis, 5-HT decreases glycogen synthesis and reduces GLUT2-mediated uptake of glucose in the liver (Sumara et al., 2012, Tudhope et al., 2012). In addition, both circulating 5-HT and hepatic 5-HT_{2B} receptor expression are increased in mice under fasting conditions (Sumara et al., 2012). This fasting-induced rise in plasma 5-HT is driven by the reduction in circulating glucose availability that

occurs under fasting conditions. Ultimately, this leads to higher EC cell TPH1 expression and 5-HT synthesis (Zelkas et al., 2015).

1.4.1.2 Adipocyte function

White adipose tissue (WAT) is an energy store that is also regulated by gut-derived 5-HT (Figure 1.3). 5-HT can mobilize free fatty acids and glycerol from adipocytes. This occurs via 5-HT_{2B} receptor-mediated phosphorylation, and consequent activation, of intracellular hormone sensitive lipase (HSL), the rate-limiting enzyme involved in lipolysis (Sumara et al., 2012). Activation of HSL is of particular importance to peripheral metabolism, as the resulting increase in lipolysis leads to an increase in circulating free fatty acids and glycerol, which are both energy substrates for peripheral tissues. HSL is stimulated through the 5-HT_{2B} receptor either indirectly by an increase in cAMP and downstream activation of cAMP-dependent PKA, or directly by phosphorylated perilipin (Kraemer and Shen, 2002). However, it is currently unknown by which of these pathways 5-HT regulates HSL. The 5-HT-induced lipolysis of stored triacylglycerol results in increased plasma levels of free fatty acids and glycerol. Glycerol can then be utilised to further fuel hepatic gluconeogenesis or can be converted, along with free fatty acids, to acetyl-CoA by β-oxidation in the liver for the synthesis of ketone bodies. Experimentally raising plasma 5-HT levels in mice significantly increases plasma glycerol and free fatty acids, an effect which is blunted in mice lacking 5-HT_{2B} receptors in adipose tissue (Sumara et al., 2012).

Serotonin hinders thermogenic capacity and energy catabolism in interscapular brown adipose tissue (iBAT), the primary tissue responsible for heat production (thermogenesis) in mice (Crane et al., 2015). Exogenous 5-HT significantly attenuates the thermogenic potential of the β-adrenergic receptor agonist, isoproterenol. 5-HT reduces cAMP levels in iBAT, lowers the activation of HSL, and reduces the expression of uncoupling protein 1 expression (UCP1), the mitochondrial protein responsible for thermogenesis) (Crane et al., 2015).

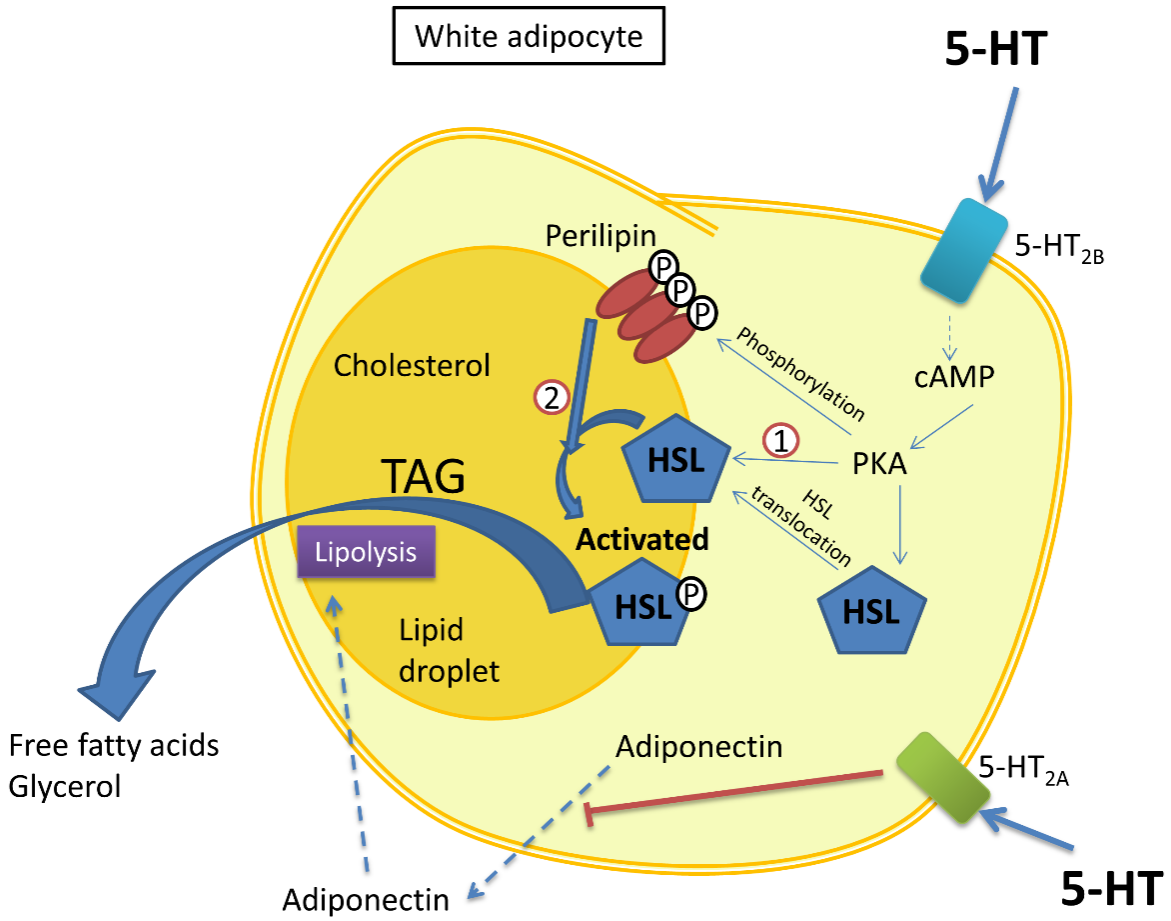

Figure 1.3 – Actions of 5-HT on adipocytes. Peripheral 5-HT stimulates lipolysis within white adipocytes, therefore increasing circulating free fatty acids and glycerol. This occurs via activation of 5-HT_{2B} receptors, which in turn results in activation of HSL by two possible mechanisms: (1) HSL translocates to the surface of lipid droplets and is activated by direct phosphorylation by cAMP-dependent protein kinase A, or (2) HSL is activated by phosphorylated (P) perilipin on the surface of lipid droplets. Whether 5-HT activates HSL by either or both of these mechanisms is currently unknown. 5-HT also inhibits the release of the metabolically active hormone adiponectin via activation of 5-HT_{2A} receptors.

In contrast, mice treated with the peripherally restricted TPH inhibitor, LP533401, display increased thermogenic capacity due to increased *Ucp1* expression in iBAT, and importantly, resistance to the glucose intolerance and insulin resistance that normally accompanies a high-fat diet (Crane et al., 2015).

In addition to direct effects on iBAT, 5-HT also inhibits the "browning" of WAT, the process through which WAT converts to a BAT-like phenotype, producing so called 'beige' adipocytes. Beige adipocytes have a higher expression of key thermogenic genes encoding for UCP1 and PGC1α compared to WAT, and consume more energy through the production of heat (Suarez-Zamorano et al., 2015). 5-HT actions on thermogenesis are partially mediated via 5-HT_{3A} receptors in BAT (Oh et al., 2015). In addition, the ablation of *Tph1* specifically in adipose tissue infers resistance in mice to high fat diet-induced obesity. These mice display reduced adipocyte mass, lower weight gain and improved glucose tolerance and insulin sensitivity under such conditions, suggesting 5-HT synthesis within WAT itself has important metabolic consequences (Oh et al., 2015).

1.4.1.3 5-HT regulates adipokine release

Serotonin can suppress adipose tissue release of adiponectin (Figure 1.3), the adipokine capable of attenuating hepatic gluconeogenesis and increasing insulin sensitivity (Fu et al., 2005, Park et al., 2011, Yoon et al., 2009). Circulating adiponectin levels are lower in rodent models of obesity and patients with T2D (Nomura et al., 2005, Weyer et al., 2001, Hotta et al., 2000, Yamauchi et al., 2001, Arita et al., 1999, Milan et al., 2002) and negatively correlate with BMI (Arita et al., 1999, Kern et al., 2003). Adiponectin acts in a paracrine manner on adipocytes to decrease lipid accumulation within WAT, to promote thermogenesis in BAT, and to induce the browning of WAT through increased UCP1 expression (Masaki et al., 2003). Activation of 5-HT_{2A} receptors on mesenteric adipose tissue suppresses adiponectin release, while increased expression of these receptors in genetically obese mice markedly reduces

adiponectin levels (Uchida-Kitajima et al., 2008). Moreover, knockdown of 5-HT_{2A} receptor expression, or pharmacological inhibition of its signalling, results in an increase in adiponectin expression in a differentiated adipocyte cell line (Uchida-Kitajima et al., 2008). Thus, peripheral 5-HT contributes to metabolic dysfunction not only through increases in hepatic gluconeogenesis and fasting blood glucose levels, but also by acting on adipocytes to mobilize free fatty acids and glycerol. In addition, peripheral 5-HT augments obesity through suppression of the "browning" of white fat, reduces *Ucp1* in BAT and suppresses secretion and expression of metabolically-beneficial adiponectin.

1.4.2 Insulin secretion and pancreatic β-cell function

Insulin-secreting β-cells in the pancreas are capable of 5-HT uptake and contain 5-HT receptors, however the primary relevant source of 5-HT signalling in islets appears to be intrinsically-derived. Pan inhibitors of TPH (and thus total body 5-HT) have no significant effect on plasma insulin during fed or fasted states in mice (Sumara et al., 2012). Similarly, plasma insulin remains unchanged in *Tph1* KO mice (Sumara et al., 2012). Pancreatic β-cells express both *Tph1* and *Tph2* and are thus able to synthesize 5-HT (Schraenen et al., 2010). This 5-HT is stored in β-cell secretory granules and is co-secreted with insulin (Ohta et al., 2011, Rosario et al., 2008, Baldeiras et al., 2006, Barbosa et al., 1996, Barbosa et al., 1998). 5-HT has intracellular effects by modifying proteins involved in exocytosis in a process termed serotonylation. This term refers to the process by which transglutaminases covalently couple 5-HT during insulin exocytosis to two key players in insulin secretion, the small GTPases Rab3a and Rab27a. This results in the augmentation of glucose-stimulated insulin secretion (GSIS) (Paulmann et al., 2009).

The most well-characterized roles of 5-HT in pancreatic islets occur through 5-HT receptor signalling. Human islets express a number of 5-HT receptors (Bennet et al., 2015), in addition to SERT, supporting functional roles for 5-HT receptor stimulation and uptake in β-

cells. 5-HT receptor activation has diverse effects on insulin secretion. The binding of 5-HT to 5-HT_{1D} receptors inhibits insulin secretion in healthy human islets and in β-cell model cell lines (Paulmann et al., 2009, Bennet et al., 2015). This is proposed to create a negative-feedback loop for both basal secretion and GSIS (Barbosa et al., 1996, Bennet et al., 2016, Baldeiras et al., 2006, Barbosa et al., 1998, Rosario et al., 2008). In contrast, activation of 5-HT_2 and 5-HT_3 receptors augments the respiratory capacity and membrane excitability of pancreatic islet cells to exert an incretin-like effect. This is through increasing insulin secretion from β-cells, while suppressing glucagon release from α-cells through activation of 5-HT_{1F} receptors (Bennet et al., 2015, Bennet et al., 2016, Ohara-Imaizumi et al., 2013, Almaca et al., 2016). Thus, the effect of 5-HT on insulin secretion will likely be dictated by the number and type of 5-HT receptors present within individual β-cells, and the affinity of each receptor subtype for 5-HT, such that small amounts of 5-HT release are targeted towards the activation threshold of specific receptors.

The diverse roles of 5-HT in pancreatic islets is also illustrated under specific conditions of metabolic change. During pregnancy, the maternal β-cell mass expands in response to increased insulin resistance. Increased β-cell proliferation drives this expansion of β-cell numbers underpinning this compensatory hyperinsulinemia. This increase in β-cell mass is due to prolactin-dependent induction of β-cell TPH1 expression. This leads to increased 5-HT production and the autocrine/paracrine activation of intrinsic 5-HT_{2B} and 5-HT_3 receptors to enhance cell proliferation (Schraenen et al., 2010, Kim et al., 2010, Ohara-Imaizumi et al., 2013). This increase in β-cell mass and insulin production plays a critical role in reducing the incidence of gestational diabetes. Serotonin can also augment β-cell function during periods of hyperglycaemia when there is an increased demand for insulin secretion. Mice with β-cell specific knockout of TPH1 have a maladaptive response to a high fat diet and display lower GSIS than control mice. This effect is driven by reduced 5-HT availability and can be rescued

by exogenous administration of 5-HT (Kim et al., 2015). The expression of a number of 5-HT receptors is also known to be altered in human islets from individuals with T2D and in islets from mice fed a high fat diet (Kim et al., 2015, Bennet et al., 2015, Bennet et al., 2016). Such changes are purported to contribute to defective insulin and glucagon secretion in human T2D. However, the mechanisms driving altered 5-HT signalling in β-cells during T2D remains unclear.

1.4.3 Osteoskeletal regulation

The skeletal system is regulated by a variety of hormonal signals and through sympathetic outflow from the CNS (Warden et al., 2005, Yadav et al., 2009). Bone renewal relies on a balance between bone reabsorption by osteoclasts and bone synthesis by osteoblasts. Alterations to this balance significantly affect bone structure. Examples of this include premature ovarian failure and menopause-associated osteoporosis, both of which are associated with a significant loss of bone density and strength (Cartwright et al., 2016).

1.4.3.1 Role of 5-HT in bone health

The relationship between 5-HT and bone structure was first identified by the decreased bone density that occurs in patients administered SSRIs for the treatment of depression (Hodge et al., 2013, Richards et al., 2007). A number of studies have shown that TPH1 is expressed in bone, but at orders of magnitude lower than within the GI tract (Chabbi-Achengli et al., 2012, Yadav et al., 2008). Gut-derived 5-HT is now clearly established as being able to inhibit bone turnover and renewal by inhibiting osteoblast and osteoclast differentiation and proliferation via actions at 5-HT_{1B} and 5-HT_{2A} receptors, and uptake via SERT (Yadav et al., 2008, Yadav et al., 2010, Nam et al., 2016, Tanaka et al., 2015, Battaglino et al., 2004, Warden et al., 2005). Correspondingly, inhibition of gut-derived 5-HT has anabolic effects on bone formation in an ovariectomized mouse model of osteoporosis, acting as both a preventative and therapeutic

treatment for bone loss (Yadav et al., 2010). Such findings demonstrate that gut-derived 5-HT is a powerful determinant of bone homeostasis.

1.4.3.2 Role of bone as an endocrine organ

Bone plays an important role in whole body metabolism through the release of osteocalcin and lipocalin 2 (LCN2) from osteoblasts. Osteocalcin is a powerful driver of β-cell proliferation and insulin production (Ferron et al., 2008). It also promotes adipocyte thermogenesis and the secretion of adiponectin (Lee et al., 2007, Ferron et al., 2008), both of which have positive metabolic effects. Circulating osteocalcin levels are inversely correlated with fasting plasma glucose, HbA_{1c}, visceral fat mass and BMI in healthy humans (Hu et al., 2014) and in individuals with T2D (Kanazawa et al., 2011, Bezerra dos Santos Magalhaes et al., 2013, Shanbhogue et al., 2016, Raghupathi et al., 2016, Ma et al., 2015, Bao et al., 2011, Hu et al., 2014). In longitudinal studies in humans both before and after the development of metabolic syndrome, plasma osteocalcin levels were found to be an independent risk factor for developing T2D (Ferron et al., 2008, Lee et al., 2007, Diaz-Lopez et al., 2013, Namkung et al., 2015, Ngarmukos et al., 2012). Administration of osteocalcin can also prevent the onset of obesity, impaired glucose tolerance and insulin insensitivity in mice fed a high fat diet (Ferron et al., 2008). Inhibition of gut-derived 5-HT in ovariectomized mice markedly increased osteoblast numbers, bone formation and serum osteocalcin (Yadav et al., 2010).

Another bone-derived hormone that has metabolic activity is LCN2, which is also released from osteoblasts and maintains glucose homeostasis by inducing insulin secretion, therefore improving glucose tolerance and insulin sensitivity (Mosialou et al., 2017). In addition to peripheral metabolic activity, centrally mediated pathways are targets for LCN2. Principally, LCN2 reduces appetite and food intake through activation of melanocortin 4 receptor in the paraventricular and ventromedial neurons of the hypothalamus, whereby activating the centrally-mediated appetite-suppression pathway (Mosialou et al., 2017).

Similarly to osteocalcin, serum LCN2 is inversely correlated with body weight HbA_{1c} in patients with T2D (Mosialou et al., 2017). Considering that plasma 5-HT levels increase in T2D (Takahashi et al., 2002), gut-derived 5-HT may promote the development of metabolic disease secondary to its inhibition of osteoblast function, by decreasing circulating levels of osteocalcin and LCN2.

1.4.4 Gastrointestinal function

EC cell-derived 5-HT has long been known to have modulatory effects on gastrointestinal motility. This occurs via activation of $5\text{-}HT_3$ and $5\text{-}HT_4$ receptors on vagal afferent nerve terminals innervating the intestinal mucosa (Hoffman et al., 2012, Bertrand et al., 2000). However, release of 5-HT from EC cells is not explicitly required for neurogenic contractions of the gut wall to occur (Spencer and Keating, 2016, Spencer et al., 2015), since propagating neurogenic contractions are maintained *in vitro* in the absence of the intestinal mucosa (Spencer et al., 2011, Keating and Spencer, 2010). Further, *in vivo* intestinal transit is maintained when TPH1 is inhibited pharmacologically (Yadav et al., 2010), and colonic migratory complexes remain in *Tph1* KO mice (Heredia et al., 2013).

Despite not being required for contractile propagation to be initiated, gut 5-HT is nevertheless a potent activator of gut motility and gastric emptying, and has established metabolic effects through such pathways. Luminal 5-HT influences intestinal nutrient and water absorption, and influences bicarbonate and electrolyte secretion into the lumen (Figure 1.4) (Imada-Shirakata et al., 1997, Tuo and Isenberg, 2003, Tuo et al., 2004). Through stimulation of $5\text{-}HT_3$ receptors on intestinal vagal afferent nerve endings which innervate the pancreas, EC cell-derived 5-HT indirectly increases post-prandial pancreatic enzyme secretion in a manner synergistic with cholecystokinin (CCK) (Cho et al., 2014). This, in turn, increases digestion and absorption of luminal nutrient contents. Intestinal fat absorption is also mediated by the release of liver-synthesized bile salts and bile acids from the gall bladder, which can be

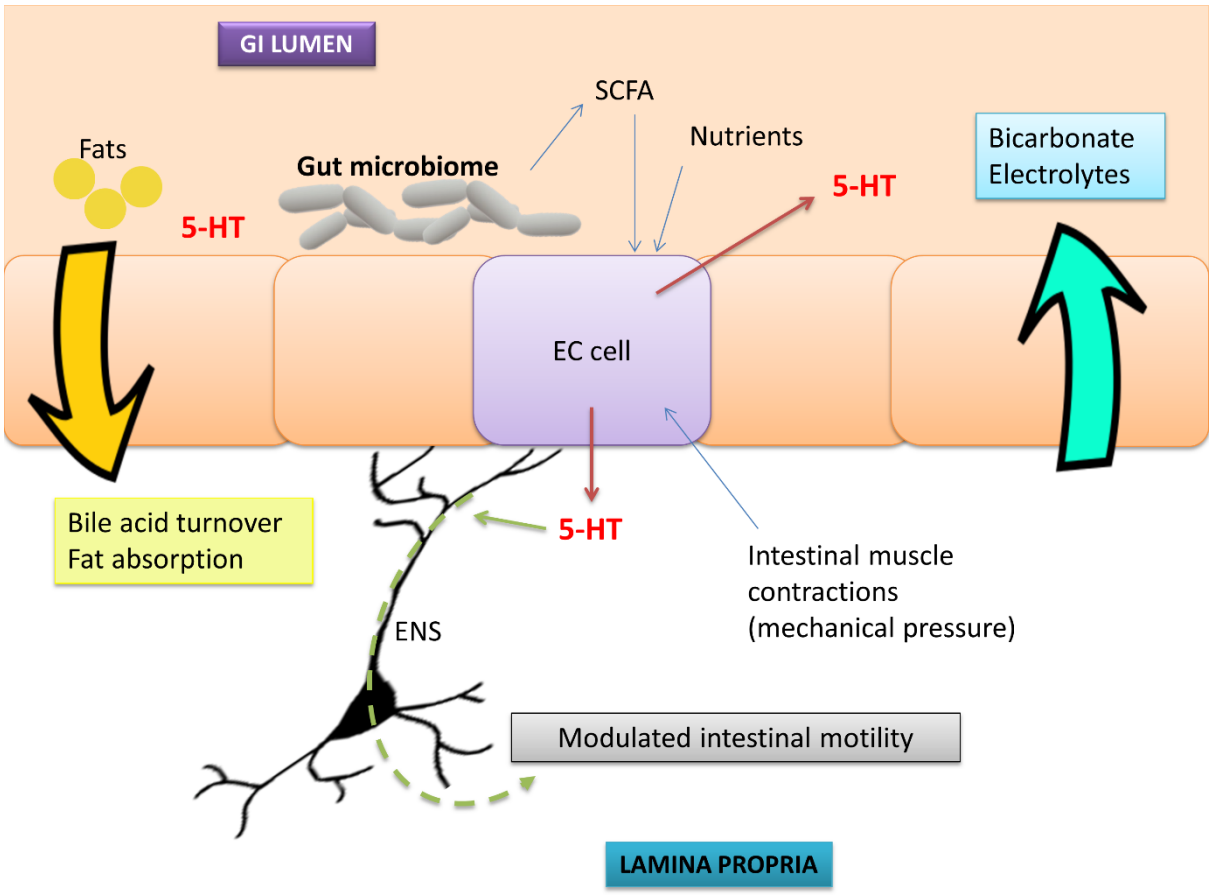

Figure 1.4 - The effects of 5-HT on GI tract absorption and motility. Release of 5-HT in response to chemical cues, such as microbially-derived short-chain fatty acids (SCFA) and luminal nutrients, and physical cues such as mechanical pressures, increases bile acid reabsorption and turnover, thereby increasing fat absorption. In addition, 5-HT release increases bicarbonate and electrolyte secretion into the GI lumen. Modulation of intestinal

reabsorbed in the intestinal lumen. Gut 5-HT increases bile acid turnover by inducing the expression of the apical sodium-dependent bile salt transporter, in addition to increasing bile acid synthesis and secretion by the liver and gall bladder (Watanabe et al., 2010). Thus, gut 5-HT indirectly increases intestinal fat absorption, and may indirectly contribute to obesity via these effects on bile acids. In turn, bile acids themselves stimulate 5-HT release via activation of the G protein-coupled bile acid receptor (TGR5), which is associated with downstream effects on colonic muscle contractility and is required for normal defecation in mice (Alemi et al., 2013).

1.4.5 Neurochemical stimuli

Cross-talk between enteric neurons and EC cells may exist, as 5-HT release from EC cells is triggered by a number of neuromodulatory agents *in vitro*, including acetylcholine and pituitary adenylate cyclase-activating peptide (PACAP) (Raghupathi et al., 2013, Kidd et al., 2009, Kidd et al., 2006, Kidd et al., 2008, Modlin et al., 2006, Kunze et al., 1995). This effect is likely mediated by activation of muscarinic M_4 and $VPAC_1$ receptors, respectively, which are expressed in enriched EC cell populations (Schäfermeyer et al., 2004, Modlin et al., 2006).

Conflicting evidence exists surrounding the effect of γ-aminobutyric acid (GABA) on EC cells. $GABA_A$ and $GABA_B$ receptors are expressed by EC cells (Kidd et al., 2006, Schäfermeyer et al., 2004) but incubation of enriched ileal EC cells from rat with GABA does not increase 5-HT release (Schäfermeyer et al., 2004). In isolated human EC cells, however,

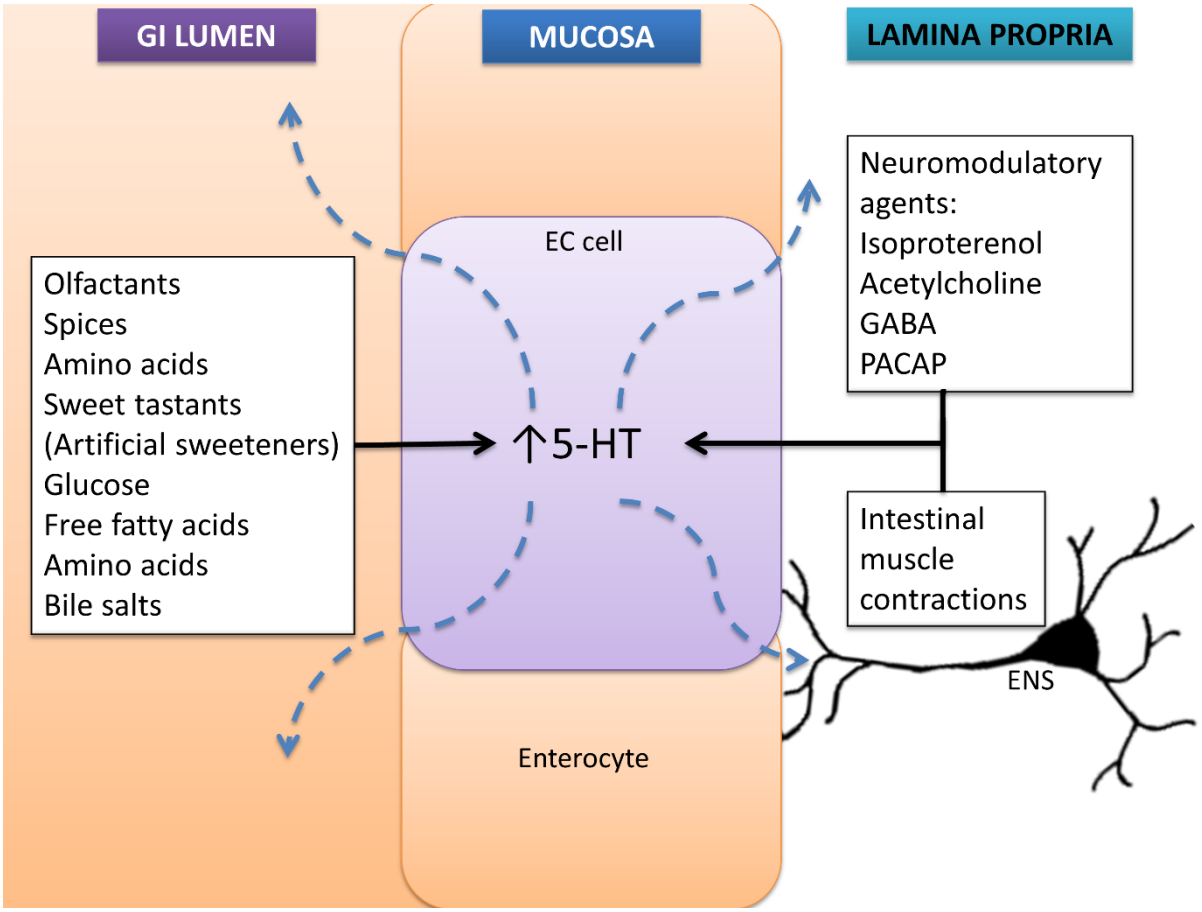

Figure 1.5 - EC cells within the mucosal lining of the GI tract. EC cells (shown in purple) act as sensory cells for a wide array of nutrient cues within the GI lumen. They also detect neuromodulatory agents from extrinsic and intrinsic afferent nerve fibres, and are responsive to mechanical stimuli, such as intestinal muscle contractions.

GABA dose-dependently inhibits isoproterenol-stimulated 5-HT secretion. Muscimol, on the other hand, is a ligand preferencing $GABA_A$ receptors and has both a stimulatory and inhibitory effect on 5-HT release from perfused rat intestine, with a biphasic stimulatory phase followed by inhibition of 5-HT release (Schworer et al., 1989). Since $GABA_A$ receptors are also present on synaptic terminals, release of other neurotransmitters may confound any observed effects of *in vivo* $GABA_A$ stimulation on 5-HT secretion. EC cells also respond to β-adrenergic stimulation, with expression of both β_1 and β_2 receptor isoforms detected in EC cells, while incubation with noradrenaline increased 5-HT release from enriched EC cells *in vitro* (Schäfermeyer et al., 2004). Correspondingly, blockade of β-adrenergic receptors attenuates 5-HT release (Kunze et al., 1995, Neunlist et al., 1999). Somatostatin (SST), derived from either enteric neuronal sources or released from the stomach following nutrient ingestion, may exert inhibitory effects on intestinal motility and nutrient absorption (Costa and Furness, 1984, Costa et al., 1980) partly through inhibiting EC cell 5-HT release (Kidd et al., 2008) via SSTR2 receptors (Modlin et al., 2006).

Consistent with the notion of neuronal-EC cell cross-talk, adrenergic, cholinergic and peptidergic nerve inputs from enteric neurons, particularly myenteric Dogiel Type 2 neurons, terminate in close apposition to EC cells (Kunze et al., 1995, Neunlist et al., 1999). Direct stimulation of neuronal inputs into the duodenal mucosa of cats also results in a significant increase in 5-HT secretion to the portal vein (France et al., 2016). Studies investigating potential neuronal stimulation of EC cells may, however, be confounded by mechanically-induced 5-HT release from EC cells. EC cells are mechanically sensitive (Kim et al., 2001b, Keating and Spencer, 2010) and 5-HT release is highly correlated with intestinal motor complexes in both *in vivo* and *ex vivo* experiments (Chin et al., 2012).

1.4.6 Mechanical stimuli

EC cells may be exposed to several different types of mechanical stimuli within the GI tract. These range from changes to membrane structure through stretch and compression, to shear stress over the surface of the bilipid layer from fluid flow. The mechanism by which EC cells detect plasma membrane distortion is thought to be through the mechanosensitive ion channel, Piezo2. Activation of this channel rapidly induces an inward cation current, membrane depolarisation and L-type calcium channel activation following a local mechanical stress stimulus (Woo et al., 2014), such as pressure due to movement of a luminal bolus or stretch from muscular contractions (Wang et al., 2016). Piezo2 is highly localised to EC cells, and the level of expression is consistent along the length of the gut (Wang et al., 2016). Genetic knockdown or pharmacological inhibition of Piezo2 almost completely attenuates mechanically-induced 5-HT secretion from QGP-1 cells, an EC cell model, suggesting this may be the major stretch or pressure mechanosensory pathway in EC cells (Wang et al., 2016). Interestingly, other mechanosensing pathways by EC cells have been suggested. In particular, a potential Gαq-coupled pathway and requirement of intracellular calcium stores has been demonstrated in BON cells, and segments of guinea pig small intestine (Kim et al., 2001b). This, in comparison to ion-channel stimulation, is less likely to give the rapid release of 5-HT observed following an acute mechanical stimulus (Bertrand, 2004). Chronic exposure of KRJ-I cells to rhythmic stretch is associated with increased biosynthesis and secretion of 5-HT, through effects on TPH1 transcription and activation. This pathway is activated by the G-protein coupled adenosine receptor 2B (ADORA2B), and downstream PKA activation (Chin et al., 2012), and may be due to adenosine released from EC cells acting in an autocrine fashion. Release of adenosine triphosphate (ATP) from either neurons, other enteroendocrine cells or possibly EC cells themselves (Linan-Rico et al., 2016) can also act in a paracrine or autocrine manner to increase 5-HT release, following mechanical stress. In segments of human colonic tissue, mechanically evoked 5-HT release is tightly regulated by co-secretion of ATP, with

several purinergic signalling mechanisms identified in subpopulations of EC cells (Linan-Rico et al., 2013). Activation of P2 receptors, namely P2X and P2Y, is associated with increased 5-HT release from guinea pig tissue and BON cells, (Patel, 2014, Linan-Rico et al., 2013). Binding of ATP to P2X ion channels initiates rapid membrane depolarisation, while P2Y receptor stimulation acts via second messenger pathway to mobilise intracellular calcium stores (Linan-Rico et al., 2013). Intriguingly, ATP-induced 5-HT secretion via P2Y receptors in response to rotational fluid flow appears to be region-specific, with responses elicited from ileal, but not colonic, tissue from guinea pig (Patel, 2014). This is suggestive that ATP-mediated mechanical stimulation via P2Y receptors is limited to the small intestine, with other mechanosensory pathways such as Piezo2 being prominent in the colon.

Varying experimental conditions, species differences, and confounding factors associated with *in vivo* experiments make it difficult to determine the precise mechanisms of EC cell mechanosensing in response to a particular type of mechanical stimulation. Functionally, the presence of several mechanosensory pathways may be due to the differing nature of mechanical stimulation over the length of the GI tract. For example, the small intestine is subjected to pressure from propulsive and segmented contractions and shear stress from fluid flow, while the colon is subjected to membrane compression due to bolus faecal mass movement and stretch from peristaltic contractions (Gayer and Basson, 2009). Mechanical-evoked 5-HT release from EC cells may have several downstream effects on intestinal motility and nutrient and electrolyte absorption, however EC cells are also sensitive to nutrients within the intestinal lumen. Determining the distinct physiological role of EC cell mechanosensing is complex, however, heightened mechanosensitivity in EC cells has been associated with intestinal inflammation and disease states such as IBD (Chin et al., 2012).

1.4.7 Nutrient sensing

1.4.7.1 Sweet tastants

EC cells are important nutrient sensors within the GI tract and have the potential to respond to an array of different luminal and circulatory nutrients. In particular, EC cells are sensitive to glucose status, responding to both acute increases and chronic reductions in glucose availability. An acute increase in glucose levels, consistent with concentrations seen in the intestinal lumen following a meal, triggers 5-HT release in intact mouse colonic tissue preparations (Zelkas et al., 2015). This illustrates that increases in ingested, but not plasma, glucose levels are detected by EC cells, through glucose sensing mechanisms located on the apical plasma membrane. Glucose-triggered 5-HT release from EC cells occurs as a result of membrane depolarisation and subsequent extracellular Ca^{2+} influx through voltage-gated L-type Ca^{2+} channels (Raghupathi et al., 2013, Zelkas et al., 2015). Cellular uptake of glucose into EC cells has been suggested to occur through the Na^{+}-dependent glucose co-transporter 1 (SGLT-1), resulting in increased 5-HT secretion in BON cells (Kim et al., 2001a). Colonic EC cells from guinea pig sense and respond to luminal concentrations of glucose, despite almost all absorption of luminal sugars occurring over the length of the small intestine (Zelkas et al., 2015). This indicates that despite glucose being absent in the colon under healthy GI physiological conditions, colonic EC cells have the capacity to detect and respond to the presence of luminal glucose during abnormal or disease states, such as those that might occur with diarrhoea or fast transit. The presence of glucose or sugars in the colon may also arise from microbial fermentation of digestion-resistant starches to simpler oligosaccharide sugars, containing monomers of glucose or fructose (Van Laere et al., 2000), or from microbial-derived succinate which can increase intestinal glucose production (De Vadder et al., 2016).

Chronic reductions in glucose availability seen during periods of fasting also increase 5-HT release from EC cells, as demonstrated in mice and guinea pig primary colonic EC cells

(Sumara et al., 2012, Zelkas et al., 2015). This effect occurs at a transcriptional level, with increased expression of *Tph1* leading to increased synthesis of 5-HT. Gut-derived 5-HT has a key role in regulating blood glucose levels, via effects on several key metabolic tissues. In particular, 5-HT increases hepatic gluconeogenesis and lipolysis from adipose tissue, while decreasing energy expenditure as heat through thermogenesis (Crane et al., 2015, Sumara et al., 2012, Watanabe et al., 2014). As such, glucose sensing by EC cells during periods of fasting acts to maintain blood glucose homeostasis. Altered glucose sensing by EC cells may therefore play a key role in diseases associated with perturbed glucose homeostasis, such as T2D.

The artificial sweetener sucralose has also been shown to increase 5-HT release from human EC cells (Kidd et al., 2008). The sweet taste receptor, a G protein-coupled receptor comprising of the T1R2 and T1R3 subunits, detects all known sweet tastants and is expressed in a subpopulation of EC cells in human duodenal mucosa (Young et al., 2013). Sweet taste-driven increase in 5-HT secretion may be particularly important for patients with T2D, who exhibit defective regulation of sweet taste receptors and exaggerated postprandial luminal glucose absorption (Young et al., 2013).

1.4.7.2 Odorants and pungent compounds

Naturally occurring olfactory compounds from a number of tastants and odorants, for example thymol and eugenol, trigger the release of 5-HT from EC cells via a number of olfactory receptors, with OR1G1 being one of the major olfactory receptors identified in both primary EC cells and BON cells (Braun et al., 2007, Kidd et al., 2008). Another olfactory receptor, Olfr558, mediates an increase in 5-HT release following exposure to pungent bacterial metabolites, such as isovalerate and isobutyrate (Bellono et al., 2017). Other naturally occurring pungent compounds such as allyl isothiocyanate from mustard and cinnamaldehyde from cinnamon stimulate 5-HT secretion by EC cells via activation of TRPA1 channels (Bellono et al., 2017, Nozawa et al., 2009). Functionally, these stimulants are associated with

increases in gut contractions; an effect possibly mediated by EC cell 5-HT release (Nozawa et al., 2009).

1.4.7.3 Lipids

Several dietary and circulating lipid molecules modulate 5-HT biosynthesis and secretion. Initially identified due to its beneficial effects on bone density and formation, the low-density lipoprotein receptor-related protein 5 (Lrp5), which binds to circulating cholesterol-laden low-density lipoproteins (LDLs), is associated with decreased TPH1 expression and reduced 5-HT synthesis in mouse duodenal EC cells (Yadav et al., 2008). While the precise mechanisms involved in this pathway are yet to be identified, internalisation of LDLs and other endogenous ligands via Lrp5-mediated endocytosis may regulate TPH1 expression through a pathway independent of β-catenin-mediated gene transcription (Yadav et al., 2008). Receptors for sensing short-chain fatty acids (SCFAs; FFAR2 and FFAR3), medium-chain fatty acids (FFAR1, GPR84) and long-chain fatty acids (FFAR1, FFAR4) are expressed in human and rat EC cells (Symonds et al., 2015, Akiba et al., 2015), and human colonic EC cells respond to amino acids and some fatty acids including lauric acid (Symonds et al., 2015). The production of SCFA by commensal bacteria within the intestine also increases 5-HT biosynthesis and secretion by EC cells (Yano et al., 2015), which likely contributes to differences in GI transit in mice with and without a native gut microbiome (Kashyap et al., 2013). The precise mechanisms responsible for this, however, are yet to be elucidated

1.4.8 GI hormonal cross-talk with EC cells

Hormonal signalling between EC cells and other enteroendocrine cells exists. A portion of EC cells express receptors for glucagon-like peptide 2 (GLP-2) (Yusta et al., 2000), a hormone secreted by intestinal L cells in response to food intake. As such, 5-HT may act as a mediator of several effects attributed to both 5-HT and GLP-2, including inhibition of gastric emptying and nutrient-stimulated gastric acid secretion (Raybould et al., 2003, LePard and

Stephens, 1994, Wojdemann et al., 1998, Wojdemann et al., 1999). In addition, GLP-2-stimulated 5-HT secretion may mediate the reported effects of GLP-2 on bone, a tissue which lacks the GLP-2 receptor, which include reductions in bone reabsorption and bone mineral density (Gottschalck et al., 2008). In contrast, 5-HT appears to have a stimulatory effect on the secretion of glucagon-like peptide 1 (GLP-1) from L cells in ileal tissue segments (Ripken et al., 2016). This effect is also seen in STC-1 cells, an immortalised L cell model, and is blocked by the addition of a broad-spectrum 5-HT receptor antagonist (Ripken et al., 2016). Through activation of 5-HT_2 and 5-HT_3 receptors innervating the submucosal plexus, 5-HT indirectly evokes intestinal CCK secretion by increasing active CCK-releasing peptide (Li and Owyang, 1996b). Together, CCK and 5-HT act to stimulate post-prandial pancreatic enzyme secretion, and contribute to the effects on bile acid regulation (Li et al., 2000, Li and Owyang, 1994, Li and Owyang, 1996a, Li et al., 2001, Zhu et al., 2001).

The expression of enteroendocrine hormones is not classically restricted to a single cell type, as co-expression of hormones has been highlighted along the length of the gut, as described previously in section 1.2. Cells containing 5-HT co-express a combination of other hormones, including substance P, secretin and CCK (Egerod et al., 2012, Cho et al., 2014, Reynaud et al., 2016, Fothergill et al., 2017a). Although, these are often stored in separate vesicles within the same cell (Fothergill et al., 2017a), suggesting selective secretion of these hormones may occur. Establishing the contributions of these subpopulations of cells to GI and peripheral physiology is complex. Individually, however, substance P and CCK act as potent stimuli within the ENS to alter GI motility and function (Holzer et al., 1981, Raybould, 1991, Raybould and Tache, 1988). Together with 5-HT, these hormones mayact synergistically with secretin to aid in nutrient digestion and absorption, partly through activation of vagal afferents innervating the pancreas, whereby increasing pancreatic enzyme secretion (Li et al., 2000, Li and Owyang, 1996a, Li et al., 2001, Zhu et al., 2001).

1.5 5-HT, the gut microbiome and metabolism

The gut is host to a densely populated and diverse commensal microbial ecosystem, composed of predominantly bacteria, with yeasts, viruses, bacteriophages and fungi (Scarpellini et al., 2015). This microbial community, together with its genetic material and traits that are encoded (collectively, the gut microbiome), perform a range of essential functions; one of which is the digestion of complex carbohydrates and plant-derived polysaccharides (Tremaroli and Backhed, 2012). The gut microbiome also regulates the development and maturation of the ENS, via the release of 5-HT and activation of 5-HT_4 receptors (De Vadder et al., 2018).

The influence of the intestinal microbiome on host-metabolism and fat storage is well established (Seeley et al., 2015, Velagapudi et al., 2010, Nieuwdorp et al., 2014, Turnbaugh et al., 2006, Suarez-Zamorano et al., 2015, Alard et al., 2016). Intervention studies involving the transplantation of faecal microbiota from lean to obese individuals, from obese individuals to germ free (GF) mice, or to mice that have reduced microbial abundance and diversity following antibiotic treatment, have clearly demonstrated a causal role of gut microbiota in the dysregulation of host glucose and lipid metabolism (Turnbaugh et al., 2006, Backhed et al., 2004, Vrieze et al., 2012, Ridaura et al., 2013). In particular, depletion of the intestinal microbiota protects mice against adverse changes in glucose tolerance and insulin sensitivity in response to genetic and diet-induced obesity, and increases thermogenesis in BAT and 'browning' of WAT (Suarez-Zamorano et al., 2015). These observations have led to intense interest in understanding the mechanistic relationship between gut microbiota and syndromes associated with metabolic dysfunction, such as obesity and T2D.

Serum, plasma, colonic and faecal concentrations of 5-HT are substantially reduced in GF and antibiotic-treated mice compared to conventionally raised controls (Sjogren et al., 2012, Wikoff et al., 2009, Yano et al., 2015, Uribe et al., 1994). These decreases in 5-HT result

from reduced gut 5-HT biosynthesis, which is supported by associated decreases in TPH1 expression and EC cell density, particularly in the colon (Uribe et al., 1994, Yano et al., 2015). The influence of the gut microbiome on EC cell density may stem from increased cell differentiation to EC cells, rather than increased EC cell proliferation. Further, the introduction of an intestinal microbiome in GF mice, for example, through the transplantation of human faecal matter, increases synthesis of EC cell 5-HT; a shift that can be attenuated by TPH inhibition (Reigstad et al., 2015).

While the intestinal microbiota can synthesize and secrete 5-HT (Karlsson et al., 1988), bacterial production of 5-HT is far exceeded by biosynthesis in EC cells. Rather, the resident microbiota of the healthy gut provides ongoing signals to host mucosal EC cells, whereby influencing gut 5-HT content and plasma 5-HT levels. Regulation of EC cell 5-HT biosynthesis by the gut microbiota appears to be maintained by the production of metabolites (Figure 1.6), including short chain fatty acids (SCFAs) and secondary bile acids (Yano et al., 2015, Reigstad et al., 2015), particularly by resident spore-forming bacteria (Yano et al., 2015, Atarashi et al., 2013, Stefka et al., 2014).

1.5.1 Short chain fatty acids

One of the major functions of commensal gut microbiota is the degradation of starches and polysaccharides, which would otherwise be indigestible by the host. The breakdown of these often plant-derived polysaccharides to metabolites primarily produces SCFA, mainly acetate, propionate and butyrate (Topping and Clifton, 2001). Microbiota-derived SCFAs have a number of physiological effects and benefits for the host, with a large proportion of SCFAs absorbed into the circulation in a concentration-dependent manner along the length of the colon (McNeil et al., 1978, Ruppin et al., 1980). Within the intestine, colonocytes use SCFA, in particular butyrate, as a major source of respiratory fuel (Roediger, 1980, Yang et al., 1970). In a chronic setting, SCFAs also may act as signalling molecules to EC cells, as butyrate

increases colonic TPH1 transcription and EC cell numbers in mice through effects on the zinc finger transcription factor, ZBP-89 (Essien et al., 2013). In addition, butyrate and propionate increase TPH1 expression and 5-HT release from the RIN14B cell line, a model of 5-HT producing cells (Yano et al., 2015), while luminal perfusion of a SCFA cocktail triggers luminal and basolateral release of 5-HT in rat colon *ex vivo* (Fukumoto et al., 2003). Cellular mechanisms by which EC cells detect and respond to microbial SCFAs remains to be established. Potential signalling pathways are through two major SCFA-sensing receptors, FFAR2 (particularly acetate and propionate) and FFAR3 (particularly propionate and butyrate). Colocalization of FFAR2 and 5-HT has been found in rat duodenal tissue (Akiba et al., 2015), and both of these receptors have been identified as SCFA sensing pathways in other enteroendocrine cell types (Nohr et al., 2013).

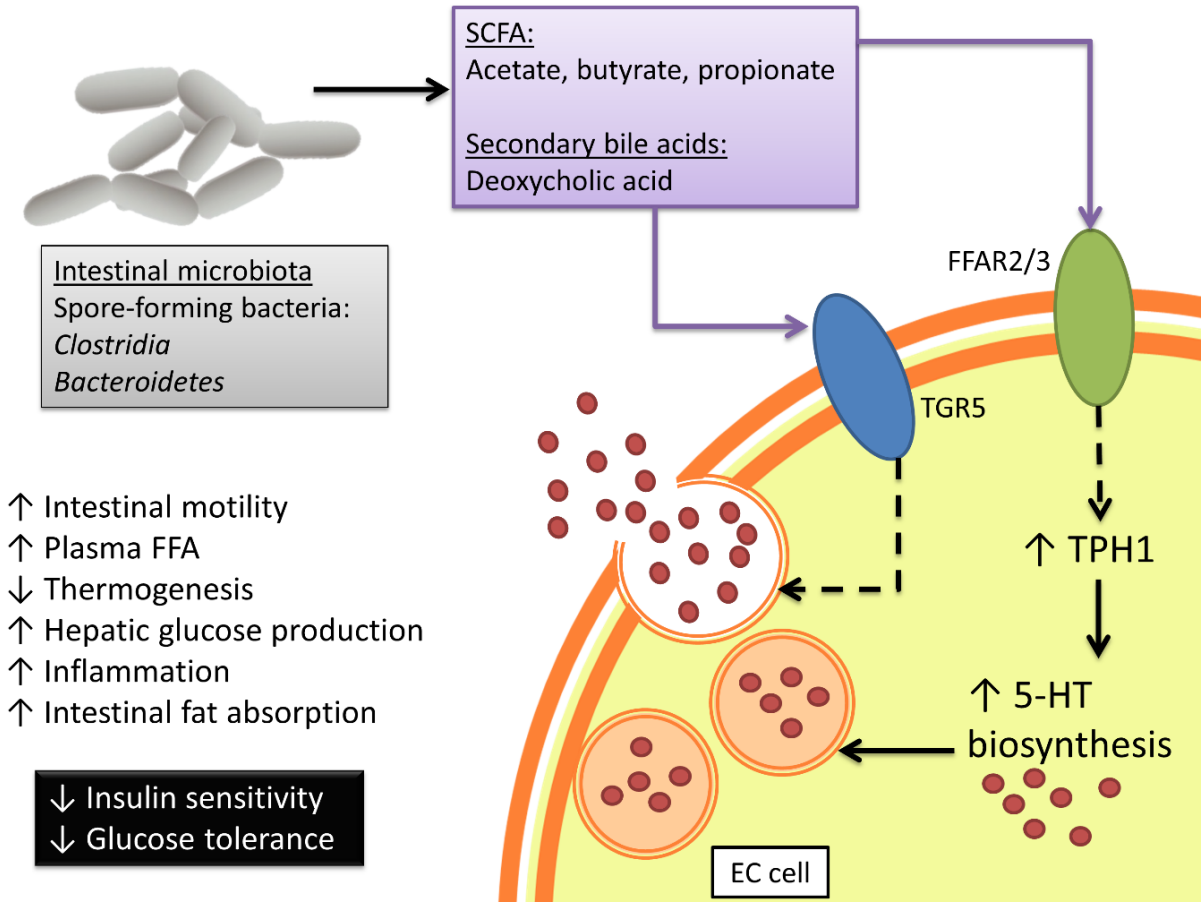

Figure 1.6 – Ramifications of the interactions between the gut microbiome and EC cells. Gut microbiota (specifically, spore-forming bacteria) play a central role in regulating EC-cell 5-HT biosynthesis and secretion through the release of secondary bile salts such as deoxycholic acid and SCFAs, particularly acetate, butyrate, and propionate. Microbial and dietary SCFAs stimulate the free fatty acid (FFA) receptors, FFAR2 and FFAR3, resulting in an increase in the expression of TPH1 and, consequently, increased 5-HT biosynthesis and secretion. Secondary bile acids activate the G protein-coupled bile acid receptor, TGR5, to stimulate the secretion of 5-HT. Increased plasma 5-HT can have detrimental consequences in the context of metabolic disease through an overall decrease in insulin sensitivity and glucose tolerance.

1.5.2 Secondary bile acids

The gut microbiome is responsible for the conversion of primary bile acids to secondary bile acids, such as the conversion of cholic acid to deoxycholic acid (DCA). Following secretion into the intestine to aid in the digestion and absorption of fats, most primary bile acids are actively reabsorbed across the mucosa of the small intestine. A small amount of bile acid does reach the colon, however, where the activities of bile tolerant Bacteroidetes and Clostridia result in the deconjugation of bile acids and conversion to secondary bile acids, which can then undergo passive reabsorption (Ridlon et al., 2006). Several secondary bile acids, such as DCA and oleanolic acid, have the capacity to increase 5-HT biosynthesis and secretion from EC cells (Alemi et al., 2013, Kidd et al., 2008). This effect is mediated through the G protein-coupled receptor, TGR5, which is expressed by EC cells, and the bile acid-mediated increase in 5-HT release is significantly ablated in mice lacking the TGR5 receptor (Alemi et al., 2013). The presence of TGR5 is required for normal defecation in mice, and TGR5-mediated 5-HT secretion may therefore contribute to the effects of bile acids on intestinal motility (Alemi et al., 2013).

1.5.3 Cellular recognition of microbial structural components

Structural components of intestinal microbiota also have the capacity to stimulate EC cell 5-HT release. Lipopolysaccharides (LPS) are a major outer surface membrane component found in almost all Gram-negative bacteria and act as potent stimuli for the intestinal inflammatory system, through the Toll-like receptor 4 (TLR4) (Alexander and Rietschel, 2001). Subpopulations of EC cells in human colonic tissue are also immunoreactive for several other functional toll-like receptors, including TLR1 and TLR2. In mice, EC cells are colocalised with TLR2 and TLR6, with the majority of these cells being found in the intestinal crypts (Bogunovic et al., 2007). LPS from *E. coli* dose-dependently increases 5-HT release

from purified human EC cells, which is exacerbated in 5-HT containing cells from patients with Crohn's disease (Kidd et al., 2009).

1.5.4 Effects of diet on gut microbiome and metabolic consequences

Given the central role that the gut microbiome plays in regulating 5-HT biosynthesis, it is unsurprising that diet-driven changes in the composition of the intestinal microbiota, as well as the associated changes in available substrates for bacterial growth, have a significant impact on gut and serum 5-HT levels. However, functional redundancy between bacterial species, as well as the ability of certain taxa to produce metabolites that stimulate 5-HT in response to varied dietary substrates, means that microbial regulation of 5-HT biosynthesis is complex. The impact of diet on microbiota-mediated 5-HT biosynthesis can be illustrated by examining the effects of increases in either plant-derived complex carbohydrates, or saturated fats; dietary components that are broadly associated with beneficial and detrimental health implications, respectively. An increased intake of non-absorbable dietary fibre results in a selective pressure for bacterial species able to utilize it for growth, notably members of the genus, Clostridium. These bacteria ferment polysaccharides in the colon to produce SCFAs which, in turn, stimulate EC cell free fatty acid receptors to trigger 5-HT biosynthesis (Fukumoto et al., 2003, Akiba et al., 2015) as well as insulin-stimulated glucose uptake and the newly-discovered process of intestinal gluconeogenesis (De Vadder et al., 2014). In humans, an increased dietary intake of saturated fats is also selective for Clostridium, as well as members of the phylum Bacteroidetes, but in this case, it results from increased levels of bile acid in the gut lumen. The activities of the bile tolerant Bacteroidetes and Clostridia result in the deconjugation of bile acids and the conversion of the secondary metabolites to DCA, respectively, which are able to stimulate EC cell 5-HT biosynthesis (Reigstad et al., 2015, Yano et al., 2015), via TGR5 (Alemi et al., 2013) (Figure 1.6). In parallel, high fat diet-driven increases in Bacteroidetes and Clostridia, and corresponding decreases in the relative abundance of *Bifidobacterium* and *Lactobacillus*, are

also likely to result in an alteration of both the absolute and relative levels of microbiota-derived SCFAs. These changes in metabolites that stimulate 5-HT biosynthesis take place in a wider context of altered bacteria-mediated energy harvest. An additional layer of complexity exists due to potential effects of the gut microbiome on the nervous system (Rogers et al., 2016), and interactions between other enteroendocrine cells. Understanding the complex interactions between diet, gut microbiota, EC cells, the nervous system and host metabolism in more detail holds the potential to have significant clinical relevance.

1.6 Physiological outcomes of acute vs chronic EC cell stimulation

There is gathering evidence that gut-derived 5-HT provides a signalling nexus between diet, gut microbiome and metabolism. Peripheral serotonin contributes to overall energy homeostasis through effects on a number of important metabolic sites including the gut, pancreas, liver, fat and bone. Plasma 5-HT increases in diabetes and obesity (Young et al., 2018), and inputs including nutrients and the gut microbiome influence gut 5-HT secretion and synthesis.

1.6.1 Acute stimulation

Acute stimulation of EC cells in response to luminal nutrients such as glucose has the capacity to increase the release of 5-HT. In this setting, increased circulating 5-HT may aid in nutrient digestion and absorption, though stimulating neuronal afferents innervating the pancreases and increasing in pancreatic enzyme secretion, and increasing bile acid reabsorption and turnover, while modulating intestinal motility to allow for maximum energy harvest. Concurrently, endogenous β-cell 5-HT contributes to GSIS to help maintain post-prandial blood glucose levels. Cross-talk between EC cells and other enteroendocrine cells is also likely to contribute to the finely tuned metabolic consequences following ingestion of certain nutrients.

1.6.2 Chronic stimulation

Alterations in energy availability during more chronic settings, such as fasting and through interactions with the gut microbiome, increases the biosynthesis of 5-HT at the level of increased *Tph1* transcription, and through an increase in stem cell progenitor differentiation to EC cells, whereby increasing EC cell density. In response to chronic exposure to such conditions, circulating 5-HT is likely to act on longer-term processes to increase blood glucose levels, and therefore energy availability, through increased hepatic gluconeogenesis and lipolysis from adipose tissue. In conjunction, 5-HT conserves energy by decreasing BAT thermogenesis and WAT browning, while also decreasing bone turnover and thus, reducing other pro-metabolic hormones such as osteocalcin, LCN2 and adiponectin. The chronic consumption of a high fat or high sugar diet may therefore shift the nature in which EC cells respond to their environment, resulting in a change from physiological outcomes associated with acute nutrient exposure to those consistent with chronic stimulation. While substantial advances have been made in understanding the role of 5-HT in metabolism and metabolic disorders, significant challenges remain.

1.7 Concluding Remarks

EC cells are tuned to a wide range of luminal stimuli, and release 5-HT in response to dietary glucose and fatty acids, however the precise mechanisms underlying this are yet to be resolved. In the face of increasing exposure to sugars, artificial sweeteners and fats in Western diets, and causal links to the development of obesity, insulin resistance and T2D, the relationship between these dietary nutrients and 5-HT release warrants deeper investigation. Our understanding of connections between the gut microbiome and metabolism are also gaining momentum, with evidence now in strong support for endogenous peripheral 5-HT as a key mediator. Further knowledge on the nature of EC cell/microbiome communication is required to shed light on the complex host-microbiota interactions that exist within the gut. In

addition to direct effects on key metabolic tissues, 5-HT may further exacerbate metabolic disorders by limiting hormones with beneficial metabolic roles, such as osteocalcin, LCN2 and adiponectin, however these mechanisms await further clarification. As such, the key question of what drives gut 5-HT synthesis in humans, and how this relates to human metabolic diseases, remains an important and clinically relevant question to be answered.

1.8 Experimental aims and hypotheses

The broad aims of the current study were to:

1. Isolate primary EC cell cultures from the duodenum and colon of mice.
2. Identify the capacity of mouse EC cells to detect and respond to certain luminal nutrients.
3. Establish whether nutrient sensing by mouse EC cells is region-specific.
4. Investigate changes to the EC-cell nutrient sensing capacity under diet-induced metabolic disease conditions.
5. Determine the role of interactions between the gut microbiome and EC cells in regulating host metabolism.

The broad hypotheses of the current study were:

1. Isolated mouse EC cells the capacity to sense and response to luminal nutrients *in vitro.*
2. Nutrient sensing by mouse EC cells is region-specific.
3. Nutrient sensing by mouse EC cells is altered in mice with diet-induced metabolic disease.
4. The gut microbiome regulates host-metabolism via mediating EC cell 5-HT synthesis and release.

CHAPTER 2: Isolation and characterisation of primary EC cells from the mouse duodenum and colon under lean and obese conditions

2.1 Introduction

A variety of physiological stimuli trigger release of 5-HT from biopsied human colonic mucosal tissue, immortalised EC cell-like cell lines and human primary 5-HT-containing cell cultures (Kidd et al., 2008, Symonds et al., 2015, Modlin et al., 2006). EC cells are exposed to GI luminal contents (e.g.; ingested nutrients, bile acids and signals produced by gut microflora) and circulating nutrients in intestinal blood vessels. An acute change in luminal glucose concentration triggers 5-HT release in intact tissue preparations and from guinea pig primary colonic EC cells (Zelkas et al., 2015). This occurs as a result of membrane depolarisation and subsequent extracellular Ca^{2+} influx through voltage-gated L-type Ca^{2+} channels (Raghupathi et al., 2013, Zelkas et al., 2015). Glucose triggers 5-HT release after uptake via the sodium-dependent glucose transporter-1 (SGLT1) in BON cells, a 5-HT secreting human carcinoid cell line, while in rodent intestine, glucose sensing by the Na^{+}/glucose co-transporter 3 (SGLT3) has been implicated in this response (Kim et al., 2001a, Freeman et al., 2006a). The GI tract shows regional differences in anatomy and function over its full length. In addition, the type, and quantity, of nutrients that the GI tract is exposed to varies throughout its length. This is exemplified by the preferential detection and absorption of simple carbohydrates in the proximal intestine, which is largely complete by the time ingested contents have reached the colon (Crane, 1960). Furthermore, the colon hosts the majority of GI microbiota, which aid in the breakdown of complex carbohydrates that are indigestible by the host and produce metabolites including SCFA and secondary bile acids. SCFAs increase 5-HT bioavailability in a number of experimental settings (Yano et al., 2015, Fukumoto et al., 2003, Alemi et al., 2013, Nzakizwanayo et al., 2015), and it is suggested that the interaction of SCFAs with free fatty acid receptor 2 (FFAR2) may mediate this response (Akiba et al., 2015). Clear evidence for this in primary EC cells has not yet been provided.

Peripheral circulating 5-HT, derived from EC cells, plays an important role in metabolic homeostasis (Young et al., 2015). In particular, 5-HT plays a key role in maintaining blood glucose levels under times of fasting, via increasing hepatic gluconeogenesis and adipocyte lipolysis (Sumara et al., 2012), while also decreasing thermogenesis to conserve energy stores (Crane et al., 2015). Hepatic glucose production is one of the main contributors to increased blood glucose levels in humans with type 2 diabetes (T2D) (DeFronzo et al., 1989). Circulating 5-HT is positively correlated with blood glucose levels in humans and a number of animal models (Takahashi et al., 2002, Tubio et al., 2010, Watanabe et al., 2014, Watanabe et al., 2010), and is significantly higher in humans with T2D (Takahashi et al., 2002). Intestinal and plasma 5-HT levels are also increased in mice with diet-induced obesity (Kim et al., 2011, Bertrand et al., 2011) and an increase in EC cell numbers precedes the onset of obesity (Le Beyec et al., 2014). As such, elevated gut-derived 5-HT is considered to be an important potential driver of obesity and metabolic disease.

Despite their role in regulating a number of important physiological functions, primary EC cells have been inadequately studied at the single cell level. Moreover, many findings on EC cell function have been based on experiments performed with pancreatic carcinoma cell lines (Kim et al., 2001a, Braun et al., 2007, Yano et al., 2015) or a human small intestinal carcinoid-derived neoplastic cell line (Kidd et al., 2007). The physiological relevance of these cell lines, and to what degree they resemble primary EC cells, is questionable. Functional studies of primary EC cells using whole tissue or isolated crypts (Lomax et al., 1999, Nozawa et al., 2009, Keating and Spencer, 2010) can also be confounded by indirect effects of non-EC cells in these preparations, such as neurons, epithelial cells and myocytes, or by contraction of the gut wall, which is known to be a major stimulus for the release of 5-HT from EC cells (Keating and Spencer, 2010). Accordingly, we have developed a technique to isolate and purify primary EC cells from guinea-pig and human colon (Raghupathi et al., 2013) and provided the

first evidence of a unique mode of 5-HT release from single vesicles within primary EC cell (Keating et al., 2008, Jackson et al., 2015, Zanin et al., 2011, Maritzen et al., 2008, Raghupathi et al., 2013, Raghupathi et al., 2016) . The approach of using isolated primary EC cells not only removes the confounding factor of motility, but also removes potential influence from other enteroendocrine cell hormones and unequal exposure to stimuli, which may be encountered in whole-tissue preparations.

The aim of the present series of experiments was to isolate primary EC cells from the duodenum and colon of mice, based on similar techniques developed from earlier work in human and guinea-pig colon (Raghupathi et al., 2013). Purified preparations of primary EC cells provide a useful tool for evaluating whether there are regional differences in EC cells by allowing for a direct comparison within an individual animal, which is yet to be achieved in humans. In addition, establishing a primary murine EC cell model will provide a solid basis for genetic manipulations, as a means of further establishing the role of these cells in various physiological processes. Since the concentrations and types of nutrients differ significantly throughout the GI tract, the sensing of nutrients may vary along the length of the gut. As such, this study aimed to interrogate the respective expression profiles of nutrient sensing receptors and transporters of duodenal and colonic EC cells and determine whether these are region-specific. Finally, this work aimed to utilise a diet-induced obese mouse model to verify increased circulating 5-HT with obesity and identify whether changes in nutrient sensing receptors and transporters occur within EC cells under obesogenic conditions.

The majority of work presented in this chapter is comprised of published work, from the following publication: Alyce M Martin *et al* (2017), ‘The nutrient-sensing repertoires of mouse enterochromaffin cells differ between colon and duodenum’, *Neurogastroenterology and Motility*, e13046. The relative author contributions to this work are as follows: AM Martin, AL Lumsden, CF Jessup and DJ Keating were involved in planning the experiments. AM Martin

performed the experiments. AM Martin and DJ Keating analysed the data. CF Jessup, RL Young and NJ Spencer provided critical input and advice. AM Martin and DJ Keating wrote the paper and all authors were involved in drafting the manuscript. This work is supported by funding from the Australian Research Council and National Health and Medical Research Council (CI: DJ Keating). No competing interests are declared.

2.2 Methods

2.2.1 Primary mouse EC cell isolation

Animal studies were performed in accordance with the guidelines of the Animal Ethics Committee of Flinders University. Male, 8-16-week-old B6:CBA mice fed a standard chow diet ad libitum on a 12-hour light-dark cycle were euthanized at approximately 10:00am by isoflurane overdose followed by cervical dislocation. Duodenum was removed by dissecting adjacent to pyloric sphincter and comprising of approximately 6 cm of proximal small intestine, and entire colon from caecum to rectum were immediately removed and EC cells isolated and enriched according to our published methods (Raghupathi et al., 2013). In brief, the mucosal layer was removed in ice-cold Krebs buffer: (in mM; NaCl 140, KCl 5, CaCl2 2, MgCl2 1, HEPES 10, D-glucose 5, pH 7.4), minced and digested in a combination of 1 part Collagenase A (3 $mg.mL^{-1}$, Roche Diagnostics GmbH, Mannheim, Germany) and 2 parts 0.05% Trypsin-EDTA (Sigma-Aldrich) at 37°C for 30-40 mins with constant agitation. Tissue digestion was inactivated by addition of equal volumes of DMEM culture media (Gibco) containing 10% FBS, 1% L-glutamine and 1% penicillin–streptomycin), and the digestion mixture was filtered through a 40 μm cell trainer (Greiner) and centrifuged at 600 × *g*. The supernatant was removed and resulting pellet resuspended in 1 mL of culture media, which was then layered on top of a Percoll® (Sigma) density gradient formed according to manufacturer's instructions. Following centrifugation at 1100 × *g* for 8 mins and slow braking, EC cells were harvested at a Percoll®

density of 1.059-1.07 $g.L^{-1}$. Harvested cells were washed once, then resuspended in culture media. EC cell viability was measured by staining with Trypan Blue (0.2% final concentration) followed by cell counting using a haemocytometer. Cells were considered viable if they completely excluded the dye. EC cell cultures were used immediately following isolation.

2.2.2 Immunocytochemical analysis of EC cell purity

To determine the purity of EC cells within the isolated population, cells were immunologically stained for 5-HT and TPH1. EC cells were cultured on glass coverslips previously coated with poly-D-lysine and poly-L-ornithine (Sigma-Aldrich), in culture medium for 2 hrs. Cells were fixed for 2 hrs in Zamboni's fixative at 4°C, followed by a series of 5 min washes (4 × 80% ethanol, 2 × 100% ethanol, 3 × DMSO and 4 × PBS). Fixed cells were incubated in 10% normal donkey serum in antibody diluent (290 mM NaCl, 7.5 mM Na_2HPO_4, 2.6 mM $Na_2HPO_4.2H_2O$, 0.1% NaN_3 in distilled water, pH 7.1) for 30 mins in a humidity chamber, followed by 24 hr incubation in a humidity chamber with either goat monoclonal anti-5-HT (Jackson Immunoresearch, 1:1500) or sheep polyclonal anti-TPH1 (Millipore, 1:200). Coverslips were washed with PBS for 3 × 5 min and incubated in a humidity chamber for 2 hrs in Cy3-labelled secondary antibodies: donkey anti-goat IgG (Jackson Immunoresearch, West Grove, PA, USA, 1:400) and donkey anti-sheep IgG (Jackson Immunoresearch, 1:200), along with the nuclear stain, DAPI (Sigma-Aldrich, 1:500). Coverslips were then washed 3 times with PBS for 5 min each and mounted on glass slides with 100% buffered glycerol and stored at 4°C.

Images were captured using an Olympus BX-50 Fluorescence microscope and ImageJ software (Bethesda, MD, USA). The purity of EC cell cultures was calculated by determining the percentage of DAPI-positive cells that were 5-HT-positive.

2.2.3 Diet-induced obesity mouse model

Animal studies were performed in accordance with the guidelines of the Animal Ethics Committee of Flinders University (Ethics number: 900/15). Male 8-week-old 186SV-Bl6 mice were individually housed on a 12-hr light-dark cycle at the School of Medicine Animal Facility and randomly assigned to control or experimental groups. At 10 weeks of age, mice were fed with either low fat (control, LFD, 4% g/kg) or high fat (HFD, 35% g/kg) diet (Table 2.1, Gordon's Speciality Stock Feeds, Yanderra, NSW, Australia) *ad libitum* for a period of 8 weeks, with food consumption and mouse weight measured weekly. Total calorie consumption per mouse was determined by calculating the total number of calories consumed after each week normalised to body weight. The efficiency of the HFD to induce weight gain was determined by analysing the amount of weight gained per calorie consumed after 8 weeks. Mice had access to water *ad libitum.* Mice were considered obese if their weight was greater than three standard deviations of the LFD control group (Enriori et al., 2007).

Table 2.1 – Dietary composition of low and high fat diets (per kg).

Dietary Component	Low Fat Diet (LFD)	High Fat Diet (HFD)
Total Protein	19.2%	26.2%
Casein, 30 Mesh	200 g	200 g
L-Cystine	3 g	3 g
Carbohydrate	67.3%	26.3%
Corn Starch	506.2 g	0 g
Maltodextrin 10	125 g	125 g
Sucrose	20 g	20 g
Fat	4.3%	34.9%
Soybean Oil	25 g	25 g
Lard	20 g	245 g
Total kcal/gm	3.85	5.24

2.2.4 Metabolic tests

2.2.4.1 Fasting glucose measurements

Mice were fasted by housing in cages without bedding or food for a period of 2 hrs. This was followed by blood collection via tail vein bleed with blood glucose measured using an ACCU-CHEK® Performa glucometer (Roche Diagnostics, Australia)

2.2.4.2 Glucose tolerance test

Mice were fasted for a period of 4 hrs, followed by blood collection via tail vein bleed for baseline blood glucose. Glucose solution was injected intraperitoneally at a concentration of 2 g/kg body weight, and blood glucose levels determined by measuring blood collected via tail bleed at 15, 30, 60, 90, 120, 150, 180 and 240 mins post-injection using an ACCU-CHEK® Performa glucometer (Roche Diagnostics, Australia).

2.2.4.3 Insulin tolerance test

Mice were fasted for a period of 2 hrs, followed by blood collection via tail vein bleed for baseline blood glucose. Insulin (Novo Nordisk, Australia) was injected intraperitoneally at a concentration of 1 unit/kg body weight, and blood glucose levels determined by measuring blood collected via tail vein bleed from 0-180 mins post-injection at 15-min intervals using an ACCU-CHEK® Performa glucometer (Roche Diagnostics, Australia).

2.2.5 Blood collection and plasma 5-HT analysis

Mice were euthanised at 18 weeks of age by isoflurane overdose followed by cervical dislocation. Blood was collected via immediate post-mortem cardiac puncture into EDTA coated blood collection vials (Microvette®, Sarstedt Australia) as per manufacturer's instructions. Plasma was immediately separated by centrifugation at room temperature at 2000 rpm for 30 mins, the top plasma fraction collected into separate tubes and stored at -80ºC until further use. Collected plasma samples were analysed for 5-HT content using the ultra-sensitive

5-HT ELISA (LDN, Germany), as per the method previously described. Plasma samples were analysed at a 1:20 dilution using the commercially available diluent buffer.

2.2.6 Quantitative real-time PCR

Quantitative real-time PCR was used to determine expression of nutrient sensing transporters and receptors (Table 2.2) in duodenal and colonic EC cells according to our previous methods (Peiris et al., 2012, Penko et al., 2015, Barreto et al., 2011). Due to the limited availability of EC cell RNA from HFD-fed mice, the nutrient sensing targets for investigation under HFD conditions were selected based on their greater abundance in the respective tissue of origin. In brief, RNA was extracted from EC cells using the RNeasy Mini Kit with on-column DNase treatment (Qiagen, Australia) according to manufacturer's instructions. RNA purity and concentration were determined using a NanoDrop 2000 (Thermo Fisher Scientific), and reverse transcription PCR performed for cDNA synthesis (see Appendix Table 6.1 for reaction components). Real-time PCR was carried out for gene transcripts using a QIAGEN Quantitect SYBR® Green PCR kit (Qiagen, Australia) and RotorGene 3000 thermocycler (Corbett Life Science, Sydney, Australia). For PCR reaction components, primer pair details and thermocycling conditions see Appendix Tables 6.2-6.4. Sample expression was normalised to that of β-actin, based on the comparable expression of this protein along different segments of the gastrointestinal tract (Vegezzi et al., 2014). A sample with no cDNA template served as the negative control, with all samples run in triplicate. Primer efficiencies were determined for each target using two-fold dilutions of pooled template DNA. Resultant PCR products were separated on a 3% agarose gel with 1Kb Plus DNA ladder (Invitrogen), and imaged using the Gel Doc EZ Imager (Bio-Rad) and Image Lab software (Bio-Rad). Target gene expression was determined relative to endogenous controls using Q-Gene analysis software as previously described (Muller et al., 2002).

Table 2.2 – Function of selected PCR targets within the GI tract.

Target	Function within the GI tract
GLUT1	High affinity, low capacity glucose transporter
GLUT2	Low affinity, high capacity glucose, fructose and galactose transporter
GLUT5	Fructose transporter
SGLT1	Na^+/glucose, Na^+/galactose co-transporter
SGLT3	Na^+/glucose, Na^+/galactose co-transporter (putative glucose sensing)
FFAR1	Medium and long chain fatty acid receptor
FFAR2	Short chain fatty acid receptor
FFAR3	Short chain fatty acid receptor
FFAR4	Long chain fatty acid receptor
GPR84	Medium chain fatty acid receptor
GPR92	Protein hydrolysate amino acid receptor
GPR119	Lipid amide and oleoylethanolamide receptor
T1R3	Sweet taste receptor subunit

2.2.7 Quantitation of EC cell size

Flow cytometry was used to determine relative size distribution of isolated EC cells. Briefly, isolated EC cells were washed once with Hank's Balanced Salt Solution (HBSS, Sigma-Aldrich) and centrifuged at 500 × *g* for 4 mins. Pellet was re-suspended in 1 mL HBSS and loaded into FACS tubes. Samples were analysed using a BD FACS Canto II flow cytometer, over a period of 3 mins. Viable EC cell populations were determined by forward scatter area (FSC-A) and side scatter area (SSC-A), which can be considered as indicative measures of relative size and granularity, respectively.

EC cell sizes were quantitatively determined by analysing the cross-sectional area of the widest part of each cell in the field of view. EC cells were plated on tissue culture petri dishes (Corning) and incubated in culture medium at 37°C for 2 hrs to adhere. Bright-field images were then taken using an Olympus CKX41 microscope and Olympus DP21 imager and cell area quantified using Image J software (Bethesda, MD, USA).

2.2.8 Statistical analysis

Analyses of data was performed using two-tailed Student's *t* tests for single comparisons using GraphPad PRISM 5.04 software. *n* indicates the number of independent cultures from different mice used. In all cases, significant differences are indicated as * $p < 0.05$, ** $p < 0.01$, *** $p < 0.001$. Data for single comparisons are presented as mean ± standard error (SEM), and correlations performed using a Pearson correlation analysis and presented as line of best fit ± 95% confidence interval.

2.3 Results

2.3.1 Isolation and purification of colonic and duodenal mouse EC cells

The described dissection protocol successfully removed intestinal mucosa whilst leaving GI musculature in-tact for both duodenal (Figure 2.1A) and colonic (Figure 2.1B) tissue segments. Separation of cell populations from digested mucosal samples using a Percoll® density gradient was successful (Figure 2.1C). Representative images of purified cell cultures are shown from the duodenum (Figure 2.2A) and colon (Figure 2.2B). The cell yield was significantly higher (Figure 2.2C) from the duodenum ($515.7\times10^4 \pm 57.1\times10^4$ cells/g tissue) compared to colon ($294.7\times10^4 \pm 61.4\times10^4$ cells/g tissue, $p < 0.01$) and cell viability (Figure 2.2D) was significantly higher (95.8 ± 1.4%) for both colon and duodenal preparations immediately after isolation. This value decreased significantly (11.9 ± 1.9%) after 24 hrs in culture.

Cells identified by DAPI showed a high degree of co-localisation between 5-HT and TPH1 in the duodenum (Figure 2.3A-B) and colon (Figure 2.3C-D). Quantification revealed that isolated EC cultures were highly enriched from the duodenum (Figure 2.3B; 5-HT: 85.9 ± 9.9%, TPH1: 93.8 ± 6.2%) and colon (Figure 2.3D; 5-HT: 97.7 ± 1.2%, TPH1: 88.8 ± 3. 7%).

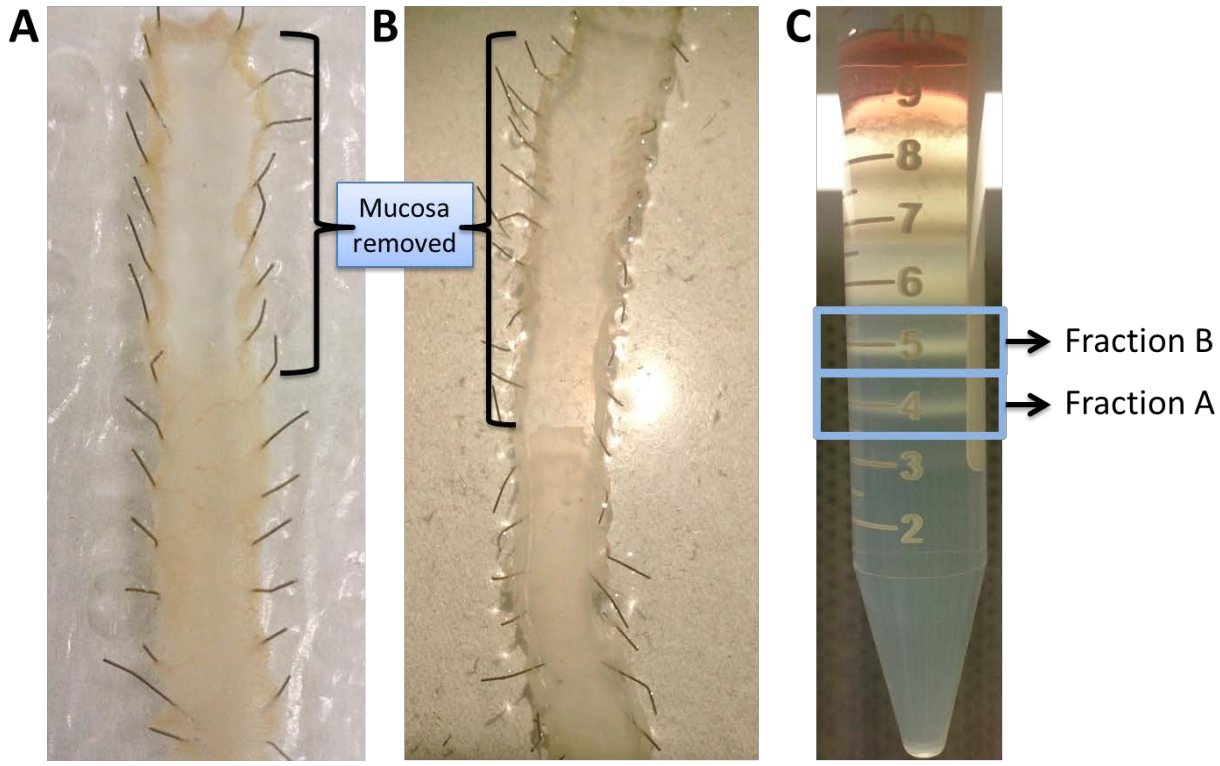

Figure 2.1 – Dissection of mucosa and fractionation of digested mucosal cells. (A) Duodenum with and without mucosa removed. (B) Colon with and without mucosa removed. (C) Distribution of digested duodenal mucosal cells through a Percoll® density gradient. EC cells are enriched in bands shown in Fraction A (1.07 g/L Percoll®) and Fraction B (1.059 g/L Percoll ®).

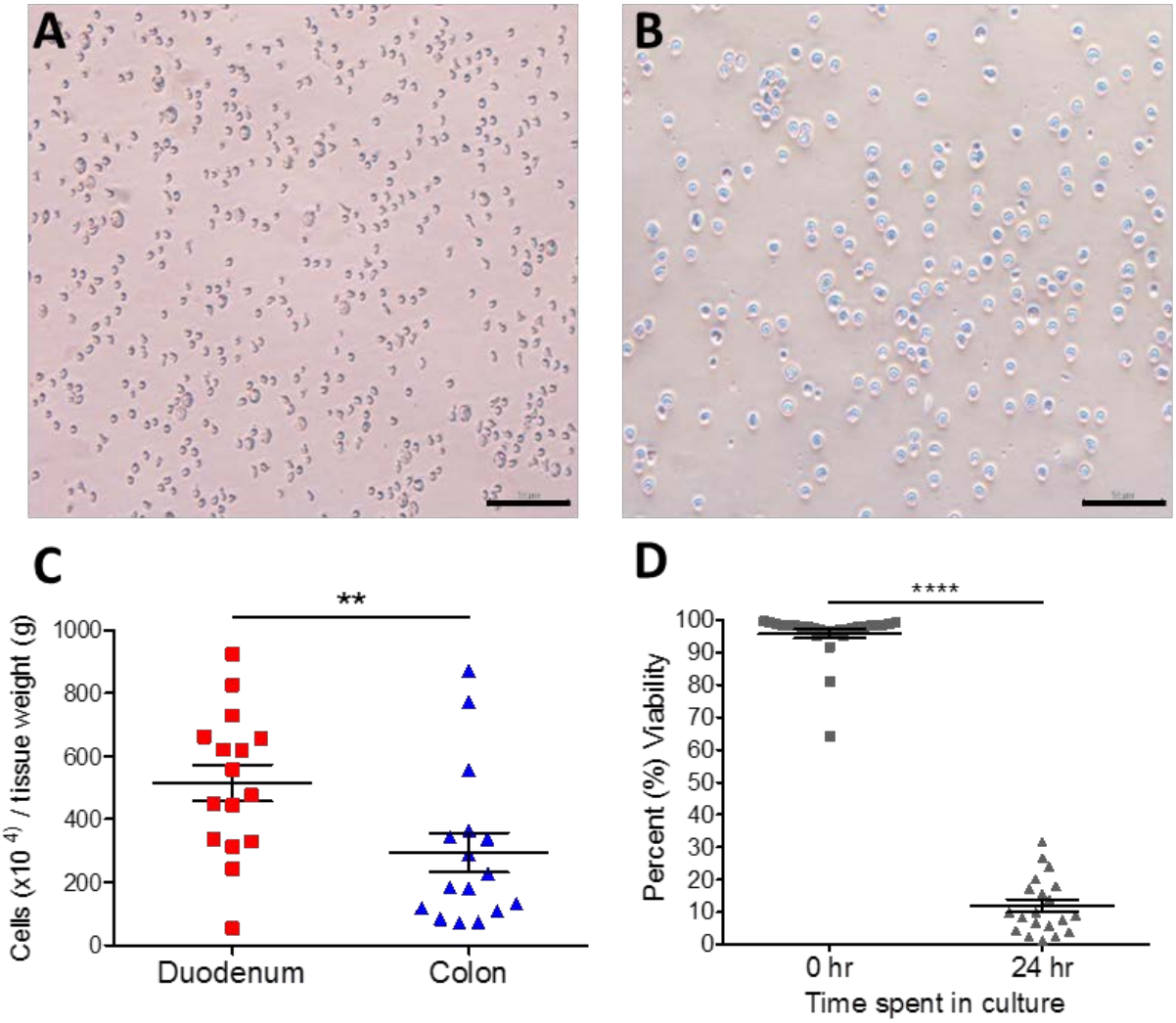

Figure 2.2 – Mouse EC cells from the GI tract can be isolated from duodenum at a greater yield when compared to colon. (A) EC cells from the duodenum and (B) colon. (C) Duodenal EC cells are isolated with greater yield per gram of tissue (n = 16 mice, **p < 0.01). (D) Isolated EC cells from duodenum and colon tissue isolations have significantly decreased viability in culture after 24 hrs (pooled duodenum and colon data, n = 20-27 mice, ****p < 0.0001). Scale bar = 50 µm.

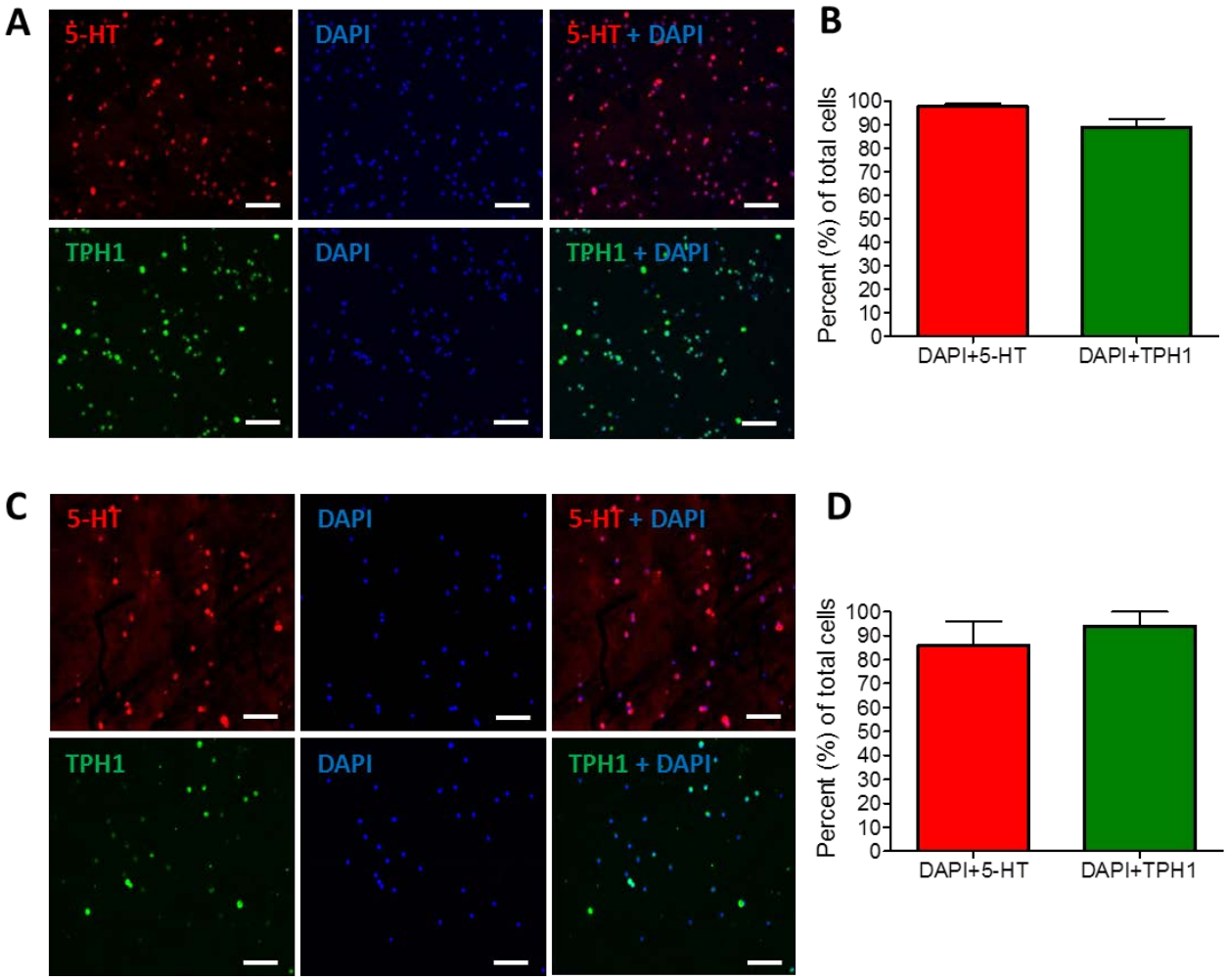

Figure 2.3 - High purity of isolated EC cells from mouse duodenum and colon. (A) Duodenal EC cells stained with DAPI and for 5-HT or TPH1. (B) The majority of isolated duodenal cells containing DAPI also expressed either 5-HT or TPH1. (C) Colonic EC cells stained with DAPI and for 5-HT or TPH1. (D) The majority of isolated colonic cells stained with DAPI also expressed either 5-HT or TPH1 (*n* = 3 mice). Scale bar = 60 μm.

2.3.1 Purified EC cells from the duodenum and colon have different size distributions

It was noted from the bright field and fluorescence images that EC cells isolated from the duodenum show two major size populations, while in the colon EC cell sizes appear to be considerably more uniform. To determine if the size distribution of EC cells differs between the duodenum and colon, EC cell populations were first interrogated by flow cytometry. Scatter plots of EC cell preparations from mouse duodenum (Figure 2.4A) and colon (Figure 2.4B) show different relative distributions with two distinct populations observed in duodenum EC cell preparations (Figure 2.4C-D). Smaller, less granular cells shown by lower relative side-scatter (SSC-A) and forward-scatter (FSC-A) constitute the majority of cells in individual preparations, averaging 69.8 ± 2.5% (n = 24 isolations) of total events detected. The FSC-A distribution of duodenal and colonic EC cells shows a binomial distribution of colonic EC cells, with duodenal EC cells having a bimodal distribution.

Given that the size distribution of duodenal EC cells differs from that of those from the colon, cross sectional cell area was quantitated to determine the average size of these populations. A significantly smaller median cell area (Figure 2.4D) was noted in EC cells from the duodenum (26.1 ± 0.5 μm) compared to colon (38.6 ± 0.5 μm, $p < 0.05$). Distributions from quantitative measurements of EC cell size show approximately the same distributions as those seen using flow cytometry.

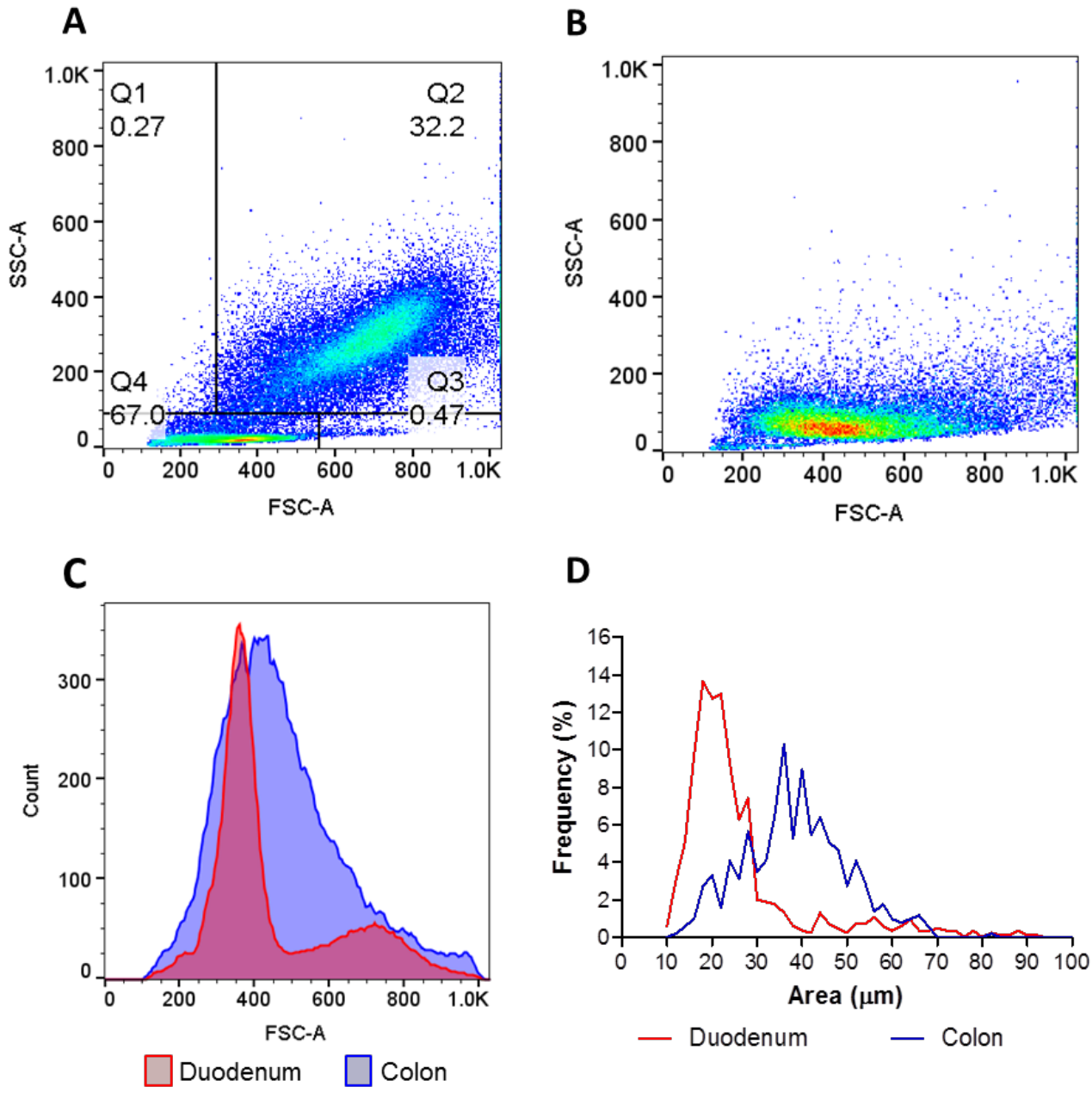

Figure 2.4 – Isolated EC cells from the mouse duodenum and colon have differing size distributions. Flow cytometry scatter plots show the distribution of enriched (A) duodenal and (B) colonic EC cells, with side scatter (SSC-A) and forward scatter (FSC-A) parameters used to identify cellular sub-populations. Sub-populations are shown by gating into quartiles (Q1-Q4), including percent of cells from the total population within each quartile. Scatter plots are representative images of isolations from one mouse. (D) The majority of EC cells in the duodenum are of a smaller size compared to the colon (n = 500-800 cells over 3 isolations).

2.3.2 Nutrient transporter and receptor gene expression in EC cells

This set of experiments characterised the expression of nutrient receptors and transporters, as well as the EC marker, TPH1, was examined in enriched EC cell cultures from the duodenum and colon of mice. A single PCR product was obtained for each transcript studied (Figure 2.5A). Transcripts for TPH1, GLUT1, GLUT2, GLUT5, SGLT1, SGLT3, T1R3, FFAR1-4, GPR84, GPR92, and GPR119 were detected in EC cells from the duodenum and colon (Figure 2.5B). GLUT1, GLUT5 and SGLT1 were the most abundantly expressed sugar transporters in EC cells from both tissues, with GLUT1 the highest expressed of all transcripts from duodenum and colon ($p < 0.05$). T1R3, SGLT3 and GLUT2 were expressed at low levels in both tissues. Another sweet taste receptor subunit, T1R2, was not detected in either duodenal or colonic EC cells.

FFAR2 was the most abundant fatty acid receptor expressed in EC cells from the duodenum and colon ($p < 0.05$). The next most abundant were transcripts for the long chain fatty acid (LCFA) receptor FFAR4, and the SCFA receptor FFAR3. The dual receptor for medium chain fatty acids (MCFA) and LCFAs, FFAR1, and the MCFA receptor GPR84 were the lowest abundance transcripts related to fatty acid sensing detected in EC cells from both tissues. GPR92 and GPR119 were also expressed at low abundance in both tissues.

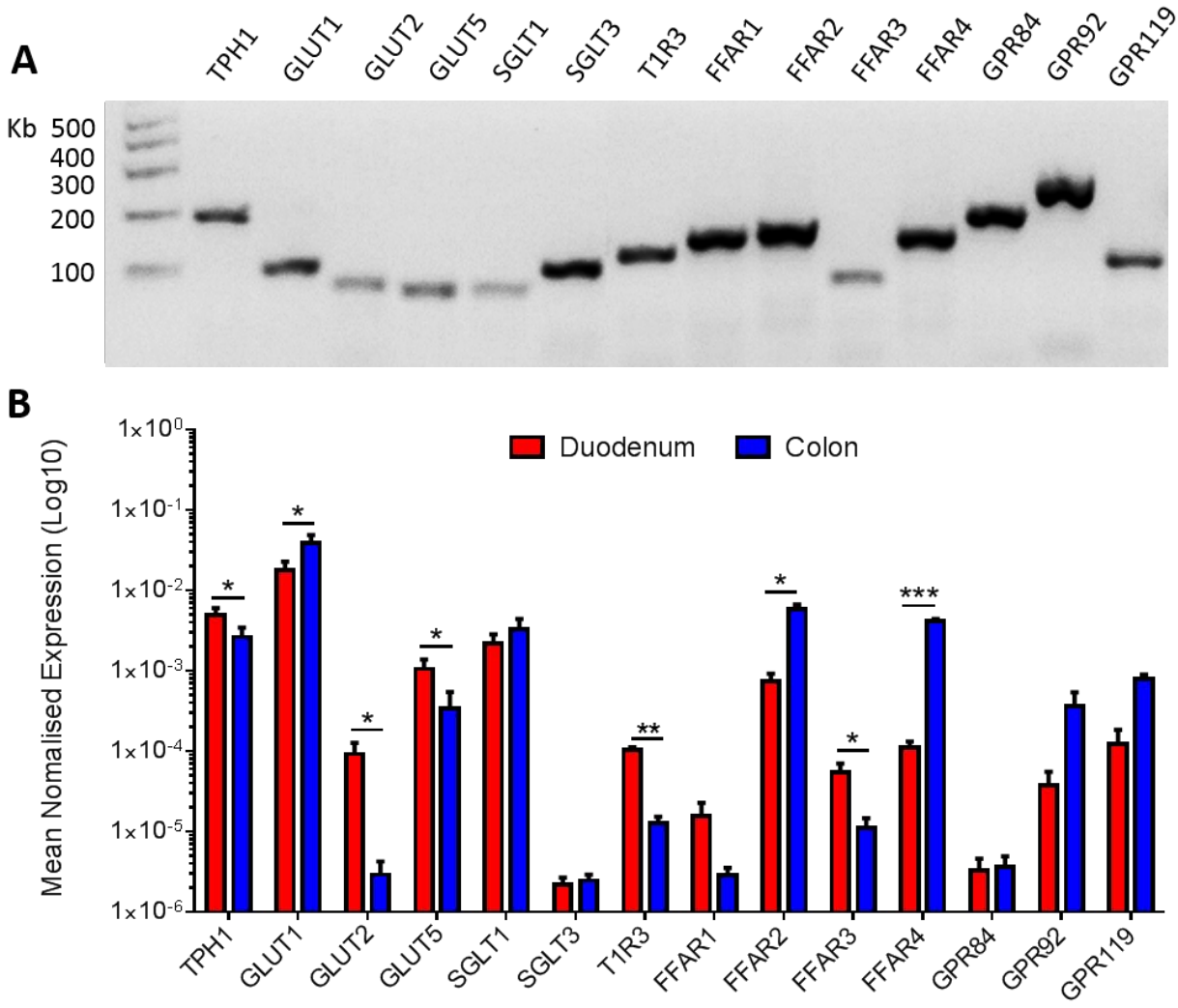

Figure 2.5 - EC cells from the mouse duodenum and colon express transcripts for nutrient receptors and transporters. (A) Agarose gel demonstrating single PCR-identified transcripts for sugar transporters (SGLT1, GLUT1, GLUT2, GLUT5), sugar sensors (T1R3, SGLT3), G-protein coupled receptors for fatty acids (FFAR1-4, GPR84), amino acids (GPR92), lipid amides (GPR119) and the EC cell marker, TPH1. (B) Relative mean expression of gene targets normalised to β-actin. (n = 3-7 mice, *$p < 0.05$, ***$p < 0.001$).

2.3.3 EC cell nutrient sensing transcript expression is region-dependent

Expression of T1R3 was 9 ± 2-fold ($p < 0.01$) higher in duodenal EC cells compared to colonic EC cells, while GLUT2 (437 ± 236-fold, $p < 0.05$) and GLUT5 (11 ± 3-fold, $p < 0.05$) were also enriched (Figure 2.6A). FFAR3 was the only SCFA receptor transcript enriched in EC cells from the duodenum, 6 ± 1-fold ($p < 0.05$) higher than in colon. Expression of TPH1 was 2 ± 1-fold higher in duodenal EC cells compared to colonic EC cells ($p < 0.05$). The LCFA receptor FFAR4 was markedly enriched in colonic EC cells compared to duodenal EC cells (45 ± 10-fold, $p < 0.001$) (Figure 2.6B). The SCFA receptor FFAR2 was also enriched 9 ± 1-fold in colonic EC cells ($p < 0.05$), while SGLT1, SGLT3, FFAR1, GRP84, GPR92 and GPR119 were equally abundant in EC cells from both tissues. GLUT1 transcript expression was 3 ± 1-fold higher in colonic EC cells ($p < 0.05$) than duodenal EC cells.

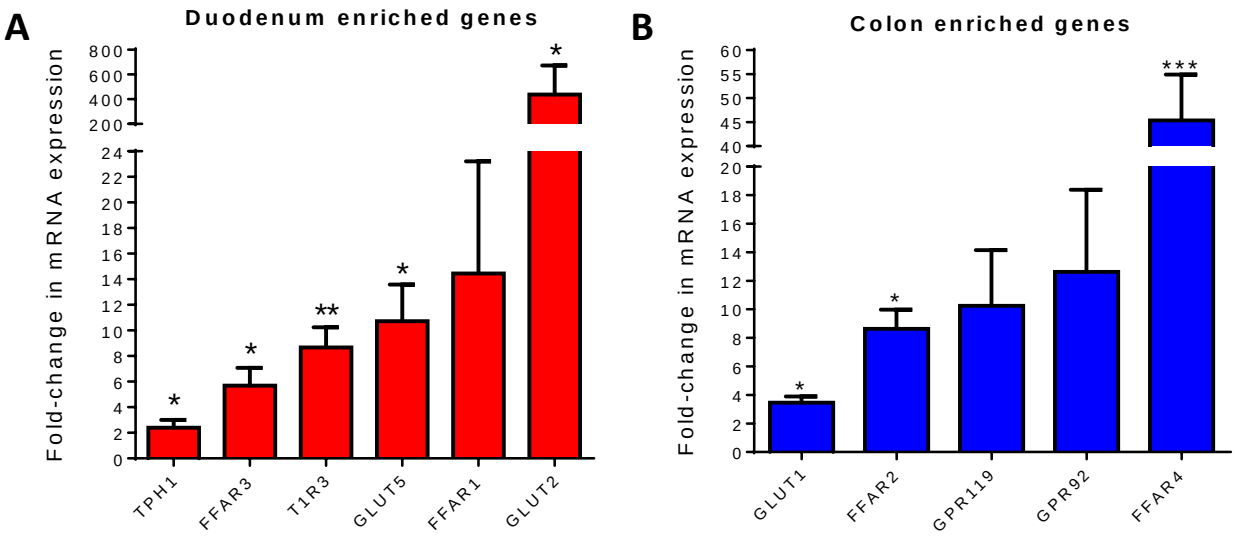

Figure 2.6 - Genes enriched within duodenal and colonic EC cells. (A) Fold-change in mRNA expression of duodenum-enriched genes relative to the colon. (B) Fold-change in mRNA expression of gene targets with higher expression in the colon compared to the duodenum. (n = 3-7 mice, *$p < 0.05$, ***$p < 0.001$).

2.3.4 High fat diet induces an obese, diabetic phenotype

Having determined the regional nutrient sensing profile of duodenal and colonic EC cells, this set of experiments aimed to establish a diet-induced obese mouse model with verified changes in circulating 5-HT, and identify whether changes to EC cell nutrient sensing occur under obesogenic conditions. Mice fed a HFD gained markedly more weight than those consuming a LFD over 8 weeks, with a significant difference in weight observed as early as 2 weeks (Figure 2.7A, $p < 0.01$). All HFD-fed mice were obese (42.6 ± 1.9 g) and weighed considerably more than LFD-fed controls (30.0 ± 0.6 g) after 8 weeks on the diet (Figure 2.7B, $p < 0.001$ *vs* LFD). While total caloric intake was similar for both diet groups, total caloric intake from fat over the 8-week period was greater in HFD-fed (487.8 ± 26.6 kcal) compared to LFD-fed (86.7 ± 2.5 kcal, $p < 0.001$) mice, while calories from carbohydrates was greater in LFD-fed mice (607 ± 17.2 kcal) compared to those fed a HFD (162.6 ± 8.9 kcal, $p < 0.001$). This indicates that the increased body weight is not due to increased calorie consumption, rather a greater efficiency of the HFD to increase weight gain for every calorie consumed (Figure 2.7C, $16.2 \times 10^{-3} \pm 1.5 \times 10^{-3}$ g/kcal) compared to the LFD ($0.7 \times 10^{-3} \pm 0.4 \times 10^{-3}$ g/kcal, $p < 0.001$).

In response to an intraperitoneal glucose challenge (Figure 2.8A), HFD-fed mice demonstrated a decreased capacity to clear glucose (Figure 2.8B, AUC: 4159 ± 140) compared to those fed a LFD (AUC: 3068 ± 51, $p < 0.001$ vs LFD). Following an intraperitoneal insulin challenge (Figure 2.8C), HFD-fed mice had impaired sensitivity to insulin (Figure 2.8D, AUC: 1220 ± 81) compared to LFD controls (AUC: 966 ± 68, $p < 0.05$ vs LFD). As such, HFD-fed mice show both insulin resistance and glucose intolerance, two hallmarks of metabolic disease progression.

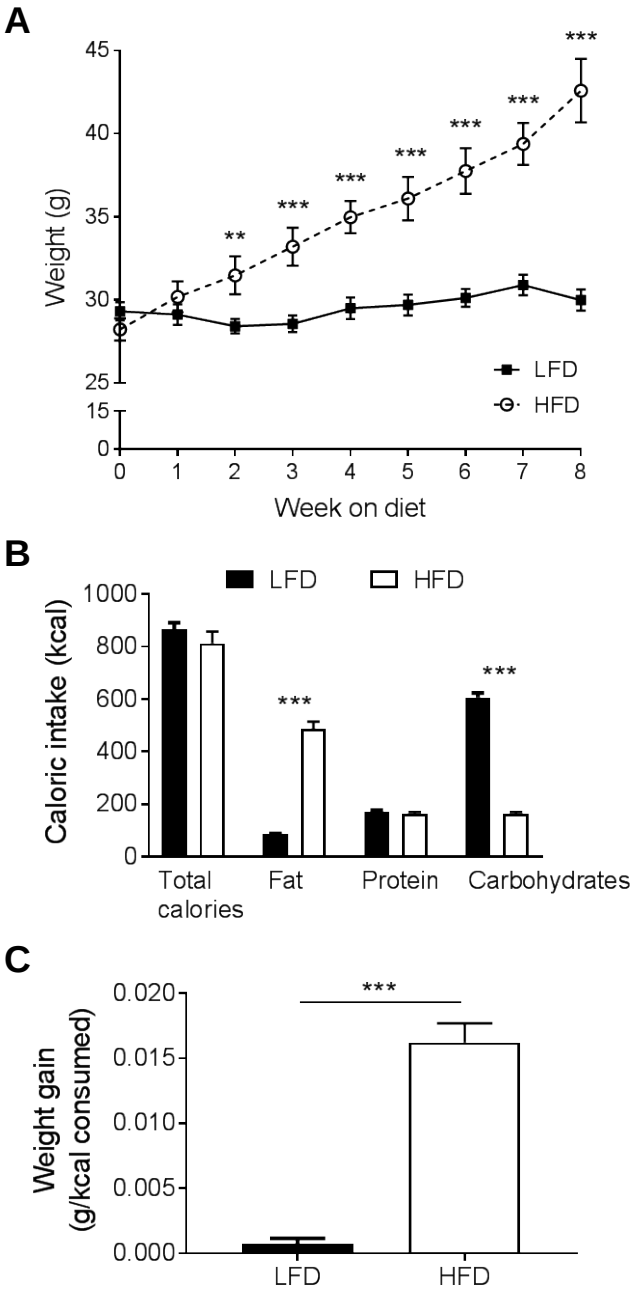

Figure 2.7 - High fat-diet consumption induced weight gain. (A) Total weight of mice fed a low-fat diet (LFD) and high fat diet (HFD) for 8 weeks. (B) Comparative breakdown of total caloric intake from fat, protein and carbohydrates for LFD and HFD. (C) Feed efficiency for LFD and HFD to induce weight gain per kcal consumed over 8 weeks (n = 5-8 mice, ** $p < 0.01$, *** $p < 0.001$ vs LFD. All data are shown as mean ± SEM.

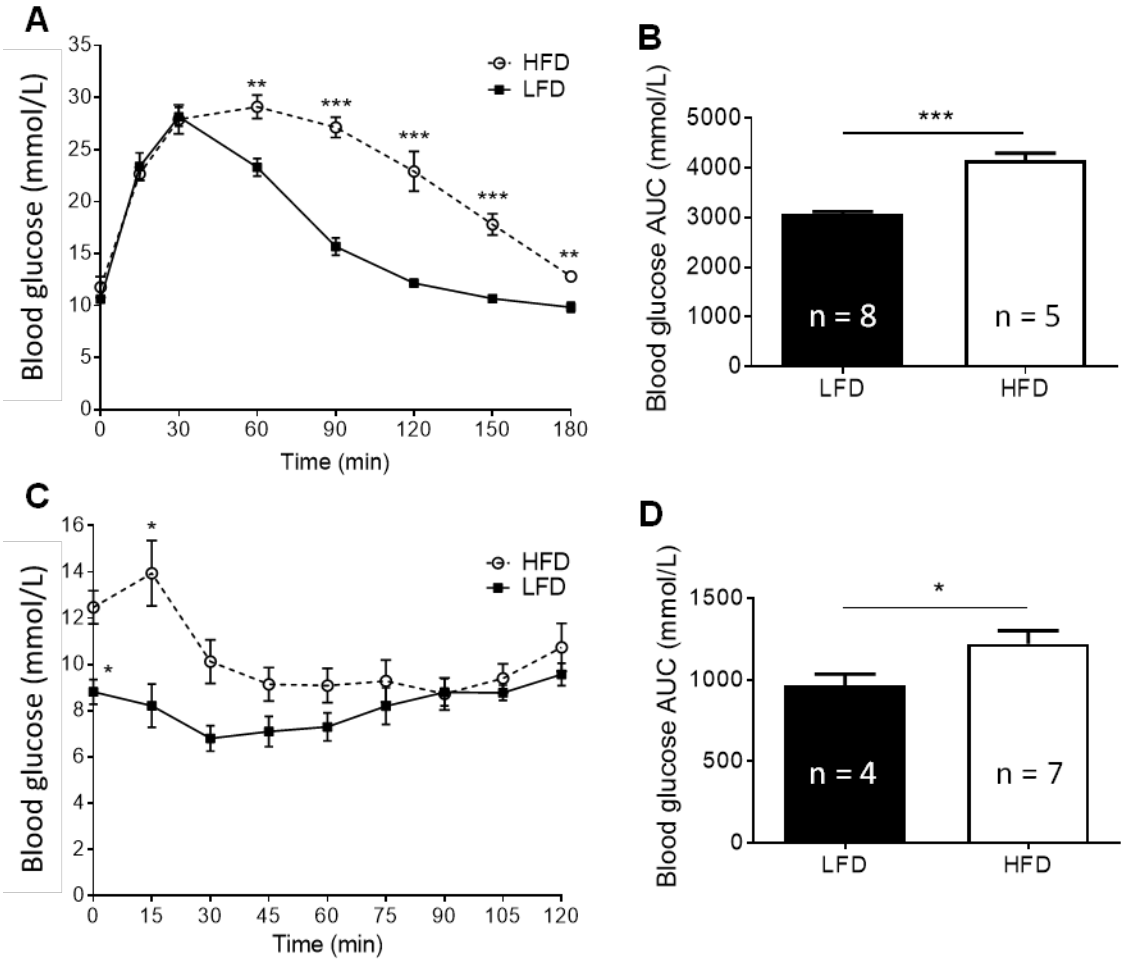

Figure 2.8 - High fat diet induces a glucose intolerant and insulin resistant phenotype. (A) Blood glucose levels over time following intraperitoneal glucose injection in LFD-fed and HFD-fed mice after 8 weeks. (B) Area under the curve (AUC) analysis for glucose tolerance test. (C) Blood glucose over time following intraperitoneal insulin tolerance test in LFD-fed and HFD-fed mice after 8 weeks. (D) Insulin tolerance test AUC. (** $p < 0.01$, *** $p < 0.001$). All data are shown as mean ± SEM.

2.3.5 Fasting blood glucose and circulating 5-HT are increased in mice with diet-induced obesity

Fasting blood glucose (Figure 2.9) was increased in HFD-fed mice (12.7 ± 0.6 mmol/L) compared to LFD mice (9.6 ± 0.5 mmol/L, $p < 0.01$) and is positively correlated with body weight (Figure 2.9B), which along with insulin resistance and glucose intolerance, is a hallmark of T2D and metabolic disease. Consistent with findings in humans with T2D, plasma 5-HT (Figure 2.9C) was higher in HFD-fed mice (130.8 ± 31.1 ng/mL) compared to those fed a LFD (40.5 ± 16.1 ng/mL, $p < 0.05$), but is not correlated with total mouse body weight (Figure 2.9D). Plasma 5-HT is positively correlated with fasting blood glucose (Figure 2.9E).

2.3.6 High fat diet consumption alters EC-cell nutrient sensing profile

Having established a mouse model of diet-induced obesity and T2D, isolated duodenal and colonic EC cells from these mice were then used to determine whether specific changes occur at a cellular level, which may underlie the increase in circulating 5-HT observed in this mouse model. Using quantitative real-time PCR for selected nutrient sensing receptors and transporters, analysis of isolated duodenal EC cells (Figure 2.10A) revealed GLUT5 fructose transporter and sweet taste receptor, T1R3, expression in EC cells from HFD-fed mice w reduced to 0.3 ± 0.1-fold ($p < 0.05$ vs LFD) of those in LFD fed mice. The SCFA-sensing receptor, FFAR3 was also decreased 0.5 ± 0.1-fold in duodenal EC cells from HFD-fed mice ($p < 0.05$ vs LFD). This effect of HFD appears to be specific to these transcripts, as expression levels of TPH1, SGLT1, GLUT1, GLUT2 and FFAR2 in duodenal EC cell were unchanged in HFD. However, SGLT1 expression positively correlates with body weight (Figure 2.10B, $R^2 = 0.623$, $p < 0.01$). Expression of T1R3 is negatively correlated with fasting blood glucose (Figure 2.10C, $R^2 = 0.623$, $p < 0.01$), which was not observed for any of the other targets of interest (Appendix Figure 6.1).

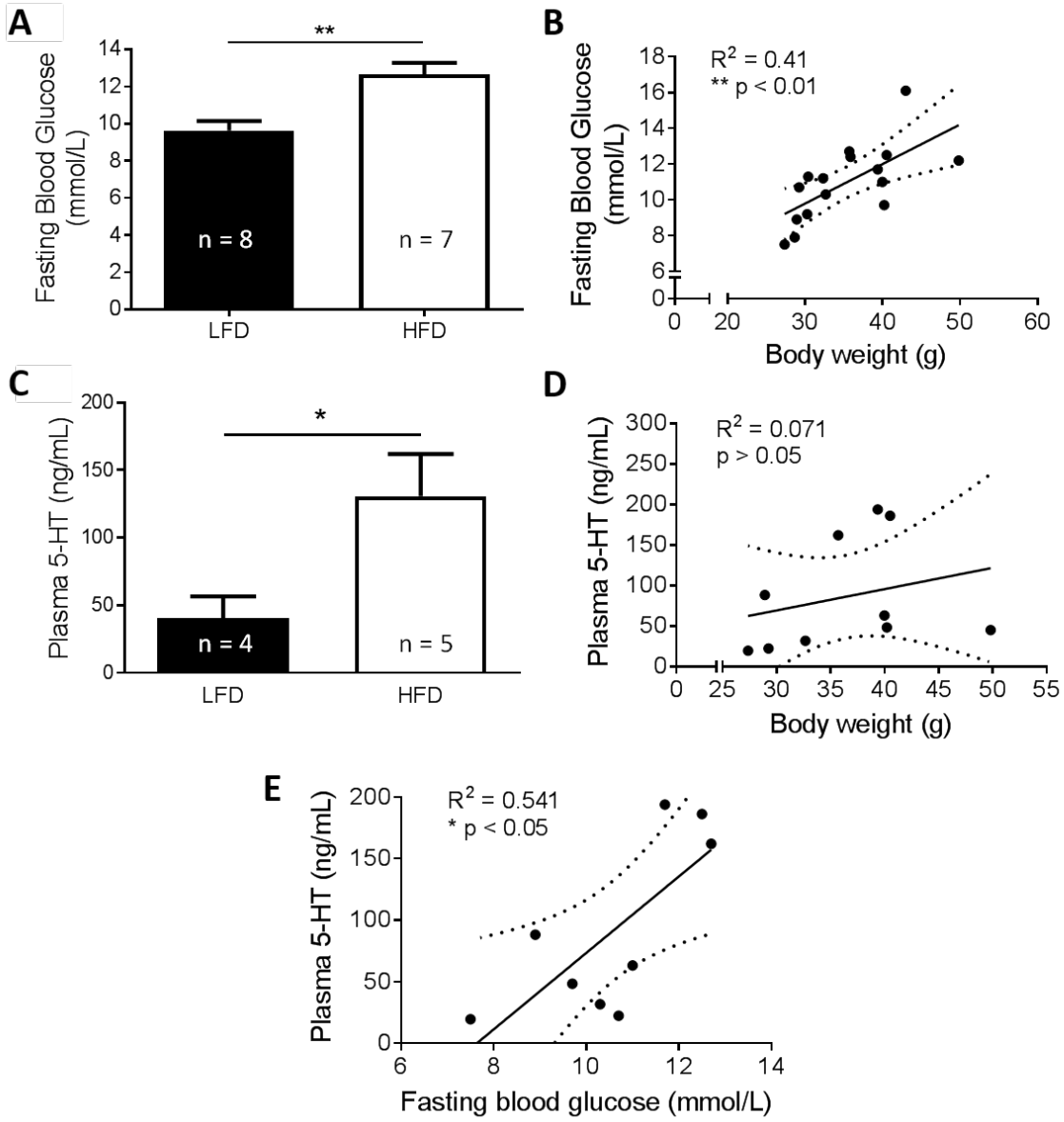

Figure 2.9 – HFD consumption increases fasting plasma glucose and 5-HT. (A) Blood glucose levels following 2-hr fast and (B) fasting blood glucose versus total mouse body weight. (C) Circulating plasma 5-HT following 8 weeks of diet consumption. (D) Plasma 5-HT versus total mouse body weight and (E) plasma 5-HT versus fasting blood glucose. (* $p < 0.01$, ** $p < 0.01$). Data (A,C) are expressed as mean ± SEM. Solid line (B,D and E) represents linear regression ± 95% confidence interval.

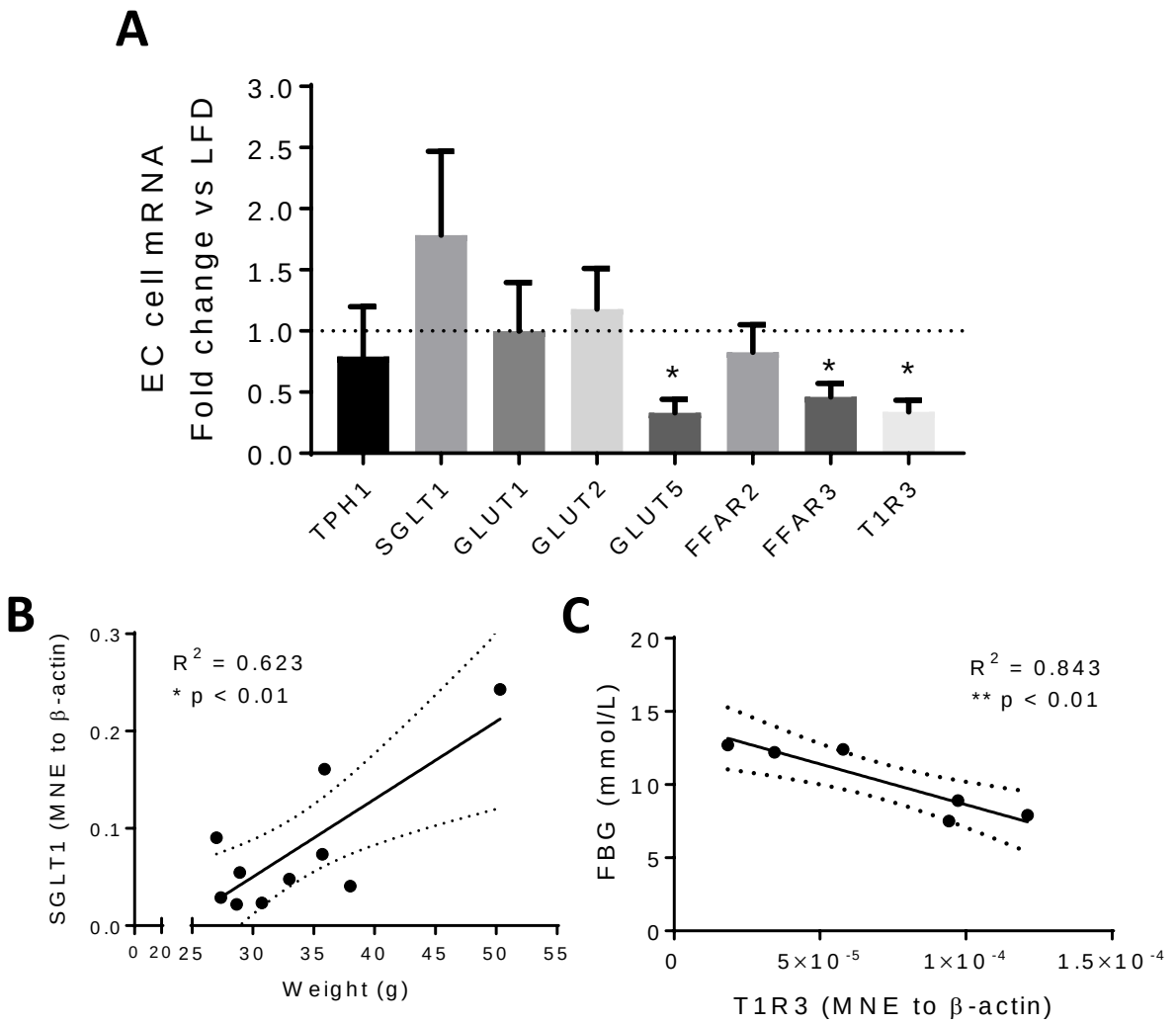

Figure 2.10 – Duodenal EC cell nutrient sensing profile is altered by HFD consumption. (A) Differences in mRNA expression in duodenal EC cells from HFD-fed mice compared to LFD-fed controls (n = 4-6 mice * $p < 0.05$ vs LFD). (B) Mean normalised expression (MNE) of SGLT1 in duodenal EC cells positively correlates with total body weight in mice. (C) MNE of T1R3 in duodenal EC cells is negatively correlated with fasting blood glucose (FBG). Data are expressed as mean ± SEM. Solid line represents linear regression ± 95% confidence interval.

In colonic EC cells (Figure 2.11A) expression of the rate-limiting enzyme for 5-HT synthesis, TPH1, was markedly higher (3.5 ± 1.4-fold) in HFD-fed mice ($p < 0.05$ vs LFD) and positively correlates with body weight (Figure 2.11B, $R^2 = 0.759$, $p < 0.001$). In addition, expression of the fructose transporter, GLUT5, is increased 1.7 ± 0.2-fold in HFD-fed mice ($p < 0.05$ vs LFD, Figure 2.12A), and is also positively correlated with body weight (Figure 2.11C, $R^2 = 0.587$, $p < 0.01$), while expression of GLUT1 is not significantly increased in the HFD-fed cohort but is positively correlated with weight (Figure 2.112D, $R^2 = 0.614$, $p < 0.01$), as is the SCFA receptor FFAR3 (Figure 2.11E, $R^2 = 0.711$, $p < 0.01$). Expression of the SCFA receptor FFAR2 is unaltered in both duodenal and colonic EC cells under high fat diet conditions, as is the medium to long chain fatty acid receptor FFAR4 in colonic EC cells and the hexose transporter GLUT2 in duodenal EC cells. No correlation was observed between colonic EC cell gene expression and fasting blood glucose for any of the targets of interest (Appendix Figure 6.2).

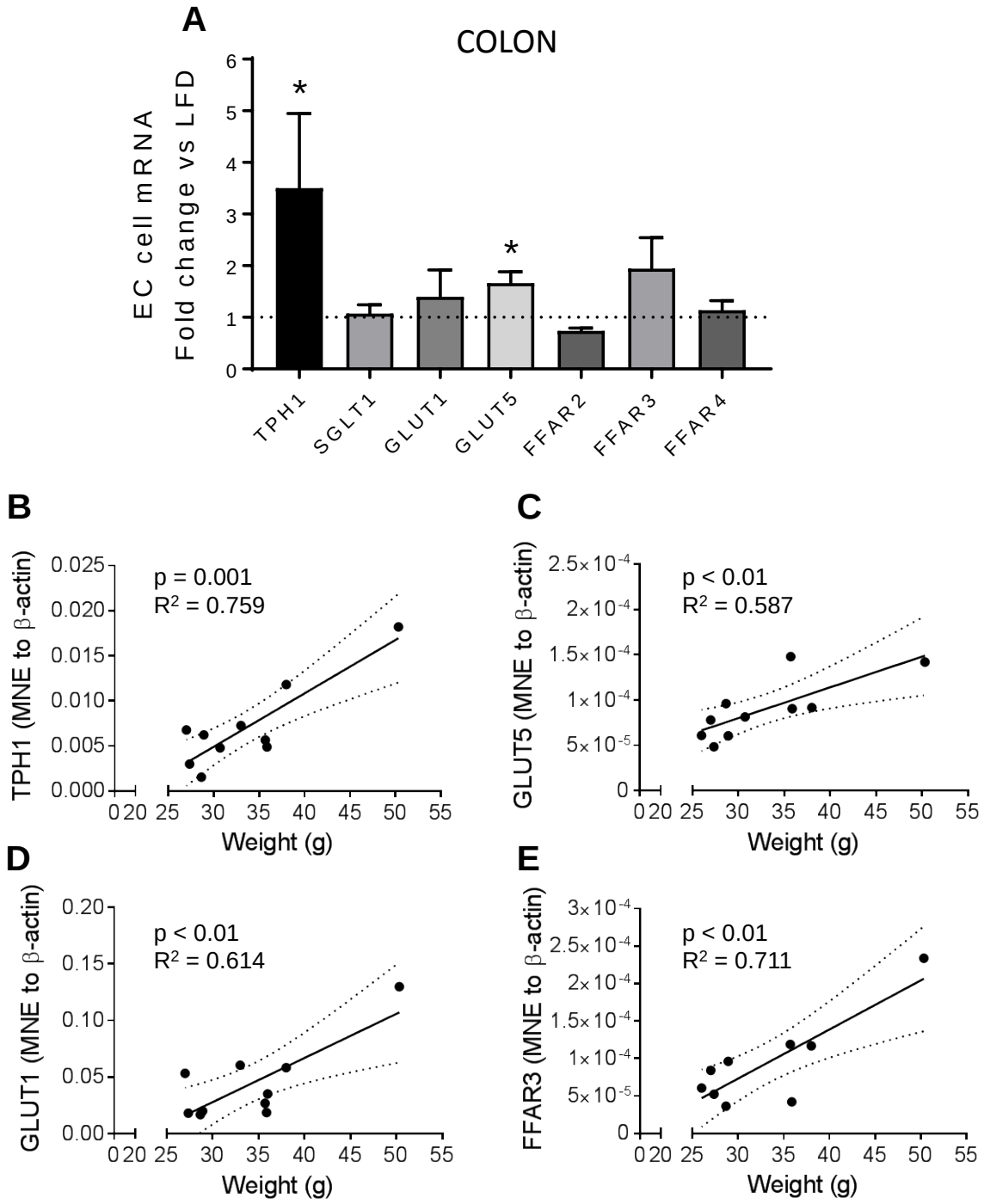

Figure 2.11 – Colonic EC cell nutrient sensing profile is altered by HFD consumption. (A) Differences in nutrient sensing receptor or transporter mRNA expression in colonic EC cells from HFD-fed mice compared to LFD-fed controls (n = 4-5 mice). * $p < 0.05$ vs LFD. (B) TPH1, (C) GLUT5, (D) GLUT1 and (E) FFAR3 mRNA expression in colonic EC cells is positively correlated with total body weight in mice fed a HFD. Data are expressed as mean ± SEM. Solid line represents linear regression ± 95% confidence interval.

2.4 Discussion

This set of experiments investigated the nutrient sensing capabilities of EC cells from two regions of the mouse gastrointestinal tract under lean and obese conditions. This is the first report of the enrichment of primary EC cells from the duodenum and colon of mice, and builds on the capacity for primary EC cell purification in humans and guinea pigs (Zelkas et al., 2015, Raghupathi et al., 2016, Raghupathi et al., 2013). This approach allows for a paired comparison of gene expression in EC cells obtained from both regions within the same mice.

The method of isolating pure EC cells from mucosal tissue yielded a greater number of EC cells per gram of tissue from the duodenum compared to the colon. This suggests a greater density of EC cells in this region of the GI tract in mice, consistent with previous findings in guinea pig (Raghupathi et al., 2013). The overall viability of mouse EC cell cultures was found to be low after 24 hrs, which therefore limits the ability to use these cultures for long-term investigations. Despite this, the use of cultures within this period provides a more accurate description of their *in vivo* characteristics. While isolated cultures show highly enriched EC cell populations, a very small percentage of 5-HT- and TPH1-negative cells remained. These cells are unidentified but may be enterocytes which are present as an artefact from the EC cell collection process. It is unknown what nutrient receptors and transporters these contaminating cells express, however the overwhelming and consistent enrichment of EC cells in both duodenum and colon isolations is likely to make the influence of these cells on the results minor.

The difference in size distribution of EC cells in the mouse duodenum and colon indicate that subpopulations of EC cells may exist. This may arise due to anatomical differences between these two regions of the GI tract, as the duodenal mucosa contains crypts and villi, while the latter are absent in the colonic mucosa (Mowat and Agace, 2014). It is possible that artefacts arising from processes which have detached from the EC cell may be observed. This

is highly unlikely to contribute to the distributions observed, however, as the smaller cells observed in the duodenal populations show the functionality of live cells, demonstrated in *Chapter 3*. Rather, the duodenal EC cell population may include smaller, less mature EC cells due to higher mucosal cell turnover in this gut region (approximately 1.5 days *versus* 3 days) (Darwich et al., 2014). Immature EC cells and EC cell subpopulations have been documented previously (Inokuchi et al., 1984), based on their morphological size, structure and number of basal or apical extensions corresponding to 'open' and 'closed'-type EC cells (Gustafsson et al., 2006). The existence of EC cell subpopulations is also supported by differential co-labelling of mouse duodenal EC cells for either or a combination of CCK and secretin (Fothergill et al., 2017a), or colonic EC cells for the amino acid-sensing and calcium-sensing receptor, CaSR (Symonds et al., 2015, Cho et al., 2014).

This study has identified that EC cells enriched from the mouse duodenum and colon express receptors and transporters capable of sensing luminal sugars and FFAs, which have previously been linked to 5-HT release (Symonds et al., 2015, Zelkas et al., 2015, Yano et al., 2015, Reigstad et al., 2015, Essien et al., 2013). These results have also showed differential expression of specific nutrient transporters and receptors in duodenal and colonic EC cells. This demonstrates that the capacity of EC cells to detect the nutrient environment of the GI tract may be dependent upon gut location.

Almost all intestinal glucose absorption is thought to be completed over the length of the small intestine, with limited glucose reaching the colon under normal conditions. The expression of sugar transporters in the colon, however, indicates a capacity for glucose absorption at this site (Yoshikawa et al., 2011). The high affinity, low capacity glucose transporter GLUT1 is highly expressed in both duodenal and colonic EC cells. GLUT1 is responsible for uptake of glucose to maintain basal cellular respiration and is upregulated in response to low glucose. The higher expression observed in the colon may be reflective of the

lower glucose exposure in this part of the GI tract compared to the duodenum and a reliance on increased sensitivity should adequate glucose levels reach this site. GLUT2 is a low affinity, high capacity glucose transporter that is upregulated in conditions of high glucose availability. Expression of GLUT2 transcript was low in isolated EC cells at both sites, but was more abundant in duodenal cells. This is in line with duodenal EC cells being more frequently exposed to high glucose conditions compared to colonic EC cells.

Expression of the sodium-glucose co-transporter-1, SGLT1, was also abundantly expressed in EC cells from both sites, highlighting that multiple routes for glucose uptake into EC cells likely exist. Previous work in the BON cell line highlighted SGLT1 as the major pathway regulating glucose-induced 5-HT release in these cells (Raybould and Zittel, 1995, Kim et al., 2001a). Whilst in rat, SGLT3 has been implicated as the most likely luminal glucose sensor for EC cell activation (Freeman et al., 2006a, Vincent et al., 2011), this study found SGLT3 to be lowly expressed in isolated mouse EC cells. Blockade of SGLT transporters inhibits glucose-dependent stimulation of EC cells and the downstream activation of intrinsic and extrinsic neurons (Vincent et al., 2011). Activation of these neural pathways leads to the inhibition of gastric motility and emptying (Raybould et al., 2003), and stimulates pancreatic exocrine secretion (Li et al., 2001). Thus, SGLT1-mediated increases to EC cell 5-HT release may play a potential pathway by which sugars and sweet tastants affect intestinal motility and digestion.

GLUT5, the primary facilitative fructose transporter, is enriched in the small intestine of humans. Localised to the brush boarder membrane (BBM) (Davidson et al., 1992), it responds to increased luminal availability of fructose in mice (Corpe et al., 1998). In addition to transporting glucose, GLUT2 can also transport fructose. Results from this study demonstrate that both GLUT5 and GLUT2 are enriched in duodenal EC cells, a site with higher exposure than the colon to ingested nutrients such as fructose.

Functional sweet taste receptors comprise of two subunits, with the most common of these being T1R2/T1R3 heterodimer. The T1R2 isoform is of low abundance compared to T1R3 (Young et al., 2013), and the detection of the transcript is dependent on subtleties in assay conditions. Immunolabelling for the T1R2 subunit has shown co-expression in only 5% of human duodenal EC cells (Young et al., 2013). The absence of T1R2, but detection of T1R3 in mouse EC cells indicates that the T1R2/T1R3 receptor is unlikely to be a significant pathway to 5-HT release (Young et al., 2013). Rather, a T1R3 homodimer may exist, which has been previously shown to act as a glucose-sensing receptor in pancreatic β-cells (Kojima et al., 2015, Egerod et al., 2012). Alternately, transcript expression can be seen without the presence of a functional protein product (Egerod et al., 2012). Thus, the expression of a functional sweet taste receptor on EC cells needs to be confirmed in future studies.

Both colonic and duodenal EC cells express G-protein coupled receptors that detect free fatty acids (FFAR), amino acids and lipid amides. These include receptors for SCFAs, which can be synthesised by gut microbiota from the breakdown of digestion-resistant starches (Wong et al., 2006). The three main SCFAs - acetate, butyrate and propionate - are present throughout the GI tract, and show peak levels in the colon in a ratio of 60:20:20 (Cummings et al., 1987, Mowat and Agace, 2014). While FFAR2 expression is known to be enriched in the mouse colon compared to duodenum (Symonds et al., 2015) and has equal affinity for all three SCFAs, we show it has a colon predominant expression pattern in mouse EC cells. In contrast, FFAR3, which has equal sensitivity for propionate and butyrate, but a 100-fold lower sensitivity for acetate (Le Poul et al., 2003), was enriched in duodenal EC cells. This is supported by findings of higher FFAR3 transcript expression in the duodenum compared to colon of both humans and mice (Symonds et al., 2015). Indeed, gut microbes have been recently shown to signal directly to EC cells via metabolic SCFA cues and, likely, activation of FFAR2 and FFAR3, to augment 5-HT synthesis and increase colonic motility (Fukumoto et al., 2003, Yano et al.,

2015, Turnbaugh et al., 2006, Reigstad et al., 2015). SCFAs generated in this context may also play an underappreciated and important role in the development of obesity (Fukumoto et al., 2003, Yano et al., 2015, Turnbaugh et al., 2006). Finally, the LCFA receptor, FFAR4, which is highly expressed in the colon compared to duodenum in both mouse and human (Symonds et al., 2015), was highly enriched in colonic EC cells. This suggests that these cells are equipped to detect FFAR4 ligands, including omega-3 FFAs (Ichimura et al., 2014). Our results also add support to work demonstrating that expression of the dual medium to long chain FFA receptor, FFAR1, is higher in the duodenum than the colon of humans (Symonds et al., 2015).

Having established the nutrient sensing capacity of duodenal and colonic EC cells under healthy, lean conditions, this study investigated how this sensing capacity changes with HFD-induced obesity and metabolic disease. This is the first investigation to identify changes in the capacity of EC cells to detect nutrients at a single-cell level in a mouse model of obesity and metabolic disease, and contributes to understanding how altered EC cell signalling may respond to, or even drive obesity and metabolic disease progression.

The mouse model of diet-induced obesity established in this study exhibited hallmarks of T2D, including impaired glucose tolerance likely due to the observed decreased peripheral insulin sensitivity, and associated increased fasting blood glucose levels which positively correlated with body weight. Increased circulating 5-HT was also present in HFD-fed obese mice, supporting the observation that the primary 5-HT metabolite, 5-HIAA, is increased in urinary samples from humans with T2D (Takahashi et al., 2002).

Despite consuming equal total calories, mice fed a HFD gained significantly more weight due to the greater efficiency of fat intake to promote weight gain. The ratio of fat to carbohydrate was substantially altered in the HFD feed, with the dominant energy source being fat in the form of lard, containing large amounts of saturated, polyunsaturated and monounsaturated fatty acids. The ratio of polyunsaturated to saturated fat influences energy

utilisation, with a low ratio consistent with our HFD decreasing fat oxidation and increasing carbohydrate oxidation, despite others observing no change in energy expenditure (Jones and Schoeller, 1988). Of the dietary fat components, polyunsaturated fats such as linoleic acid are preferentially oxidised within the liver, while saturated fats such as palmitic acid are diverted to triacylglycerol synthesis and storage within adipocytes (Nestel and Steinberg, 1963). The substantially increased adiposity within HFD-fed mice is therefore likely due to increased consumption and storage of saturated fats within visceral and subcutaneous adipocytes. The absorption and storage of dietary fats may be further contributed to by increased circulating 5-HT, via increased intestinal bile acid turnover (Watanabe et al., 2010). Secretion of bile acids into the intestinal lumen contributes significantly to the digestion and uptake of lipids across the intestinal mucosa. Circulating 5-HT acts to increase bile acid turnover by upregulating bile acid transporters along the brush border membrane to increase bile acid reuptake from the intestinal lumen and enhance luminal fat absorption (Watanabe et al., 2010).

It is unknown if the increased circulating 5-HT observed in this study precedes the increased adiposity in diet-induced obese mice. However, other mouse models have demonstrated an increase in EC cell number at the onset of obesity, resulting from increased gastric leptin secretion (Le Beyec et al., 2014). Circulating leptin levels in the obese mouse model were not investigated in this study. Increased circulating leptin has been observed, however, in other models of diet-induced obese mice (Hoffler et al., 2009, Le Beyec et al., 2014), and has been demonstrated to influence feeding behaviour and satiety (Enriori et al., 2007). Total caloric intake was unchanged with HFD consumption, suggesting that the normal satiety signalling pathways exist in the obese mouse model used in this study. It is not known, however, if HFD-induced weight gain also results from reduced physical activity and, therefore, changes in energy expenditure, altered basal metabolic rate and thermogenic capacity. It is possible that increased adiposity is accompanied by alterations to these

parameters, as others have demonstrated in diet-induced obese mouse models (Kohsaka et al., 2007, Feldmann et al., 2009). Gut-derived 5-HT plays a key role in inhibiting BAT thermogenic capacity and the browning of WAT, as evidenced when inhibiting gut-derived 5-HT either genetically or pharmacologically (Crane et al., 2015). Whether this pathway contributes to the altered metabolism observed in mice within this study is unknown, however.

The primary aim of this model was to provide an obesogenic model to test whether the EC cell nutrient sensing capacity changes in a dynamic manner during obesity. The capacity for fructose transport, and sweet tastant and SCFA sensing by duodenal EC cells appears to be downregulated in mice with HFD-induced obesity, while colonic EC cells have an upregulated capacity to transport fructose, along with increased 5-HT biosynthesis.

The finding that the capacity for fructose transport via GLUT5 is differentially altered in duodenal and colonic EC cells from diet-induced obese mice suggests that EC cells are receptive to changes in dietary fructose. The reduction in GLUT5 expression in duodenal EC cells from HFD-fed mice is in line with downregulated GLUT5 expression in whole-tissue segments of jejunum from morbidly obese humans (Deal et al., 2016, Deal et al., 2017) and from the small intestine of streptozotocin-induced diabetic rats (Miyamoto et al., 1991). These findings suggest an overall reduction in fructose transport and absorption across the small intestine with obesity.

Colonic EC cells, on the other hand, demonstrated increased GLUT5 expression with obesity, suggesting an increased sensitivity to fructose in the colon; whether this is the case is investigated in *Chapter 3*. The presence of fructose within the intestinal lumen with consumption of HFD is likely to be derived from the hydrolysis of sucrose to monomers of glucose and fructose. As almost all fructose absorption occurs over the length of the small intestine, it is therefore unlikely that fructose will reach the colon under healthy GI conditions. As such, the increased GLUT5 expression in colonic EC cells from diet-induced obese mice

suggests changes to luminal and/or circulating fructose may occur, as the expression of GLUT5 is regulated by the availability of fructose (Corpe et al., 1998). Since the level of dietary fructose is unchanged between LFD and HFD, increased colonic EC cell GLUT5 expression may be an indication of altered GI function and small intestinal fructose absorption. It is unknown, however, whether changes in the sensitivity of EC cells to fructose conveys changes to EC cell 5-HT release.

Expression of the sweet taste receptor subunit, T1R3, is downregulated in duodenal EC cells from obese mice compared to lean controls, and is negatively correlated with fasting blood glucose levels. In obese human duodenal biopsies, expression of functional sweet taste receptors, comprising of T1R2 and T1R3, is also negatively correlated with fasting blood glucose levels (Young et al., 2009). A reduction in T1R3 expression may, therefore, convey reduced sensitivity of duodenal EC cells to sweet taste stimuli, such as sucrose and the D-glucose polymer, maltodextrin, which are components of the HFD. While the absence of T1R2 in mouse EC cells suggests that a T1R3 homodimer may exist as a low-efficiency sweet taste receptor (Kojima et al., 2015), it is unknown whether downregulation of T1R3 with HFD-induced obesity is associated with a compensatory increase in T1R2 expression. Furthermore, it is unknown whether changes in T1R3 expression correspond to altered 5-HT secretion.

A positive correlation exists between duodenal EC cell SGLT1 expression and mouse weight, suggesting a relationship between duodenal EC cell glucose uptake via SGLT1 and body weight. Others have found an upregulation of SGLT1 expression in proximal small intestinal biopsies from obese humans, compared to those who are lean (Nguyen et al., 2015), and in rats with long-term streptozotocin-induced diabetes (Miyamoto et al., 1991). Acute exposure to glucose consistent with high luminal concentrations triggers 5-HT release from colonic EC cells (Zelkas et al., 2015), but whether SGLT1 is responsible for this and whether the same response is seen for duodenal EC cells is unknown. As such, it is unknown to what

extent altered duodenal EC cell SGLT1 expression may have on 5-HT secretion, which could contribute to the overall weight gain with HFD.

The effect of HFD-induced obesity on EC cell nutrient sensing appears to be both pathway-specific and region-specific, as GLUT1 is unchanged in duodenal and colonic EC cells from obese mice. Expression of GLUT1 is enriched in colonic EC cells and is, however, positively correlated with mouse total body weight, suggesting a relationship between glucose transport via GLUT1 and weight. Whether glucose uptake via GLUT1 is the pathway responsible for the effects of acute glucose on colonic EC cells (Zelkas et al., 2015) is unknown. Although, GLUT1-mediated glucose uptake maintains basal cellular respiration, GLUT1 is also upregulated in tissues such as the blood brain barrier in response to low glucose (Kumagai et al., 1995), but is upregulated in jejunal enterocytes from diabetic rats (Boyer et al., 1996). Obese mice in the present study exhibit increased fasting blood glucose levels, with increased colonic GLUT1, indicative that defective glucose sensing pathways may exist in colonic EC cells. Why this is unique to colonic, and not duodenal EC cells, and what drives this differential relationship with weight is unknown.

Sensing of SCFA by duodenal EC cells via FFAR3 may be downregulated in diet-induced obese mice. With the majority of SCFA-producing bacteria residing in the colon, as elaborated on further in *Chapter 4*, the presence of SCFA in the small intestine is largely derived from fermentation by oral bacteria and from dietary sources (Hoverstad et al., 1984). Almost all dietary-derived SCFAs are absorbed in the small intestine, with very little reaching the colon. In rats, distinct regional differences in microbial communities exist between the small and large intestine, with the cecum having significantly higher abundance of Bacteroidetes and Tenericutes than the ileum, which has a significantly greater abundance of Firmicutes, Actinobacteria, Proteobacteria and Cyanobacteria. The microbial communities in these regions are also differentially affected by HFD (Hamilton et al., 2015). Decreased FFAR3 expression

in duodenal EC cells from HFD-induced obese mice highlights that, in response to changes in the luminal and circulating nutrients, EC cells can alter their capacity to detect SCFA. Downregulation of FFAR3 may convey reduced sensing for SCFA of longer carbon length, particular propionate and butyrate, as FFAR3 shows preferential affinity for propionate over butyrate and substantially lower preference for acetate (Offermanns, 2014). While possible diet-induced changes to microbial communities are unknown in the present study, this may contribute to regional changes in SCFA-sensing by EC cells. Whether isolated EC cells can indeed directly sense SCFA is investigated in *Chapter 3*.

Diet-induced obesity differentially effects 5-HT biosynthesis in a region-specific manner. That is, the capacity for duodenal EC cell 5-HT synthesis by TPH1 appears to be unaltered. Colonic EC cells, on the other hand, have upregulated expression of TPH1 with HFD, and therefore a greater capacity for 5-HT biosynthesis, compared to those from LFD-fed mice. While others find a decrease in colonic EC cell numbers in rats fed a Western diet, this is not reflected in expression levels of TPH1 in whole biopsies (Bertrand et al., 2012). The reason for these differences is unclear but may be a reflection of species differences. The increased expression of TPH1 in colonic EC cells may be responsible for the increased circulating 5-HT in HFD-fed mice. While duodenal EC cell TPH1 is not increased at a cellular level, others have demonstrated the number of EC cells to increase in the small intestine with obesity (Le Beyec et al., 2014). TPH1 mRNA expression is increased in whole-tissue small intestine biopsies from obese humans (Ritze et al., 2015), but since this current study in duodenum has found that EC cell TPH1 expression at a cellular level is unchanged, the increased TPH1 expression observed in whole human jejunum (Ritze et al., 2015) is likely due to increased EC cell numbers in the small intestine. Paired with increased 5-HT biosynthesis in the colon, a rise in EC cell numbers in the small intestine likely further contributes to the augmented circulating 5-HT in obesity and diabetes.

Transcriptional changes affecting colonic EC cell TPH1 expression in obese mice may be through microbial-produced SCFA, signalling to EC cells via FFAR3. In the intestine, FFAR2 and FFAR3 detect SCFA which are present at the highest concentrations within the colon, and are primarily derived from resident intestinal microbiota. Exposure of mice lacking a native microbiome to microbiota from donor mice increases the expression of TPH1 in intestinal mucosal segments (Yano et al., 2015). In addition, incubation of cell lines with microbial metabolites increased TPH1 expression and 5-HT release (Essien et al., 2013, Reigstad et al., 2015), with the microbial production of secondary bile salts also being a stimulant for EC cell 5-HT synthesis via TGR5 (Alemi et al., 2013). Alterations to dietary intake, such as with HFD consumption, induce a shift in the composition of commensal microbial populations (Turnbaugh et al., 2009, David et al., 2014, Hildebrandt et al., 2009). The microbial composition of HFD-fed mice was not analysed as part of this study. Microbial analysis of obese humans, however, demonstrates a diet-induced shift that is aligned with an increase in capacity for bacteria to harvest more energy per mass of food intake, whereby increasing the relative types and abundance of SCFA and secondary bile acids (Turnbaugh et al., 2006).

Functional implications of altered nutrient sensing by EC cells are broad and may have both acute influences within the GI tract, but also peripheral effects – particularly with respect to the effects of increased circulating 5-HT on metabolism. Changes to EC cell nutrient sensing may potentially alter signalling to enteric neurons, thereby modulating GI motility (Keating and Spencer, 2010). In addition, net fluid/electrolyte flux across the mucosa may be altered (Imada-Shirakata et al., 1997) and may underlie symptoms of GI dysfunction, such as vomiting, constipation, diarrhoea and faecal incontinence, all of which are associated with altered 5-HT signalling. Such symptoms are often reported by patients with diabetes and are associated with poor glycaemic control and diabetic complications (Bytzer et al., 2002). Increased circulating

5-HT levels, as a result of increased 5-HT biosynthesis, has the potential to chronically affect blood glucose control, as described previously in *Chapter 1*.

2.5 Conclusion

This study has demonstrated that subtypes of EC cells exist with respect to their size and nutrient sensing capacity, and that this is dictated by location within the GI tract. In addition, functionally defined subpopulations of EC cells also exist. Several studies have shown regional-dependent co-localisation of 5-HT with other enteroendocrine hormones, particularly substance P, secretin and CCK (Roth and Gordon, 1990, Reynaud et al., 2016, Cho et al., 2014, Fothergill et al., 2017a). Whether these subpopulations play specific physiological roles within the GI tract is unknown. Within the duodenal and colonic EC cell populations examined, functional subpopulations may also have unique nutrient sensing capacities, however this has not been resolved using the preparations in this study. Duodenal and colonic EC cells have the capacity to detect a number of dietary nutrients that they may be exposed to within the gut lumen. In particular, they contain a number of hexose transporters and free fatty acid sensing receptors. Whether these nutrients trigger an increase in 5-HT secretion from EC cells is unknown.

Findings from this study also highlight that the capacity of duodenal and colonic EC cells to transport luminal sugars, and detect sweet tastants and SCFAs is differentially altered by dietary changes, such as with HFD consumption. This is the first evidence that, at a cellular level, dietary changes influence EC cell nutrient sensing. Duodenal EC cells have reduced capacity to detect fructose and SCFA, which may convey reduced sensitivity to these stimuli in this region of the gut. On the other hand, colonic EC cells have an increased capacity to detect fructose, and a relationship may exist between colonic EC cell SCFA and glucose sensing and total body weight. One of the most significant findings from this study is that the

increased circulating 5-HT seen with obesity and T2D may be due to increased 5-HT synthesis in colonic, but not duodenal EC cells. Whether the transcriptional changes observed in HFD-fed obese mice relate to altered EC cell signalling, and the downstream effects on 5-HT signalling, requires further investigation. In addition, analysis of nutrient sensing changes in EC cells at a cellular level in obese humans is also warranted. This study has provided novel insight into the potential mechanisms by which HFD consumption can increase circulating 5-HT, which may contribute to the development of obesity and metabolic disease.

CHAPTER 3: Characterising the nutrient sensing capabilities of EC cells from the duodenum and colon of mice

3.1 Introduction

Details related to how EC cells respond to ingested nutrients are scarce. Given that the nutrient environment and expression of nutrient receptors and transporters by EC cells changes significantly along the length of the gut, as demonstrated in *Chapter 2*, whether EC responses to nutrients are dependent upon their GI location is unknown. The aim of the present study was to expand on work in *Chapter 2* to identify whether the capacity of EC cells to detect nutrients conveys an ability of nutrients to increase 5-HT release, and whether regional differences in nutrient-induced 5-HT secretion exist in mouse EC cells. In particular, this set of experiments uses mouse EC cells from duodenum and colon, which were shown in the previous chapter to have the capacity to detect nutrients, to demonstrate differential responses to nutrients depending on location. Using a combination of intracellular calcium measurements and 5-HT secretion, paired responses from mouse duodenal and colonic EC cells to selected sugars and free fatty acids were made.

The majority of work presented in this chapter is comprised of published work, from the following publication: Alyce M Martin *et al.* (2017), 'Regional differences in nutrient-induced secretion of gut serotonin, *Physiological Reports*, e13199. The relative author contributions to this work are as follows: AM Martin, AL Lumsden, CF Jessup and DJ Keating were involved in planning the experiments. AM Martin performed the experiments. AM Martin and DJ Keating analysed the data. CF Jessup, RL Young and NJ Spencer provided critical input and advice. AM Martin and DJ Keating wrote the paper and all authors were involved in drafting the manuscript. This work is supported by funding from the Australian Research Council and National Health and Medical Research Council (CI: DJ Keating). No competing interests are declared.

3.2 Methods

3.2.1 Primary mouse EC cell isolation

Animal studies were performed in accordance with the guidelines of the Animal Ethics Committee of Flinders University. Male, 8-16-week-old C57BL/6 mice fed a standard chow diet were euthanised by isoflurane overdose and cervical dislocation. Duodenum and colon were immediately removed and EC cells isolated and purified according to methods previously described (see *Chapter 2*) (Raghupathi et al., 2013, Zelkas et al., 2015, Martin et al., 2017).

3.2.2 Ca^{2+} flux by flow cytometry

Isolated EC cells were centrifuged at 500 × *g* for 4 mins, then resuspended in 1 mL of Hank's Balanced Salt Solution (HBSS, Sigma) supplemented with 1 mM Ca^{2+} and 20 mM HEPES. EC cells were incubated at 37°C for 35 min in the presence of the Ca^{2+} indicators, Fluo-3 and Fura Red, washed once with HBSS, centrifuged at 450 × *g* for 4 min, then resuspended in HBSS at a final volume of 150 µL per FACS tube, with 1.0 to 3.0×10^5 cells per tube. Intracellular Ca^{2+} ($Ca^{2+}_{(i)}$) flux determined using BD FACSCanto II (BD Biosciences). Following a 10 sec baseline recording, a stimulation solution containing 100-500 mM of one of the hexoses: glucose, fructose, sucrose, α-methyl glucoside (α-MG), or 1-100 mM of the SCFA: acetate, butyrate or propionate, was added and recording continued for a further 150 sec, by which time all cells were collected. The concentrations of hexoses were chosen based on luminal glucose concentrations within the GI tract having been proposed to reach 300 mM at the brush-border membrane (BBM) following a meal (Pappenheimer, 1993), while the sucrose concentration of a standard sugar-sweetened beverage can exceed 600 mM (Varsamis et al., 2017). In colon preparations, however, the concentration of the different sugar stimulants did not exceed 300 mM, as concentrations higher than this significantly altered cell morphology, as a substantial shift in the size and granularity of EC cell populations was observed with flow cytometry. SCFA concentrations were based on the concentrations reported

in the lumen of the colon under healthy conditions (Yajima and Sakata, 1992, Alex et al., 2013, Cummings et al., 1987, Topping and Clifton, 2001). The Ca^{2+}-ATPase blocker, thapsigargin (TG) was used as a positive control to test the ability of cells to respond and to test for adequate Ca^{2+} indicator loading. In doing this, subpopulations of EC cells were further observed, as the larger cells noted in duodenal isolations constituting approximately 30% of total cells, showed full Ca2+ flux prior to flow cytometry interrogation (Appendix Figure 6.3). As such, they were not responsive to stimulation with TG, and were excluded from further analysis. Data was expressed as the relative change in the ratio of Fluo-3/Fura Red over time using FlowJo V10 (LLC, USA) for analyses. Changes in Fluo-3/Fura Red were compared to the baseline time period for each recording and compared to responses in unstimulated conditions (control). Baseline-subtracted net area under the curve (AUC) was quantified using GraphPad PRISM 5.04 software.

3.2.3 5-HT secretion by ELISA

Isolated EC cells were suspended in pre-warmed Krebs solution containing 5-HT stabiliser buffer (Labor Diagnosticka Nord) and 1 μM fluoxetine, to block potential 5-HT reuptake via SERT, and added to a 96-well plate at a density of 1.5 to 2×10^4 cells in 120 μl per well. Cells were incubated to adhere and equilibrate for 30 min at 37°C, 5% CO_2. From each well, half the volume was collected (representing 0 mins) and replaced with an equal volume of stimulation solution at two times concentration to achieve the desired assay concentration. Influence of osmotic pressures on 5-HT release was assessed by using equimolar concentrations of the non-metabolisable glucose analogue, alpha-methylglucoside (α-MG) (see Appendix Table 7.5 for calculated osmotic pressures). To determine the minimum incubation time for detectable changes in 5-HT concentration using 5-HT ELISA, a time course was determined with exposure to glucose, sampling at 2, 5, 10, 20 and 120 min intervals. Since 20 mins was the minimum incubation time for detectable changes in 5-HT secretion by ELISA (Appendix

Figure 6.4), this timeframe was used as the bases for all hexose-stimulation experiments. Since the potential pathways for SCFA-sensing are via G-protein coupled receptors and second messenger signalling, and effects were not seen rapidly within 20 mins, incubation of EC cells with SCFA was performed for 2 hrs. Following incubation with the respective hexoses and SCFA stimuli, 40 µl of solution was collected from each well, placed on ice and immediately stored at -20°C until further analysis. 5-HT content of each sample was measured using a 5-HT ELISA kit (BA E-5900, BioStrategy) according to manufacturer's instructions. Preliminary experiments were performed to confirm that later addition of stimuli to supernatant does not alter ELISA results (data not shown). Data are expressed as net 5-HT secretion from 0 mins, normalised to cell number.

3.2.4 Intestinal motility

Mouse duodenal and colonic tissues were dissected and nutrient-evoked changes in motility were assessed using a distention-evoked peristalsis method as previously described (Spencer et al., 2011). Briefly, 6 cm of proximal small intestine (duodenum) and whole-colon, which had mesenteric fat was removed, were secured at each end to inlets of an organ bath containing pre-warmed oxygenated Krebs perfused at a constant temperature (36ºC) and rate of 1.5 mL/min. The lumen of duodenum and colon was also perfused with Krebs solutions at 36ºC with a flow rate of 0.24 µl/min. Distention-evoked peristaltic motility was achieved with 12 mm/H_2O backpressure. Preparations were equilibrated for 10 mins with luminal perfusion of control solution (Krebs containing 5 mM glucose), followed by a 10-minute baseline recording of motility patterns using Gastrointestinal Motility Monitor video recorder and software (Med Associates, USA). High glucose (300 mM and 500 mM) solutions were then luminally perfused and motility patterns recorded for a further 10 mins. To ensure results were not confounded by loss of tissue integrity, recordings did not exceed 30 mins. Analysis of motility patterns and generation of spatiotemporal diameter maps (D-Maps) were carried out

using MATLAB software (MathWorks, USA). Duodenal and colonic contractile events were excluded from analysis if reduction in diameter was less than 50%, and in the colon, were excluded if propagation was less than 50%.

3.3 Results

3.3.1 Response of EC cells to glucose

Intracellular calcium flux was monitored by flow cytometry as measure of cell activation in isolated EC cells. Cells were pre-loaded with the Ca^{2+} indicators Fluo-3 and Fura Red. These sensors increase and decrease fluorescence upon exposure to Ca^{2+}, respectively, allowing a ratiometric analysis to be performed (Dustin, 2000). The Fluo-3/Fura red ratio was used to represent a comparable unit of intracellular Ca^{2+} level ($Ca^{2+}_{(i)}$). The net AUC for the stimulation period was calculated by subtracting the mean baseline value for each respective recording, and represented a measure of total net Ca^{2+} flux within the stimulation time period. For unstimulated control cells (in 5 mM glucose) $Ca^{2+}_{(i)}$ and AUC was relatively unchanged across the 160-sec time period (Figure 3.3). Stimulation of duodenal EC cells with 100 mM glucose caused a sustained reduction in $Ca^{2+}_{(i)}$ compared to pre-stimulation baseline (Figure 3.1A), resulting in a negative total net flux compared to the unstimulated control (Figure 3.1B, AUC $p < 0.01$,). No change in $Ca^{2+}_{(i)}$ from baseline, or change in AUC compared to unstimulated (5 mM) control was observed in response to 300 mM glucose. However, 500 mM glucose increased $Ca^{2+}_{(i)}$ (Figure 3.1A,B, $p < 0.001$ *vs* control), exceeding that observed with positive stimulatory control, thapsigargin ($p < 0.05$ *vs* control).

In order to relate these findings to 5-HT secretion, 5-HT release was determined by ELISA. 5-HT release from duodenal EC cells increased 20 mins after exposure to 500 mM glucose (Figure 3.1C, 0.36 ± 0.09 nmol/10^4 cells), in comparison to 500 mM of the non-metabolisable

sugar, α-MG (0.01 ± 0.07 nmol/10^4 cells, $p < 0.01$) or 5 mM glucose exposure (control group, 0.04 ± 0.04 nmol/10^4 cells, $p < 0.01$). Neither 100 mM glucose (0.16 ± 0.03 nmol/10^4 cells) nor 300 mM glucose (0.17 ± 0.56 nmol/10^4 cells) elicited an increase in 5-HT from duodenal EC cells.

In colonic cells, exposure to 100 mM glucose had no effect on $Ca^{2+}_{(i)}$ levels. However, 300 mM glucose transiently raised $Ca^{2+}_{(i)}$ (Figure 3.1D) resulting in increased total net Ca^{2+} flux (Figure 3.1E, AUC $p < 0.01$ *vs* control). Release of 5-HT from colonic EC cells was increased when exposed to 300 mM glucose (0.46 ± 0.12 nmol/10^4 cells), in comparison to 100 mM glucose (0.11 ± 0.03 nmol/10^4 cells, $p < 0.01$), 300 mM α-MG (0.11 ± 0.05 nmol/10^4 cells, $p < 0.01$) or to the 5 mM glucose control (Figure 3.1F, 0.06 ± 0.05 nmol/10^4 cells, $p < 0.01$).

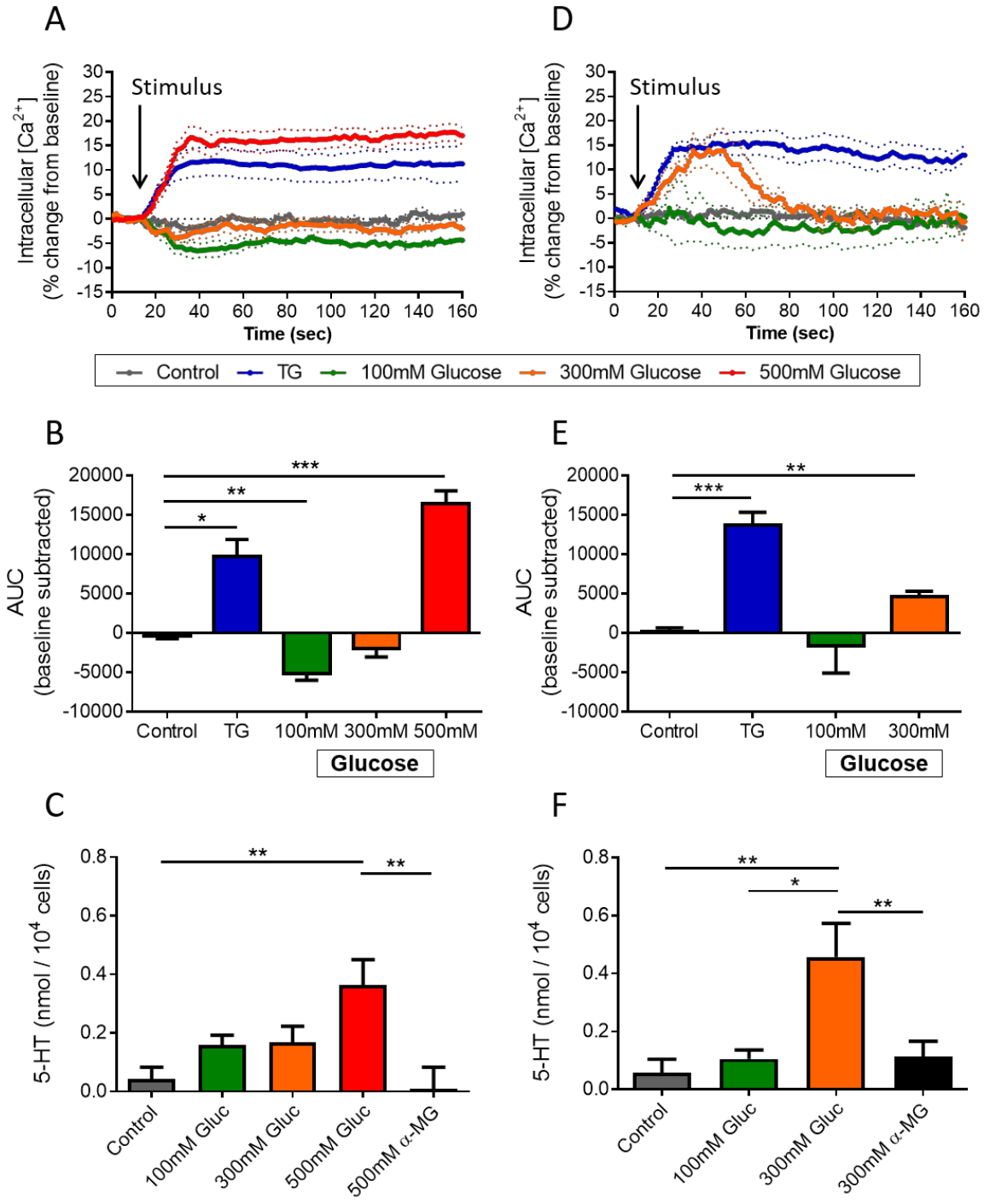
A
D
Stimulus
Intracellular [Ca2+] (% change from baseline)
Time (sec)
Control
TG
100mM Glucose
300mM Glucose
500mM Glucose
B
E
AUC (baseline subtracted)
Control
TG
100mM
300mM
500mM
Glucose
C
F
5-HT (nmol / 10^4 cells)
Control
100mM Gluc
300mM Gluc
500mM Gluc
500mM α-MG
300mM α-MG

Figure 3.1 - Effect of acute glucose stimulation on duodenal and colonic EC cells. (A) Time course of $Ca^{2+}_{(i)}$ changes in duodenal EC cells in response to glucose, shown as % change from baseline. Dotted lines indicate SEM. Arrow indicates time of stimulus addition (*n* = 3-8 mice). TG, Thapsigargin. (B) Area under the curve (AUC) of $Ca^{2+}_{(i)}$ in duodenal EC cells. (*n* = 3-8 mice, **p* < 0.05, ***p* < 0.01, ****p* < 0.001 *vs* control). (C) Release of 5-HT from duodenal EC cells in culture following 20 min exposure to glucose (Gluc) or α-MG. (*n* = 4-7 mice, ***p* < 0.01: 500 mM Gluc *vs* control and 500 mM α-MG). (D) Time course of $Ca^{2+}_{(i)}$ changes in colonic EC cells in response to glucose, shown as % change from baseline. Arrow indicates time of stimulus addition at 10 mins (*n* = 4-6 mice). (E) Area under the curve (AUC) of $Ca^{2+}_{(i)}$ in colonic EC cells. (*n* = 4-6 mice, ***p* < 0.01: 300 mM Gluc *vs* control, ****p* < 0.001: TG *vs* control). (F) Release of 5-HT from colonic EC cells in culture following 20 min exposure to glucose (Gluc) or α-MG. (*n* = 6-7 mice, **p* < 0.05: 100 mM Gluc *vs* 300 mM Gluc., ***p* < 0.01: 300 mM Gluc *vs* control and 300 mM α-MG). All data are shown as mean ± SEM.

3.3.2 Response of EC cells to fructose

Exposure of duodenal EC cells to 100 mM fructose did not change $Ca^{2+}_{(i)}$. However, dose-dependent increases in $Ca^{2+}_{(i)}$ were observed in response to 300 mM (AUC $p < 0.05$ *vs* control) and 500 mM fructose (AUC $p < 0.05$ *vs* control), with the latter response comparable to that seen with TG (Figure 3.2A,B, $p < 0.01$ *vs* control). Fructose exposure also increased 5-HT secretion from duodenal EC cells at both 300 mM (0.88 ± 0.12 nmol/10^4 cells, $p < 0.001$ *vs* control and α-MG) and 500 mM fructose (0.79 ± 0.18 nmol/10^4 cells, $p < 0.001$ *vs* control and α-MG). No change in 5-HT secretion was seen with α-MG exposure (Figure 3.2C).

The $Ca^{2+}_{(i)}$ response to fructose in colonic EC cells differed to that in duodenal EC cells (Figure 3.2D). Exposure to 100 mM fructose decreased $Ca^{2+}_{(i)}$ in colonic EC cells (AUC $p < 0.001$ *vs* control) but $Ca^{2+}_{(i)}$ did not change in the presence of 300 mM fructose (Figure 3.2E), as occurred in duodenal EC cells. 5-HT secretion, however, was triggered from colonic EC cells after 20 mins exposure to 300 mM fructose (0.34 ± 0.13 nmol/10^4 cells, $p < 0.01$ *vs* control, Figure 3.2F), while 5-HT release did not increase following exposure to 100 mM fructose (0.14 ± 0.09 nmol/10^4 cells).

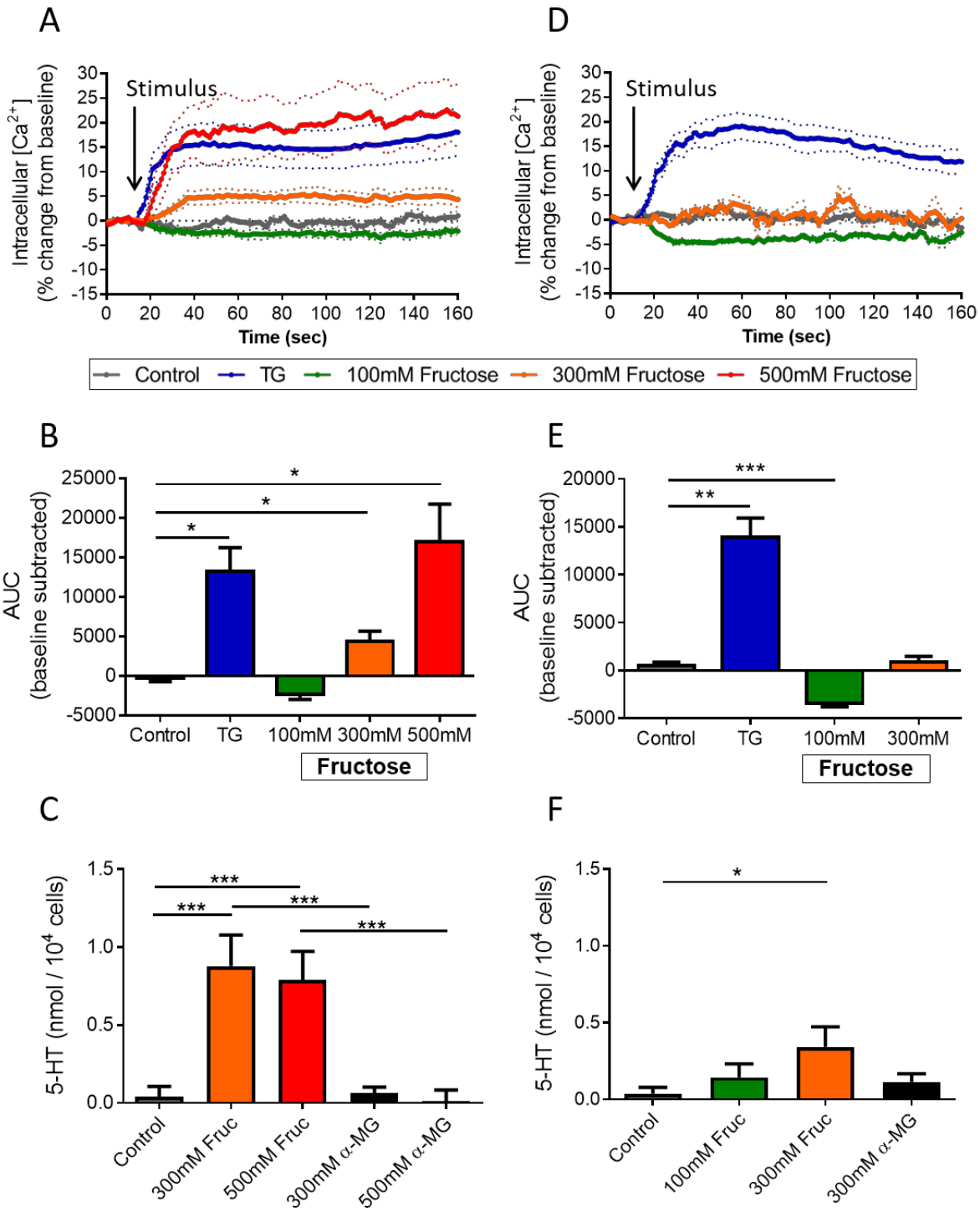
A
D
Intracellular [Ca2+] (% change from baseline)
Stimulus
Time (sec)
Control
TG
100mM Fructose
300mM Fructose
500mM Fructose
B
E
AUC (baseline subtracted)
Control
TG
100mM
300mM
500mM
Fructose
C
F
5-HT (nmol / 10^4 cells)
Control
300mM Fruc
500mM Fruc
300mM α-MG
500mM α-MG
100mM Fruc

Figure 3.2 - Effect of acute fructose stimulation on duodenal and colonic EC cells. (A) Time course of $Ca^{2+}_{(i)}$ changes in duodenal EC cells in response to fructose, shown as % change from baseline. Dotted lines indicate SEM. Arrow indicates time of stimulus addition (*n* = 3-9 mice). (B) Area under the curve (AUC) of $Ca^{2+}_{(i)}$ in duodenal EC cells. (*n* = 3-9 mice, **p* < 0.05). (C) Release of 5-HT from duodenal EC cells in culture following 20 min exposure to fructose (Fruc) or α-MG. (*n* = 4-9 mice, ****p* < 0.001). (D) Time course of $Ca^{2+}_{(i)}$ changes in colonic EC cells in response to fructose, shown as % change from baseline. Arrow indicates time of stimulus addition at 10 mins (*n* = 4-8 mice). (E) Area under the curve (AUC) of $Ca^{2+}_{(i)}$ in colonic EC cells. (*n* = 4-8 mice, ****p* < 0.001). (F) Release of 5-HT from colonic EC cells in culture following 20 min exposure to fructose (Fruc) or α-MG. (*n* = 3-9 mice, **p* < 0.05: 300 mM Fruc *vs* control). All data are shown as mean ± SEM.

3.3.3 Response of EC cells to sucrose

Exposure of duodenal EC cells to 300 mM sucrose induced a rapid and sustained increase in $Ca^{2+}_{(i)}$ (AUC $p < 0.01$ *vs* control), comparable with that seen with TG (Figure 3.3A,B, $p < 0.01$ *vs* control,). An increase in 5-HT secretion from duodenal EC cells was also seen with exposure to 300 mM sucrose (0.61 ± 0.18 nmol/10^4 cells, $p < 0.01$ *vs* control), which did not occur with exposure to 300 mM α-MG (Figure 3.3C, $p < 0.05$ *vs* 300mM sucrose,).

A decrease in $Ca^{2+}_{(i)}$ was observed in colonic EC cells in response to both 100 mM sucrose ($p < 0.01$ *vs* control) and 300 mM sucrose ($p < 0.001$ *vs* control) (Figure 3.3D,E). No increase in 5-HT secretion was observed at any of the sucrose concentrations (Figure 3.3F).

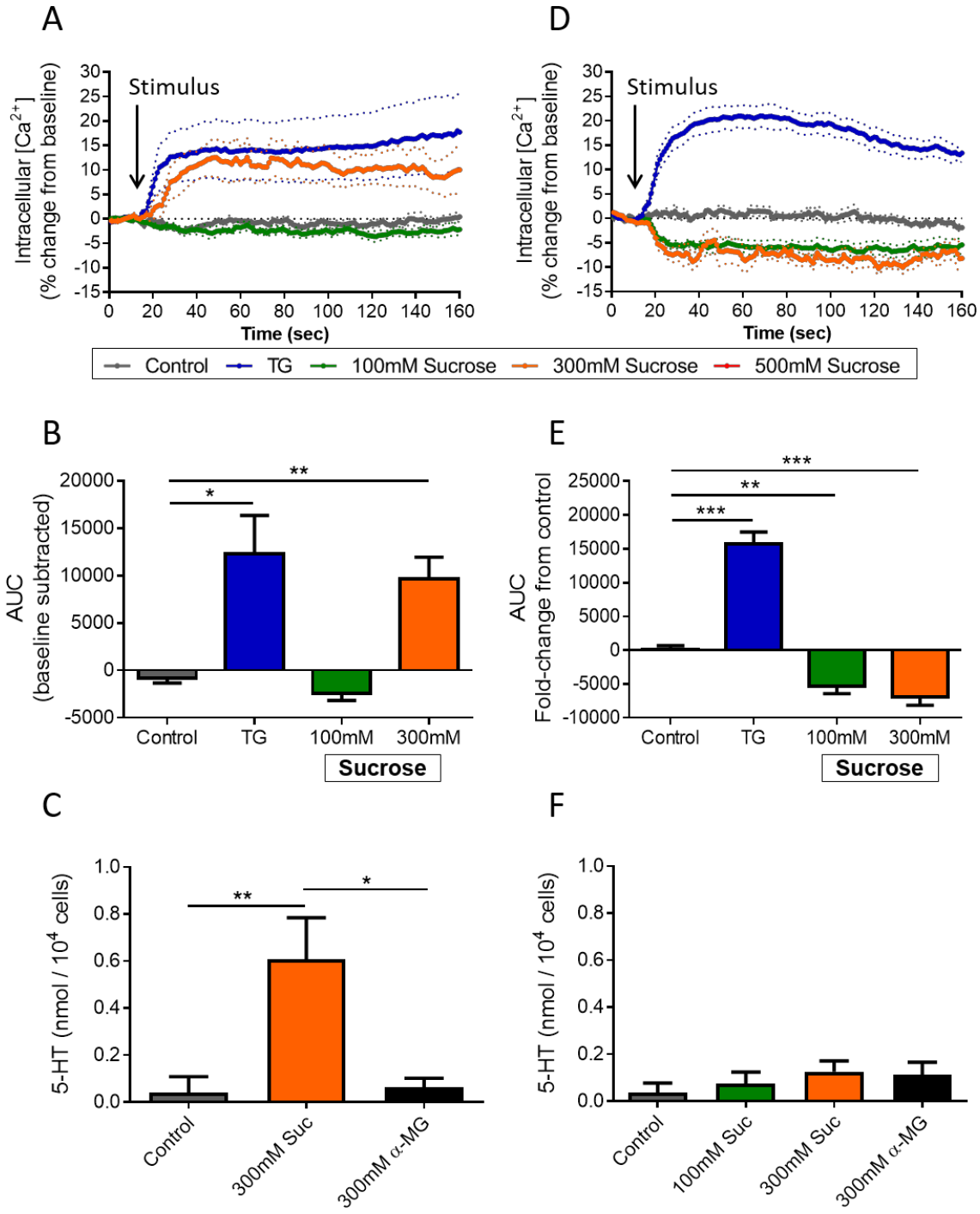
A
D
Stimulus
Intracellular [Ca2+] (% change from baseline)
Time (sec)
Control
TG
100mM Sucrose
300mM Sucrose
500mM Sucrose
B
E
AUC (baseline subtracted)
Fold-change from control
Control
TG
100mM
300mM
Sucrose
C
F
5-HT (nmol / 10^4 cells)
Control
300mM Suc
300mM α-MG
100mM Suc

Figure 3.3 - Effect of acute sucrose stimulation on duodenal and colonic EC cells. (A) Time course of $Ca^{2+}_{(i)}$ changes in duodenal EC cells in response to sucrose, shown as % change from baseline. Dotted lines indicate SEM. Arrow indicates time of stimulus addition (n = 4-5 mice). (B) Area under the curve (AUC) of $Ca^{2+}_{(i)}$ in duodenal EC cells. (n = 4-5 mice, $*p < 0.05$, $**p < 0.01$). (C) Release of 5-HT from duodenal EC cells in culture following 20 min exposure to sucrose (Suc) or α-MG. (n = 6-11 mice, $*p < 0.05$, $**p < 0.01$). (D) Time course of $Ca^{2+}_{(i)}$ changes in colonic EC cells in response to sucrose, shown as % change from baseline. Arrow indicates time of stimulus addition at 10 mins (n = 5 mice). (E) Area under the curve (AUC) of $Ca^{2+}_{(i)}$ in colonic EC cells. (n = 5 mice, $**p < 0.01$, $***p < 0.001$). (F) Release of 5-HT from colonic EC cells in culture following 20 min exposure to sucrose (Suc) or α-MG (n = 3-9 mice). All data are shown as mean ± SEM.

3.3.4 Response of EC cells to SCFA

EC cells were tested for responses to the short chain fatty acids acetate, butyrate and propionate. Duodenal EC cells did not alter $Ca^{2+}_{(i)}$ or cause secretion of 5-HT in response to a range of acetate concentrations from 1 to 100 mM (Figure 3.4A-C). $Ca^{2+}_{(i)}$ was reduced in colonic EC cells in response to 1 mM ($p < 0.05$ *vs* control) and 100 mM acetate (Figure 3.4D,E, $p < 0.05$ *vs* control), however this was not associated with any changes in 5-HT secretion (Figure 3.4F).

Exposure to increasing concentrations of butyrate from 1-30 mM did not alter $Ca^{2+}_{(i)}$ or release 5-HT from duodenal EC cells (Figure 3.5A-C). In colonic EC cells, however, $Ca^{2+}_{(i)}$ was reduced after exposure to both 15 mM (Figure 3.5D, $p < 0.05$ *vs* control,) and 30 mM butyrate (Figure 3.7E, $p < 0.05$ *vs* control). No change in 5-HT secretion was observed after 2 hrs incubation with butyrate (Figure 3.5F).

Duodenal EC cells did not change $Ca^{2+}_{(i)}$ or secrete 5-HT in response to increasing concentrations of propionate from 1-30 mM (Figure 3.6A-C). Colonic EC cells were unresponsive to 1 mM propionate, however $Ca^{2+}_{(i)}$ decreased upon exposure to 15 mM ($p < 0.05$ *vs* control) and 30 mM propionate (Figure 3.6D,E, $p < 0.05$ *vs* control,). This was not associated with any change in 5-HT secretion after 2 hrs exposure to propionate (Figure 3.6F).

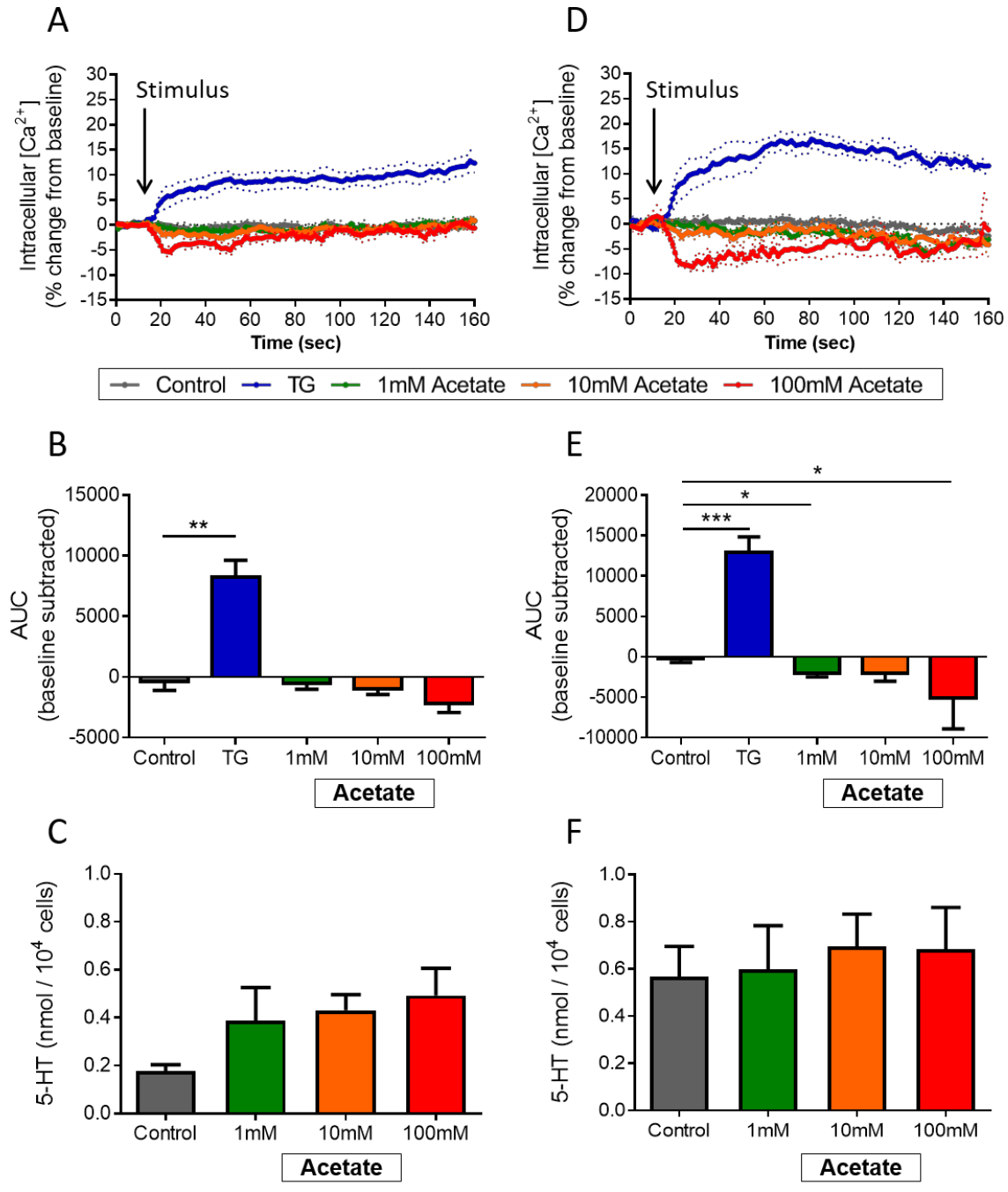
A
D
Stimulus
Intracellular [Ca2+] (% change from baseline)
Time (sec)
Control
TG
1mM Acetate
10mM Acetate
100mM Acetate
B
E
AUC (baseline subtracted)
**
*
***
Control
TG
1mM
10mM
100mM
Acetate
C
F
5-HT (nmol / 10^4 cells)
Control
1mM
10mM
100mM
Acetate

Figure 3.4 - Effect of acetate stimulation on duodenal and colonic EC cells. (A) Time course of $Ca^{2+}_{(i)}$ changes in duodenal EC cells in response to acetate, shown as % change from baseline. Dotted lines indicate SEM. Arrow indicates time of stimulus addition (n = 4-5 mice). (B) Area under the curve (AUC) of $Ca^{2+}_{(i)}$ in duodenal EC cells. (n = 5 mice, $^{**}p < 0.01$). (C) Release of 5-HT from duodenal EC cells in culture following 2 hr exposure to acetate (Acet) or α-MG. (n = 5-6 mice). (D) Time course of $Ca^{2+}_{(i)}$ changes in colonic EC cells in response to sucrose, shown as % change from baseline. Arrow indicates time of stimulus addition at 10 mins (n = 4-7 mice). (E) Area under the curve (AUC) of $Ca^{2+}_{(i)}$ in colonic EC cells. (n = 4-7 mice, $^{*}p < 0.05$, $^{***}p < 0.001$). (F) Release of 5-HT from colonic EC cells in culture following 2 hr exposure to acetate (n = 5-8 mice). All data are shown as mean ± SEM.

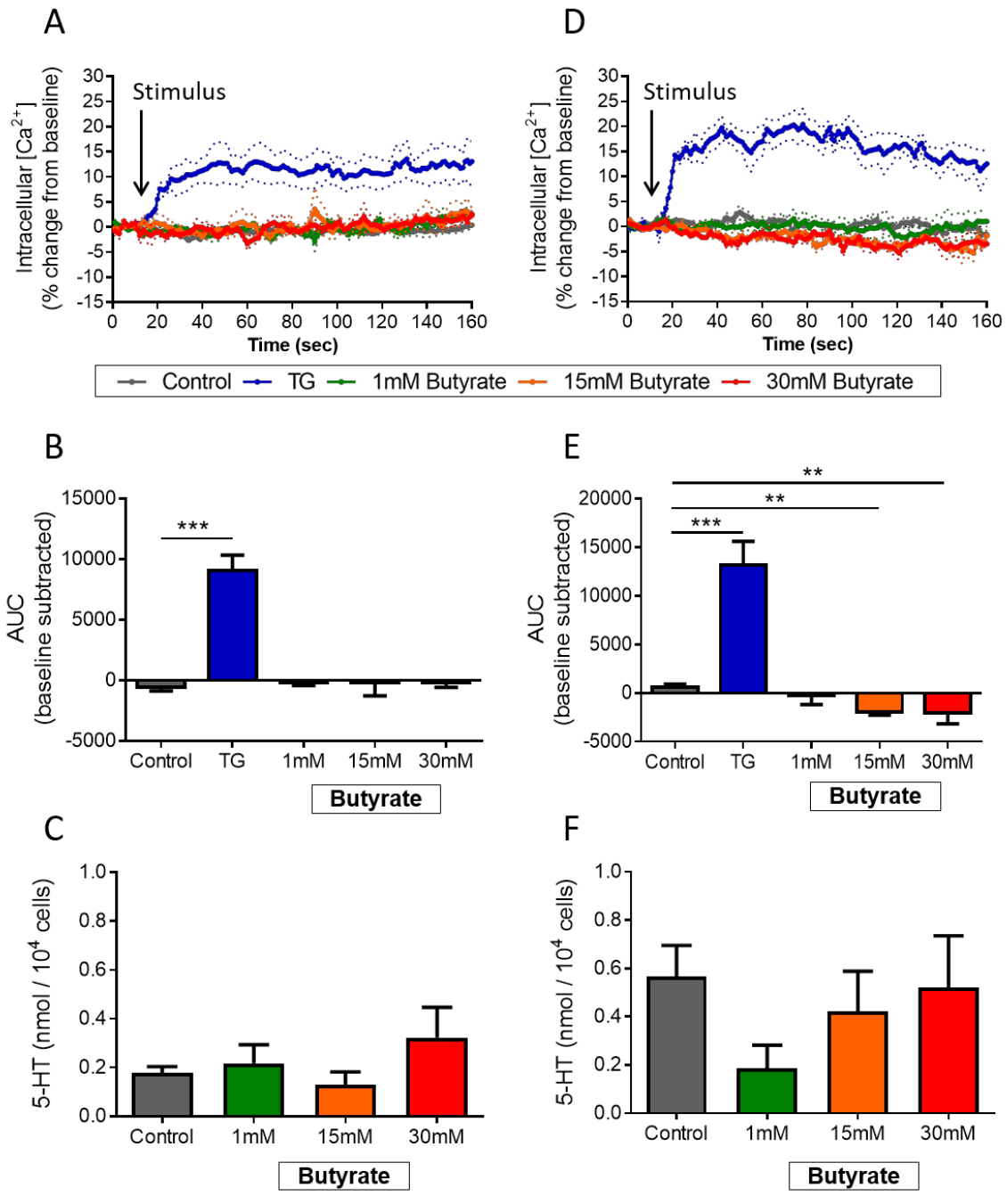
A
D
Stimulus
Intracellular [Ca2+] (% change from baseline)
Time (sec)
Control
TG
1mM Butyrate
15mM Butyrate
30mM Butyrate
B
E
AUC (baseline subtracted)
***
**
Control
TG
1mM
15mM
30mM
Butyrate
C
F
5-HT (nmol / 10^4 cells)
Control
1mM
15mM
30mM
Butyrate

Figure 3.5 - Effect of butyrate stimulation on duodenal and colonic EC cells. (A) Time course of $Ca^{2+}_{(i)}$ changes in duodenal EC cells in response to butyrate, shown as % change from baseline. Dotted lines indicate SEM. Arrow indicates time of stimulus addition (*n* = 4-5 mice). (B) Area under the curve (AUC) of $Ca^{2+}_{(i)}$ in duodenal EC cells. (*n* = 4-5 mice, ***$p < 0.001$). (C) Release of 5-HT from duodenal EC cells in culture following 2 hr exposure to butyrate (But) or α-MG (*n* = 5 mice). (D) Time course of $Ca^{2+}_{(i)}$ changes in colonic EC cells in response to butyrate, shown as % change from baseline. Arrow indicates time of stimulus addition at 10 mins (*n* = 3-4 mice). (E) Area under the curve (AUC) of $Ca^{2+}_{(i)}$ in colonic EC cells. (*n* = 3-4 mice, **$p < 0.01$). (F) Release of 5-HT from colonic EC cells in culture following 2 hr exposure to butyrate. (*n* = 5-7 mice). All data are shown as mean ± SEM.

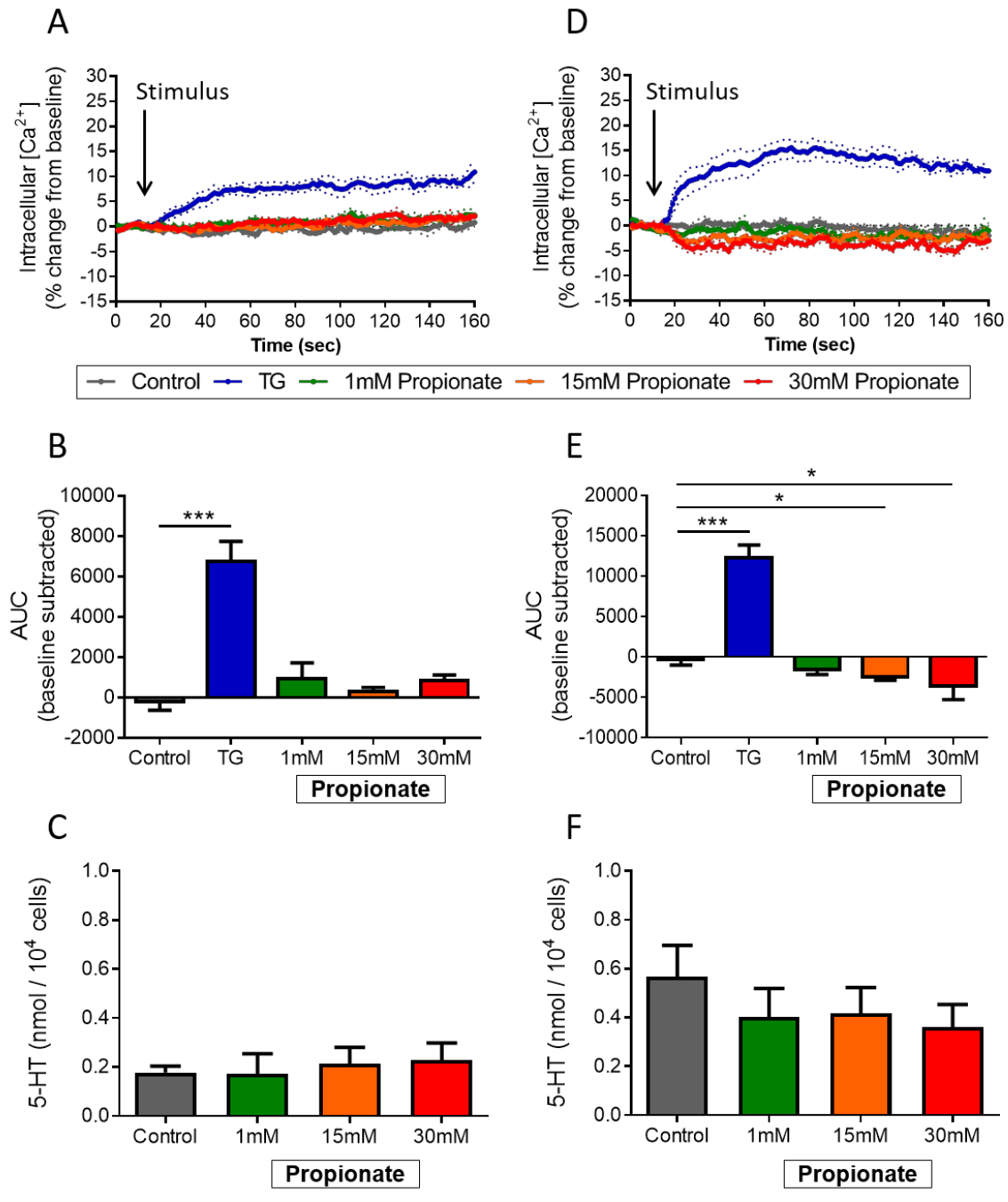
A
D
Stimulus
Intracellular [Ca2+] (% change from baseline)
Time (sec)
Control
TG
1mM Propionate
15mM Propionate
30mM Propionate
B
E
AUC (baseline subtracted)
***
*
Control
TG
1mM
15mM
30mM
Propionate
C
F
5-HT (nmol / 10^4 cells)
Control
1mM
15mM
30mM
Propionate

Figure 3.6 - Effect of propionate stimulation on duodenal and colonic EC cells. (A) Time course of $Ca^{2+}_{(i)}$ changes in duodenal EC cells in response to propionate, shown as % change from baseline. Dotted lines indicate SEM. Arrow indicates time of stimulus addition (n = 4 mice). (B) Area under the curve (AUC) of $Ca^{2+}_{(i)}$ in duodenal EC cells. (n = 4 mice, *p < 0.05, ***p < 0.001). (C) Release of 5-HT from duodenal EC cells in culture following 2 hr exposure to propionate (Prop) or α-MG (n = 5 mice). (D) Time course of $Ca^{2+}_{(i)}$ changes in colonic EC cells in response to propionate, shown as % change from baseline. Arrow indicates time of stimulus addition at 10 mins (n = 5 mice). (E) Area under the curve (AUC) of $Ca^{2+}_{(i)}$ in colonic EC cells. (n = 5 mice, *p < 0.05, ***p < 0.001). (F) Release of 5-HT from colonic EC cells in culture following 2 hr exposure to propionate (n = 5-6 mice). All data are shown as mean ± SEM.

3.3.5 Intestinal motility

To determine whether glucose-induced 5-HT secretion alters intestinal motility, duodenal and colonic motility was examined *ex vivo* in response to glucose concentrations which showed to increase 5-HT release in culture. Duodenal motility patterns consisted of intermittent clusters of contractions (Figure 3.7A), which were inhibited following infusion of 500 mM glucose (Figure 3.7B-C, 0.04 ± 0.04 contractions per minute) compared to 5 mM glucose (0.92 ± 0.1 contractions per minute, $p < 0.001$). Luminal perfusion of 300 mM glucose did not elicit any change in the frequency of contractions (0.67 ± 0.24 contractions per minute).

In *ex vivo* colonic preparations, propagating contractions observed with 5mM glucose (Figure 3.8A,C, 0.66 ± 0.07 contractions per minute) were inhibited following luminal perfusion with 500mM glucose (Figure 3.8B,C, 0.133 ± 0.133 contractions per minute, $p < 0.05$), but not 300 mM glucose (0.5 ± 0.15 contractions per minute).

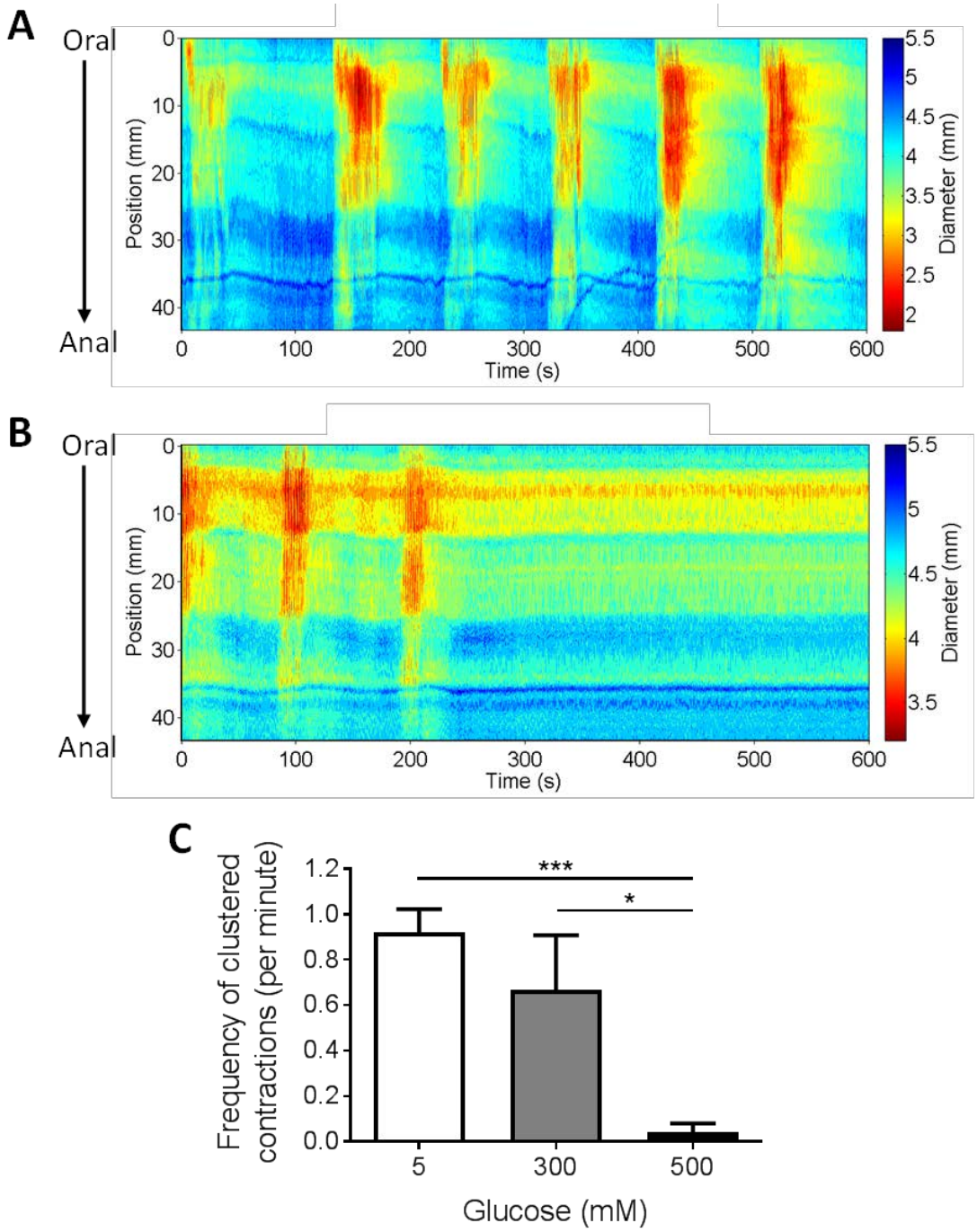

Figure 3.7 – High luminal glucose inhibits mouse duodenal motility *ex vivo*. (A) Diameter map (D-Map) of clustered contractions over time in duodenum with luminal perfusion of 5 mM glucose. (B) D-map of duodenal contractions over time with luminal infusion of 500 mM glucose. (C) Frequency of duodenal clustered contractions is decreased with 500 mM glucose. (n = 3-5 mice, * $p < 0.05$, **** $p < 0.0001$). Data are shown as mean ± SEM.

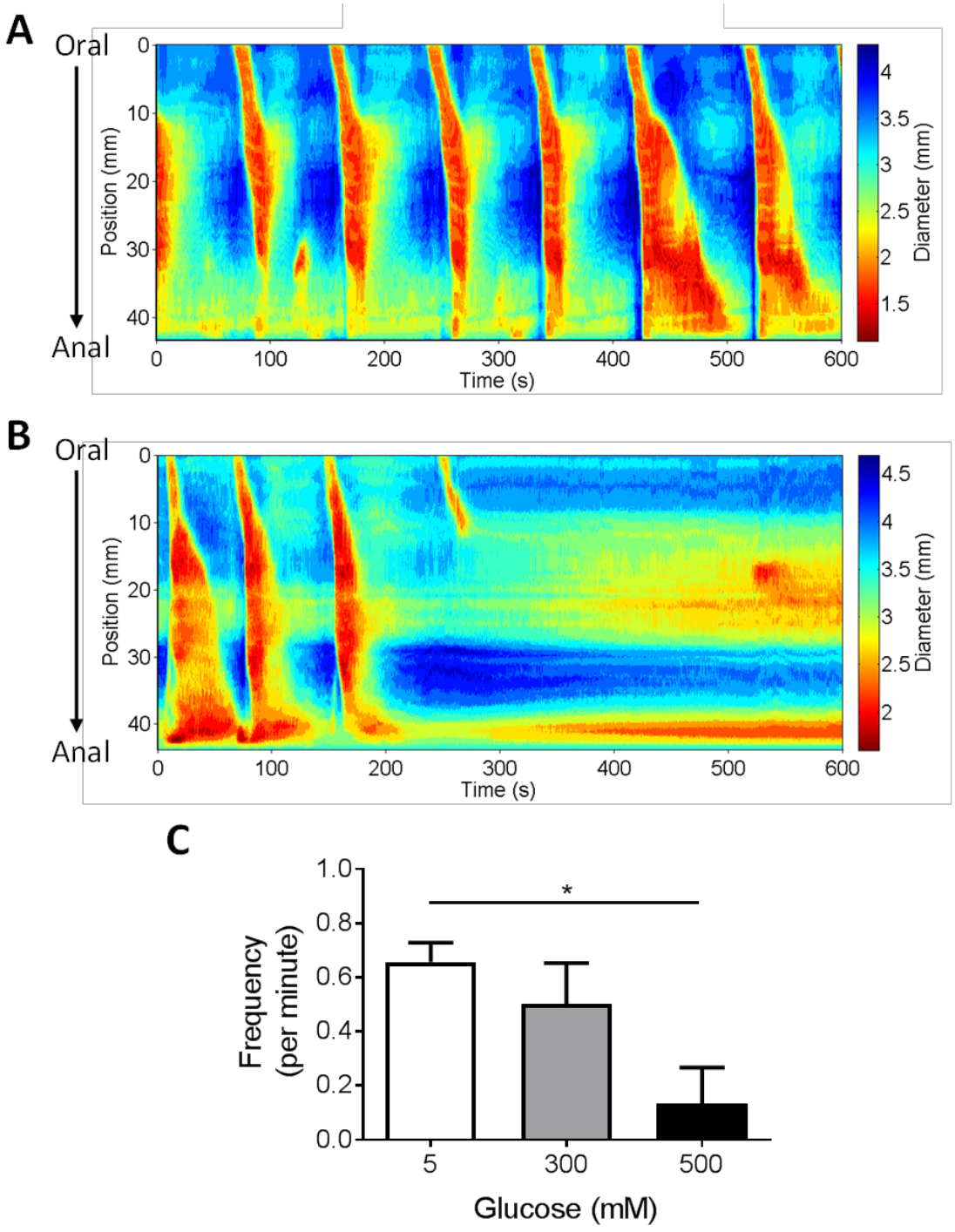

Figure 3.8 – High luminal glucose inhibits colonic motility *ex vivo*. (A) D-Map of colonic contractions over time with luminal perfusion of 5 mM glucose. (B) D-map of colonic contractions over time with luminal infusion of 500 mM glucose. (C) Frequency of propulsive colonic contractions is decreased with 500 mM glucose. (n = 3-7 mice, * $p < 0.05$). Data are shown as mean ± SEM.

3.4 Discussion

This study compared differences in nutrient sensing capacity in primary mouse EC cells obtained from duodenum and colon of the same animal. This provides a powerful approach allowing for a paired comparison of nutrient responses in EC cells obtained from different regions of the GI tract. A major finding is the demonstration of region-specific responses of duodenal and colonic EC cells to sugars, as evidenced by differential increases and decreases in $Ca^{2+}_{(i)}$ and 5-HT release. In particular, colonic EC cells showed higher sensitivity to glucose, while duodenal EC cells were more sensitive to fructose and sucrose. While sugars were found to elicit secretion of gut 5-HT, acute exposure to SCFAs did not. Importantly, this 5-HT secretion was nutrient-dependent and did not occur secondary to osmotic influences, as the non-metabolisable glucose analogue, α-MG, did not increase 5-HT secretion in either duodenal or colonic EC cells at effective sugar doses to 500 mM. This provides support for a receptor- or transporter-mediated response underlying nutrient-induced 5-HT secretion. In addition to directly increasing EC cell 5-HT release, exposure to high luminal glucose inhibited both duodenal and colonic motility patterns *ex vivo*, however it is unknown if this is directly due to EC cell 5-HT release and activation of neuronal 5-HT receptors.

These data demonstrate that mouse EC cells respond to levels that would occur within the GI tract following nutrient ingestion. The discrepancy in 5-HT release in response to 100 mM glucose between this study and previous work (Zelkas et al., 2015) is likely due to the sensitivity of techniques used to detect 5-HT release, as previous work used the highly sensitive technique of amperometry to detect single-vesicle release events. As such, any potential increases in 5-HT release with 100 mM glucose seen by others may be below detection threshold for the techniques used in this study. While the concentration of sugars used to stimulate cells in this study appear high, luminal glucose concentrations within the GI tract have been proposed to reach 300 mM at the brush-border membrane (BBM) following a meal

(Pappenheimer, 1993), and active transport accounts for around 77% of absorption of a 400 mM glucose solution (Uhing and Kimura, 1995), while the sucrose concentration of a standard sugar-sweetened beverage can exceed 600 mM (Varsamis et al., 2017). The fact that this study finds duodenal EC cells are less sensitive to glucose than the colon, with 5-HT secretion occurring in response to 500 mM, but not 300 mM glucose, is likely a reflection of duodenal EC cells being exposed to the high concentrations of glucose following a meal.

The decrease in intracellular Ca^{2+} levels observed following stimulus exposure in some preparations, predominantly in response to lower stimulant concentrations, was unexpected and cannot be explained with the current methodology. Removal of Ca^{2+} from the cytoplasm may be due to the re-sequestering of Ca^{2+} to endoplasmic stores, or to the movement of Ca^{2+} from the cells due to changes in membrane permeability, Ca^{2+} transporters or ion channels. It is plausible that this is an effort to maintain Ca^{2+} homeostasis through clearance of intracellular Ca^{2+}, a mechanism shown to terminate a stimulus response in isolated mouse taste receptor cells through Na^{+}- Ca^{2+} exchange (Szebenyi et al., 2010). As the current methodology for Ca^{2+} flux analysis by flow cytometry does not allow for cell recovery and Ca^{2+} level observation following stimulus-removal, there is a possibility that the continuous Ca^{2+} signal seen in duodenal EC cells with 500 mM glucose and fructose may induce a cell apoptosis or cell death pathway (Pinton et al., 2008). However, the Ca^{2+} levels observed with this concentration of glucose and fructose are consistent with that seen for the positive control, thapsigargin, which is a strong and continuous stimulus for intracellular Ca^{2+} and acts via blocking Ca^{2+} uptake into the endoplasmic reticulum stores. As such, continuous Ca^{2+} seen with 500 mM glucose and fructose may also be a reflection of the strength of this stimulus for intracellular Ca^{2+}-driven 5-HT release, rather than induction of a terminal cell state. This is supported by significant increases in 5-HT secretion with this concentration of glucose and fructose.

This study found that duodenal EC cells were more responsive to fructose than colonic EC cells. Fructose triggered Ca^{2+} entry and 5-HT release in duodenal cells at 300 and 500 mM. Despite equivalent 5-HT secretion, intracellular Ca^{2+} influx in response to 300 mM fructose stimulation was, however, significantly lower compared to 500 mM fructose stimulation. The lower Ca^{2+} influx but equal 5-HT secretion at 300 mM compared to 500 mM fructose may be due to the level of Ca^{2+} needed for peak 5-HT secretion occurring at 300 mM, with increased Ca^{2+} above this level causing no further increase in 5-HT secretion. However, while 300 mM fructose triggered a small increase in 5-HT release in colonic EC cells, it did so in the absence of an increase in cellular Ca^{2+} levels. It is possible that this difference is a result of the different duration of experiments used to measure intracellular calcium and 5-HT secretion, and that significant amounts of Ca^{2+} may enter the cell in response to fructose over 20 min. Such a long duration was not possible to measure with the Ca^{2+} imaging approach used in this study. Exposure to fructose for 20 min in culture could also have permitted translocation of GLUT2/GLUT5 transporters to the plasma membrane (Mace et al., 2007) to increase 5-HT release in colonic EC cells, a process unlikely to be evident during the Ca^{2+} measurement time frame. Alternatively, fructose may trigger 5-HT release from colonic EC cells via Ca^{2+}-independent mechanisms, such as an increase in cyclic AMP (cAMP), which acts directly to increase the sensitivity of exocytotic machinery to Ca^{2+}. As a result, exocytosis is triggered in the absence of increased intracellular Ca^{2+}, as observed in pancreatic β-cells (Ammala et al., 1993). The greater sensitivity of duodenal EC cells to fructose stimulation may be underlined by the greater expression of the GLUT5 transporter found in duodenal EC cells, as demonstrated in *Chapter 2.*

High sucrose concentrations triggered 5-HT release from duodenal, but not colonic EC cells, similar to that seen following fructose stimulation of duodenal EC cells. Unlike exposure of colonic EC cells to 300 mM glucose, 300 mM sucrose did not trigger Ca^{2+} entry or 5-HT

release. Hexose sugars and sweeteners are detected by the sweet taste receptor family of proteins, which are comprised of T1R2 and T1R3 and form as either heterodimers or homodimers. While the T1R2/T1R3 receptor heterodimer is expressed in the duodenum of humans (Young et al., 2009), T1R2 has been immuno-localised to only a small subset of human duodenal EC cells (Young et al., 2013), and T1R2 gene expression has not been detected in EC cells, as shown in *Chapter 2*. The lack of T1R2 suggests that the ability of duodenal EC cells to detect sucrose may occur via a T1R3 receptor homodimer, which has been identified as a low affinity glucose sensor in pancreatic β-cells (Kojima et al., 2015). Another possible mechanism, which has not been tested in the current study, is the potential for enzymatic breakdown of sucrose by EC cell-derived sucrase, resulting in equal units of glucose and fructose, both of which increase duodenal EC cell 5-HT release.

Intraduodenal infusion of sugars slows gastric emptying and nutrient intake in rodents and humans (Rayner et al., 2000) and, in this study, high concentrations of luminal glucose inhibit duodenal motility patterns *ex vivo.* Such glucose-induced release of 5-HT also stimulates duodenal bicarbonate secretion (Tuo et al., 2004) and suppresses the uptake of sodium from the lumen, thus affecting luminal water and electrolyte absorption (Imada-Shirakata et al., 1997, Gill et al., 2005). Others have demonstrated that inhibition of gastric emptying occurs via an extrinsic nerve reflex, which is triggered, in part, by stimulation of 5-HT_3 receptors on vagal sensory neurons (Rayner et al., 2000, Raybould et al., 2003, Savastano et al., 2005). Release of 5-HT from duodenal EC cells in response to luminal sugars is therefore likely to be central to this pathway. Another possible mechanism for the glucose-associated inhibition of gut motility is that high glucose increased 5-HT release, which inhibits motility via saturation and, subsequently, internalisation of 5-HT_3 receptors. 5-HT_3 receptor desensitisation and internalisation is observed with the 5-HT_3 agonist, 3-methyl-5-HT, and is blocked by the 5-HT_3 antagonist, ondansetron (Freeman et al., 2006b). Whether 5-HT is acting directly to

inhibit motility following high luminal glucose could be evaluated using these pharmacological agents, in particular ondansetron to assess the role of 5-HT_3 receptors.

The ability of glucose to trigger colonic EC cell 5-HT release is surprising, as this region would have limited exposure to luminal glucose under situations of normal GI transit. However, in disease states such as short bowel syndrome (Mayeur et al., 2016) with reduced intestinal transit time or reduced glucose absorption across the small intestine, higher luminal concentrations of ingested sugars may occur in the colon. Indeed, luminal infusion of high glucose inhibited colonic motility, similar to what was observed in the duodenum following luminal glucose infusion. Whether this is directly due to increased 5-HT release remains to be seen, but may underlie a nutrient-induced halt to colonic motility similar to the "ileal brake" mechanism that exists following exposure to nutrients in the ileum, which allows for increased nutrient absorption (Spiller et al., 1988). Such a mechanism has been described as a 'colonic brake' in patients with short bowel syndrome (Nightingale et al., 1993). The increased sensitivity of colonic EC cells to glucose may also play a role in the side effects often observed in patients following Roux-en-Y gastric bypass surgery, including diarrhoea and nausea (Tack and Deloose, 2014), and the often-occurring complication of dumping syndrome (Tobe et al., 1967). These processes are also mediated by innervation of enteric nerve terminals that contain 5-HT receptors, within the intestinal mucosa. This is best demonstrated by the antiemetic and anti-diarrhoeal activity of 5-HT_3 antagonists such as ondansetron (Bunce and Tyers, 1992, Lin et al., 2012, Garsed et al., 2014).

The finding that SCFAs do not acutely stimulate EC cell 5-HT secretion is, perhaps, not surprising given the potential for SCFAs signal to these cells via FFAR2/3. As demonstrated in *Chapter* 2, EC cells express FFAR2 and FFAR3, both of which are G protein-coupled receptors and signal via second messenger pathways (Brown et al., 2003). FFAR2 is coupled to either G_q (Brown et al., 2003) to increase IP_3-mediated Ca^{2+} release from ER stores (Billups

et al., 2006), or to $G_{i/o}$ (Brown et al., 2003), which inhibits the adenylate cyclase pathway and has the potential to increase gene transcription via activation of PLC (Berger et al., 2015). FFAR3 is exclusively coupled to $G_{i/o}$ (Brown et al., 2003). This study found that exposure of EC cells to luminal concentrations of SCFAs to not increase intracellular calcium or 5-HT secretion in an acute setting. Others have found that chronic stimulation does not have a direct secretory effect on EC cells but, rather, results in SCFA-dependent increases in *Tph1* expression and 5-HT synthesis (Yano et al., 2015, Reigstad et al., 2015, Essien et al., 2013). Further investigation is required into the precise signalling pathways involved; however, these findings are strongly indicative that the mechanisms by which SCFA signal to EC cells to augment 5-HT release are likely to be via influencing 5-HT biosynthesis.

The approach used in this study demonstrates a direct influence of nutrients on EC cell 5-HT release, although the polarity of 5-HT secretion from EC cells in response to luminal cues has not been established. Cell polarity has been shown to play an important role in luminal nutrient sensing in L-cells, with sensing via the apical membrane required for glucose-induced GLP-1 secretion (Kuhre et al., 2015). In addition, nutrient sensing receptors and transporters exhibit localised expression on either brush-border or basolateral membranes (Mace et al., 2007). Possible differences in nutrient sensing between the apical and basolateral membrane of EC cells are not established using these single-cell preparations, in which the polarity of EC cells becomes lost. In addition, intercellular interactions within the native environment of the gut, which could potentially modulate the response to luminal nutrients, are also lost. How changes to cell polarity and environment affect the basic cellular responses of EC cells to nutrients in culture remains unknown. However, the findings in this study of glucose sensing by isolated colonic EC cells is consistent with previous work showing high luminal concentrations of glucose increases quantal 5-HT release from intact colonic tissue

preparations, in which cell-to-cell interactions and cell polarity are maintained (Zelkas et al., 2015).

3.5 Conclusion

This study provides the first comparative analysis of the capacity of EC cells from the mouse duodenum and colon to respond to rapid nutrient exposure. It is also the first to demonstrate the capacity for isolated primary EC cells from mice to respond to nutrients. This approach has revealed that duodenal EC cells are more responsive than colonic EC cells to fructose and sucrose, while the opposite is true for glucose responses. It has also revealed that SCFAs do not trigger acute Ca^{2+} entry or 5-HT secretion at either intestinal site. Correspondingly, the responsiveness of intestinal EC cells to ingested nutrients is likely to be diverse and region-dependent.

CHAPTER 4: Gut-derived 5-HT is a signalling nexus between the microbiome and host metabolism

4.1 Introduction

The role of the gut microbiome in the development and progression of obesity has attracted intense research interest. The established paradigm suggests that alteration to the composition of gut microbiota (Ridaura et al., 2013, Turnbaugh et al., 2006) and gut-derived 5-HT (Sumara et al., 2012, Crane et al., 2015) can independently affect whole-body metabolism. Intervention studies using germ-free (GF) mice or antibiotic-induced intestinal dysbiosis have demonstrated a causal role of the gut microbiome in the dysregulation of host metabolism (Turnbaugh et al., 2006, Backhed et al., 2004, Vrieze et al., 2012, Ridaura et al., 2013). In particular, colonisation of GF mice with microbiota from obese mice (Turnbaugh et al., 2006) and humans (Ridaura et al., 2013) conveys an obese metabolic phenotype, resulting in increased fat mass, insulin resistance and glucose intolerance, while gut microbiome ablation improves host insulin sensitivity and glucose tolerance, and reduces fat mass and obesity (Backhed et al., 2007, Carvalho et al., 2012). One mechanism underlying this involves increased thermogenic capacity in brown adipocytes, and the browning of white to "beige" adipocytes via increased expression of the key thermoregulatory genes, *Ucp1* and *Pgc1α* (Suarez-Zamorano et al., 2015).

A role for gut 5-HT in metabolism and glucose homeostasis is also evident, as previously described in *Chapter 1*. Notably, depletion of gut-derived 5-HT through genetic ablation or pharmacological inhibition of TPH1 in mice conveys protection against diet-induced obesity, in a manner similar to that seen in GF mice. Increased blood glucose levels are observed following intraperitoneal injection of 5-HT (Watanabe et al., 2010). Mechanisms by which 5-HT modulates blood glucose are through the activation of 5-HT receptors on hepatocytes to increase hepatic gluconeogenesis, while increasing circulating free fatty acids and glycerol via lipolysis within adipocytes (Sumara et al., 2012). Circulating 5-HT also suppresses thermogenic capacity, as evidenced by pharmacological inhibition of TPH1 resulting in

increased brown adipose thermogenesis and increased browning of white adipocytes (Crane et al., 2015).

Increased circulating 5-HT (both free and platelet-derived) and colonic EC cell 5-HT synthesis is observed with diet-induced obesity, as shown in *Chapter 2*. Both circulating and mucosal 5-HT are substantially reduced in GF and antibiotic-treated mice due to decreased EC cell numbers and reduced biosynthesis within EC cells (Yano et al., 2015), highlighting a dynamic relationship between the gut microbiome and EC cells. In particular, the resident gut microbiome signals to EC cells through a number of microbial metabolites including SCFA and secondary bile acids (Reigstad et al., 2015). This indicates a potential role for gut-derived 5-HT in acting as a signalling mediator between the gut microbiome and host metabolism.

The use of GF models has highlighted potential pathways by which the gut microbiome effects metabolism, however GF mice exhibit altered enteric neuronal activity (Neufeld et al., 2011) intestinal motility (Ge et al., 2017, Yano et al., 2015) and abnormal behavioural development (Diaz Heijtz et al., 2011, Luczynski et al., 2016). It is unknown to what extent this culmination of developmental differences alters whole-body metabolism. Depletion of the gut microbiome through the use of antibiotics allows for normal post-natal development, whereby the changes in metabolism with antibiotic treatment can be directly associated with the gut microbiome. Whole-body and gut-specific ablation of TPH1 by genetic knock-down in mice have established the role of peripheral 5-HT in metabolism. TPH1 is also expressed at low levels in a number of other tissues, including the metabolically active BAT (Crane et al., 2015), WAT (Sumara et al., 2012), pancreatic β-cells (Almaca et al., 2016) and bone (Yadav et al., 2008), and it is unknown to what extent 5-HT in these tissues contributes to metabolism. The TPH inhibitor, LP533401, has been used previously to dose-dependently reduce circulating 5-HT (Yadav et al., 2010). The poor bioavailability of LP533401 largely restricts the activity of the drug to the intestinal lumen, when delivered by oral gavage (Liu et al., 2008,

Shi et al., 2008), making it a useful tool for inhibiting 5-HT synthesis within EC cells. By pharmacologically targeting intestinal 5-HT biosynthesis, secondary effects associated with altered intestinal physiology and removing TPH1 activity in other tissues are avoided.

The gut microbiome and gut-derived 5-HT have been independently demonstrated to regulate metabolism, and a dynamic relationship exists whereby the gut microbiome can increase EC cell 5-HT synthesis. As such, the broad aim of this study was to determine whether the gut microbiome affects host metabolism through a gut 5-HT-dependent pathway. Specifically, this study aimed to:

1. Use a combination of antibiotics to induce intestinal dysbiosis and verify the metabolic outcomes and changes in gut-derived 5-HT seen in other models.
2. Use a combination of antibiotic-induced dysbiosis and pharmacological inhibition of gut-derived 5-HT to determine whether the microbiome alters host metabolism via a 5-HT pathway within the GI tract.

4.2 Methods

4.2.1 Animal housing and experimental rationale

4.2.1.1 Animal housing

All experiments were approved by the SAHMRI Animal Ethics Committee (SAM163 and SAM218) and conducted under the NHMRC guidelines for animal research. Male C57/BL6 mice were housed in SAHMRI Bioresources under specific pathogen–free conditions at 20-22°C on a 12-hr light-dark cycle. All treatment groups were randomised to control or treatment groups at the initiation of the experiment. All mice were fed a standard chow diet and had access to water *ad libitum*.

4.2.1.2 Experimental rationale

To establish a mouse model of intestinal dysbiosis and verify changes in host-metabolism, antibiotics were used as a means of depleting the gut microbiome and metabolic parameters were assessed. This model was then used to establish the role of gut-derived 5-HT as a signalling mediator between the gut microbiome and host metabolism. To test the influence of gut-derived 5-HT on metabolism, the TPH inhibitor, LP533401, was used orally to deplete EC cell 5-HT synthesis. To determine whether the gut microbiome affects host metabolism by increasing gut-derived 5-HT, co-treatment with antibiotics and LP533401 was used to deplete both the gut microbiome and gut-derived 5-HT (Figure 4.1). Starting at 8 weeks of age, mice were exposed to their respective treatments for a period of 28 days. Mice in the antibiotic-treated (Abx) group had their normal drinking water substituted with antibiotic water containing 1.0 mg/mL Ampicillin (sodium salt, Sigma Aldrich, Australia) and 0.5 mg/mL Neomycin (triphosphate salt, Sigma Aldrich). Mice in the TPH inhibitor group received daily oral gavage of LP533401 (30 mg/kg body weight, Dalton Pharma Services, Canada) dissolved in DMSO (0.8%) and polyethylene glycol 400 (Sigma Aldrich, Australia) and diluted 1:2.5 with 5% (w/v) dextrose in PBS to achieve a final concentration of 3 mg/mL. Control and Abx

treated groups received daily vehicle gavage (0.8% DMSO in PEG 400 diluted 1:2.5 with 5% dextrose/PBS). Metabolic testing, faecal sampling and blood collection was undertaken at specified time points over the course of the treatment.

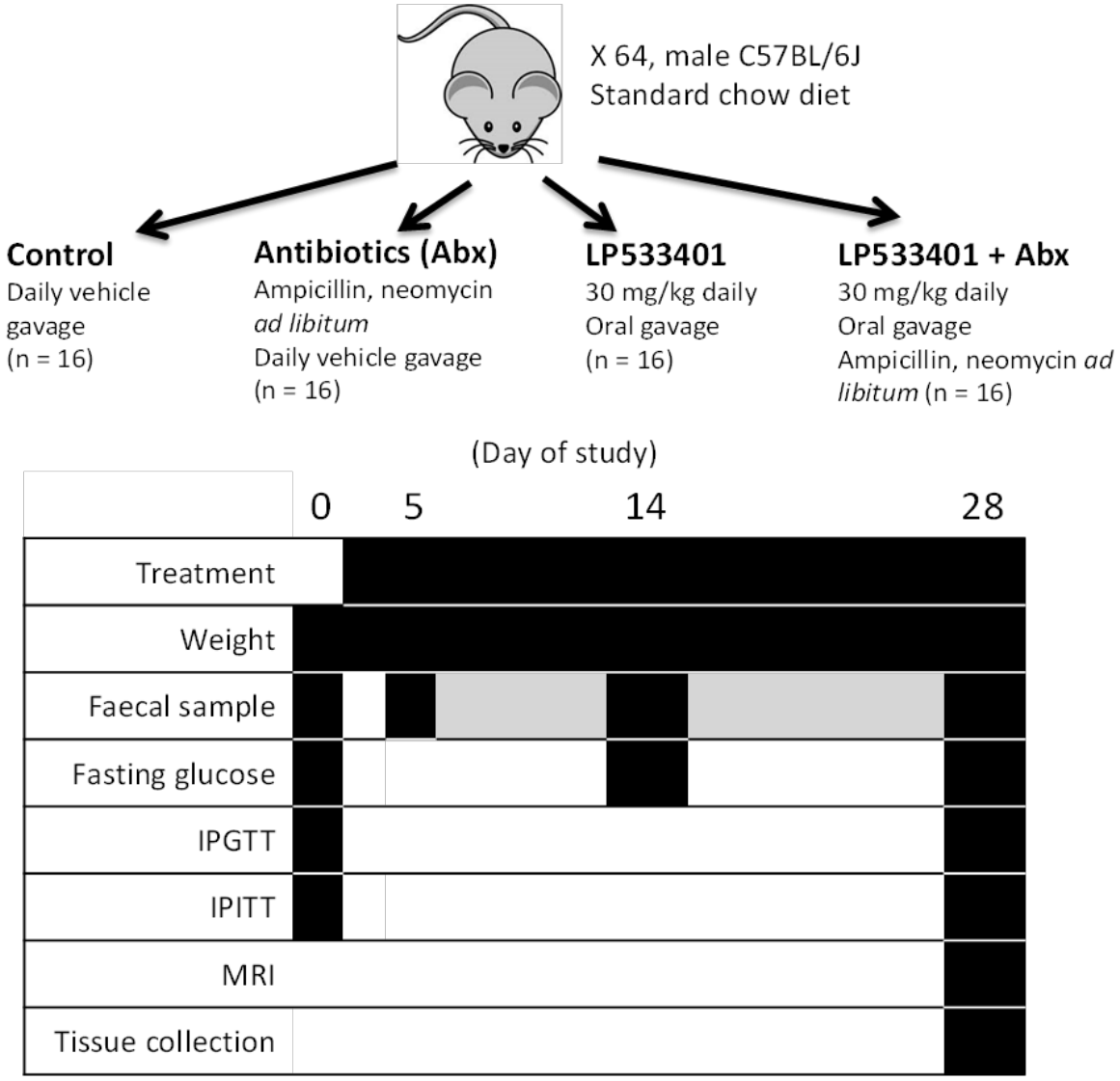

Figure 4.1 – Experimental study design to investigate the role of gut 5-HT in the effects of the gut microbiome on host metabolism. Antibiotics were used to induce intestinal dysbiosis, while the TPH inhibitor, LP533401, was administered orally to strictly reduce intestinal 5-HT synthesis. Areas shaded in black represent days in which the specific tests were performed.

4.2.2 Fasting blood glucose, and glucose and insulin tolerance tests

4.2.2.1 Fasting glucose

Mice were fasted for a period of 3 hrs by housing in bedding- and feed-free cages with fasting trays. This was followed for 5 mins in a Thermacage™ at 35°C, and blood glucose measured via tail vein bleed using an ACCU-CHEK® Performa glucometer (Roche Diagnostics, Australia)

4.2.2.2 Glucose tolerance test

Mice were fasted for a period of 4 hrs by housing in bedding- and feed-free cages with fasting trays, followed by brief heat exposure for 5 mins in a Thermacage™ at 35°C, and baseline blood glucose measured via tail vein bleed using an ACCU-CHEK® Performa glucometer (Roche Diagnostics, Australia). Glucose solution was injected intraperitoneally at a concentration of 2 g/kg body weight, and blood glucose levels determined by measuring blood collected via tail bleed at 15, 30, 60, 90, 120, 150, 180 and 240 mins post-injection.

4.2.2.3 Insulin tolerance test

Mice were fasted for a period of 3 hrs by housing in bedding and feed-free cages with fasting trays, followed by brief heat exposure for 5 mins in a Thermacage™ at 35°C, and baseline blood glucose measured via tail vein bleed using an ACCU-CHEK® Performa glucometer (Roche Diagnostics, Australia). Insulin (NovoRapid®, Novo Nordisk, Australia) was injected intraperitoneally at a concentration of 0.75 unit/kg body weight, and blood glucose levels measuring via tail vein bleed at 15-minute intervals from 30 to 240 mins post-injection.

4.2.3 Metabolic chambers and body composition

Whole body metabolic rates were assessed at the end of the 28-day treatment. Mice were housed individually in Promethion™ Metabolic Cages housed at a room temperature of 20-22°C on a 12-hr light-dark cycle for a period of 2 days, with 24 hrs allowed for acclimatisation. Mice had access to food and water *ad libitum*. Data was analysed over light phase (LP) and dark phase (DP) using ExpeData-P data analysis software (Sable Systems International). Body composition parameters were measured post-mortem using magnetic resonance imaging (MRI). Mice were humanely euthanized by CO_2 overdose and were scanned using the rat body coil in a benchtop 1T Bruker Icon MR system with an advance III spectrometer. ParaVision software (Bruker, Germany) was used to acquire and reconstruct scans. A 3D T1-weighted gradient scan with 4 averages, TR/TE = 378.364/6.210 ms, FOV = 75 mm, matrix = 256^2, and 2 mm slice thickness was used. MRI analysis was carried out using ITK-SNAP (Yushkevich et al., 2006). Subcutaneous adipose tissue was manually segmented slice-by-slice on the basis of differences in signal intensity and anatomical location. Due to interference from undigested intestinal contents within the caecum, visceral adipose tissue could not be accurately measured and was thus excluded from analysis. Subcutaneous fat volume was determined by total voxel volume (mm^3).

4.2.4 Blood collection and analysis

Whole blood was collected via tail vein bleed during the experiment and by terminal cardiac puncture under isoflurane anaesthesia at the end of the experiment. Time-of-day for blood collection was consistent across all experimental groups. For plasma collection, blood was collected into EDTA-coated collection vials (Sarstedt, Australia) and immediately centrifuged at room temperature for 15 mins at 2000 rpm using an Eppendorf Minispin. Due to the potential for platelet 5-HT to contaminate plasma samples, serum was collected as an indication of total circulating 5-HT. For serum sample analysis, whole blood was collected into

serum tubes containing a clotting agent (Microvette®, Sarstedt Australia), followed by immediate addition of a 1:100 cocktail mixture of DPP-IV inhibitor (Merck Millipore), EDTA-free protease inhibitor (Roche Diagnostics, Australia) cocktail and commercially available 5-HT stabiliser (LDN, Germany). Blood samples were incubated for 30 mins at room temperature to allow for complete clotting, mediated by 5-HT release from platelets, and serum collected by centrifugation at room temperature for 10 mins at 10,000 rpm. Plasma and serum samples were immediately snap-frozen on dry ice and stored at -80°C until further analysis.

4.2.4.1 Serum analyte analysis

Serum metabolic hormone content was analysed using a mouse multiplex ELISA (MMHMAG-44K, Merck Millipore) according to manufacturer's instructions. All incubations were performed with orbital shaking. Briefly, 10 µL of serum was loaded onto wells of a prepared multiplex ELISA plate containing assay buffer, followed by addition of antibody-coated magnetic assay beads into each well. Serum matrix effects were accounted for my addition of a serum matrix solution to standards and controls. Following incubation for 20 hrs at 4°C, the ELISA plate was washed three times while on a hand-held magnet. 50 µL of detection antibodies was added to each well and incubated for 30 mins at room temperature. This was followed by addition of 50 µL of streptavidin-phycoerythrin and a further 30 mins incubation at room temperature. Well contents were removed, and the plate washed three times while on a hand-held magnet, and 100 µL of Drive Fluid added to each well. After 5 mins, the ELISA plate was assayed using a MAGPIX® System with xPONENT software. A standard curve of median fluorescence intensity using a 5-parameter log method was used to calculate serum sample analyte concentrations.

4.2.5 Mucosal and blood 5-HT analysis

Proximal small intestine, comprising of tissue beginning adjacent to the pylorus and ending 6 cm distally, and the entire colon from caecum to rectum was dissected and mucosal tissue removed as per methods previously described in *Chapter 2*. Mucosal tissue was lysed in 0.5 mL of RIPA Lysis Buffer (Sigma Aldrich) containing 5-HT stabiliser (1:100, LDN, Germany), and tissue disrupted by gentle repetitive pipetting to ensure minimal 5-HT degradation, as agitation increases the rate of 5-HT oxidation. Lysed tissue was centrifuged at 14,000 rpm for 20 mins at 4°C, and supernatant collected and stored at -80°C until further analysis.

4.2.5.1 5-HT analysis

Mucosal and serum 5-HT content was measured by 5-HT ELISA, as per previous methods, at a 1:2000 dilution, while plasma 5-HT content was analysed at a 1:100 dilution. Mucosal 5-HT content was normalised to total protein, measured by EZQ Protein Quantitation Kit (BioRad) according to manufacturer's instructions.

4.2.6 Faecal collection and bacterial load analysis

Faecal samples were routinely collected at 8:00 am at Days 0, 5, 14 and 28, immediately snap frozen on dry ice and stored at -80°C until further analysis. Raw data collection of faecal pellet microbial load and composition was performed by Dr. Jocelyn Choo, from the SAHMRI Microbiome Research Laboratory, based at Flinders University.

4.2.6.1 DNA extraction

Faecal samples were individually weighed, washed in 1mL of phosphate buffered saline (PBS) (pH 7.2) by vortexing, and pelleted by centrifugation at 13,000 × *g* for 5 min. DNA extraction was performed on the faecal pellets using a PowerSoil®-htp 96 Well Soil DNA Isolation kit (MoBio Laboratories, USA) with minor modifications. Briefly, the faecal pellets were resuspended in 750 μL of Powersoil® bead solution and 60 μL solution C1 in a

Powersoil® bead plate. The bead plate was then incubated at 65°C for 30 mins prior to bead beating. Subsequent DNA extraction procedures were performed according to the manufacturer's instructions.

4.2.6.2 Quantitative real-time PCR analysis to determine bacterial load

Real-time PCR was performed using primers that targeted conserved regions of the 16S rRNA gene as previously described (Nadkarni et al., 2002) on a Quant Studio™ 7 Flex Real-time PCR system (Thermofisher Scientific, USA). A no template DNA control containing sterile water was included in each run. Real-time PCR reaction of each sample was performed in triplicates, and a melting curve analysis was performed at the end of the program. For real-time PCR reaction components and thermocycling conditions, see Appendix Tables 6.5-6.6. The total bacterial load was quantitated against a standard curve of serial dilutions of *E. coli* genomic DNA from 3 to 3×10^6 cells performed in the same run.

4.2.6.3 Analysis to determine bacterial composition

To determine whether a bi-directional relationship exists between the gut microbiome and EC-cell 5-HT, the composition of gut microbiota at Day 0 and Day 28 were assessed for control and LP533401 treated mice. Since analysis of variation at Day 0 across control and LP533401 mice collected over different days was not significant, suggesting low day-to-day variability, only two time-points were selected for analysis. Using extracted faecal DNA, operational taxonomic units (OTUs) were assigned based on 16S rRNA sequences from the Silva123 database. Nonmetric multidimensional (NMDS) plots were generated and permutational multivariate analysis of variance (PERMANOVA) statistical analysis was performed using PRIMER v5 software (Clarke, 1993). DESeq analysis was generated based on OTU counts to identify taxa that potentially contribute to the differences between groups. Comparisons were performed between Day 0 and Day 28 for control, as well as Day 0 and Day 28 for LP533401.

4.2.7 Thermogenesis gene expression

Changes in BAT thermogenic capacity with antibiotics and LP533401 treatment was analysed by determining the mRNA expression of uncoupling protein 1 (UCP1), one of the key genes involved in regulating thermogenesis. Briefly, 30 mg of iBAT tissue was lysed by QIAzol treatment and homogenisation using a QIAGEN TissueLyser II at 30 Hz for 5 mins. RNA was extracted as previously described with several modifications using the QIAGEN Lipid RNeasy kit as per manufacturer's instructions, with off-column DNase digest. RNA concentration was quantified using the Nanodrop and cDNA was synthesised, and quantitative real-time PCR performed for UCP1 (Fwd: GCCAAAGTCCGCCTTCAGAT, Rev: TGATTTGCCTCTGAATGCCC) as per previous method outlined in Chapter 2.

4.3 Results

4.3.1 Establishing a mouse model of gut dysbiosis and verifying changes to host metabolism and gut-derived 5-HT

4.3.1.1 Antibiotic-induced gut dysbiosis

To produce a conventionally raised mouse model of gut bacteria depletion (intestinal dysbiosis), a combination of antibiotics (ampicillin and neomycin) was used to deplete the gut microbiome. Faecal DNA content, as a measure of intestinal bacteria content (Figure 4.2), was almost completely depleted with antibiotic treatment after 5 days (0.02 ± 0.004 ng/mg vs control: 37.49 ± 4.12 ng/mg) and this reduction was sustained at Day 14 (0.006 ± 0.001 ng/mg vs control: 17.82 ± 2.36 ng/mg) and Day 28 (0.05 ± 0.05 ng/mg vs control: 29.05 ± 5.65 ng/mg). This is indicative that antibiotic administration depleted intestinal bacterial, therefore inducing intestinal dysbiosis. Consistent with previous reports from GF mice and mouse models of antibiotic-induced dysbiosis, antibiotic treatment was associated with abnormal intestinal physiology and a substantially enlarged caecum (Figure 4.3) (Yano et al., 2015). While intestinal content appeared darker in colour in antibiotic-treated mice, faecal pellet formation within the colon appeared normal. However, faecal pellet output and size was not quantitatively measured.

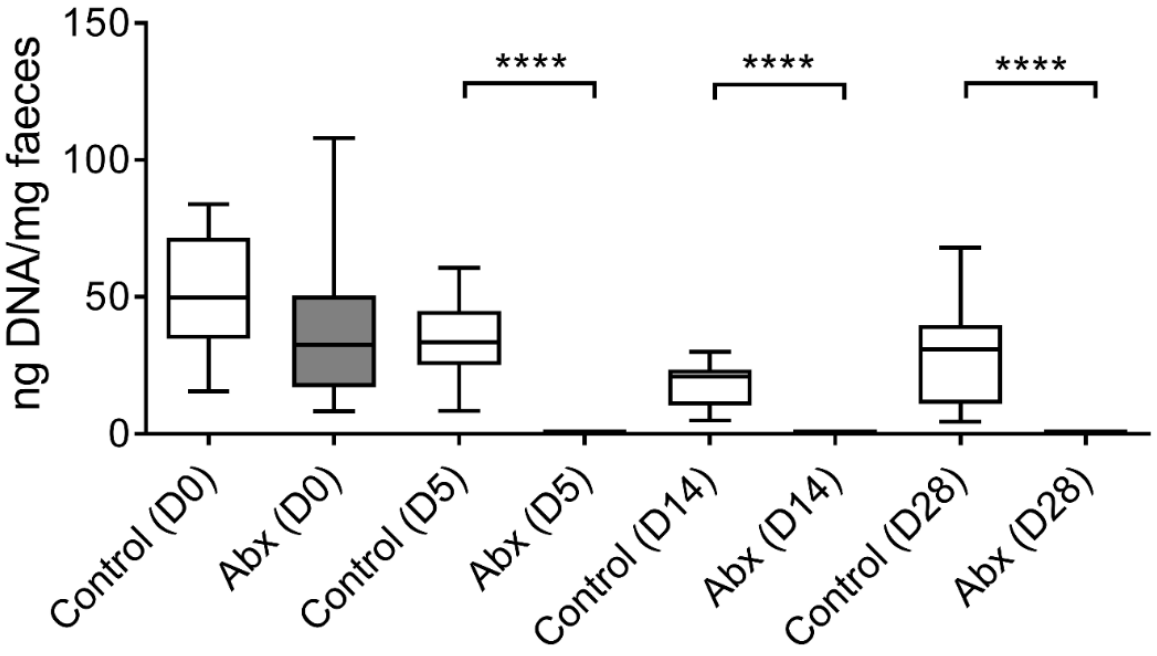

Figure 4.2 – **Quantification of faecal bacterial load.** Faecal bacterial load at specified time points with (Abx) and without (Control) *ad libitum* antibiotics. Complete bacterial ablation (dysbiosis) was achieved after 5 days of antibiotic treatment, which was sustained over 28 days (n = 11 – 16 mice, **** $p < 0.0001$). Data are shown as mean ± upper and lower quartiles.

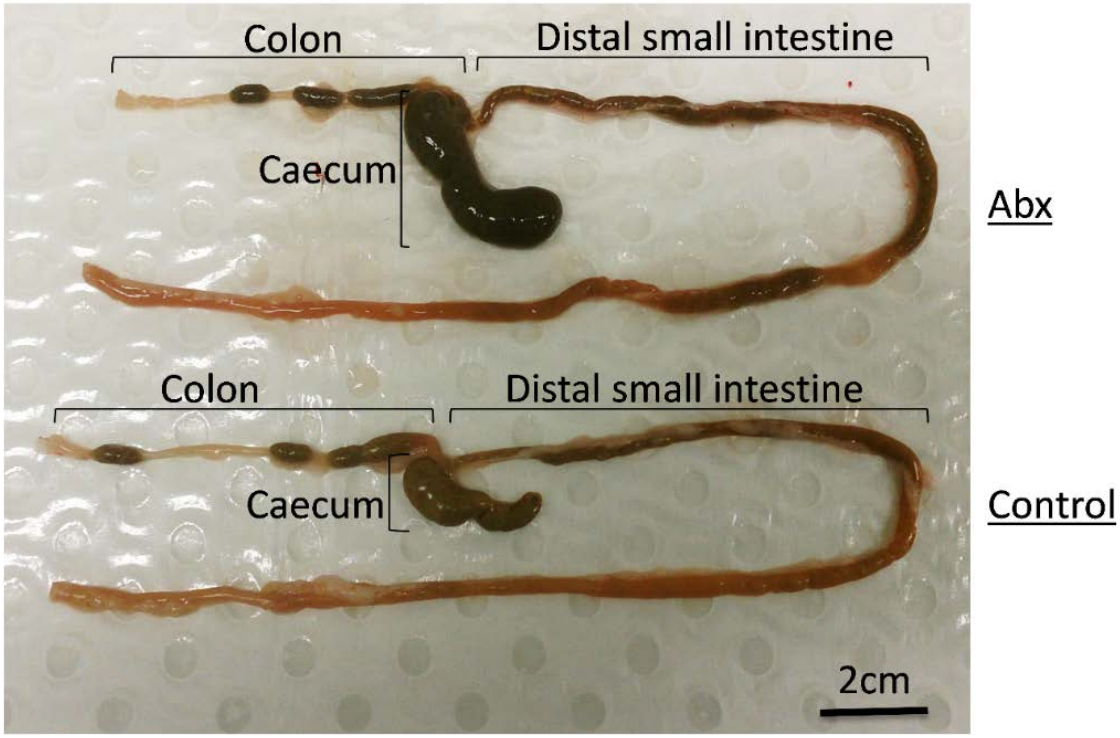

Figure 4.3 – Representative anatomical samples of mouse intestine with (Abx) and without (Control) antibiotic treatment. Abx-treated mice (top) had a considerably enlarged caecum compared to controls (bottom), with faecal content also being darker in colour.

4.3.1.2 Gut microbiome depletion reduces weight gain, fasting blood glucose levels and improves blood glucose clearance and insulin sensitivity

Consistent with other findings with antibiotic-induced gut dysbiosis, and in mice devoid of natural gut microbiota, natural weight gain of ~1-2 g over 28 days seen in control mice (Figure 4.4A) was inhibited with antibiotic treatment, such that antibiotic-treated mice weight less than controls at Day 14 (29.3 ± 0.3 g *vs* control: 30.9 ± 0.5 g) and Day 28 (29.8 ± 0.5 g *vs* control: 31.6 ± 0.6 g). Fasting blood glucose levels (Figure 4.4B) were also reduced with antibiotic treatment, with differences evident at Day 14 (6.9 ± 0.2 mM vs control: 8.9 ± 0.4 mM) and Day 28 (5.9 ± 0.3 mM vs control: 7.9 ± 0.5 mM).

In response to an intraperitoneal glucose challenge (Figure 4.5) no difference in blood glucose clearance was observed between control or antibiotic treated groups prior to commencing treatment (Figure 4.5A). Following microbiome depletion, blood glucose clearance was significantly improved (Figure 4.5B, AUC: 109.1 ± 6.55) compared to controls (AUC: 144.6 ± 8.9). Responses to intraperitoneal insulin challenge (Figure 4.6) were similar in both control and antibiotic treated groups prior to treatment, and an improvement in peripheral insulin sensitivity following microbiome depletion with antibiotic treatment (Figure 4.6A, AUC: 32.5 ± 1.1) compared to controls (Figure 4.56B, AUC: 59.0 ± 2.7).

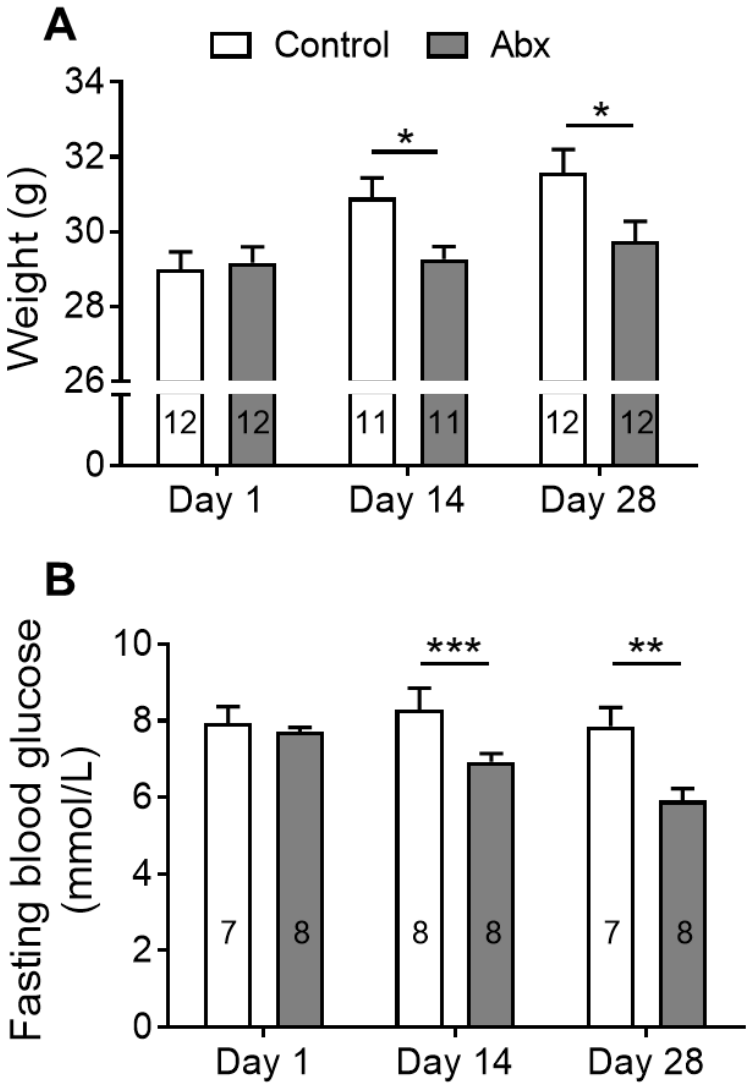

Figure 4.4 – Weight and fasting blood glucose over 28 days. (A) Antibiotic treatment (Abx) over 28 days inhibited natural weight gain on a standard chow diet and (B) reduced 2 hr fasting blood glucose levels compared to control mice. (*$p < 0.05$, **$p < 0.01$, ***$p < 0.001$). Data are shown as mean ± SEM.

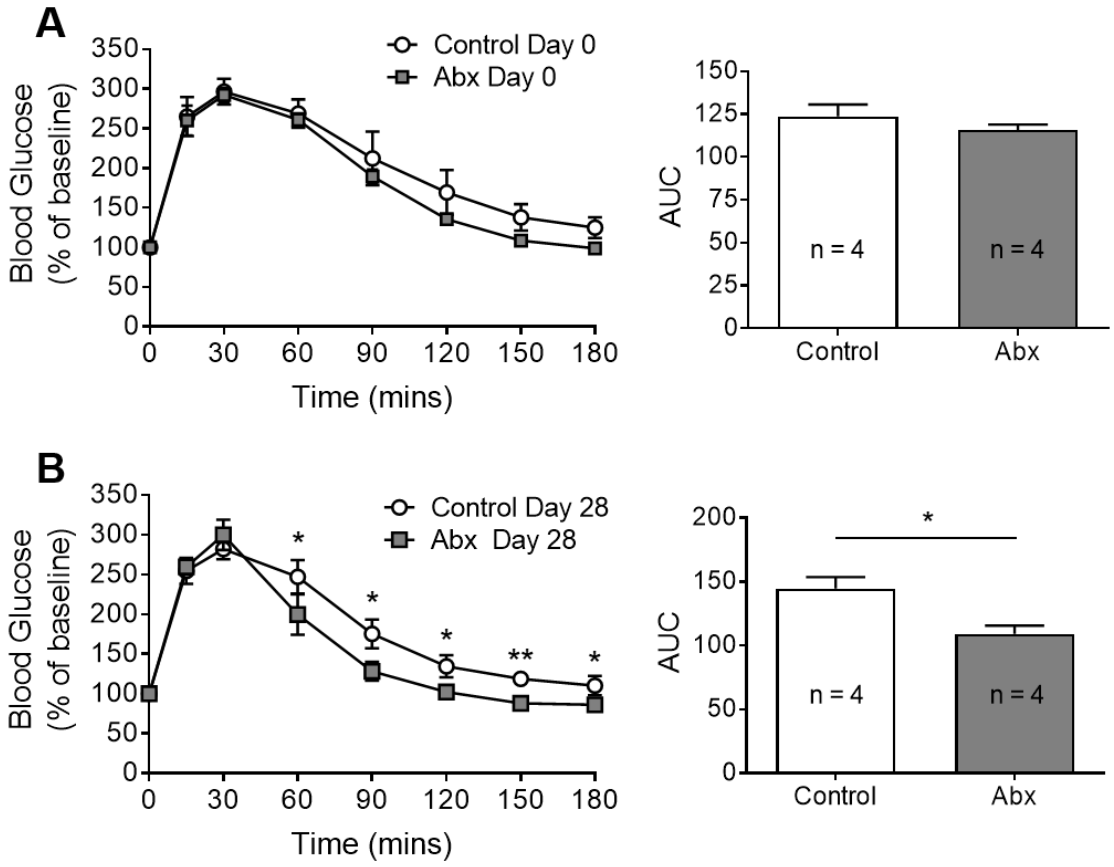

Figure 4.5 – Glucose tolerance tests (GTT) of control and Abx-treated mice at Day 0 and Day 28. (A) Blood glucose clearance following an intraperitoneal GTT did not differ between control and Abx groups prior to treatment, but was significantly improved with (B) Abx treatment for 28 days**.** (*$p < 0.05$, **$p < 0.01$). Data are shown as mean ± SEM.

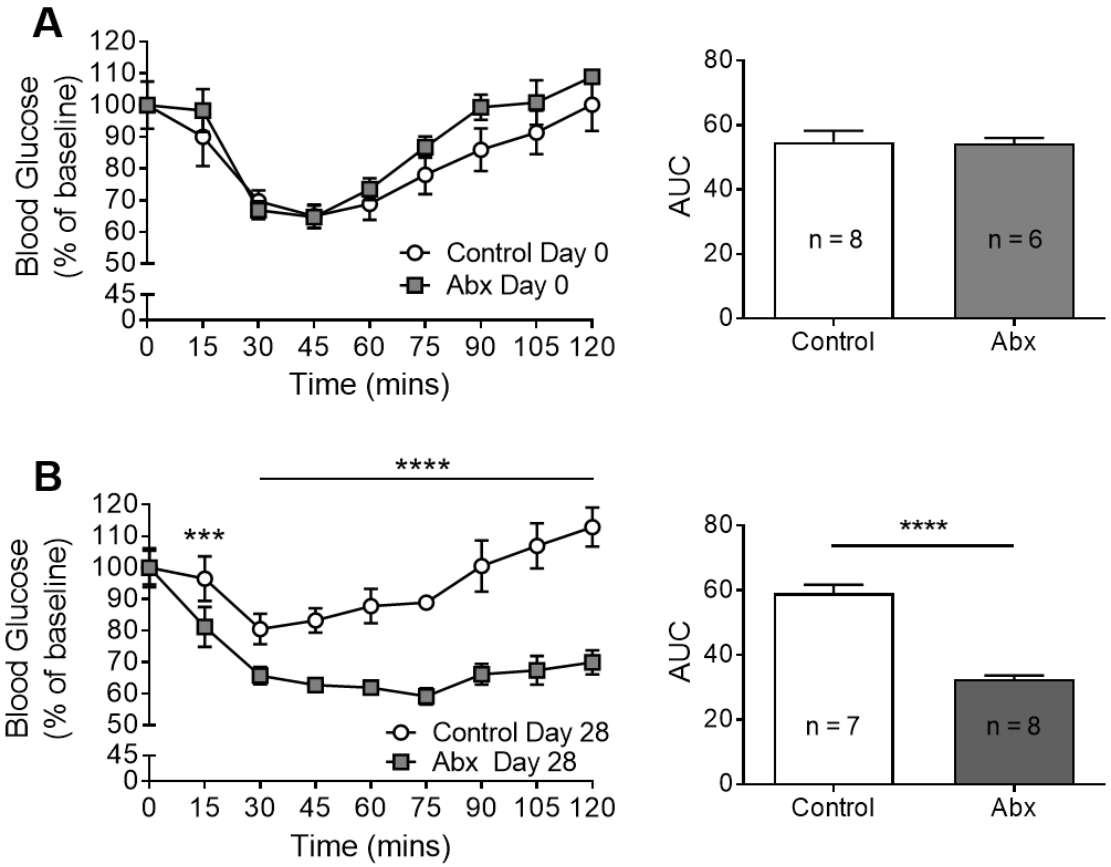

Figure 4.6 – Insulin tolerance tests (ITT) of control and Abx-treated mice at Day 0 and Day 28. (A) Sensitivity to insulin following an intraperitoneal insulin tolerance test was equal across both control and Abx treated groups at Day 0, but was increased in (B) Abx mice compared to controls after 28 days treatment. (****$p < 0.0001$). Data are shown as mean ± SEM.

4.3.1.3 Changes in peripheral metabolism with gut dysbiosis are not due to changes in activity or feeding behaviour

Metabolic parameters were assessed over a 24-hr period to determine if the changes in glucose tolerance and insulin sensitivity with microbiome depletion were associated with altered feeding behaviour and activity (Figure 4.7). Total food intake, determined by number and size of individual meals, and mouse activity did not differ between control and antibiotic groups. The ratio of oxygen consumption to carbon dioxide output, termed the respiratory quotient (RQ), is used as an indirect measure of which fuel source is relied upon for energy. A value approaching 0.7 is indicative of fatty acid oxidation being the predominant source of energy, whereas 1.0 indicates the exclusive use of carbohydrates. No difference was observed in the RQ between antibiotic treated mice and control mice. Similarly, no differences in energy expenditure or water consumption were observed between groups. This is indicative that the improvements in glucose tolerance and insulin sensitivity with Abx treatment were not associated with changes in respiration or basal metabolic rate. Differences were seen between light cycle and dark cycle phases, with all parameters increased in the dark cycle phase compared to light cycle due to mice being nocturnal.

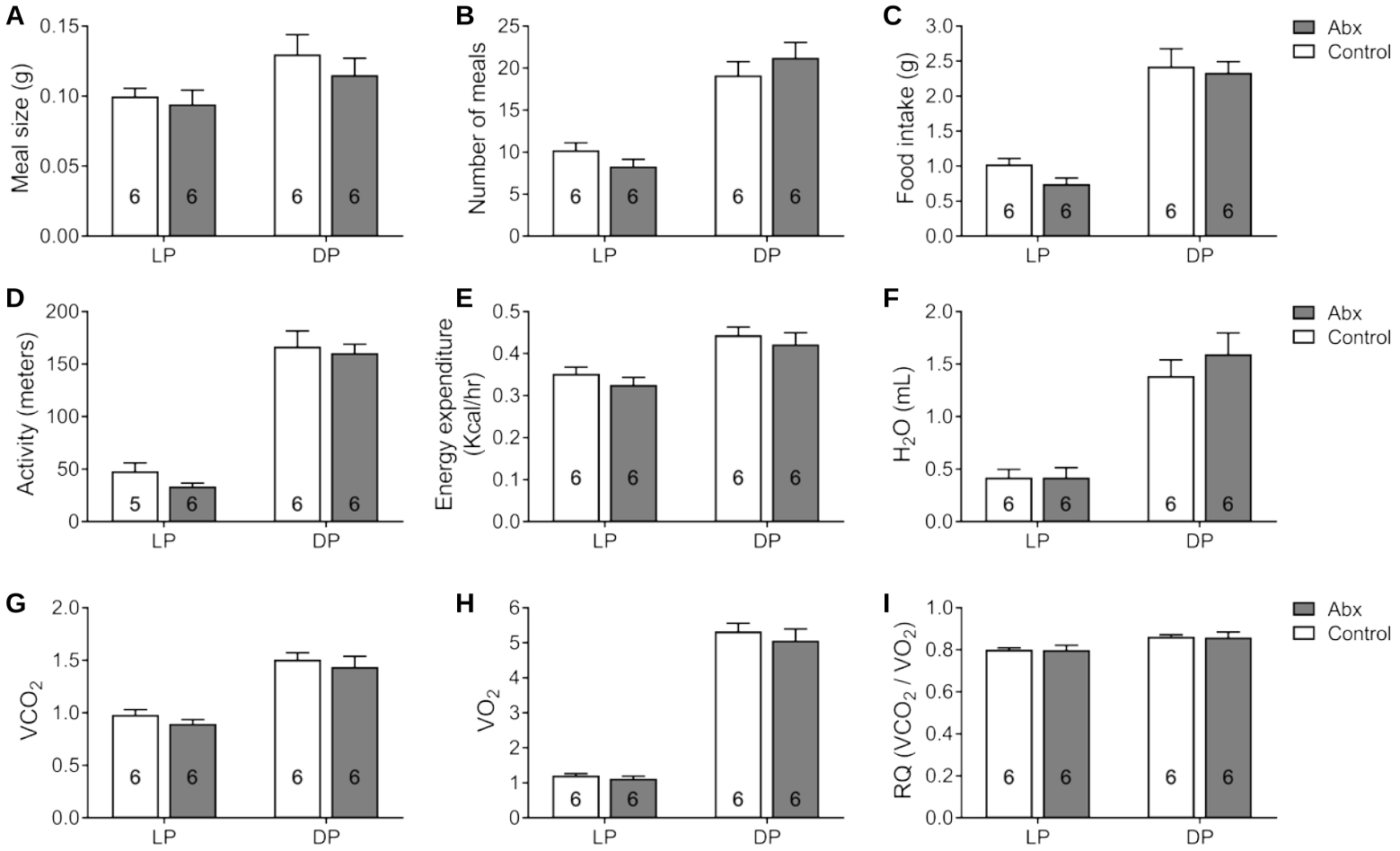

Figure 4.7 – Metabolic cage analysis at Day 28. (A) Individual meal size, (B) number of meals and (C) total food intake did not differ between control and Abx treated groups. (D) Physical activity, (E) energy expenditure and (F) water consumption were also unaffected by Abx treatment. (G) Carbon dioxide output, (H) oxygen consumption and (I) respiratory quotient (RQ), were unchanged by Abx treatment. LP: light phase, DP: dark phase. Data are shown as mean ± SEM.

4.3.1.4 Gut microbiome depletion reduces intestinal 5-HT content

Circulating plasma 5-HT and mucosal 5-HT content were assessed to verify changes in host gut-derived 5-HT previously observed in other models of intestinal dysbiosis (Figure 4.8). Depletion of the gut microbiome did not significantly alter plasma 5-HT after 28 days; however, plasma levels of 5-HT were highly variable, possibly as a result of contaminating platelet 5-HT during sample collection. Mucosal 5-HT content was reduced in both the proximal small intestine (5.0 ± 1.5 pg/µg protein vs control: 15.8 ± 4.6 pg/µg protein) and colon (1.5 ± 0.1 pg/µg protein vs control: 2.2 ± 0.3 pg/µg protein) from antibiotic treated mice. Mucosal content was higher in the small intestine, likely due to the density of EC cells and cell 5-HT content being greater in this region.

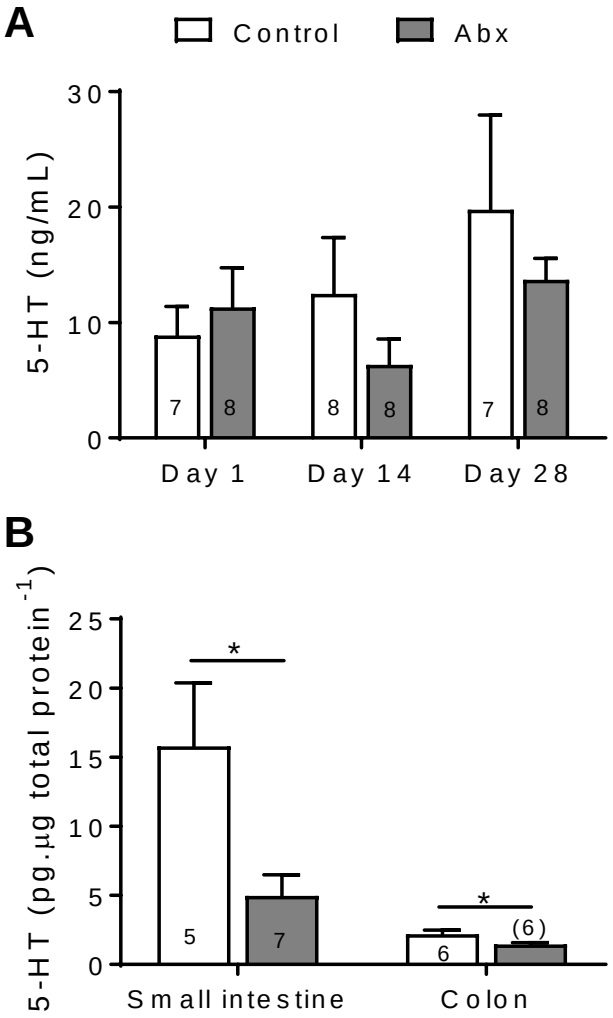

Figure 4.8 – 5-HT levels in control and Abx treated mice. (A) Circulating plasma 5-HT at specified time points and (B) mucosal 5-HT content at Day 28. (*$p < 0.05$). Data are shown as mean ± SEM.

4.3.2 Establishing the role of gut-derived 5-HT in dysbiosis-induced effects on host metabolism

Having established a mouse model of antibiotic-induced gut dysbiosis and verified changes to host metabolism and gut 5-HT, this model was used to determine whether the gut microbiome alters host metabolism via EC-cell 5-HT signalling. To establish the role of gut-derived 5-HT in the microbiome-host metabolism pathway, the TPH antagonist, LP533401, was used to inhibit EC-cell 5-HT biosynthesis. The poor oral bioavailability of LP533401 limits the activity to the gastrointestinal tract when delivered via oral gavage (Liu et al., 2008). The combination of LP533401 with antibiotic treatment was used to determine whether the gut microbiome and gut-derived 5-HT act via the same pathway to impact host metabolism. To provide an internally-controlled comparison, and thus increase the statistical strength of the experiment, comparisons were made between Day 0 and Day 28 for each individual mouse.

4.3.2.1 Effects on glucose tolerance

The blood glucose response to intraperitoneal glucose challenge (Figure 4.9) was unchanged in vehicle-treated control mice at Day 28 compared to Day 0. Improvements in blood glucose clearance after 28 days were observed in mice treated with LP533401 (Figure 4.9B), Abx (Figure 4.9C) and the combined LP533401 and Abx treatment (Figure 4.9D) compared to Day 0. While all treatments improved glucose tolerance compared to controls, the degree to which LP533401 (62.8 ± 8.2% vs Day 0), Abx (59.4 ± 6.7% vs Day 0) and LP533401 + Abx (63.2 ± 9.4% vs Day 0) improved glucose tolerance did not differ between groups, demonstrating no additive effect of combining the two treatments.

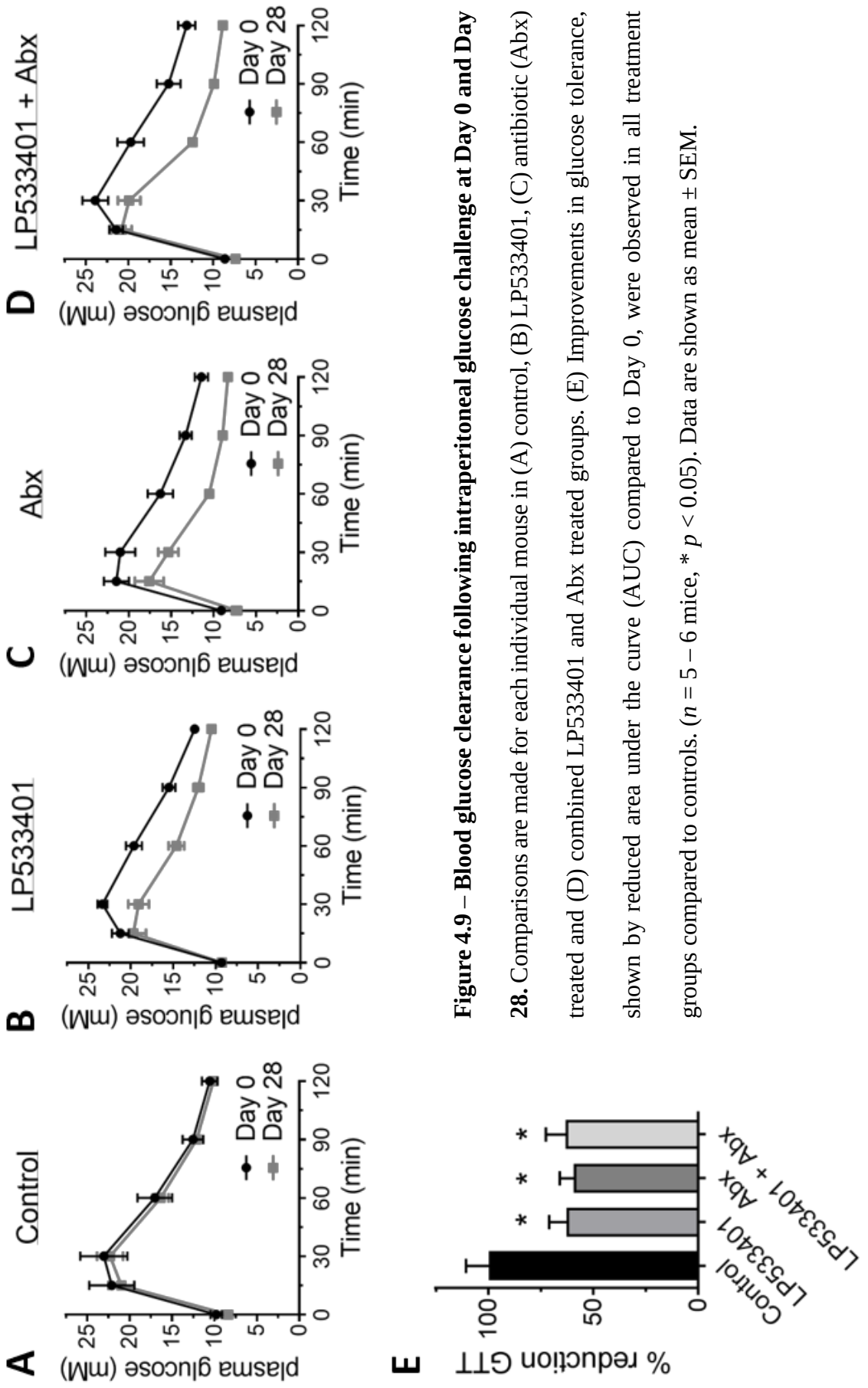

Figure 4.9 – Blood glucose clearance following intraperitoneal glucose challenge at Day 0 and Day 28. Comparisons are made for each individual mouse in (A) control, (B) LP533401, (C) antibiotic (Abx) treated and (D) combined LP533401 and Abx treated groups. (E) Improvements in glucose tolerance, shown by reduced area under the curve (AUC) compared to Day 0, were observed in all treatment groups compared to controls. (n = 5 – 6 mice, * $p < 0.05$). Data are shown as mean ± SEM.

4.3.2.2 Effects on insulin sensitivity

Blood glucose responses to intraperitoneal insulin at Day 28 were unchanged in control mice (Figure 4.10A) compared to Day 0, while LP533401 treated (Figure 4.10B), Abx treated (Figure 4.10C) and the combined LP533401 + Abx treated (Figure 4.10D) groups all exhibited increased insulin sensitivity. Notably, the effect of antibiotic treatment (53.5 ± 2.8% of control) and combined LP533401 and antibiotics (47.1 ± 2.5% of control) on insulin sensitivity was significantly greater than LP533401 treatment alone (Figure 4.10-E, 78.9 ± 2.6% of control), however no difference was observed between the two antibiotic treated groups. This is indicative that the gut microbiome may be acting, at least in part, via gut-derived 5-HT to affect peripheral insulin sensitivity.

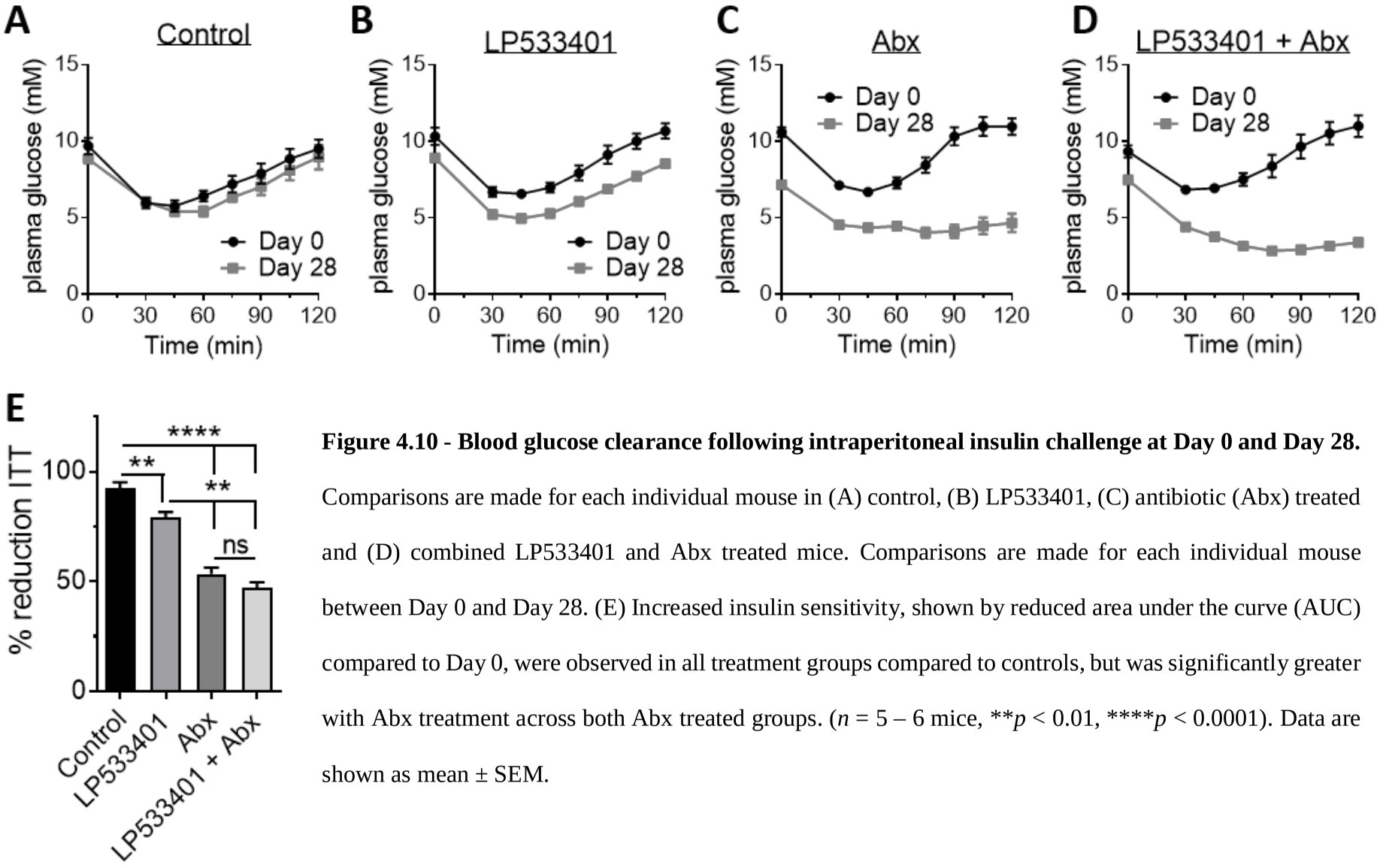

Figure 4.10 - Blood glucose clearance following intraperitoneal insulin challenge at Day 0 and Day 28. Comparisons are made for each individual mouse in (A) control, (B) LP533401, (C) antibiotic (Abx) treated and (D) combined LP533401 and Abx treated mice. Comparisons are made for each individual mouse between Day 0 and Day 28. (E) Increased insulin sensitivity, shown by reduced area under the curve (AUC) compared to Day 0, were observed in all treatment groups compared to controls, but was significantly greater with Abx treatment across both Abx treated groups. (n = 5 – 6 mice, $^{**}p < 0.01$, $^{****}p < 0.0001$). Data are shown as mean ± SEM.

4.3.2.3 Effects on feeding behaviour, activity, and basal metabolic rate

The effects of gut microbiome and 5-HT depletion on feeding behaviour, activity, and basal metabolic rate were also investigated (Figure 4.11) to determine whether these underlie the changes in host metabolism observed. Consistent with results from the established antibiotic-induced dysbiosis mouse model in this study, the effects on host metabolism seen in all treatment groups were not associated with changes to feeding behaviour, as feeding frequency, meal size and total food intake were consistent across groups. Administration of LP533401 increased water intake, likely due to reduced water absorption caused by gut 5-HT depletion. Changes in peripheral metabolism were not due to increased activity or altered basal metabolic rate, as oxygen consumption, carbon dioxide output and energy expenditure did not differ across all groups. To further establish whether thermogenic capacity was altered with gut dysbiosis and/or 5-HT depletion (Crane et al., 2015), expression of the key thermoregulatory gene, *Ucp1*, in BAT was investigated. An increase in BAT *Ucp1* expression was observed with LP533401 treatment alone, but not with Abx alone or combined Abx and LP533401 treatment. In contrast with mice administered antibiotics in the absence of a vehicle gavage (Figure 4.4), and findings from previous studies (Crane et al., 2015, Oh et al., 2015), no difference in weight was observed across all groups (Figure 4.11J). However, weight gain in the vehicle gavaged control group alone was significantly lower than the previous non-gavaged control group, likely due to some level of gavage-induced stress.

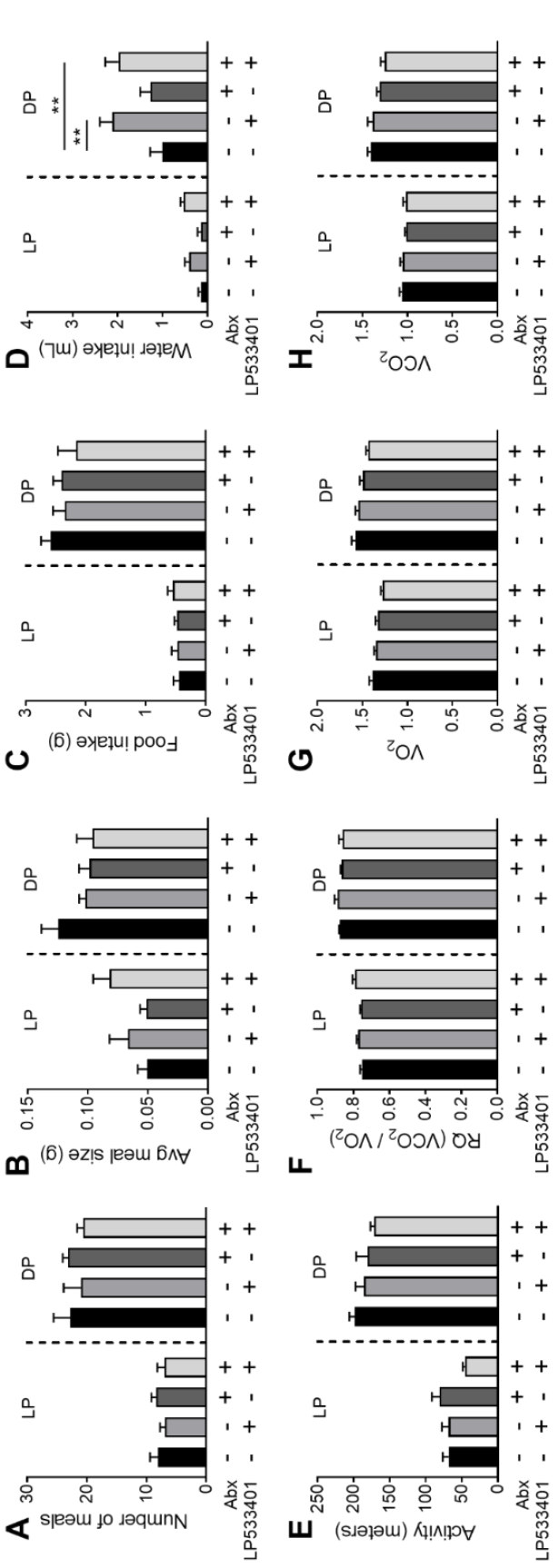

Figure 4.11 – Metabolic cage analysis of control, LP533401, Abx and LP533401+Abx treated mice. Analysis of (A) individual meal size, (B) number of meals and (C) total food intake, (D) water intake, (E) physical activity, (F) respiratory quotient (RQ), (G) oxygen consumption, (H) carbon dioxide output, (I) energy expenditure and (J) body weight across all groups at Day 28. (K) Expression of a key regulator of thermogenesis, uncoupling protein 1 (*Ucp1*), in BAT. LP: light phase, DP: dark phase. (n = 4 – 5 mice per treatment group, $^{**}p < 0.01$). Two-way ANOVA with Tukey's multiple comparison test. Data are shown as mean ± SEM.

4.3.2.4 Effects on gut-derived 5-HT and other metabolic hormones

All three treatment groups demonstrated reduced EC-cell 5-HT synthesis. LP533401 reduced circulating serum 5-HT levels (Figure 4.12A) by ~40% when given alone (3338 ± 95 ng/mL) and in combination with Abx treatment (3213 ± 165 ng/mL). Abx treatment alone had a lesser effect on circulating 5-HT, reducing serum 5-HT by ~25% (4139 ± 190 ng/mL) compared to controls (5568 ± 357 ng/mL). To confirm that the reduction in circulating 5-HT is due to reduced EC cell 5-HT synthesis, mucosal 5-HT content was measured from the small intestine and the colon. While a trend for decreased 5-HT content was seen in the proximal small intestine (Figure 4.12B) with all three treatments, this was not significantly lower. All three treatments reduced colonic mucosal 5-HT by ~30-40% (Figure 4.12C) compared to controls, and did not differ significantly from each other.

To determine what other mechanisms may underlie the increased insulin sensitivity seen with microbiome depletion, and whether EC-cell 5-HT alters metabolism via effecting release of other endocrine hormones, metabolic hormones were measured in serum from all groups (Figure 4.13). Circulating C-peptide, a measure of active insulin levels, did not differ between treatments and controls. Similarly, gastric inhibitory polypeptide (GIP) and leptin were unaffected by Abx and LP533401 treatment. Gut microbiome depletion dramatically increased circulating glucagon, active GLP-1 and PYY, which were undetectable in control and LP533401 treated groups.

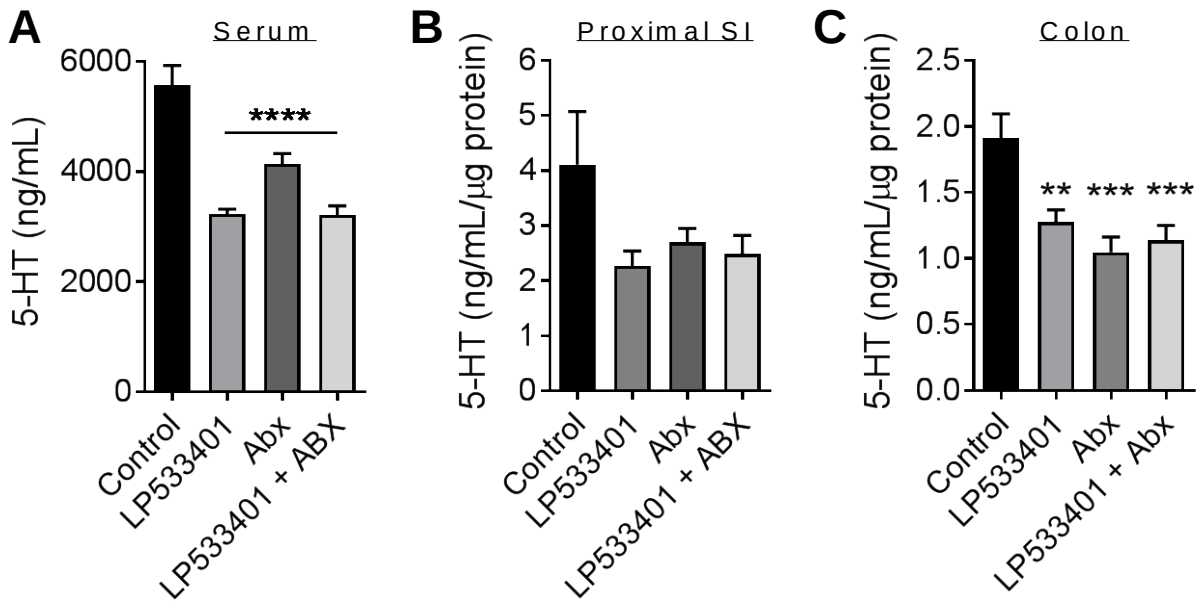

Figure 4.12 – 5-HT levels in Control, LP533401, Abx and LP533401+Abx treated mice at Day 28. (A) Circulating serum 5-HT (n = 12 – 16 mice, ****p < 0.0001 *vs* control). (B) Mucosal 5-HT content in the proximal small intestine (SI) and (C) colon (n = 8 – 11 mice, ** p < 0.01, *** p < 0.001 vs control). One-way ANOVA with Tukey's multiple comparison test. Data are shown as mean ± SEM.

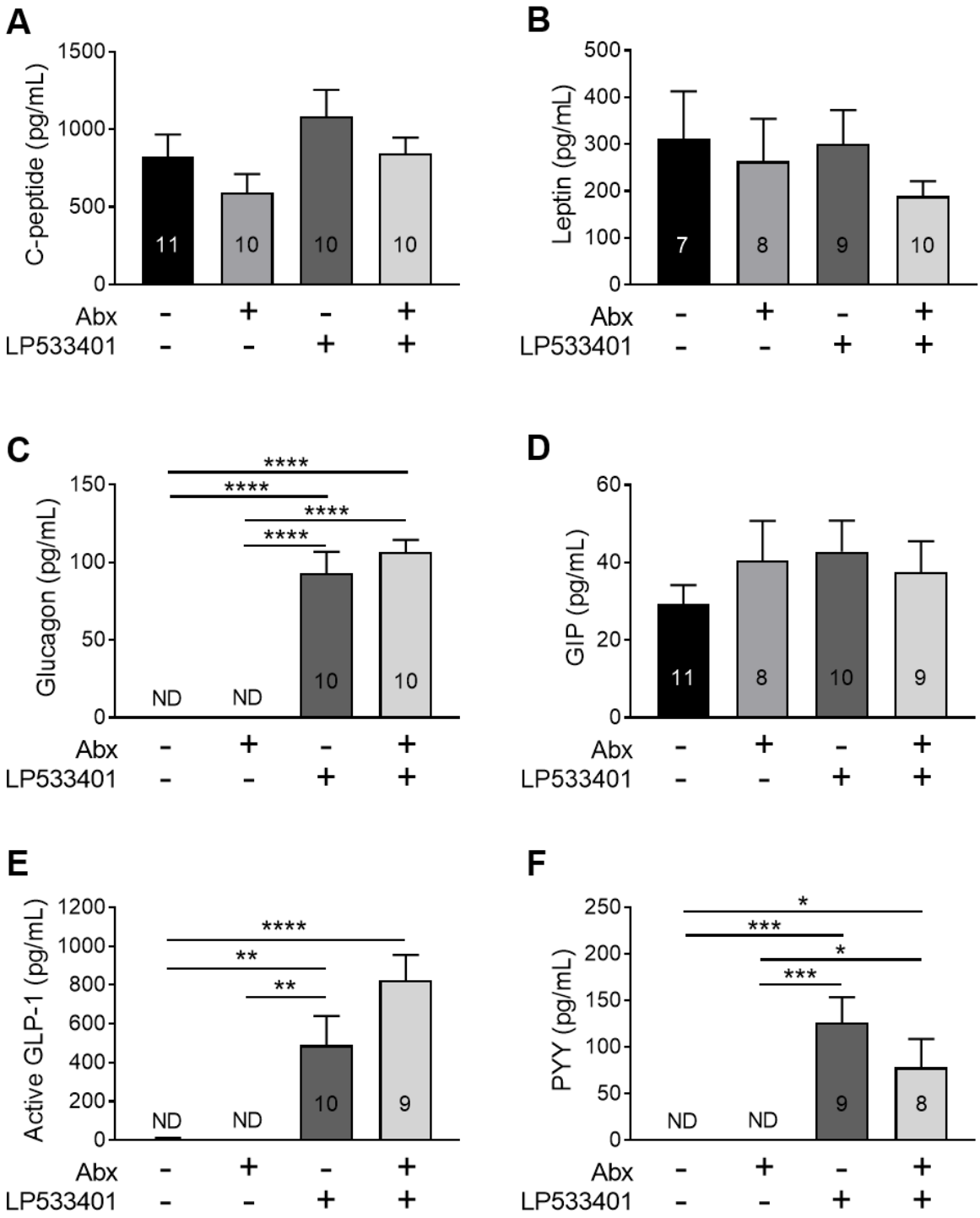

Figure 4.13 – **Multiplex metabolic hormone analysis of Day 28 serum**. (A) C-peptide, a measure of circulating active insulin, (B) leptin, (C) glucagon, (D) gastrin inhibitory peptide (GIP), (E) active glucagon like peptide 1 (GLP-1) and (F) peptide YY (PYY). ND: not detected, indicates samples below level of detection. *p < 0.05, **p < 0.01, ***p < 0.001, ****p < 0.0001. One-way ANOVA with Tukey's multiple comparison test. Data are shown as mean ± SEM

4.3.2.5 Effects on subcutaneous adiposity

Despite having no difference in body weight, MRI analysis of fat volume (Figure 4.14A) revealed that all three treatment groups had a substantial ~40-70% reduction in subcutaneous fat volume compared to controls (Figure 4.14B). Abx (44.8 ± 6.8% of control) and combined LP533401+Abx- (32.4 ± 4.4% of control) treated mice exhibited the greatest reduction in subcutaneous fat, but none of the 3 treatment groups differed from each other. Subcutaneous white adipose tissue volume has a strong (R^2 = 0.355) and significant ($p < 0.01$) positive correlation with circulating serum 5-HT levels (Figure 4.14C).

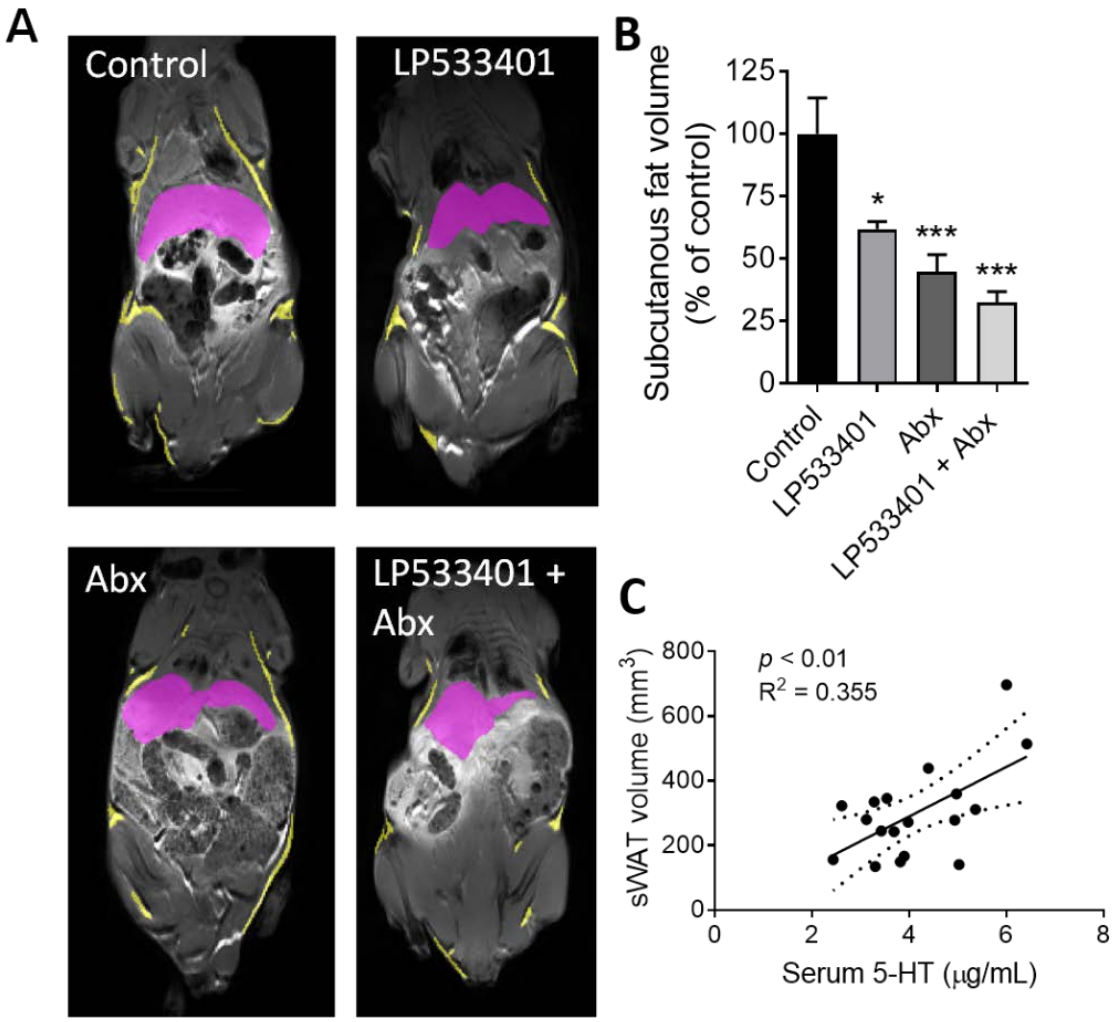

Figure 4.14 – Effects of LP533401, Abx and combined LP533401 + Abx treatment on adiposity. (A) Representative magnetic resonance imaging (MRI) scans showing subcutaneous adipose tissue (yellow) at Day 28. (B) Quantification of subcutaneous fat volume revealed an effect of all treatment groups on subcutaneous adiposity. (n = 5 mice per group, *$p < 0.05$, ***$p < 0.001$). Data are shown as mean ± SEM. (C) Circulating serum 5-HT is positively correlated with subcutaneous white adipose tissue (sWAT) volume. Liver (purple) is shown for anatomic orientation. Solid line represents linear regression ± 95% confidence interval.

4.3.2.6 Effects of gut-derived 5-HT depletion on microbial composition

To establish whether a bi-directional relationship exists between the gut microbiome and EC cells, the effects of TPH1 inhibition on the faecal microbiome composition were examined. Following 28 days of LP533401 treatment, the microbial composition was significantly altered within each mouse compared to their original microbial composition (Figure 4.15). Mice in the vehicle-treated control group exhibited greater microbial diversity between individuals at both Day 0 and Day 28 compared to LP533401-treated mice at Day 0 and Day 28. Despite this, no significant shift was observed in the overall composition at Day 28, with changes ($p < 0.05$) in abundance occurring only for specific members of the *Firmicutes* (Clostridiaceae1, Lachnospiraceae, Ruminococcaceae) and *Proteobacteria* (Rhodospirillaceae) phyla (Figure 4.16). Compared to vehicle-treated control mice, changes to microbial abundance in LP533401-treated mice at Day 28 were significantly ($p < 0.05$) more diverse (Figure 4.17), but were predominantly due to shifts in a number of genera from the *Firmicutes* phyla, in particular a ~9.5-fold increase in Allobactum. Other genera which showed large increases in abundance with LP533401 treatment were Bacteroides (~13-fold) and Akkermansia (~11-fold).

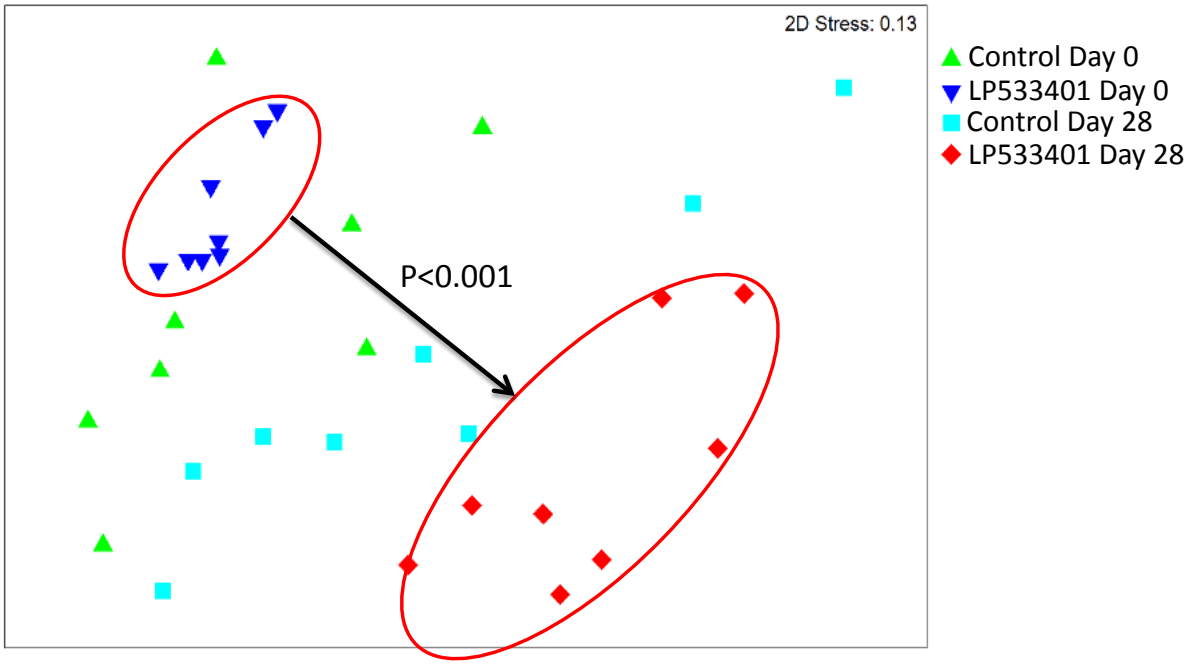

Figure 4.15 – Non-metric multidimensional scaling (NMDS) ordination plot representing the dissimilarity between faecal microbial composition in control and LP533401 treated mice at Day 28 compared to Day 0. Individual points are representative of individual mice. The distance between individual points is indicative of how similar (close proximity) or dissimilar (far proximity) the microbial compositions are to each other. Statistical significance determined by PERMANOVA pairwise test for time and treatment.

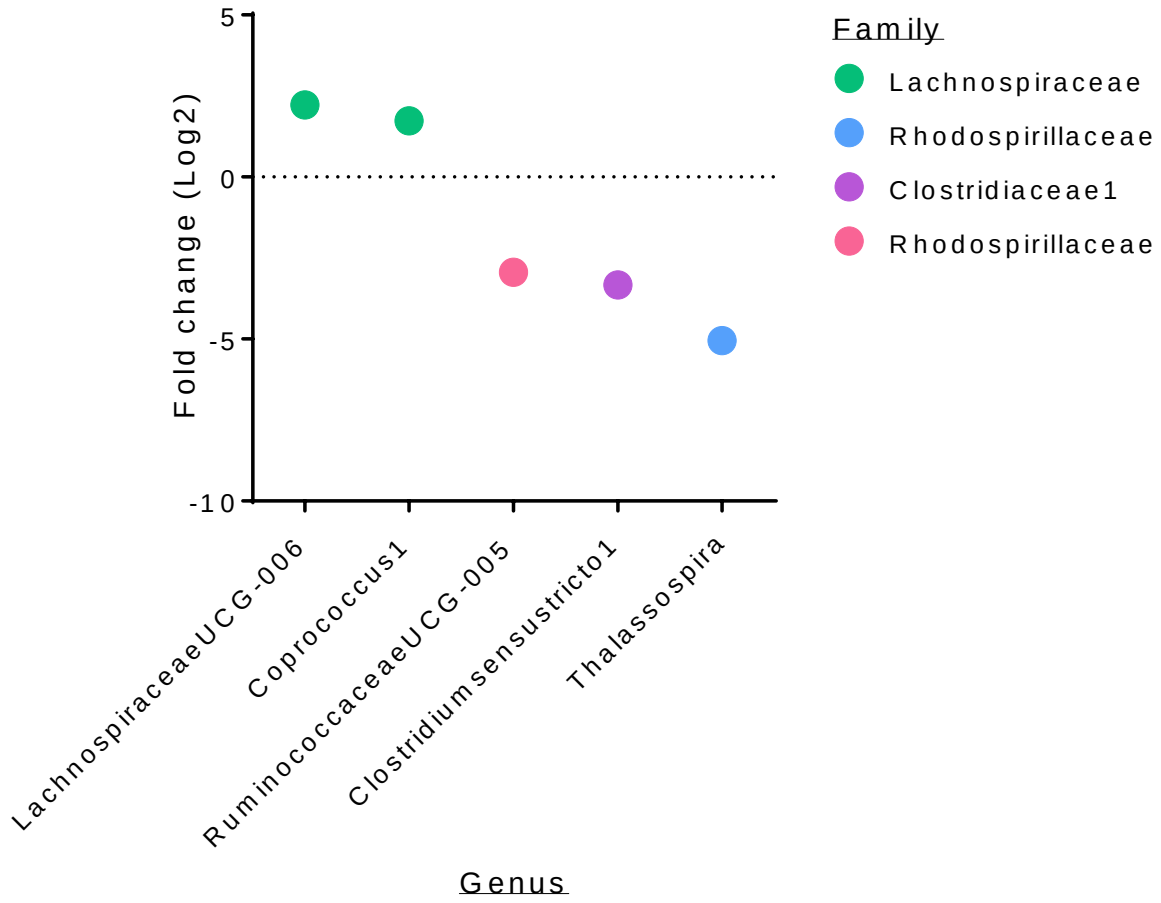

Figure 4.16 – Changes in microbial taxa abundance in control mice at Day 28 compared to Day 0. Data are shown as fold change (Log2 scale) for genera that have a significant shift in abundance after 28 days.

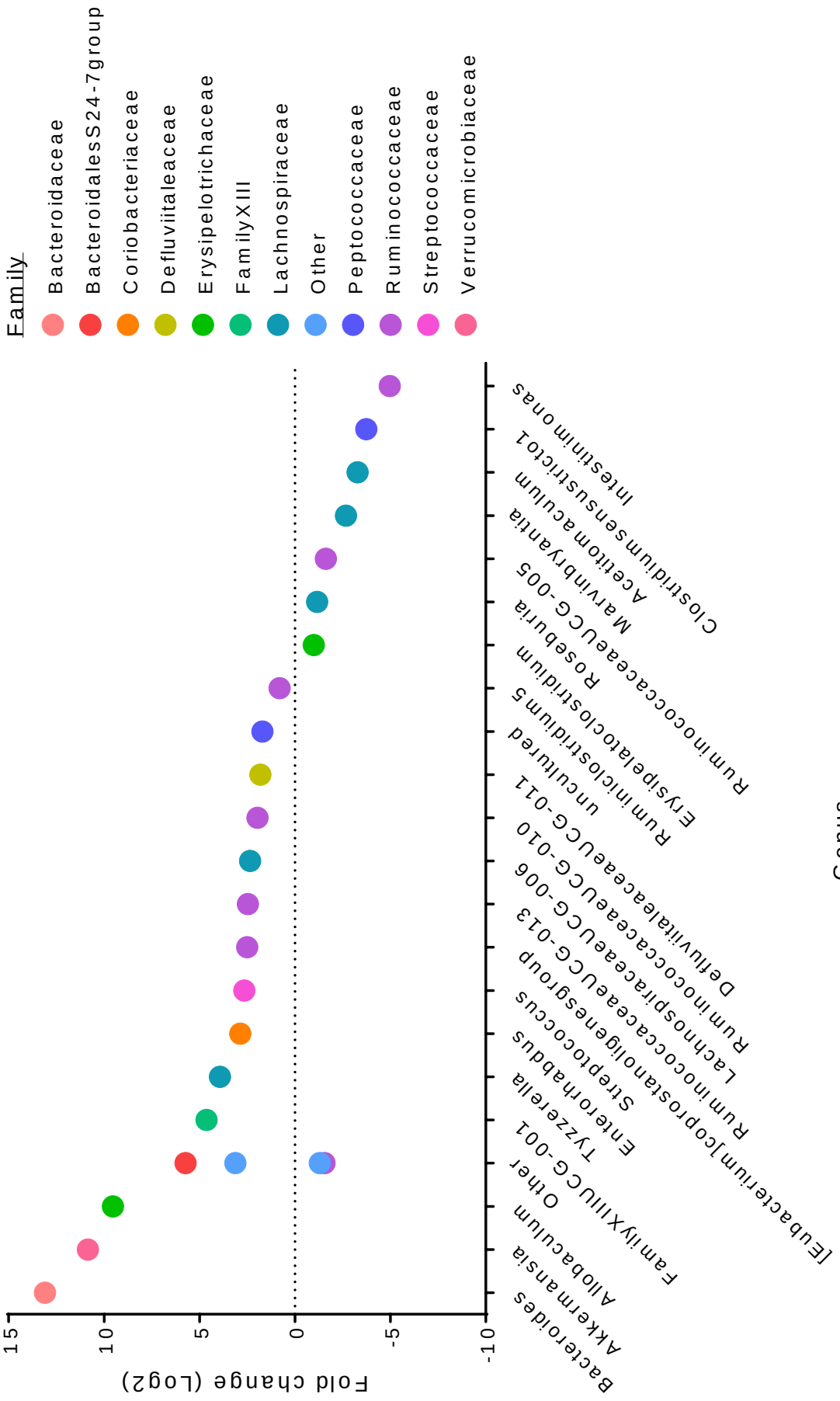

Figure 4.17 – Changes in microbial taxa abundance in LP533401-treated mice at Day 28 compared to Day 0. Data are shown as fold change (Log2 scale) for genera that have a significant shift in abundance after 28 days.

4.4 Discussion

This study investigated the role of gut-derived 5-HT as a signalling nexus between the gut microbiome and host metabolism. This is the first study to verify dysbiosis-induced changes in gut-derived 5-HT and host metabolism within the same mouse model. Treatment of conventionally raised mice with an antibiotic regimen successfully induced intestinal microbial dysbiosis. Enlargement of the caecum, as observed in this study, is associated with antibiotic treatment (Ge et al., 2017). This is a result of the accumulation of soluble and insoluble proteins and carbohydrates (Loesche, 1969) which are normally broken down and digested by the intestinal microbiota, resulting in reduced fluid absorption and enhanced smooth muscle relaxation (Bleich and Fox, 2015).

Ablation of the gut microbiome in antibiotic treated mice was associated with improved blood glucose clearance following a glucose challenge. The improved glucose clearance is likely due to increased sensitivity to insulin at peripheral tissues, as blood glucose clearance following an insulin challenge was also improved with antibiotic treatment. This has also been observed by others with antibiotic modulation of the intestinal microbiome, particularly in diet-induced obese mice (Carvalho et al., 2012). Possible differences in glucose induced insulin secretion (GSIS) which may also underlie an improved clearance of blood glucose were not investigated in this study. However, a marked (~70%) reduction in GSIS with hyperglycaemic clamp following antibiotic administration has been described, with the presence of microbial metabolites (predominantly acetate) substantially increasing GSIS (Perry et al., 2016). Such decreases in GSIS may be a result of improved insulin signalling at peripheral tissues, such that less insulin is required to maintain blood glucose levels following a glucose challenge.

Mice lacking a gut microbiome are protected from developing obesity and metabolic disease, as microbial dysbiosis prevents weight gain in GF and antibiotic-treated mice fed a high fat diet (Backhed et al., 2007, Carvalho et al., 2012). This current study found that this

effect of microbial dysbiosis on weight gain is evident even on a standard chow diet, as natural weight gain in antibiotic-treated mice was inhibited. This was due to a significant reduction in subcutaneous WAT fat volume, supporting similar findings from others in GF mice and in mice with antibiotic-induced dysbiosis showing reduced adiposity (Backhed et al., 2007). Others have also observed the improvement in metabolism following antibiotic treatment (Suarez-Zamorano et al., 2015), however, it is unknown whether the changes in metabolism with microbial dysbiosis are solely a result of reduced adiposity.

Having validated that intestinal dysbiosis influences host metabolism, the present study also aimed to validate whether this is associated changes in host gut-derived 5-HT within the same mouse model. Microbiome depletion reduced both mucosal and circulating 5-HT levels, comparable with other mouse models of intestinal dysbiosis including GF and antibiotic-treated (Yano et al., 2015). This finding further highlights an important interaction between the gut microbiome and host 5-HT, and may have been a result of reduced microbial signalling to EC cells within the intestinal mucosa. An absence of gut bacteria would result in reduced luminal SCFA and secondary bile acid production (Ge et al., 2017) – both of which increase 5-HT biosynthesis (Reigstad et al., 2015, Yano et al., 2015). Gut-derived 5-HT plays a key metabolic role through augmenting blood glucose levels, and thus reduced gut-derived 5-HT seen with microbial dysbiosis may underlie the improvements in blood glucose control and host metabolism.

To investigate if the intestinal microbiome influences host metabolism by augmenting 5-HT synthesis and secretion, this study produced a second mouse model with combined gut microbiome and mucosal 5-HT depletion. The reduction in circulating serum and colonic 5-HT in the mouse model used in this study is comparable with other mouse models of TPH inhibition with LP533401 (Liu et al., 2008). The variability of 5-HT content observed in the small intestine of controls may reflect the differences in nutrient content in the small intestine,

as tissue was collected from un-fasted mice. Independently, intestinal dysbiosis and reduced gut-derived 5-HT induced a positive shift in metabolism, with increased glucose tolerance and insulin sensitivity. Importantly, the combination of reduced EC-cell 5-HT and depleted gut microbiome did not show any additive effect compared to the individual treatments alone. This highlights that the gut microbiome and EC-cell 5-HT are likely to be acting via the same pathway to modulate host metabolism.

The improvement in blood glucose clearance following a glucose challenge in both antibiotic and LP533401 treatment is evidenced by improved insulin signalling, specifically the sensitivity of peripheral tissues following an insulin challenge. Depletion of the gut microbiome, alone or in combination with LP533401 had more of an effect on insulin sensitivity than LP533401 alone, highlighting that the gut microbiome may act via additional mechanisms not involving gut-derived 5-HT to modulate peripheral insulin sensitivity. Importantly, no additive effect on insulin sensitivity was observed when combining antibiotics and LP533401 treatment, demonstrating that gut-derived 5-HT is acting, in part, to modulate the effects of the gut microbiome on host insulin sensitivity. It is possible, however, that the increased insulin sensitivity with antibiotic treatment results in a 'ceiling effect', such that the blood glucose levels cannot decrease any further in chow-fed mice as part of a homeostatic mechanism that is protective against severe hypoglycaemic excursions. This is supported by the increase in serum glucagon observed in both groups treated with antibiotics, as pancreatic glucagon acts to increase blood glucose levels by triggering hepatic gluconeogenesis in response to hypoglycaemia. Repetition of this experiment in mice fed a HFD may negate these glucohomeostatic mechanisms, as this would raise fasting blood glucose and would avoid severe hypoglycaemic excursions following an insulin challenge.

Serum metabolic hormone analysis revealed that circulating levels of active insulin, represented by the level of C-peptide, are unchanged in all treatment groups. C-peptide is a

component of proinsulin that is cleaved when insulin becomes active. It has far greater stability than insulin in plasma and is therefore a more stable surrogate marker of circulating plasma insulin levels. This data indicates that basal insulin secretion is unaffected by gut microbiome or 5-HT depletion, and is consistent with gut-specific genetic TPH1 knock-out models which have unchanged fed and fasting levels of circulating insulin (Sumara et al., 2012). While no global effect on insulin secretion was observed, it is unknown whether antibiotics or LP533401 treatments alter acute dynamic changes in plasma insulin levels, particularly GSIS. Whether other pathways exist which may contribute to increased insulin sensitivity following antibiotic treatment remains unclear.

Increased circulating GLP-1 was observed with antibiotic treatment in the present study. GLP-1 has been shown previously to be associated with increased insulin sensitivity (Zander et al., 2002). Increased basal plasma GLP-1 observed in GF mice (Wichmann et al., 2013), other rodent models (Tolessa et al., 1998, I˙meryüz et al., 1997) and humans (Nauck et al., 1997, Zander et al., 2002) is also associated with slowed gastric emptying and small intestinal motility, via innervation of central and enteric neurons. This effect of GLP-1 is independent of its role as an incretin to increase insulin secretion (Nauck et al., 1997, Wichmann et al., 2013). The present study also found that gut microbiome depletion increased serum PYY. Mice lacking endogenous PYY demonstrate increased upper GI motility (Tough et al., 2011). In humans, gastric emptying and small intestinal transit time are also reduced following exogenous PYY infusion (Savage et al., 1987). This indicates that PYY acts to reduce intestinal motility in this region. The effect of PYY on colonic motility, on the other hand, is dependent on the type of Y receptor (Tough et al., 2011) and the active isoform of PYY, with colonic motility inhibited by the mature isoform, PYY_{3-36} (Tough et al., 2011) and stimulated by the naïve PYY_{1-36} (Ferrier et al., 2000). While gastric emptying and intestinal motility in antibiotic-treated mice were not assessed in the present study, it is plausible that the increase in circulating

GLP-1 and PYY is an adaptive response to slow intestinal motility. In this case, intestinal nutrient absorption would be increased, maintaining energy balance in the absence of microbial fermentation (Wichmann et al., 2013).

Food intake, physical activity, energy expenditure, and circulating levels of the satiety hormone, leptin, are unaltered by gut microbiome depletion or reduced gut 5-HT synthesis. Both GLP-1 and PYY have been demonstrated to act via centrally mediated satiety pathways to decrease food intake and increase energy expenditure (Abbott et al., 2005). However, given that food intake and energy expenditure were unaltered with microbiome depletion in this study, increases in GLP-1 and PYY may precede the changes in CNS pathways observed in other models such as GF mice, including altered satiety signalling (Backhed et al., 2004) and physical activity/locomotion (Backhed et al., 2007). The observed changes in glucose tolerance and insulin sensitivity with both gut microbiome and 5-HT depletion are therefore unlikely to be caused by altered satiety and energy utilisation. Such findings are consistent with those from mice with gut-specific genetic ablation of TPH1, which exhibit no change in energy expenditure compared to wild-type mice on a standard diet (Sumara et al., 2012). Food intake and physical activity are also unaltered in whole body TPH1 KO mice on a high fat diet (Crane et al., 2015). GF mice, however, have higher locomotive activity and lower food intake and basal metabolic rate compared to conventionalized mice (Backhed et al., 2004). The differences in locomotion, satiety and basal metabolic rate seen in GF, but not antibiotic-treated, mice are possibly a result of developmental effects in GF mice (Diaz Heijtz et al., 2011). These developmental effects are avoided in the antibiotic model used in this study, as ablation of the microbiome followed maturation.

Despite the equal consumption of food across all groups in this study, mice with ablated gut microbiota may have a decreased capacity for microbial-mediated energy harvest per gram of ingested food and, therefore, less energy availability to peripheral tissues. The

concentrations of circulating microbial metabolites across all groups were not measured within this study, however others have found that microbial fermentation of undigested nutrients contributes to approximately 6-10% of total energy intake in healthy, lean humans (McNeil et al., 1978). As such, a decrease in energy availability from food would enhance the utilisation of endogenous energy stores such as glycogen and adipocyte triglycerides, thereby decreasing adipose fat mass. Gut-derived 5-HT plays a key role in fasting adaptation, and acts to maintain blood glucose levels during times of low energy availability by increasing hepatic glucose production and mobilisation of free fatty acids (Sumara et al., 2012). The reduction in circulating 5-HT with antibiotic treatment, given independently and in combination with LP533401, would conversely decrease the rate of hepatic gluconeogenesis (Sumara et al., 2012). It is plausible that, with the combination of reduced energy availability from microbial fermentation and reduced 5-HT-mediated hepatic gluconeogenesis, compensatory mechanisms such as increased glucagon secretion are upregulated with antibiotic treatment. Such a mechanism would maintain energy availability to peripheral tissues. Indeed, greater circulating glucagon was observed in both groups treated with antibiotics after 28 days, and may therefore act to maintain blood glucose levels under reduced dietary energy availability.

Increased BAT thermogenesis has been demonstrated in a high fat diet model, with pharmacological inhibition of TPH through intraperitoneal injection delivery and whole-body genetic knockdown of TPH1 (Crane et al., 2015). BAT itself expresses TPH1 (Crane et al., 2015), however, and the effects observed in these studies may reflect the autocrine activity of 5-HT on BAT. In the present study, where oral administration of LP533401 limits the pharmacological inhibition of TPH to the intestine, *Ucp1* expression in BAT significantly increased only in mice treated with LP533401 alone, but not in combination with antibiotics. The difference between the two LP533401 treated groups in the current work is the presence of a gut microbiome in the LP533401-treated, but not antibiotic-treated or the combined group.

This suggests that an association with the gut microbiome in LP533401-treated mice may underlie the increased BAT *Ucp1* expression. It is unknown whether this increase in mRNA expression reflects increased protein expression of UCP1. However, it does not appear to reflect differences in total thermogenic capacity, as basal metabolic rate is unchanged across all groups.

The present study did not examine the expression of thermogenic genes in WAT. It is possible that the reduced adiposity seen with all treatment groups may be due to increased browning of WAT and increased WAT thermogenesis. However, this would be expected to result in a change in the basal metabolic rate, which was not observed in this study or in other studies using gut-specific TPH1 KO mice (Sumara et al., 2012). It is possible that the discrepancy in altered thermogenesis in mice from this study versus that seen by others is due to the duration of the study, with others being 12 weeks in duration (Sumara et al., 2012, Crane et al., 2015). It may also reflect the moderate degree of 5-HT depletion within this study, compared to the absolute ablation of 5-HT in TPH1 KO mice (Sumara et al., 2012, Crane et al., 2015). In addition, the difference in findings between the model used in this study and other models may be due to the thermal conditions at which the study was performed. Mice within this study were housed at 22-25°C for the duration of the study and for all metabolic testing. This is below what is considered the thermoneutral zone (30°C) for mice (Speakman and Keijer, 2012), and as such may have caused a moderate and sustained induction of thermogenesis in all mice when compared to other studies in which metabolic tests were carried out under thermoneutral conditions (Crane et al., 2015).

No change in body weight was found across all treatment groups compared to controls. This is consistent with other studies using LP533401 on a standard chow diet (Yadav et al., 2010, Sumara et al., 2012). Despite this, all treatment regimens resulted in lower subcutaneous adiposity compared to controls. Subcutaneous fat is the largest adipose tissue store

(Tchoukalova et al., 2010, Abate et al., 1995) and the major source of circulating triglycerides and free fatty acids (Ebbert and Jensen, 2013, Jensen and Johnson, 1996). The contribution of subcutaneous fat to total body fat mass is a predictor of metabolic disease risk compared to visceral adipose fat, and subcutaneous fat plays a major role in the development of insulin resistance with obesity (Goodpaster et al., 1997, Abate et al., 1995). Antibiotics and LP533401 treatment, individually and in combination, were associated with significantly reduced circulating 5-HT, at consistent levels across all treatment groups. Similarly, reductions in subcutaneous fat volume were also consistent across all treatments, suggesting a role of 5-HT in mediating the effects of the gut microbiome on adipose tissue accumulation, specifically subcutaneous adiposity. GF and TPH1 KO mouse models also display reduced body fat, which is associated with a reduction in adipose inflammation and macrophage accumulation (Caesar et al., 2012, Crane et al., 2015). Chronic inflammation and macrophage infiltration in adipose tissue is associated with reduced insulin sensitivity in an obese setting (Xu et al., 2003). While the expression of inflammatory markers within adipose tissue is unknown in this present study, circulating 5-HT contributes to inflammation and immunity via a variety of 5-HT receptors on immune cells, with one of the downstream effects being the recruitment of macrophages (Shajib and Khan, 2015). Gut-derived 5-HT may also contribute to adiposity by increasing bile acid turnover thereby increasing the absorption of fats from the lumen (Watanabe et al., 2010). Indeed, pharmacological inhibition of intestinal 5-HT synthesis has been shown to decrease circulating FFA (Sumara et al., 2012). Lipid clearance from the circulation is also reduced in the absence of gut microbiota, thereby decreasing lipid uptake and storage within adipocytes (Velagapudi et al., 2010, Backhed et al., 2007), however whether this is due to reduced 5-HT in these mice is unknown. Reductions in mucosal 5-HT may, therefore, decrease the absorption and storage of dietary fats, thus reducing the subcutaneous adiposity observed in all treatment groups in this study. This was independent of changes in weight, however, and it is unknown whether changes in visceral adiposity occurred in mice within this study.

Having established that the gut microbiome influences host metabolism, at least in part, via influencing gut-derived 5-HT, this study also aimed to determine for the first time whether a bidirectional relationship exists between the gut microbiome and EC-cell 5-HT. A significant shift in a number of genera was observed following pharmacological reduction of gut-derived 5-HT. In particular, there was a significant increase in the abundance of *Bacteroides*, *Akkermansia* and *Allobaculum*. *Akkermansia muciniphila* has been positively linked with improved metabolism in both lean and high fat diet-fed mouse models (Plovier et al., 2017, Schneeberger et al., 2015, Zhao et al., 2017) and with reduced lipid metabolism occurring via fatty acid oxidation (Schneeberger et al., 2015). It is also associated with reduced chronic low grade inflammation in adipose tissue (Zhao et al., 2017), possibly through interactions of a bacterial outer membrane protein with Toll-like receptor 2 (Plovier et al., 2017). Increased abundance of *Allobaculum*, a genus within the Firmicutes phylum, is also potentially beneficial for host physiology. *Allobaculum* is negatively correlated with metabolic disease (Wang et al., 2015), improves insulin sensitivity in a high fat diet rodent model (Zhang et al., 2012) and is responsive to changes in dietary intake (Everard et al., 2014, Ravussin et al., 2012, Zhang et al., 2012). The present study did not assess changes in concentrations of microbial metabolites following LP533401 treatment; however, the shift in the specific microbial genera within this group correlates with increased production of certain microbial metabolites. *Bacteroides, Akkermansia and Allobaculum* contain key SCFA (particularly propionate) producing species (Derrien et al., 2004, Rios-Covian et al., 2017), with members of the Bacteroidetes phylum being the largest producers of propionate within the human gut (Salonen et al., 2014, Aguirre et al., 2016). While the types and abundance of SCFAs and other microbial metabolites are highly influenced by diet and the existing microbial composition, increased propionate synthesis from *Bacteroides* and *Akkermansia* may be partly responsible for improved glucose homeostasis (De Vadder et al., 2014). In addition to acting as signalling molecules within the lumen, intestinal SCFAs can enter the hepatic circulation where they are metabolised by the

liver and other peripheral tissues (den Besten et al., 2014, den Besten et al., 2013). Within the liver, three major SCFA (acetate, propionate and butyrate) act in concert to modulate hepatic gluconeogenesis and lipogenesis, with propionate in particular shown to reduce visceral and hepatic adiposity by decreasing triglyceride accumulation in obese humans (Chambers et al., 2015). Further to this, intestinal gluconeogenesis, triggered by propionate, provides negative feedback to the liver in a homeostatic mechanism to reduce hepatic glucose production and maintain plasma glucose levels (De Vadder et al., 2014).

The modulation of microbial populations through the reduction of intestinal 5-HT highlights a bidirectional relationship between the gut microbiome and gut-derived 5-HT. Certain species of gut microbiota have the capacity to synthesise 5-HT themselves, and although the exact molecular pathway has not yet been elucidated, it is believed to be via pathways independent of TPH (Tsavkelova et al., 2006). As such, the oral-delivery of the TPH inhibitor, LP533401, is unlikely to directly influence bacterial 5-HT synthesis. Locally within commensal microbial populations, 5-HT stimulates bacterial growth and cell aggregation within certain species (Oleskin et al., 2016). It is unknown, however, whether microbial-derived 5-HT influences host physiology.

While the results from the present study using a mouse model of antibiotic-induced dysbiosis demonstrate for the first time that gut 5-HT is a signalling mediator between the gut microbiome and host metabolism, there is not yet clear evidence of antibiotic-induced changes to host metabolism in humans. Investigations involving antibiotic administration in humans have provided negative results in terms of metabolic benefits, showing no changes to host metabolism with microbiota manipulation in spite of longer-lasting effects on the composition of gut microbiome (Mikkelsen et al., 2015, Reijnders et al., 2016), and even a negative effect on insulin sensitivity with vancomycin treatment (Vrieze et al., 2014). This may be due to the extremely acute duration of these studies (≤ 7 days), which likely negates any changes to EC

cell numbers seen with intestinal dysbiosis (Yano et al., 2015), as endocrine cell differentiation occurs over a longer period of time. In addition, humans have inherent intestinal microbiome variability, and studies on humans do not completely deplete the gut microbiome (Reijnders et al., 2016, Vrieze et al., 2014, Mikkelsen et al., 2015). As such, remaining bacterial populations may have an unknown impact on host metabolism. The complete ablation of gut microbiota cannot be used as a potential treatment option, as commensal microbiota are needed to aid in the digestion of complex carbohydrates and starches and contribute to mucosal integrity. Rather, the complex, bidirectional relationship between the gut microbiome and gut-derived 5-HT represents a novel potential therapeutic avenue to improve host metabolism.

4.5 Conclusion

This study has highlighted a novel and dynamic bi-directional relationship between 5-HT and the gut microbiome, and provides new knowledge into the pathway by which the gut microbiome influences host metabolism. Independently, both microbial dysbiosis and reduced 5-HT improve blood glucose maintenance and subcutaneous adiposity. Combining microbial dysbiosis and 5-HT depletion showed no additive effects on glucose tolerance or insulin sensitivity compared to dysbiosis alone, suggesting that the gut microbiome is influencing host metabolism by augmenting gut 5-HT. However, it is likely that other additional mechanisms are involved, particularly associated with insulin sensitivity. It is unclear what these mechanisms are, although they may involve increased GLP-1, PYY and glucagon. These hormones are all increased with dysbiosis, but are not associated with changes to centrally mediated satiety and physical activity. Thermogenic capacity is unaltered by 5-HT depletion or microbial dysbiosis, however increased browning or reduced lipid storage may contribute to improved host metabolism by augmenting adiposity within white adipose stores.

CHAPTER 5: General Discussion

The aim of this work was to characterise EC cells from the mouse gut, with particular respect to the role they play as sensory cells within the GI lumen. Using a combination of isolated primary mouse EC cell cultures, and mouse models of diet-induced obesity and antibiotic-induced microbial dysbiosis, this work specifically aimed to answer the following questions:

1. Do EC cells possess the capacity to detect and respond to nutrients within the gastrointestinal lumen?
2. Do the nutrient-sensing capabilities of EC cells depend on their location within the gastrointestinal tract?
3. How does the nutrient-sensing capacity of EC cells change with diet-induced obesity and development of metabolic disease?
4. Does EC cell-derived 5-HT act as a signalling nexus between the gut microbiome and host metabolism?

This chapter describes how the above questions have been addressed and highlights the contributions to the field made by this thesis.

5.1 Summary of results and implications

5.1.1 EC cells are luminal nutrient sensors within the gut

Previous investigations into the ability of EC cells to detect and respond to luminal nutrient cues have relied upon the use of stable 5-HT-secreting cell lines, such as BON and RIN14B cells, or whole-tissue preparations in which release of 5-HT may also be influenced by confounding factors such as muscular contractions. Neither of these models has demonstrated, at a cellular level, the mechanisms by which native EC cells detect luminal nutrients. This body of work is the first to isolate primary EC cells from unique regions of the mouse GI tract, using a method of isolation that provides highly enriched EC cell populations. This has allowed for a paired comparison of EC cells from two distinct regions of the gut: the duodenum and colon. This thesis has demonstrated, in *Chapter 2,* the novel finding that EC cells from the duodenum and colon of mice have the capacity to detect a number of luminal nutrients, through the use of real-time PCR to detect mRNA expression of receptors and transporters for sensing sugars and sweet tastants, as well as short-, medium- and long-chain fatty acids and protein metabolites.

To determine whether the expression of nutrient sensing receptors and transporters conveys an ability of nutrients to trigger 5-HT release, the present study in *Chapter 3* used a highly sensitive 5-HT ELISA to examine the outcomes of acute (20 mins) exposure of duodenal and colon EC cells to high (100-300 μM) luminal concentrations of dietary sugars. Indeed, high glucose triggered 5-HT release from both duodenal and colonic EC cells, while sensitivity to fructose and sucrose stimulation was unique to duodenal EC cells. The increased 5-HT release observed following nutrient stimulation was also associated with an increase in intracellular calcium, as detected by flow cytometry, and importantly was not simply caused by osmotic stress. As such, findings from this thesis highlight potential mechanistic pathways by which sugars increase 5-HT release, via metabolic processes and through changes in intracellular calcium. Given the increased sugar consumption in Western society, and the role that gut-

derived 5-HT plays in obesity and metabolic disease, findings from this study are of particular consequence, and provide novel insight into the role of increased dietary sugar consumption in the pathogenesis of disease. A role for EC cell 5-HT has been established in altered gastrointestinal function, such as slowed gastric emptying or gastroparesis, which is commonly associated with diabetes and has implications on glycaemic control. The present study in *Chapter 2* also investigated the impact of luminal nutrient exposure on motility patterns in *ex vivo* duodenal and colonic preparations. Both duodenal and colonic motility were inhibited with exposure to high luminal glucose; however, whether this is due to a direct effect of EC cell 5-HT was not able to be evaluated due to time constraints.

In accordance with the findings from others, my research demonstrates a dynamic relationship between intestinal bacteria and EC cells, as the presence of the gut microbiome is associated with increased mucosal and circulating 5-HT. The underlying mechanisms by which native EC cells detect the gut microbiome are unknown; however, EC cells appear to be stimulated by chronic exposure to luminal microbial metabolites such as SCFA. This study has shown that EC cells express the two main SCFA-sensing receptors, and that exposure of primary duodenal and colonic EC cells to luminal concentrations of acetate, propionate and butyrate (the three major SCFAs) does not acutely trigger 5-HT release. These findings are therefore supportive of evidence that chronic, but not acute, exposure to SCFAs increases 5-HT biosynthesis, through a transcriptionally mediated pathway, and contributes to understanding the mechanisms by which dietary and microbiota-derived SCFAs can increase 5-HT synthesis and secretion.

5.1.2 Nutrient sensing by EC cells is region-specific

EC cells are present throughout the length of the gut; however, the luminal environment varies substantially over the length of the digestive tract. To date, no study has investigated how EC cells differ at a cellular level between two distinctly different regions of the gut. To

determine this, I made paired comparisons between EC cells from two vastly different luminal environments: the duodenum and colon. The work in *Chapter* 2 and *Chapter 3* has revealed, for the first time, distinct nutrient sensing repertoires of EC cells located in these two regions. In particular, sugar transporters and sweet taste receptors were enriched in duodenal EC cells, indicative that cells in this region are tuned to sensing a variety of luminal sugars compared to the colon. Colonic EC cells, on the other hand, are more highly tuned to detect free fatty acids compared to those in the duodenum. Intriguingly, colonic EC cells are more sensitive to luminal glucose, while duodenal EC cells are more sensitive to fructose and sucrose. The preference of colonic EC cells to glucose, which rarely reaches the colon under healthy conditions, may therefore represent a mechanism by which colonic EC cells detect and respond to, abnormal gastrointestinal function.

5.1.3 Diet-induced obesity alters EC cell nutrient sensing

These novel insights into how duodenal and colonic EC cells differentially detect luminal nutrients, also contributes to understanding how changes in EC cell nutrient sensing may respond to obesity and metabolic disease progression. The high fat diet-induced obese, diabetic mouse model used in *Chapter 2* of this study resembles the metabolic syndrome in humans, with accompanying increased circulating 5-HT. To determine whether changes in EC cell nutrient sensing underlie the increased circulating 5-HT, mRNA expression of nutrient receptors and transporters in duodenal and colonic EC cells were analysed using real-time PCR in mice fed a control diet or HFD. Duodenal EC cells from HFD mice have a reduced capacity to detect fructose, sweet tastants and SCFAs, while colonic EC cells from HFD mice have an increased capacity to detect fructose, and display a positive correlation between SCFA sensing capacity and weight gain. Of note, expression of TPH1 was greater in colonic EC cells from obese mice compared to lean controls; an effect not observed in duodenal EC cells. The findings presented in this thesis are the first to demonstrate, at a cellular level, changes in

nutrient signalling to EC cells which may influence the release of 5-HT under high fat diet conditions, with changes in colonic 5-HT biosynthesis likely contributing to increased circulating 5-HT.

5.1.4 Gut-derived 5-HT acts as a signalling nexus between the gut microbiome and host metabolism

The described increase in colonic TPH1 expression with high fat diet shown in *Chapter 2* may be due to diet-induced alterations to the intestinal microbiome. The evidence presented in *Chapter 4* of this thesis is the first to demonstrate the existence of a microbiome - gut 5-HT - host metabolism axis, through both selectively and concurrently targeting the gut microbiome and intestinal 5-HT synthesis. Depletion of the gut microbiome, associated with reduced EC cell 5-HT, has a positive effect on host metabolism, improving blood glucose control and reducing subcutaneous adiposity. Inhibition of 5-HT synthesis also has a positive effect on whole-body metabolism, similar to that observed with microbiome depletion. Notably, the combined depletion of the gut microbiome and reduced gut-derived 5-HT did not show any additive effects on improving host metabolism, highlighting that the microbiome signals through EC cells to influence host metabolism. Microbiome depletion caused greater improvements in insulin sensitivity compared to only reducing 5-HT, indicative that the microbiome alters insulin sensitivity through EC cells and additional pathways. Serum glucagon, GLP-1 and PYY were all increased by antibiotic-induced dysbiosis, but not by reduced 5-HT synthesis. However, the mechanisms underlying this, and whether they contribute to the increased insulin sensitivity is unknown.

Another significant and highly novel finding from *Chapter 4* of this work is that inhibition of EC cell 5-HT synthesis alters the type and abundance of gut microbes. This demonstrates for the first time the existence of a bi-directional relationship between EC cells and the intestinal microbiome. This raises the notion that 5-HT may be influencing host metabolism

via a direct effect on the gut microbiome. Given that EC cell 5-HT is increased in human obesity and T2D, which are also driven by microbial changes, regulation of the gut microbiome by 5-HT is an interesting phenomenon with examining. Together, the findings presented in this thesis provide a significant insight into how the gut microbiome influences host metabolism, which is through signalling to EC cells and mediating 5-HT release. This also provides a platform for further understanding the precise mechanisms by which the gut microbiome signal to EC cells, which may provide novel therapeutic targets for obesity and metabolic disease.

5.2 Future directions

The current body of work has provided significant insight into the role of EC cells as sensory cells within the GI tract, the changes that occur within EC cells that may contribute to obesity and metabolic disease, and the role of gut 5-HT as a mediator through which the gut microbiome effects host metabolism. The current work may be complemented in the future by investigations focusing on mechanistic pathways of EC cell activation by luminal nutrients, principally the transport of sugars intracellularly to trigger an increase in 5-HT release, and the physiological implications of this increased 5-HT release.

The mechanisms underlying sugar-induced 5-HT release are yet to be determined. Future work may utilise pharmacological approaches to selectively target specific signalling pathways. The non-metabolisable sugar, α-MG, does not increase 5-HT secretion, highlighting a potential metabolic pathway regulating sugar-induced 5-HT secretion. Pharmacological antagonists for hexose transporters, such as phloretin (GLUT1&2 inhibitor) and phloridzin (SGLT1 inhibitor), could also be used to determine the specific pathways for cellular uptake of sugars. EC cells contain L-type calcium channels, however the extent to which extracellular and intracellular calcium stores contribute to 5-HT release is unknown. This could be determined by assessing the release of 5-HT in the absence of intracellular calcium, through the use of thapsigargin to deplete calcium stores within the endoplasmic reticulum, and in

absence of extracellular calcium, by removing calcium from the extracellular media or by blocking voltage-gated calcium channels.

Findings from this study highlight that the capacity for EC cells to detect luminal sugars, sweet tastants and SCFAs is altered by exposure to a HFD, and that duodenal and colonic EC cells are differentially affected with diet-induced obesity. Further investigation is needed to determine whether the transcriptional changes observed in EC cells from obese, diabetic mice relate to altered EC cell signalling, and the downstream effects on 5-HT secretion. In addition, a comprehensive transcriptome profile, using an RNASeq approach, could be used to determine the full extent to which EC cells are altered under obesogenic conditions. The use of EC cells derived from mice for this particular technique is beneficial compared to using EC cells derived from humans, as there is less genetic variability in mice of the same genetic background compared to that in humans, and could therefore more readily highlight changes specifically caused by diet-induced obesity. Along with this, future studies are needed to determine the cellular mechanisms by which HFD consumption drives changes in EC cell nutrient sensing profile, and particularly increased colonic EC cell 5-HT biosynthesis and increased colonic EC cell numbers. A possible, and important, avenue of investigation into this is the communication between the gut microbiome and EC cells.

The work presented in this thesis has demonstrated a key role of gut 5-HT in mediating the effects of the gut microbiome on host metabolism. As such, changes to the composition of bacterial species, and the relative abundance and types of bacterial metabolites, has significant implications for host metabolism. Diet influences the composition of the gut microbiome, the number of EC cells and the nutrient sensing profile of EC cells. Further investigation is needed to definitively determine whether gut 5-HT is a key intermediary through which the microbiome influences host metabolism under obesogenic conditions. Such studies could include the use of Tph1 KO mice to remove all gut 5-HT, as well as the use of germ-free mice,

as an alternative model of dysbiosis to the antibiotic model used here. The addition of high fat diet mouse cohorts in each of these studies will also be beneficial. This work has demonstrated that microbial SCFAs do not acutely stimulate 5-HT release over 20 minutes. Rather, the chronic exposure of EC cells to microbial metabolites likely mediates the increased in circulating and mucosal 5-HT. Future interrogation of the mechanisms by which the gut microbiome signal to mucosal EC cells is needed. This could be achieved using an intestinal organoid culture approach, to observe whether chronic exposure to specific microbial metabolites increase EC cell density and/or 5-HT synthesis in individual cells. The inhibition of 5-HT synthesis alters the abundance of several metabolically significant microbial genera. However, mechanisms surrounding this bidirectional relationship are unknown. Further investigation is needed to determine how 5-HT alters the composition of the gut microbiome and what the physiological implications of this are. This may be answered through the use of faecal microbiota transplantation from donor mice exhibiting altered microbial composition following 5-HT depletion, and assessing the metabolic outcomes.

This study has described several significant findings within mouse models. However, to determine the therapeutic implications of targeting EC cells and gut-derived 5-HT pathways in health and disease, future work is needed to determine if these signalling pathways described in mice also exist in humans. The techniques described in this study using pure primary EC cell cultures from mice are directly transferrable to human tissue, which also allows for a comparison between the physiological characteristics of EC cells in mice compared to humans. Previous antibiotic intervention studies in humans has yielded negative results regarding the impact of the gut microbiome on host metabolism (Vrieze et al., 2014, Mikkelsen et al., 2015), likely as a result of the short duration of these studies. In mice, however, interventions of longer duration provide clear evidence that the composition of the gut microbiome strongly influences metabolic status (Carvalho et al., 2012, Membrez et al., 2008, Cox et al., 2014).

Future studies are therefore needed to determine whether the interaction between the gut microbiome and 5-HT exist in humans. A possible approach for this is to determine whether correlations exist between intestinal microbial composition, circulating and mucosal 5-HT, and host metabolism within individuals in cohorts of lean and obese individuals.

5.3 Concluding remarks

The results of this study have demonstrated that EC cells act as region-dependent nutrient sensors within the gut lumen. This work also shows that subtypes of EC cells may exist, as EC cells from two unique regions of the gut have the capacity to detect a number of dietary nutrients, and this is dependent upon their location within the GI tract. Using a single cell approach, this study has revealed that duodenal EC cells are more responsive than colonic EC cells to fructose and sucrose, while the opposite is observed for responses to glucose. It has also been revealed that acute stimulation to luminal concentrations of SCFA do not trigger increases in intracellular calcium or 5-HT secretion from either duodenal or colonic EC cells. Using a mouse model of diet-induced obesity and metabolic dysfunction, this study highlights that in duodenal and colonic EC cells, expression of nutrient receptors and transporters to detect luminal sugars, sweet tastants and SCFAs is differentially affected by dietary changes, along with increased colonic EC cell numbers, which ultimately leads to increased circulating 5-HT. These findings provide insight into how changes within individual EC cells may contribute to increases in circulating 5-HT with obesity and metabolic disease. This study provides ground breaking evidence that gut 5-HT acts as a signalling nexus between the gut microbiome and host metabolism. This is through improving glucose tolerance and, in part, insulin sensitivity, and reducing subcutaneous adiposity under normal diet conditions. This work also provides the first evidence for the existence of a bidirectional relationship between the gut microbiome and 5-HT. In light of these observations, this study has demonstrated that EC cells are important, region-specific sensory cells that can detect and respond to changes in the luminal

environment of the GI tract, and that this can have significant consequences for regulating host metabolism and potentially human health.

References

ABATE, N., GARG, A., PESHOCK, R. M., STRAY-GUNDERSEN, J. & GRUNDY, S. M. 1995. Relationships of generalized and regional adiposity to insulin sensitivity in men. *Journal of Clinical Investigation,* 96**,** 88-98.

ABBOTT, C. R., MONTEIRO, M., SMALL, C. J., SAJEDI, A., SMITH, K. L., PARKINSON, J. R., GHATEI, M. A. & BLOOM, S. R. 2005. The inhibitory effects of peripheral administration of peptide YY(3-36) and glucagon-like peptide-1 on food intake are attenuated by ablation of the vagal-brainstem-hypothalamic pathway. *Brain Res,* 1044**,** 127-31.

ABDOUH, M., STORRING, J. M., RIAD, M., PAQUETTE, Y., ALBERT, P. R., DROBETSKY, E. & KOUASSI, E. 2001. Transcriptional mechanisms for induction of 5-HT1A receptor mRNA and protein in activated B and T lymphocytes. *J Biol Chem,* 276**,** 4382-8.

AGUIRRE, M., ECK, A., KOENEN, M. E., SAVELKOUL, P. H., BUDDING, A. E. & VENEMA, K. 2016. Diet drives quick changes in the metabolic activity and composition of human gut microbiota in a validated in vitro gut model. *Res Microbiol,* 167**,** 114-25.

AHERN, G. P. 2011. 5-HT and the immune system. *Curr Opin Pharmacol,* 11**,** 29-33.

AHLMAN, H. & NILSSON, O. 2001. The gut as the largest endocrine organ in the body. *Annals of Oncology,* 12**,** S63-S68.

AKIBA, Y., INOUE, T., KAJI, I., HIGASHIYAMA, M., NARIMATSU, K., IWAMOTO, K., WATANABE, M., GUTH, P. H., ENGEL, E., KUWAHARA, A. & KAUNITZ, J. D. 2015. Short-chain fatty acid sensing in rat duodenum. *J Physiol,* 593**,** 585-99.

ALARD, J., LEHRTER, V., RHIMI, M., MANGIN, I., PEUCELLE, V., ABRAHAM, A. L., MARIADASSOU, M., MAGUIN, E., WALIGORA-DUPRIET, A. J., POT, B., WOLOWCZUK, I. & GRANGETTE, C. 2016. Beneficial metabolic effects of selected probiotics on diet-induced obesity and insulin resistance in mice are associated with improvement of dysbiotic gut microbiota. *Environ Microbiol,* 18**,** 1484-97.

ALBERT, P. R., SAJEDI, N., LEMONDE, S. & GHAHREMANI, M. H. 1999. Constitutive G(i2)-dependent activation of adenylyl cyclase type II by the 5-HT1A receptor. Inhibition by anxiolytic partial agonists. *J Biol Chem,* 274**,** 35469-74.

ALBILLOS, A., DERNICK, G., HORSTMANN, H., ALMERS, W., ALVAREZ DE TOLEDO, G. & LINDAU, M. 1997. The exocytotic event in chromaffin cells revealed by patch amperometry. *Nature,* 389**,** 509-12.

ALEMI, F., POOLE, D. P., CHIU, J., SCHOONJANS, K., CATTARUZZA, F., GRIDER, J. R., BUNNETT, N. W. & CORVERA, C. U. 2013. The receptor TGR5 mediates the prokinetic actions of intestinal bile acids and is required for normal defecation in mice. *Gastroenterology,* 144**,** 145-54.

ALEX, S., LANGE, K., AMOLO, T., GRINSTEAD, J. S., HAAKONSSON, A. K., SZALOWSKA, E., KOPPEN, A., MUDDE, K., HAENEN, D., AL-LAHHAM, S., ROELOFSEN, H., HOUTMAN, R., VAN DER BURG, B., MANDRUP, S., BONVIN, A. M., KALKHOVEN, E., MULLER, M., HOOIVELD, G. J. & KERSTEN, S. 2013. Short-chain fatty acids stimulate angiopoietin-like 4 synthesis in human colon adenocarcinoma cells by activating peroxisome proliferator-activated receptor gamma. *Mol Cell Biol,* 33**,** 1303-16.

ALEXANDER, C. & RIETSCHEL, E. T. 2001. Bacterial lipopolysaccharides and innate immunity. *J Endotoxin Res,* 7**,** 167-202.

ALMACA, J., MOLINA, J., MENEGAZ, D., PRONIN, A. N., TAMAYO, A., SLEPAK, V., BERGGREN, P. O. & CAICEDO, A. 2016. Human Beta Cells Produce and Release Serotonin to Inhibit Glucagon Secretion from Alpha Cells. *Cell Rep,* 17**,** 3281-3291.

AMIREAULT, P., BAYARD, E., LAUNAY, J. M., SIBON, D., LE VAN KIM, C., COLIN, Y., DY, M., HERMINE, O. & COTE, F. 2013. Serotonin is a key factor for mouse red blood cell survival. *PLoS One,* 8**,** e83010.

AMIREAULT, P. & DUBE, F. 2005. Intracellular cAMP and calcium signaling by serotonin in mouse cumulus-oocyte complexes. *Mol Pharmacol,* 68**,** 1678-87.

AMIREAULT, P., HATIA, S., BAYARD, E., BERNEX, F., COLLET, C., CALLEBERT, J., LAUNAY, J. M., HERMINE, O., SCHNEIDER, E., MALLET, J., DY, M. & COTE, F. 2011. Ineffective erythropoiesis with reduced red blood cell survival in serotonin-deficient mice. *Proc Natl Acad Sci U S A,* 108**,** 13141-6.

AMMALA, C., ASHCROFT, F. M. & RORSMAN, P. 1993. Calcium-independent potentiation of insulin release by cyclic AMP in single beta-cells. *Nature,* 363**,** 356-8.

ARITA, Y., KIHARA, S., OUCHI, N., TAKAHASHI, M., MAEDA, K., MIYAGAWA, J., HOTTA, K., SHIMOMURA, I., NAKAMURA, T., MIYAOKA, K., KURIYAMA, H., NISHIDA, M., YAMASHITA, S., OKUBO, K., MATSUBARA, K., MURAGUCHI, M., OHMOTO, Y., FUNAHASHI, T. & MATSUZAWA, Y. 1999. Paradoxical decrease of an adipose-specific protein, adiponectin, in obesity. *Biochem Biophys Res Commun,* 257**,** 79-83.

ATARASHI, K., TANOUE, T., OSHIMA, K., SUDA, W., NAGANO, Y., NISHIKAWA, H., FUKUDA, S., SAITO, T., NARUSHIMA, S., HASE, K., KIM, S., FRITZ, J. V., WILMES, P., UEHA, S., MATSUSHIMA, K., OHNO, H., OLLE, B., SAKAGUCHI, S., TANIGUCHI, T., MORITA, H., HATTORI, M. & HONDA, K. 2013. Treg induction by a rationally selected mixture of Clostridia strains from the human microbiota. *Nature,* 500**,** 232-6.

BACKHED, F., DING, H., WANG, T., HOOPER, L. V., KOH, G. Y., NAGY, A., SEMENKOVICH, C. F. & GORDON, J. I. 2004. The gut microbiota as an environmental factor that regulates fat storage. *Proc Natl Acad Sci U S A,* 101**,** 15718-23.

BACKHED, F., MANCHESTER, J. K., SEMENKOVICH, C. F. & GORDON, J. I. 2007. Mechanisms underlying the resistance to diet-induced obesity in germ-free mice. *Proc Natl Acad Sci U S A,* 104**,** 979-84.

BAGANZ, N. L. & BLAKELY, R. D. 2013. A dialogue between the immune system and brain, spoken in the language of serotonin. *ACS Chem Neurosci,* 4**,** 48-63.

BALDEIRAS, I. E., SANTOS, R. M. & ROSARIO, L. M. 2006. Protein kinase C isoform specificity of cholinergic potentiation of glucose-induced pulsatile 5-HT/ insulin release from mouse pancreatic islets. *Biol Res,* 39**,** 531-9.

BANSAL, S. 1988. Sexual dysfunction in hypertensive men. A critical review of the literature. *Hypertension,* 12**,** 1-10.

BAO, Y. Q., ZHOU, M., ZHOU, J., LU, W., GAO, Y. C., PAN, X. P., TANG, J. L., LU, H. J. & JIA, W. P. 2011. Relationship between serum osteocalcin and glycaemic variability in Type 2 diabetes. *Clin Exp Pharmacol Physiol,* 38**,** 50-4.

BARBOSA, R. M., SILVA, A. M., TOME, A. R., STAMFORD, J. A., SANTOS, R. M. & ROSARIO, L. M. 1996. Real time electrochemical detection of 5-HT/insulin secretion from single pancreatic islets: effect of glucose and K+ depolarization. *Biochem Biophys Res Commun,* 228**,** 100-4.

BARBOSA, R. M., SILVA, A. M., TOME, A. R., STAMFORD, J. A., SANTOS, R. M. & ROSARIO, L. M. 1998. Control of pulsatile 5-HT/insulin secretion from single mouse pancreatic islets by intracellular calcium dynamics. *J Physiol,* 510 (Pt 1)**,** 135-43.

BARKER, N. 2014. Adult intestinal stem cells: critical drivers of epithelial homeostasis and regeneration. *Nat Rev Mol Cell Biol,* 15**,** 19-33.

BARRETO, S. G., BAZARGAN, M., ZOTTI, M., HUSSEY, D. J., SUKOCHEVA, O. A., PEIRIS, H., LEONG, M., KEATING, D. J., SCHLOITHE, A. C., CARATI, C. J., SMITH, C., TOOULI, J. & SACCONE, G. T. 2011. Galanin receptor 3--a potential target for acute pancreatitis therapy. *Neurogastroenterol Motil,* 23**,** e141-51.

BATTAGLINO, R., FU, J., SPATE, U., ERSOY, U., JOE, M., SEDAGHAT, L. & STASHENKO, P. 2004. Serotonin regulates osteoclast differentiation through its transporter. *J Bone Miner Res,* 19**,** 1420-31.

BELLONO, N. W., BAYRER, J. R., LEITCH, D. B., CASTRO, J., ZHANG, C., O'DONNELL, T. A., BRIERLEY, S. M., INGRAHAM, H. A. & JULIUS, D. 2017. Enterochromaffin Cells Are Gut Chemosensors that Couple to Sensory Neural Pathways. *Cell*.

BENNET, H., BALHUIZEN, A., MEDINA, A., DEKKER NITERT, M., OTTOSSON LAAKSO, E., ESSEN, S., SPEGEL, P., STORM, P., KRUS, U., WIERUP, N. & FEX, M. 2015. Altered serotonin (5-HT) 1D and 2A receptor expression may contribute to defective insulin and glucagon secretion in human type 2 diabetes. *Peptides,* 71**,** 113-20.

BENNET, H., MOLLET, I. G., BALHUIZEN, A., MEDINA, A., NAGORNY, C., BAGGE, A., FADISTA, J., OTTOSSON-LAAKSO, E., VIKMAN, P., DEKKER-NITERT, M., ELIASSON, L., WIERUP, N., ARTNER, I. & FEX, M. 2016. Serotonin (5-HT) receptor 2b activation augments glucose-stimulated insulin secretion in human and mouse islets of Langerhans. *Diabetologia,* 59**,** 744-54.

BERGER, M., SCHEEL, D. W., MACIAS, H., MIYATSUKA, T., KIM, H., HOANG, P., KU, G. M., HONIG, G., LIOU, A., TANG, Y., REGARD, J. B., SHARIFNIA, P., YU, L., WANG, J., COUGHLIN, S. R., CONKLIN, B. R., DENERIS, E. S., TECOTT, L. H. & GERMAN, M. S. 2015. Gαi/o-coupled receptor signaling restricts pancreatic β-cell expansion. *Proceedings of the National Academy of Sciences,* 112**,** 2888-2893.

BERTRAND, P. P. 2004. Real-time detection of serotonin release from enterochromaffin cells of the guinea-pig ileum. *Neurogastroenterol Motil,* 16**,** 511-4.

BERTRAND, P. P. 2006. Real-time measurement of serotonin release and motility in guinea pig ileum. *J Physiol,* 577**,** 689-704.

BERTRAND, P. P. & BERTRAND, R. L. 2010. Serotonin release and uptake in the gastrointestinal tract. *Auton Neurosci,* 153**,** 47-57.

BERTRAND, P. P., KUNZE, W. A., FURNESS, J. B. & BORNSTEIN, J. C. 2000. The terminals of myenteric intrinsic primary afferent neurons of the guinea-pig ileum are excited by 5-hydroxytryptamine acting at 5-hydroxytryptamine-3 receptors. *Neuroscience,* 101**,** 459-69.

BERTRAND, R. L., SENADHEERA, S., MARKUS, I., LIU, L., HOWITT, L., CHEN, H., MURPHY, T. V., SANDOW, S. L. & BERTRAND, P. P. 2011. A Western diet increases serotonin availability in rat small intestine. *Endocrinology,* 152**,** 36-47.

BERTRAND, R. L., SENADHEERA, S., TANOTO, A., TAN, K. L., HOWITT, L., CHEN, H., MURPHY, T. V., SANDOW, S. L., LIU, L. & BERTRAND, P. P. 2012. Serotonin availability in rat colon is reduced during a Western diet model of obesity. *Am J Physiol Gastrointest Liver Physiol,* 303**,** G424-G434.

BEZERRA DOS SANTOS MAGALHAES, K., MAGALHAES, M. M., DINIZ, E. T., LUCENA, C. S., GRIZ, L. & BANDEIRA, F. 2013. Metabolic syndrome and central fat distribution are related to lower serum osteocalcin concentrations. *Ann Nutr Metab,* 62**,** 183-8.

BHASKARAN, S., ZALUSKI, J. & BANES-BERCELI, A. 2014. Molecular interactions of serotonin (5-HT) and endothelin-1 in vascular smooth muscle cells: in vitro and ex vivo analyses. *Am J Physiol Cell Physiol,* 306**,** C143-51.

BILLUPS, D., BILLUPS, B., CHALLISS, R. A. & NAHORSKI, S. R. 2006. Modulation of Gq-protein-coupled inositol trisphosphate and Ca2+ signaling by the membrane potential. *J Neurosci,* 26**,** 9983-95.

BISCHOFF, S. C., MAILER, R., PABST, O., WEIER, G., SEDLIK, W., LI, Z., CHEN, J. J., MURPHY, D. L. & GERSHON, M. D. 2009. Role of serotonin in intestinal inflammation: knockout of serotonin reuptake transporter exacerbates 2,4,6-trinitrobenzene sulfonic acid colitis in mice. *Am J Physiol Gastrointest Liver Physiol,* 296**,** G685-95.

BLEICH, A. & FOX, J. G. 2015. The Mammalian Microbiome and Its Importance in Laboratory Animal Research. *ILAR J,* 56**,** 153-8.

BLUM, I., NESSIEL, L., DAVID, A., GRAFF, E., HARSAT, A., WEISSGLAS, L., GABBAY, U., SULKES, J., YERUSHALMY, Y. & VERED, Y. 1992. Plasma neurotransmitter profile during different phases of the ovulatory cycle. *J Clin Endocrinol Metab,* 75**,** 924-9.

BOEHME, S. A., LIO, F. M., SIKORA, L., PANDIT, T. S., LAVRADOR, K., RAO, S. P. & SRIRAMARAO, P. 2004. Cutting edge: serotonin is a chemotactic factor for eosinophils and functions additively with eotaxin. *J Immunol,* 173**,** 3599-603.

BOGUNOVIC, M., DAVE, S. H., TILSTRA, J. S., CHANG, D. T., HARPAZ, N., XIONG, H., MAYER, L. F. & PLEVY, S. E. 2007. Enteroendocrine cells express functional Toll-like receptors. *Am J Physiol Gastrointest Liver Physiol,* 292**,** G1770-83.

BOYER, S., SHARP, P. A., DEBNAM, E. S., BALDWIN, S. A. & SRAI, S. K. 1996. Streptozotocin diabetes and the expression of GLUT1 at the brush border and basolateral membranes of intestinal enterocytes. *FEBS Lett,* 396**,** 218-22.

BRAUN, T., VOLAND, P., KUNZ, L., PRINZ, C. & GRATZL, M. 2007. Enterochromaffin cells of the human gut: sensors for spices and odorants. *Gastroenterology,* 132**,** 1890-901.

BROWN, A. J., GOLDSWORTHY, S. M., BARNES, A. A., EILERT, M. M., TCHEANG, L., DANIELS, D., MUIR, A. I., WIGGLESWORTH, M. J., KINGHORN, I., FRASER, N. J., PIKE, N. B., STRUM, J. C., STEPLEWSKI, K. M., MURDOCK, P. R., HOLDER, J. C., MARSHALL, F. H., SZEKERES, P. G., WILSON, S., IGNAR, D. M., FOORD, S. M., WISE, A. & DOWELL, S. J. 2003. The Orphan G protein-coupled receptors GPR41 and GPR43 are activated by propionate and other short chain carboxylic acids. *J Biol Chem,* 278**,** 11312-9.

BUNCE, K. T. & TYERS, M. B. 1992. The Role of 5-HT in Postoperative Nausea and Vomiting. *BJA: British Journal of Anaesthesia,* 69**,** 60S-62S.

BYTZER, P., TALLEY, N. J., HAMMER, J., YOUNG, L. J., JONES, M. P. & HOROWITZ, M. 2002. GI symptoms in diabetes mellitus are associated with both poor glycemic control and diabetic complications. *Am J Gastroenterol,* 97**,** 604-611.

CAESAR, R., REIGSTAD, C. S., BACKHED, H. K., REINHARDT, C., KETONEN, M., LUNDEN, G. O., CANI, P. D. & BACKHED, F. 2012. Gut-derived lipopolysaccharide augments adipose macrophage accumulation but is not essential for impaired glucose or insulin tolerance in mice. *Gut,* 61**,** 1701-7.

CARTWRIGHT, B., ROBINSON, J., SEED, P. T., FOGELMAN, I. & RYMER, J. 2016. Hormone replacement therapy versus the combined oral contraceptive pill in premature ovarian failure: a randomised controlled trial of the effects on bone mineral density. *J Clin Endocrinol Metab***,** jc20154063.

CARVALHO, B. M., GUADAGNINI, D., TSUKUMO, D. M. L., SCHENKA, A. A., LATUF-FILHO, P., VASSALLO, J., DIAS, J. C., KUBOTA, L. T., CARVALHEIRA, J. B. C. & SAAD, M. J. A. 2012. Modulation of gut microbiota by antibiotics improves insulin signalling in high-fat fed mice. *Diabetologia,* 55**,** 2823-2834.

CASTEJON, A. M., PAEZ, X., HERNANDEZ, L. & CUBEDDU, L. X. 1999. Use of intravenous microdialysis to monitor changes in serotonin release and metabolism induced by cisplatin in cancer patients: Comparative effects of granisetron and ondansetron. *Journal of Pharmacology and Experimental Therapeutics,* 291**,** 960-966.

CHABBI-ACHENGLI, Y., COUDERT, A. E., CALLEBERT, J., GEOFFROY, V., COTE, F., COLLET, C. & DE VERNEJOUL, M. C. 2012. Decreased osteoclastogenesis in serotonin-deficient mice. *Proc Natl Acad Sci U S A,* 109**,** 2567-72.

CHAMBERS, E. S., VIARDOT, A., PSICHAS, A., MORRISON, D. J., MURPHY, K. G., ZAC-VARGHESE, S. E. K., MACDOUGALL, K., PRESTON, T., TEDFORD, C., FINLAYSON, G. S., BLUNDELL, J. E., BELL, J. D., THOMAS, E. L., MT-ISA, S., ASHBY, D., GIBSON, G. R., KOLIDA, S., DHILLO, W. S., BLOOM, S. R., MORLEY, W., CLEGG, S. & FROST, G. 2015. Effects of targeted delivery of propionate to the human colon on appetite regulation, body weight maintenance and adiposity in overweight adults. *Gut,* 64**,** 1744-1754.

CHANG, C. F., YANG, J., ZHAO, W. M., LI, Y., GUO, P. J., LI, M. H., ZHOU, Y. & XU, C. S. 2015. Gene expression profiling analysis of 5-hydroxytryptamine signaling pathway in rat regenerating liver and different types of liver cells. *Genet Mol Res,* 14**,** 3409-20.

CHEN, Y., LEON-PONTE, M., PINGLE, S. C., O'CONNELL, P. J. & AHERN, G. P. 2015. T lymphocytes possess the machinery for 5-HT synthesis, storage, degradation and release. *Acta Physiol (Oxf),* 213**,** 860-7.

CHIN, A., SVEJDA, B., GUSTAFSSON, B. I., GRANLUND, A. B., SANDVIK, A. K., TIMBERLAKE, A., SUMPIO, B., PFRAGNER, R., MODLIN, I. M. & KIDD, M. 2012. The role of mechanical forces and adenosine in the regulation of intestinal enterochromaffin cell serotonin secretion. *Am J Physiol Gastrointest Liver Physiol,* 302**,** G397-405.

CHO, H. J., CALLAGHAN, B., BRON, R., BRAVO, D. M. & FURNESS, J. B. 2014. Identification of enteroendocrine cells that express TRPA1 channels in the mouse intestine. *Cell Tissue Res,* 356**,** 77-82.

CLARKE, K. R. 1993. Nonparametric Multivariate Analyses of Changes in Community Structure. *Australian Journal of Ecology,* 18**,** 117-143.

COLEMAN, J. A., GREEN, E. M. & GOUAUX, E. 2016. X-ray structures and mechanism of the human serotonin transporter. *Nature,* 532**,** 334-9.

CORONA, G., RICCA, V., BANDINI, E., MANNUCCI, E., LOTTI, F., BODDI, V., RASTRELLI, G., SFORZA, A., FARAVELLI, C., FORTI, G. & MAGGI, M. 2009. Selective serotonin reuptake inhibitor-induced sexual dysfunction. *J Sex Med,* 6**,** 1259-69.

CORPE, C. P., BOVELANDER, F. J., HOEKSTRA, J. H. & BURANT, C. F. 1998. The small intestinal fructose transporters: site of dietary perception and evidence for diurnal and fructose sensitive control elements. *Biochim Biophys Acta,* 1402**,** 229-38.

COSTA, M., BROOKES, S. J., STEELE, P. A., GIBBINS, I., BURCHER, E. & KANDIAH, C. J. 1996. Neurochemical classification of myenteric neurons in the guinea-pig ileum. *Neuroscience,* 75**,** 949-67.

COSTA, M. & FURNESS, J. B. 1984. Somatostatin is present in a subpopulation of noradrenergic nerve fibres supplying the intestine. *Neuroscience,* 13**,** 911-919.

COSTA, M., FURNESS, J. B., SMITH, I. J., DAVIES, B. & OLIVER, J. 1980. An immunohistochemical study of the projections of somatostatin-containing neurons in the guinea-pig intestine. *Neuroscience,* 5**,** 841-52.

COTE, F., FLIGNY, C., BAYARD, E., LAUNAY, J. M., GERSHON, M. D., MALLET, J. & VODJDANI, G. 2007. Maternal serotonin is crucial for murine embryonic development. *Proc Natl Acad Sci U S A,* 104**,** 329-34.

COX, L. M., YAMANISHI, S., SOHN, J., ALEKSEYENKO, A. V., LEUNG, J. M., CHO, I., KIM, S. G., LI, H., GAO, Z., MAHANA, D., ZARATE RODRIGUEZ, J. G., ROGERS, A. B., ROBINE, N., LOKE, P. & BLASER, M. J. 2014. Altering the intestinal microbiota during a critical developmental window has lasting metabolic consequences. *Cell,* 158**,** 705-721.

CRANE, J. D., PALANIVEL, R., MOTTILLO, E. P., BUJAK, A. L., WANG, H., FORD, R. J., COLLINS, A., BLUMER, R. M., FULLERTON, M. D., YABUT, J. M., KIM, J. J., GHIA, J. E., HAMZA, S. M., MORRISON, K. M., SCHERTZER, J. D., DYCK, J. R., KHAN, W. I. & STEINBERG, G. R. 2015. Inhibiting peripheral serotonin synthesis reduces obesity and metabolic dysfunction by promoting brown adipose tissue thermogenesis. *Nat Med,* 21**,** 166-72.

CRANE, R. K. 1960. Intestinal absorption of sugars. *Physiol Rev,* 40**,** 789-825.

CUBEDDU, L. X., HOFFMANN, I. S., FUENMAYOR, N. T. & MALAVE, J. J. 1992. Changes in serotonin metabolism in cancer patients: its relationship to nausea and vomiting induced by chemotherapeutic drugs. *Br J Cancer,* 66**,** 198-203.

CUMMINGS, J. H., POMARE, E. W., BRANCH, W. J., NAYLOR, C. P. & MACFARLANE, G. T. 1987. Short chain fatty acids in human large intestine, portal, hepatic and venous blood. *Gut,* 28**,** 1221-7.

DALE, G. L. 2005. Coated-platelets: an emerging component of the procoagulant response. *J Thromb Haemost,* 3**,** 2185-92.

DARWICH, A. S., ASLAM, U., ASHCROFT, D. M. & ROSTAMI-HODJEGAN, A. 2014. Meta-analysis of the turnover of intestinal epithelia in preclinical animal species and humans. *Drug Metab Dispos,* 42**,** 2016-22.

DAVID, L. A., MAURICE, C. F., CARMODY, R. N., GOOTENBERG, D. B., BUTTON, J. E., WOLFE, B. E., LING, A. V., DEVLIN, A. S., VARMA, Y., FISCHBACH, M. A., BIDDINGER, S. B., DUTTON, R. J. & TURNBAUGH, P. J. 2014. Diet rapidly and reproducibly alters the human gut microbiome. *Nature,* 505**,** 559-63.

DAVIDSON, N. O., HAUSMAN, A. M., IFKOVITS, C. A., BUSE, J. B., GOULD, G. W., BURANT, C. F. & BELL, G. I. 1992. Human intestinal glucose transporter expression and localization of GLUT5. *Am J Physiol,* 262**,** C795-800.

DE FRANCISCIS, P., MAININI, G., MESSALLI, E. M., TROTTA, C., LUISI, A., LAUDANDO, E., MARINO, G., DELLA PUCA, G., CERRETO, F. V. & TORELLA, M. 2013. Arterial hypertension and female sexual dysfunction in postmenopausal women. *Clin Exp Obstet Gynecol,* 40**,** 58-60.

DE VADDER, F., GRASSET, E., MANNERAS HOLM, L., KARSENTY, G., MACPHERSON, A. J., OLOFSSON, L. E. & BACKHED, F. 2018. Gut microbiota regulates maturation of the adult enteric nervous system via enteric serotonin networks. *Proc Natl Acad Sci U S A*.

DE VADDER, F., KOVATCHEVA-DATCHARY, P., GONCALVES, D., VINERA, J., ZITOUN, C., DUCHAMPT, A., BACKHED, F. & MITHIEUX, G. 2014. Microbiota-generated metabolites promote metabolic benefits via gut-brain neural circuits. *Cell,* 156**,** 84-96.

DE VADDER, F., KOVATCHEVA-DATCHARY, P., ZITOUN, C., DUCHAMPT, A., BACKHED, F. & MITHIEUX, G. 2016. Microbiota-Produced Succinate Improves Glucose Homeostasis via Intestinal Gluconeogenesis. *Cell Metab,* 24**,** 151-7.

DEAL, R., TANG, Y., FLETCHER, R., TORQUATI, A. & OMOTOSHO, P. 2016. Intestinal glucose transporters GLUT-1 and GLUT-5 expression in obese and non-obese subjects and potential impact on Type 2 diabetes remission following bariatric surgery. *Surgery for Obesity and Related Diseases,* 12**,** S63-S65.

DEAL, R. A., TANG, Y., FLETCHER, R., TORQUATI, A. & OMOTOSHO, P. 2017. Understanding intestinal glucose transporter expression in obese compared to non-obese subjects. *Surg Endosc*.

DEFRONZO, R. A., FERRANNINI, E. & SIMONSON, D. C. 1989. Fasting hyperglycemia in non-insulin-dependent diabetes mellitus: contributions of excessive hepatic glucose production and impaired tissue glucose uptake. *Metabolism,* 38**,** 387-95.

DEN BESTEN, G., HAVINGA, R., BLEEKER, A., RAO, S., GERDING, A., VAN EUNEN, K., GROEN, A. K., REIJNGOUD, D. J. & BAKKER, B. M. 2014. The short-chain fatty acid uptake fluxes by mice on a guar gum supplemented diet associate with amelioration of major biomarkers of the metabolic syndrome. *PLoS One,* 9**,** e107392.

DEN BESTEN, G., LANGE, K., HAVINGA, R., VAN DIJK, T. H., GERDING, A., VAN EUNEN, K., MULLER, M., GROEN, A. K., HOOIVELD, G. J., BAKKER, B. M. & REIJNGOUD, D. J. 2013. Gut-derived short-chain fatty acids are vividly assimilated into host carbohydrates and lipids. *Am J Physiol Gastrointest Liver Physiol,* 305**,** G900-10.

DERRIEN, M., VAUGHAN, E. E., PLUGGE, C. M. & DE VOS, W. M. 2004. Akkermansia muciniphila gen. nov., sp. nov., a human intestinal mucin-degrading bacterium. *Int J Syst Evol Microbiol,* 54**,** 1469-76.

DIAZ-LOPEZ, A., BULLO, M., JUANOLA-FALGARONA, M., MARTINEZ-GONZALEZ, M. A., ESTRUCH, R., COVAS, M. I., AROS, F. & SALAS-SALVADO, J. 2013. Reduced serum concentrations of carboxylated and undercarboxylated osteocalcin are associated with risk of developing type 2 diabetes mellitus in a high cardiovascular risk population: a nested case-control study. *J Clin Endocrinol Metab,* 98**,** 4524-31.

DIAZ HEIJTZ, R., WANG, S., ANUAR, F., QIAN, Y., BJORKHOLM, B., SAMUELSSON, A., HIBBERD, M. L., FORSSBERG, H. & PETTERSSON, S. 2011. Normal gut microbiota modulates brain development and behavior. *Proc Natl Acad Sci U S A,* 108**,** 3047-52.

DIWAKARLA, S., FOTHERGILL, L. J., FAKHRY, J., CALLAGHAN, B. & FURNESS, J. B. 2017. Heterogeneity of enterochromaffin cells within the gastrointestinal tract. *Neurogastroenterol Motil,* 29.

DUSING, R. 2005. Sexual dysfunction in male patients with hypertension: influence of antihypertensive drugs. *Drugs,* 65**,** 773-86.

DUSTIN, L. B. 2000. Ratiometric analysis of calcium mobilization. *Clinical and Applied Immunology Reviews,* 1**,** 5-15.

EBBERT, J. O. & JENSEN, M. D. 2013. Fat depots, free fatty acids, and dyslipidemia. *Nutrients,* 5**,** 498-508.

EDDAHIBI, S., HUMBERT, M., FADEL, E., RAFFESTIN, B., DARMON, M., CAPRON, F., SIMONNEAU, G., DARTEVELLE, P., HAMON, M. & ADNOT, S. 2001. Serotonin transporter overexpression is responsible for pulmonary artery smooth muscle hyperplasia in primary pulmonary hypertension. *J Clin Invest,* 108**,** 1141-50.

EGEROD, K. L., ENGELSTOFT, M. S., GRUNDDAL, K. V., NOHR, M. K., SECHER, A., SAKATA, I., PEDERSEN, J., WINDELOV, J. A., FUCHTBAUER, E. M., OLSEN, J., SUNDLER, F., CHRISTENSEN, J. P., WIERUP, N., OLSEN, J. V., HOLST, J. J., ZIGMAN, J. M., POULSEN, S. S. & SCHWARTZ, T. W. 2012. A major

lineage of enteroendocrine cells coexpress CCK, secretin, GIP, GLP-1, PYY, and neurotensin but not somatostatin. *Endocrinology,* 153**,** 5782-95.

EL-SALHY, M., DANIELSSON, A., STENLING, R. & GRIMELIUS, L. 1997. Colonic endocrine cells in inflammatory bowel disease. *J Intern Med,* 242**,** 413-9.

ENRIORI, P. J., EVANS, A. E., SINNAYAH, P., JOBST, E. E., TONELLI-LEMOS, L., BILLES, S. K., GLAVAS, M. M., GRAYSON, B. E., PERELLO, M., NILLNI, E. A., GROVE, K. L. & COWLEY, M. A. 2007. Diet-induced obesity causes severe but reversible leptin resistance in arcuate melanocortin neurons. *Cell Metab,* 5**,** 181-94.

ERSPAMER, V. 1954. Pharmacology of indole-alkylamines. *Pharmacol Rev,* 6**,** 425-87.

ESSIEN, B. E., GRASBERGER, H., ROMAIN, R. D., LAW, D. J., VENIAMINOVA, N. A., SAQUI-SALCES, M., EL-ZAATARI, M., TESSIER, A., HAYES, M. M., YANG, A. C. & MERCHANT, J. L. 2013. ZBP-89 regulates expression of tryptophan hydroxylase I and mucosal defense against Salmonella typhimurium in mice. *Gastroenterology,* 144**,** 1466-77, 1477 e1-9.

EVANS, D. L., LYNCH, K. G., BENTON, T., DUBE, B., GETTES, D. R., TUSTIN, N. B., LAI, J. P., METZGER, D. & DOUGLAS, S. D. 2008. Selective serotonin reuptake inhibitor and substance P antagonist enhancement of natural killer cell innate immunity in human immunodeficiency virus/acquired immunodeficiency syndrome. *Biol Psychiatry,* 63**,** 899-905.

EVERARD, A., LAZAREVIC, V., GAIA, N., JOHANSSON, M., STAHLMAN, M., BACKHED, F., DELZENNE, N. M., SCHRENZEL, J., FRANCOIS, P. & CANI, P. D. 2014. Microbiome of prebiotic-treated mice reveals novel targets involved in host response during obesity. *ISME J,* 8**,** 2116-2130.

FARGIN, A., RAYMOND, J. R., REGAN, J. W., COTECCHIA, S., LEFKOWITZ, R. J. & CARON, M. G. 1989. Effector coupling mechanisms of the cloned 5-HT1A receptor. *J Biol Chem,* 264**,** 14848-52.

FAUSTO, N., CAMPBELL, J. S. & RIEHLE, K. J. 2006. Liver regeneration. *Hepatology,* 43**,** S45-53.

FELDMANN, H. M., GOLOZOUBOVA, V., CANNON, B. & NEDERGAARD, J. 2009. UCP1 ablation induces obesity and abolishes diet-induced thermogenesis in mice exempt from thermal stress by living at thermoneutrality. *Cell Metab,* 9**,** 203-9.

FERRIER, L., SEGAIN, J. P., PACAUD, P., CHERBUT, C., LOIRAND, G., GALMICHE, J. P. & BLOTTIERE, H. M. 2000. Pathways and receptors involved in peptide YY induced contraction of rat proximal colonic muscle in vitro. *Gut,* 46**,** 370-5.

FERRON, M., HINOI, E., KARSENTY, G. & DUCY, P. 2008. Osteocalcin differentially regulates beta cell and adipocyte gene expression and affects the development of metabolic diseases in wild-type mice. *Proc Natl Acad Sci U S A,* 105**,** 5266-70.

FOLEY, S., GARSED, K., SINGH, G., DUROUDIER, N. P., SWAN, C., HALL, I. P., ZAITOUN, A., BENNETT, A., MARSDEN, C., HOLMES, G., WALLS, A. & SPILLER, R. C. 2011. Impaired uptake of serotonin by platelets from patients with irritable bowel syndrome correlates with duodenal immune activation. *Gastroenterology,* 140**,** 1434-43 e1.

FOTHERGILL, L. J., CALLAGHAN, B., HUNNE, B., BRAVO, D. M. & FURNESS, J. B. 2017a. Co-storage of enteroendocrine hormones evaluated at the cell and subcellular levels in male mice. *Endocrinology*.

FOTHERGILL, L. J., CALLAGHAN, B., HUNNE, B., BRAVO, D. M. & FURNESS, J. B. 2017b. Costorage of Enteroendocrine Hormones Evaluated at the Cell and Subcellular Levels in Male Mice. *Endocrinology,* 158**,** 2113-2123.

FRANCE, M., SKORICH, E., KADROFSKE, M., SWAIN, G. M. & GALLIGAN, J. J. 2016. Sex-related differences in small intestinal transit and serotonin dynamics in high-fat-diet-induced obesity in mice. *Exp Physiol,* 101**,** 81-99.

FREEMAN, S. L., BOHAN, D., DARCEL, N. & RAYBOULD, H. E. 2006a. Luminal glucose sensing in the rat intestine has characteristics of a sodium-glucose cotransporter. *Am J Physiol Gastrointest Liver Physiol,* 291**,** G439-45.

FREEMAN, S. L., GLATZLE, J., ROBIN, C. S., VALDELLON, M., STERNINI, C., SHARP, J. W. & RAYBOULD, H. E. 2006b. Ligand-induced 5-HT3 receptor internalization in enteric neurons in rat ileum. *Gastroenterology,* 131**,** 97-107.

FROHLICH, P. F. & MESTON, C. M. 2000. Evidence that serotonin affects female sexual functioning via peripheral mechanisms. *Physiol Behav,* 71**,** 383-93.

FU, Y., LUO, N., KLEIN, R. L. & GARVEY, W. T. 2005. Adiponectin promotes adipocyte differentiation, insulin sensitivity, and lipid accumulation. *J Lipid Res,* 46**,** 1369-79.

FUJIMIYA, M., MAEDA, T. & KIMURA, H. 1991. Serotonin-containing epithelial cells in rat duodenum. I. Quantitative morphometric study of the distribution density. *Histochemistry,* 95**,** 217-24.

FUKUMOTO, S., TATEWAKI, M., YAMADA, T., FUJIMIYA, M., MANTYH, C., VOSS, M., EUBANKS, S., HARRIS, M., PAPPAS, T. N. & TAKAHASHI, T. 2003. Short-chain fatty acids stimulate colonic transit via intraluminal 5-HT release in rats. *Am J Physiol Regul Integr Comp Physiol,* 284**,** R1269-76.

GARSED, K., CHERNOVA, J., HASTINGS, M., LAM, C., MARCIANI, L., SINGH, G., HENRY, A., HALL, I., WHORWELL, P. & SPILLER, R. 2014. A randomised trial of ondansetron for the treatment of irritable bowel syndrome with diarrhoea. *Gut,* 63**,** 1617-25.

GAYER, C. P. & BASSON, M. D. 2009. The effects of mechanical forces on intestinal physiology and pathology. *Cell Signal,* 21**,** 1237-44.

GE, X., DING, C., ZHAO, W., XU, L., TIAN, H., GONG, J., ZHU, M., LI, J. & LI, N. 2017. Antibiotics-induced depletion of mice microbiota induces changes in host serotonin biosynthesis and intestinal motility. *J Transl Med,* 15**,** 13.

GENTILCORE, D., LITTLE, T. J., FEINLE-BISSET, C., SAMSOM, M., SMOUT, A. J., HOROWITZ, M. & JONES, K. L. 2007. Role of 5-hydroxytryptamine mechanisms in mediating the effects of small intestinal glucose on blood pressure and antropyloroduodenal motility in older subjects. *Am J Physiol Gastrointest Liver Physiol,* 293**,** G692-8.

GERSHON, M. D., DRAKONTIDES, A. B. & ROSS, L. L. 1965. Serotonin: Synthesis and Release from the Myenteric Plexus of the Mouse Intestine. *Science,* 149**,** 197-199.

GERSHON, M. D. & TACK, J. 2007. The serotonin signaling system: from basic understanding to drug development for functional GI disorders. *Gastroenterology,* 132**,** 397-414.

GILL, R. K., SAKSENA, S., TYAGI, S., ALREFAI, W. A., MALAKOOTI, J., SARWAR, Z., TURNER, J. R., RAMASWAMY, K. & DUDEJA, P. K. 2005. Serotonin inhibits Na+/H+ exchange activity via 5-HT4 receptors and activation of PKC alpha in human intestinal epithelial cells. *Gastroenterology,* 128**,** 962-74.

GOODPASTER, B. H., THAETE, F. L., SIMONEAU, J. A. & KELLEY, D. E. 1997. Subcutaneous abdominal fat and thigh muscle composition predict insulin sensitivity independently of visceral fat. *Diabetes,* 46**,** 1579-85.

GORDON, J. & BARNES, N. M. 2003. Lymphocytes transport serotonin and dopamine: agony or ecstasy? *Trends in Immunology,* 24**,** 438-443.

GOTTSCHALCK, I. B., JEPPESEN, P. B., HARTMANN, B., HOLST, J. J. & HENRIKSEN, D. B. 2008. Effects of treatment with glucagon-like peptide-2 on bone resorption in colectomized patients with distal ileostomy or jejunostomy and short-bowel syndrome. *Scand J Gastroenterol,* 43**,** 1304-10.

GUSTAFSSON, B. I., BAKKE, I., TOMMERAS, K. & WALDUM, H. L. 2006. A new method for visualization of gut mucosal cells, describing the enterochromaffin cell in the rat gastrointestinal tract. *Scand J Gastroenterol,* 41**,** 390-5.

HAAHR, M. E., HANSEN, D. L., FISHER, P. M., SVARER, C., STENBAEK, D. S., MADSEN, K., MADSEN, J., HOLST, J. J., BAARE, W. F., HOJGAARD, L., ALMDAL, T. & KNUDSEN, G. M. 2015. Central 5-HT neurotransmission modulates weight loss following gastric bypass surgery in obese individuals. *J Neurosci,* 35**,** 5884-9.

HAMILTON, M. K., BOUDRY, G., LEMAY, D. G. & RAYBOULD, H. E. 2015. Changes in intestinal barrier function and gut microbiota in high-fat diet-fed rats are dynamic and region dependent. *Am J Physiol Gastrointest Liver Physiol,* 308**,** G840-51.

HANNON, J. & HOYER, D. 2008. Molecular biology of 5-HT receptors. *Behav Brain Res,* 195**,** 198-213.

HANSEN, M. & WITTE, A. B. 2008. The role of serotonin in intestinal luminal sensing and secretion. *Acta physiologica (Oxford, England),* 193**,** 311-323.

HAUB, S., RITZE, Y., BERGHEIM, I., PABST, O., GERSHON, M. D. & BISCHOFF, S. C. 2010. Enhancement of intestinal inflammation in mice lacking interleukin 10 by deletion of the serotonin reuptake transporter. *Neurogastroenterol Motil,* 22**,** 826-34, e229.

HELLSTRAND, K. & HERMODSSON, S. 1990. Enhancement of human natural killer cell cytotoxicity by serotonin: role of non-T/CD16+ NK cells, accessory monocytes, and 5-HT1A receptors. *Cell Immunol,* 127**,** 199-214.

HEREDIA, D. J., GERSHON, M. D., KOH, S. D., CORRIGAN, R. D., OKAMOTO, T. & SMITH, T. K. 2013. Important role of mucosal serotonin in colonic propulsion and peristaltic reflexes: in vitro analyses in mice lacking tryptophan hydroxylase 1. *J Physiol,* 591**,** 5939-57.

HERNANDEZ, M. E., MARTINEZ-FONG, D., PEREZ-TAPIA, M., ESTRADA-GARCIA, I., ESTRADA-PARRA, S. & PAVON, L. 2010. Evaluation of the effect of selective serotonin-reuptake inhibitors on lymphocyte subsets in patients with a major depressive disorder. *Eur Neuropsychopharmacol,* 20**,** 88-95.

HERRICK-DAVIS, K. 2013. Functional significance of serotonin receptor dimerization. *Exp Brain Res,* 230**,** 375-86.

HILDEBRANDT, M. A., HOFFMANN, C., SHERRILL-MIX, S. A., KEILBAUGH, S. A., HAMADY, M., CHEN, Y. Y., KNIGHT, R., AHIMA, R. S., BUSHMAN, F. & WU, G. D. 2009. High-fat diet determines the composition of the murine gut microbiome independently of obesity. *Gastroenterology,* 137**,** 1716-24 e1-2.

HODGE, J. M., WANG, Y., BERK, M., COLLIER, F. M., FERNANDES, T. J., CONSTABLE, M. J., PASCO, J. A., DODD, S., NICHOLSON, G. C., KENNEDY, R. L. & WILLIAMS, L. J. 2013. Selective serotonin reuptake inhibitors inhibit human osteoclast and osteoblast formation and function. *Biol Psychiatry,* 74**,** 32-9.

HOFFLER, U., HOBBIE, K., WILSON, R., BAI, R., RAHMAN, A., MALARKEY, D., TRAVLOS, G. & GHANAYEM, B. I. 2009. Diet-induced obesity is associated with hyperleptinemia, hyperinsulinemia, hepatic steatosis, and glomerulopathy in C57Bl/6J mice. *Endocrine,* 36**,** 311-25.

HOFFMAN, J. M., TYLER, K., MACEACHERN, S. J., BALEMBA, O. B., JOHNSON, A. C., BROOKS, E. M., ZHAO, H., SWAIN, G. M., MOSES, P. L., GALLIGAN, J. J., SHARKEY, K. A., GREENWOOD-VAN MEERVELD, B. & MAWE, G. M. 2012. Activation of colonic mucosal 5-HT(4) receptors accelerates propulsive motility and inhibits visceral hypersensitivity. *Gastroenterology,* 142**,** 844-854 e4.

HOLZER, P., EMSON, P. C., IVERSEN, L. L. & SHARMAN, D. F. 1981. Regional differences in the response to substance P on the longitudinal muscle and the concentration of substance P in the digestive tract of the guinea-pig. *Neuroscience,* 6**,** 1433-41.

HOTTA, K., FUNAHASHI, T., ARITA, Y., TAKAHASHI, M., MATSUDA, M., OKAMOTO, Y., IWAHASHI, H., KURIYAMA, H., OUCHI, N., MAEDA, K., NISHIDA, M., KIHARA, S., SAKAI, N., NAKAJIMA, T., HASEGAWA, K., MURAGUCHI, M., OHMOTO, Y., NAKAMURA, T., YAMASHITA, S., HANAFUSA, T. & MATSUZAWA, Y. 2000. Plasma concentrations of a novel, adipose-specific protein, adiponectin, in type 2 diabetic patients. *Arterioscler Thromb Vasc Biol,* 20**,** 1595-9.

HOVERSTAD, T., BJORNEKLETT, A., MIDTVEDT, T., FAUSA, O. & BOHMER, T. 1984. Short-chain fatty acids in the proximal gastrointestinal tract of healthy subjects. *Scand J Gastroenterol,* 19**,** 1053-8.

HOYER, D., HANNON, J. P. & MARTIN, G. R. 2002. Molecular, pharmacological and functional diversity of 5-HT receptors. *Pharmacol Biochem Behav,* 71**,** 533-54.

HU, W. W., KE, Y. H., HE, J. W., FU, W. Z., LIU, Y. J., CHEN, D. & ZHANG, Z. L. 2014. Serum osteocalcin levels are inversely associated with plasma glucose and body mass index in healthy Chinese women. *Acta Pharmacol Sin,* 35**,** 1521-6.

I˙MERYÜZ, N., YEĞEN, B. Ç., BOZKURT, A., COŞKUN, T., VILLANUEVA-PEÑACARRILLO, M. L. & ULUSOY, N. B. 1997. Glucagon-like peptide-1 inhibits gastric emptying via vagal afferent-mediated central mechanisms. *American Journal of Physiology - Gastrointestinal and Liver Physiology,* 273**,** G920-G927.

ICHIMURA, A., HASEGAWA, S., KASUBUCHI, M. & KIMURA, I. 2014. Free fatty acid receptors as therapeutic targets for the treatment of diabetes. *Frontiers in Pharmacology,* 5.

IMADA-SHIRAKATA, Y., KOTERA, T., UEDA, S. & OKUMA, M. 1997. Serotonin activates electrolyte transport via 5-HT2A receptor in rat colonic crypt cells. *Biochem Biophys Res Commun,* 230**,** 437-41.

INOKUCHI, H., AZUMA, T., KAWAI, K., TAKEUCHI, Y. & SANO, Y. 1984. Serotonin immunohistochemistry reveals immature EC cells. *Histochemistry,* 80**,** 517-8.

JACKSON, J., PAPADOPULOS, A., MEUNIER, F. A., MCCLUSKEY, A., ROBINSON, P. J. & KEATING, D. J. 2015. Small molecules demonstrate the role of dynamin as a bi-directional regulator of the exocytosis fusion pore and vesicle release. *Mol Psychiatry,* 20**,** 810-9.

JENSEN, M. D. & JOHNSON, C. M. 1996. Contribution of leg and splanchnic free fatty acid (FFA) kinetics to postabsorptive FFA flux in men and women. *Metabolism,* 45**,** 662-6.

JONES, P. J. & SCHOELLER, D. A. 1988. Polyunsaturated:saturated ratio of diet fat influences energy substrate utilization in the human. *Metabolism,* 37**,** 145-51.

JORGENSEN, T. N., CHRISTENSEN, P. M. & GETHER, U. 2014. Serotonin-induced down-regulation of cell surface serotonin transporter. *Neurochem Int,* 73**,** 107-12.

KANAZAWA, I., YAMAGUCHI, T., YAMAUCHI, M., YAMAMOTO, M., KURIOKA, S., YANO, S. & SUGIMOTO, T. 2011. Serum undercarboxylated osteocalcin was inversely associated with plasma glucose level and fat mass in type 2 diabetes mellitus. *Osteoporos Int,* 22**,** 187-94.

KARLSSON, S., BANHIDI, Z. G. & ALBERTSSON, A. C. 1988. Detection by high-performance liquid chromatography of polyamines formed by clostridial putrefaction of caseins. *J Chromatogr,* 442**,** 267-77.

KASHYAP, P. C., MARCOBAL, A., URSELL, L. K., LARAUCHE, M., DUBOC, H., EARLE, K. A., SONNENBURG, E. D., FERREYRA, J. A., HIGGINBOTTOM, S. K., MILLION, M., TACHE, Y., PASRICHA, P. J., KNIGHT, R., FARRUGIA, G. & SONNENBURG, J. L. 2013. Complex interactions among diet, gastrointestinal transit, and gut microbiota in humanized mice. *Gastroenterology,* 144**,** 967-77.

KAUMANN, A. J. & LEVY, F. O. 2006. 5-hydroxytryptamine receptors in the human cardiovascular system. *Pharmacol Ther,* 111**,** 674-706.

KEATING, D. J., DUBACH, D., ZANIN, M. P., YU, Y., MARTIN, K., ZHAO, Y. F., CHEN, C., PORTA, S., ARBONES, M. L., MITTAZ, L. & PRITCHARD, M. A. 2008. DSCR1/RCAN1 regulates vesicle exocytosis and fusion pore kinetics: implications for Down syndrome and Alzheimer's disease. *Hum Mol Genet,* 17**,** 1020-30.

KEATING, D. J. & SPENCER, N. J. 2010. Release of 5-hydroxytryptamine from the mucosa is not required for the generation or propagation of colonic migrating motor complexes. *Gastroenterology,* 138**,** 659-70 670 e1-2.

KERN, P. A., DI GREGORIO, G. B., LU, T., RASSOULI, N. & RANGANATHAN, G. 2003. Adiponectin expression from human adipose tissue: relation to obesity, insulin resistance, and tumor necrosis factor-alpha expression. *Diabetes,* 52**,** 1779-85.

KIDD, M., EICK, G. N., MODLIN, I. M., PFRAGNER, R., CHAMPANERIA, M. C. & MURREN, J. 2007. Further delineation of the continuous human neoplastic enterochromaffin cell line, KRJ-I, and the inhibitory effects of lanreotide and rapamycin. *J Mol Endocrinol,* 38**,** 181-92.

KIDD, M., GUSTAFSSON, B. I., DROZDOV, I. & MODLIN, I. M. 2009. IL1beta- and LPS-induced serotonin secretion is increased in EC cells derived from Crohn's disease. *Neurogastroenterol Motil,* 21**,** 439-50.

KIDD, M., MODLIN, I. M., EICK, G. N. & CHAMPANERIA, M. C. 2006. Isolation, functional characterization, and transcriptome of Mastomys ileal enterochromaffin cells. *Am J Physiol Gastrointest Liver Physiol,* 291**,** G778-91.

KIDD, M., MODLIN, I. M., GUSTAFSSON, B. I., DROZDOV, I., HAUSO, O. & PFRAGNER, R. 2008. Luminal regulation of normal and neoplastic human EC cell serotonin release is mediated by bile salts, amines, tastants, and olfactants. *Am J Physiol Gastrointest Liver Physiol,* 295**,** G260-72.

KIM, H., TOYOFUKU, Y., LYNN, F. C., CHAK, E., UCHIDA, T., MIZUKAMI, H., FUJITANI, Y., KAWAMORI, R., MIYATSUKA, T., KOSAKA, Y., YANG, K., HONIG, G., VAN DER HART, M., KISHIMOTO, N., WANG, J., YAGIHASHI, S., TECOTT, L. H., WATADA, H. & GERMAN, M. S. 2010. Serotonin regulates pancreatic beta cell mass during pregnancy. *Nat Med,* 16**,** 804-8.

KIM, H. J., KIM, J. H., NOH, S., HUR, H. J., SUNG, M. J., HWANG, J. T., PARK, J. H., YANG, H. J., KIM, M. S., KWON, D. Y. & YOON, S. H. 2011. Metabolomic analysis of livers and serum from high-fat diet induced obese mice. *J Proteome Res,* 10**,** 722-31.

KIM, K., OH, C. M., OHARA-IMAIZUMI, M., PARK, S., NAMKUNG, J., YADAV, V. K., TAMARINA, N. A., ROE, M. W., PHILIPSON, L. H., KARSENTY, G., NAGAMATSU, S., GERMAN, M. S. & KIM, H. 2015. Functional role of serotonin in insulin secretion in a diet-induced insulin-resistant state. *Endocrinology,* 156**,** 444-52.

KIM, M., COOKE, H. J., JAVED, N. H., CAREY, H. V., CHRISTOFI, F. & RAYBOULD, H. E. 2001a. D-glucose releases 5-hydroxytryptamine from human BON cells as a model of enterochromaffin cells. *Gastroenterology,* 121**,** 1400-6.

KIM, M., JAVED, N. H., YU, J. G., CHRISTOFI, F. & COOKE, H. J. 2001b. Mechanical stimulation activates Galphaq signaling pathways and 5-hydroxytryptamine release from human carcinoid BON cells. *J Clin Invest,* 108**,** 1051-9.

KOHSAKA, A., LAPOSKY, A. D., RAMSEY, K. M., ESTRADA, C., JOSHU, C., KOBAYASHI, Y., TUREK, F. W. & BASS, J. 2007. High-fat diet disrupts behavioral and molecular circadian rhythms in mice. *Cell Metab,* 6**,** 414-21.

KOJIMA, I., NAKAGAWA, Y., HAMANO, K., MEDINA, J., LI, L. & NAGASAWA, M. 2015. Glucose-Sensing Receptor T1R3: A New Signaling Receptor Activated by Glucose in Pancreatic beta-Cells. *Biol Pharm Bull,* 38**,** 674-9.

KORF, J. & SEBENS, J. B. 1970. Determination of O-conjugates of 5-hydroxytryptamine in human urine. *Clin Chim Acta,* 27**,** 149-53.

KRAEMER, F. B. & SHEN, W. J. 2002. Hormone-sensitive lipase: control of intracellular tri-(di-)acylglycerol and cholesteryl ester hydrolysis. *J Lipid Res,* 43**,** 1585-94.

KUHRE, R. E., FROST, C. R., SVENDSEN, B. & HOLST, J. J. 2015. Molecular mechanisms of glucose-stimulated GLP-1 secretion from perfused rat small intestine. *Diabetes,* 64**,** 370-82.

KUMAGAI, A. K., KANG, Y. S., BOADO, R. J. & PARDRIDGE, W. M. 1995. Upregulation of blood-brain barrier GLUT1 glucose transporter protein and mRNA in experimental chronic hypoglycemia. *Diabetes,* 44**,** 1399-404.

KUNZE, W. A., BORNSTEIN, J. C. & FURNESS, J. B. 1995. Identification of sensory nerve cells in a peripheral organ (the intestine) of a mammal. *Neuroscience,* 66**,** 1-4.

KUSHNIR-SUKHOV, N. M., GILFILLAN, A. M., COLEMAN, J. W., BROWN, J. M., BRUENING, S., TOTH, M. & METCALFE, D. D. 2006. 5-hydroxytryptamine induces mast cell adhesion and migration. *J Immunol,* 177**,** 6422-32.

KUSUMOTO, Y., GRUBE, D., SATO, A. G., KANEDA, K. & NAKAMAE, E. 1988. Cytology and arrangement of enterochromaffin (EC) cells in the human stomach. *Arch Histol Cytol,* 51**,** 271-6.

KWAK, S. H., PARK, B. L., KIM, H., GERMAN, M. S., GO, M. J., JUNG, H. S., KOO, B. K., CHO, Y. M., CHOI, S. H., CHO, Y. S., SHIN, H. D., JANG, H. C. & PARK, K. S. 2012. Association of variations in TPH1 and HTR2B with gestational weight gain and measures of obesity. *Obesity (Silver Spring),* 20**,** 233-8.

LAPORTA, J., PETERS, T. L., MERRIMAN, K. E., VEZINA, C. M. & HERNANDEZ, L. L. 2013. Serotonin (5-HT) affects expression of liver metabolic enzymes and mammary gland glucose transporters during the transition from pregnancy to lactation. *PLoS One,* 8**,** e57847.

LAUDER, J. M., WILKIE, M. B., WU, C. & SINGH, S. 2000. Expression of 5-HT(2A), 5-HT(2B) and 5-HT(2C) receptors in the mouse embryo. *Int J Dev Neurosci,* 18**,** 653-62.

LE BEYEC, J., PELLETIER, A. L., ARAPIS, K., HOURSEAU, M., CLUZEAUD, F., DESCATOIRE, V., DUCROC, R., APARICIO, T., JOLY, F., COUVELARD, A., MARMUSE, J. P., LE GALL, M. & BADO, A. 2014. Overexpression of gastric leptin precedes adipocyte leptin during high-fat diet and is linked to 5HT-containing enterochromaffin cells. *Int J Obes (Lond),* 38**,** 1357-64.

LE CHATELIER, E., NIELSEN, T., QIN, J., PRIFTI, E., HILDEBRAND, F., FALONY, G., ALMEIDA, M., ARUMUGAM, M., BATTO, J. M., KENNEDY, S., LEONARD, P., LI, J., BURGDORF, K., GRARUP, N., JORGENSEN, T., BRANDSLUND, I., NIELSEN, H. B., JUNCKER, A. S., BERTALAN, M., LEVENEZ, F., PONS, N., RASMUSSEN, S., SUNAGAWA, S., TAP, J., TIMS, S., ZOETENDAL, E. G., BRUNAK, S., CLEMENT, K., DORE, J., KLEEREBEZEM, M., KRISTIANSEN, K., RENAULT, P., SICHERITZ-PONTEN, T., DE VOS, W. M., ZUCKER, J. D., RAES, J., HANSEN, T., META, H. I. T. C., BORK, P., WANG, J., EHRLICH, S. D. & PEDERSEN, O. 2013. Richness of human gut microbiome correlates with metabolic markers. *Nature,* 500**,** 541-6.

LE POUL, E., LOISON, C., STRUYF, S., SPRINGAEL, J. Y., LANNOY, V., DECOBECQ, M. E., BREZILLON, S., DUPRIEZ, V., VASSART, G., VAN DAMME, J., PARMENTIER, M. & DETHEUX, M. 2003. Functional characterization of human receptors for short chain fatty acids and their role in polymorphonuclear cell activation. *J Biol Chem,* 278**,** 25481-9.

LEE, N. K., SOWA, H., HINOI, E., FERRON, M., AHN, J. D., CONFAVREUX, C., DACQUIN, R., MEE, P. J., MCKEE, M. D., JUNG, D. Y., ZHANG, Z., KIM, J. K., MAUVAIS-JARVIS, F., DUCY, P. & KARSENTY, G. 2007. Endocrine regulation of energy metabolism by the skeleton. *Cell,* 130**,** 456-69.

LEON-PONTE, M., AHERN, G. P. & O'CONNELL, P. J. 2007. Serotonin provides an accessory signal to enhance T-cell activation by signaling through the 5-HT7 receptor. *Blood,* 109**,** 3139-46.

LEPARD, K. J. & STEPHENS, R. L. 1994. Serotonin inhibits gastric acid secretion through a 5-hydroxytryptamine1-like receptor in the rat. *Journal of Pharmacology and Experimental Therapeutics,* 270**,** 1139-1144.

LESURTEL, M., GRAF, R., ALEIL, B., WALTHER, D. J., TIAN, Y., JOCHUM, W., GACHET, C., BADER, M. & CLAVIEN, P. A. 2006. Platelet-derived serotonin mediates liver regeneration. *Science,* 312**,** 104-7.

LI, Y., HAO, Y., ZHU, J. & OWYANG, C. 2000. Serotonin released from intestinal enterochromaffin cells mediates luminal non-cholecystokinin-stimulated pancreatic secretion in rats. *Gastroenterology,* 118**,** 1197-207.

LI, Y. & OWYANG, C. 1994. Endogenous cholecystokinin stimulates pancreatic enzyme secretion via vagal afferent pathway in rats. *Gastroenterology,* 107**,** 525-31.

LI, Y. & OWYANG, C. 1996a. Pancreatic secretion evoked by cholecystokinin and non-cholecystokinin-dependent duodenal stimuli via vagal afferent fibres in the rat. *J Physiol,* 494 (Pt 3)**,** 773-82.

LI, Y. & OWYANG, C. 1996b. Peptone stimulates CCK-releasing peptide secretion by activating intestinal submucosal cholinergic neurons. *Journal of Clinical Investigation,* 97**,** 1463-1470.

LI, Y., WU, X. Y., ZHU, J. X. & OWYANG, C. 2001. Intestinal serotonin acts as paracrine substance to mediate pancreatic secretion stimulated by luminal factors. *Am J Physiol Gastrointest Liver Physiol,* 281**,** G916-23.

LI, Z., CHALAZONITIS, A., HUANG, Y. Y., MANN, J. J., MARGOLIS, K. G., YANG, Q. M., KIM, D. O., COTE, F., MALLET, J. & GERSHON, M. D. 2011. Essential roles of enteric neuronal serotonin in gastrointestinal motility and the development/survival of enteric dopaminergic neurons. *J Neurosci,* 31**,** 8998-9009.

LIN, B., MORRIS, D. W. & CHOU, J. Y. 1997. The role of HNF1alpha, HNF3gamma, and cyclic AMP in glucose-6-phosphatase gene activation. *Biochemistry,* 36**,** 14096-106.

LIN, S. J., HATOUM, H. T., BUCHNER, D., COX, D. & BALU, S. 2012. Impact of 5-HT3 receptor antagonists on chemotherapy-induced nausea and vomiting: a retrospective cohort study. *BMC Health Serv Res,* 12**,** 215.

LINAN-RICO, A., OCHOA-CORTES, F., BEYDER, A., SOGHOMONYAN, S., ZULETA-ALARCON, A., COPPOLA, V. & CHRISTOFI, F. L. 2016. Mechanosensory Signaling in Enterochromaffin Cells and 5-HT Release: Potential Implications for Gut Inflammation. *Front Neurosci,* 10**,** 564.

LINAN-RICO, A., WUNDERLICH, J. E., GRANTS, I. S., FRANKEL, W. L., XUE, J., WILLIAMS, K. C., HARZMAN, A. E., ENNEKING, J. T., COOKE, H. J. & CHRISTOFI, F. L. 2013. Purinergic autocrine regulation of mechanosensitivity and serotonin release in a human EC model: ATP-gated P2X3 channels in EC are downregulated in ulcerative colitis. *Inflamm Bowel Dis,* 19**,** 2366-79.

LINDEN, D. R., CHEN, J. X., GERSHON, M. D., SHARKEY, K. A. & MAWE, G. M. 2003. Serotonin availability is increased in mucosa of guinea pigs with TNBS-induced colitis. *Am J Physiol Gastrointest Liver Physiol,* 285**,** G207-16.

LIU, Q., YANG, Q., SUN, W., VOGEL, P., HEYDORN, W., YU, X. Q., HU, Z., YU, W., JONAS, B., PINEDA, R., CALDERON-GAY, V., GERMANN, M., O'NEILL, E., BROMMAGE, R., CULLINAN, E., PLATT, K., WILSON, A., POWELL, D., SANDS, A., ZAMBROWICZ, B. & SHI, Z. C. 2008. Discovery and characterization of novel tryptophan hydroxylase inhibitors that selectively inhibit serotonin synthesis in the gastrointestinal tract. *J Pharmacol Exp Ther,* 325**,** 47-55.

LOESCHE, W. J. 1969. Effect of bacterial contamination on cecal size and cecal contents of gnotobiotic rodents. *J Bacteriol,* 99**,** 520-6.

LOMAX, R. B., GALLEGO, S., NOVALBOS, J., GARCIA, A. G. & WARHURST, G. 1999. L-Type calcium channels in enterochromaffin cells from guinea pig and human duodenal crypts: an in situ study. *Gastroenterology,* 117**,** 1363-9.

LUCZYNSKI, P., MCVEY NEUFELD, K. A., ORIACH, C. S., CLARKE, G., DINAN, T. G. & CRYAN, J. F. 2016. Growing up in a Bubble: Using Germ-Free Animals to Assess the Influence of the Gut Microbiota on Brain and Behavior. *Int J Neuropsychopharmacol,* 19**,** pyw020.

LYCHKOVA, A. E. & PAVONE, L. M. 2013. Role of serotonin receptors in regulation of contractile activity of urinary bladder in rabbits. *Urology,* 81**,** 696 e13-8.

MA, X. Y., CHEN, F. Q., HONG, H., LV, X. J., DONG, M. & WANG, Q. Y. 2015. The Relationship between Serum Osteocalcin Concentration and Glucose and Lipid Metabolism in Patients with Type 2 Diabetes Mellitus - The Role of Osteocalcin in Energy Metabolism. *Ann Nutr Metab,* 66**,** 110-6.

MACE, O. J., AFFLECK, J., PATEL, N. & KELLETT, G. L. 2007. Sweet taste receptors in rat small intestine stimulate glucose absorption through apical GLUT2. *J Physiol,* 582**,** 379-92.

MAIGAARD, S., FORMAN, A. & ANDERSSON, K. E. 1986. Relaxant and contractile effects of some amines and prostanoids in myometrial and vascular smooth muscle within the human uteroplacental unit. *Acta Physiol Scand,* 128**,** 33-40.

MANOCHA, M., SHAJIB, M. S., RAHMAN, M. M., WANG, H., RENGASAMY, P., BOGUNOVIC, M., JORDANA, M., MAYER, L. & KHAN, W. I. 2013. IL-13-mediated immunological control of enterochromaffin cell hyperplasia and serotonin production in the gut. *Mucosal Immunol,* 6**,** 146-55.

MARGOLIS, K. G., STEVANOVIC, K., LI, Z., YANG, Q. M., ORAVECZ, T., ZAMBROWICZ, B., JHAVER, K. G., DIACOU, A. & GERSHON, M. D. 2014. Pharmacological reduction of mucosal but not neuronal serotonin opposes inflammation in mouse intestine. *Gut,* 63**,** 928-37.

MARITZEN, T., KEATING, D. J., NEAGOE, I., ZDEBIK, A. A. & JENTSCH, T. J. 2008. Role of the vesicular chloride transporter ClC-3 in neuroendocrine tissue. *J Neurosci,* 28**,** 10587-98.

MARKSTEIN, R., MATSUMOTO, M., KOHLER, C., TOGASHI, H., YOSHIOKA, M. & HOYER, D. 1999. Pharmacological characterisation of 5-HT receptors positively coupled to adenylyl cyclase in the rat hippocampus. *Naunyn Schmiedebergs Arch Pharmacol,* 359**,** 454-9.

MARSHALL, A. M., HERNANDEZ, L. L. & HORSEMAN, N. D. 2014. Serotonin and serotonin transport in the regulation of lactation. *J Mammary Gland Biol Neoplasia,* 19**,** 139-46.

MARTIN, A. M., LUMSDEN, A. L., YOUNG, R. L., JESSUP, C. F., SPENCER, N. J. & KEATING, D. J. 2017. The nutrient-sensing repertoires of mouse enterochromaffin cells differ between duodenum and colon. *Neurogastroenterol Motil,* e13046.

MARTINS, P., FAKHRY, J., DE OLIVEIRA, E. C., HUNNE, B., FOTHERGILL, L. J., RINGUET, M., REIS, D. D., REHFELD, J. F., CALLAGHAN, B. & FURNESS, J. B. 2017. Analysis of enteroendocrine cell populations in the human colon. *Cell Tissue Res,* 367**,** 161-168.

MASAKI, T., CHIBA, S., YASUDA, T., TSUBONE, T., KAKUMA, T., SHIMOMURA, I., FUNAHASHI, T., MATSUZAWA, Y. & YOSHIMATSU, H. 2003. Peripheral, But Not Central, Administration of Adiponectin Reduces Visceral Adiposity and Upregulates the Expression of Uncoupling Protein in Agouti Yellow (Ay/a) Obese Mice. *Diabetes,* 52**,** 2266-2273.

MASSON, J., EMERIT, M. B., HAMON, M. & DARMON, M. 2012. Serotonergic signaling: multiple effectors and pleiotropic effects. *Wiley Interdisciplinary Reviews: Membrane Transport and Signaling,* 1**,** 685-713.

MATSUDA, M., IMAOKA, T., VOMACHKA, A. J., GUDELSKY, G. A., HOU, Z., MISTRY, M., BAILEY, J. P., NIEPORT, K. M., WALTHER, D. J., BADER, M. & HORSEMAN, N. D. 2004. Serotonin regulates mammary gland development via an autocrine-paracrine loop. *Dev Cell,* 6**,** 193-203.

MAYEUR, C., GILLARD, L., LE BEYEC, J., BADO, A., JOLY, F. & THOMAS, M. 2016. Extensive Intestinal Resection Triggers Behavioral Adaptation, Intestinal Remodeling and Microbiota Transition in Short Bowel Syndrome. *Microorganisms,* 4**,** 16.

MCNEIL, N. I., CUMMINGS, J. H. & JAMES, W. P. 1978. Short chain fatty acid absorption by the human large intestine. *Gut,* 19**,** 819-22.

MEMBREZ, M., BLANCHER, F., JAQUET, M., BIBILONI, R., CANI, P. D., BURCELIN, R. G., CORTHESY, I., MACE, K. & CHOU, C. J. 2008. Gut microbiota modulation with norfloxacin and ampicillin enhances glucose tolerance in mice. *FASEB J,* 22**,** 2416-26.

MERCADO, C. P., QUINTERO, M. V., LI, Y., SINGH, P., BYRD, A. K., TALABNIN, K., ISHIHARA, M., AZADI, P., RUSCH, N. J., KUBERAN, B., MAROTEAUX, L. & KILIC, F. 2013. A serotonin-induced N-glycan switch regulates platelet aggregation. *Sci Rep,* 3**,** 2795.

MIKKELSEN, K. H., FROST, M., BAHL, M. I., LICHT, T. R., JENSEN, U. S., ROSENBERG, J., PEDERSEN, O., HANSEN, T., REHFELD, J. F., HOLST, J. J., VILSBOLL, T. & KNOP, F. K. 2015. Effect of Antibiotics on Gut Microbiota, Gut Hormones and Glucose Metabolism. *PLoS One,* 10**,** e0142352.

MILAN, G., GRANZOTTO, M., SCARDA, A., CALCAGNO, A., PAGANO, C., FEDERSPIL, G. & VETTOR, R. 2002. Resistin and adiponectin expression in visceral fat of obese rats: effect of weight loss. *Obes Res,* 10**,** 1095-103.

MIYAMOTO, K., HASE, K., TAKETANI, Y., MINAMI, H., OKA, T., NAKABOU, Y. & HAGIHIRA, H. 1991. Diabetes and glucose transporter gene expression in rat small intestine. *Biochem Biophys Res Commun,* 181**,** 1110-7.

MODLIN, I. M., KIDD, M., PFRAGNER, R., EICK, G. N. & CHAMPANERIA, M. C. 2006. The functional characterization of normal and neoplastic human enterochromaffin cells. *J Clin Endocrinol Metab,* 91**,** 2340-8.

MOORE, M., KIMURA, K., SHIBATA, H., HONJOH, T., SAITO, M., EVERETT, C., SMITH, M. & CHERRINGTON, A. 2005. Portal 5-hydroxytryptophan infusion enhances glucose disposal in conscious dogs. *American journal of physiology. Endocrinology and metabolism,* 289**,** 31.

MOSIALOU, I., SHIKHEL, S., LIU, J. M., MAURIZI, A., LUO, N., HE, Z., HUANG, Y., ZONG, H., FRIEDMAN, R. A., BARASCH, J., LANZANO, P., DENG, L., LEIBEL, R. L., RUBIN, M., NICHOLAS, T., CHUNG, W., ZELTSER, L. M., WILLIAMS, K. W., PESSIN, J. E. & KOUSTENI, S. 2017. MC4R-dependent suppression of appetite by bone-derived lipocalin 2. *Nature,* 543**,** 385-390.

MOWAT, A. M. & AGACE, W. W. 2014. Regional specialization within the intestinal immune system. *Nat Rev Immunol,* 14**,** 667-85.

MULLER, P. Y., JANOVJAK, H., MISEREZ, A. R. & DOBBIE, Z. 2002. Processing of gene expression data generated by quantitative real-time RT-PCR. *Biotechniques,* 32**,** 1372-4, 1376, 1378-9.

MULLER, T., DURK, T., BLUMENTHAL, B., GRIMM, M., CICKO, S., PANTHER, E., SORICHTER, S., HEROUY, Y., DI VIRGILIO, F., FERRARI, D., NORGAUER, J. & IDZKO, M. 2009. 5-hydroxytryptamine modulates migration, cytokine and chemokine release and T-cell priming capacity of dendritic cells in vitro and in vivo. *PLoS One,* 4**,** e6453.

MURRAY, K. C., STEPHENS, M. J., BALLOU, E. W., HECKMAN, C. J. & BENNETT, D. J. 2011. Motoneuron excitability and muscle spasms are regulated by 5-HT2B and 5-HT2C receptor activity. *J Neurophysiol,* 105**,** 731-48.

NADKARNI, M. A., MARTIN, F. E., JACQUES, N. A. & HUNTER, N. 2002. Determination of bacterial load by real-time PCR using a broad-range (universal) probe and primers set. *Microbiology,* 148**,** 257-66.

NAKATANI, Y., SATO-SUZUKI, I., TSUJINO, N., NAKASATO, A., SEKI, Y., FUMOTO, M. & ARITA, H. 2008. Augmented brain 5-HT crosses the blood-brain barrier through the 5-HT transporter in rat. *Eur J Neurosci,* 27**,** 2466-72.

NAM, S. S., LEE, J. C., KIM, H. J., PARK, J. W., LEE, J. M., SUH, J. Y., UM, H. S., KIM, J. Y., LEE, Y. & KIM, Y. G. 2016. Serotonin Inhibits Osteoblast Differentiation and Bone Regeneration in Rats. *J Periodontol,* 87**,** 461-9.

NAMKUNG, J., KIM, H. & PARK, S. 2015. Peripheral Serotonin: a New Player in Systemic Energy Homeostasis. *Mol Cells,* 38**,** 1023-8.

NASCIMENTO, E. R., MAIA, A. C., NARDI, A. E. & SILVA, A. C. 2015. Sexual dysfunction in arterial hypertension women: The role of depression and anxiety. *J Affect Disord,* 181**,** 96-100.

NAUCK, M. A., NIEDEREICHHOLZ, U., ETTLER, R., HOLST, J. J., ORSKOV, C., RITZEL, R. & SCHMIEGEL, W. H. 1997. Glucagon-like peptide 1 inhibition of gastric emptying outweighs its insulinotropic effects in healthy humans. *Am J Physiol,* 273**,** E981-8.

NEBIGIL, C. G., CHOI, D. S., DIERICH, A., HICKEL, P., LE MEUR, M., MESSADDEQ, N., LAUNAY, J. M. & MAROTEAUX, L. 2000. Serotonin 2B receptor is required for heart development. *Proc Natl Acad Sci U S A,* 97**,** 9508-9513.

NESTEL, P. J. & STEINBERG, D. 1963. Fate of Palmitate and of Linoleate Perfused through the Isolated Rat Liver at High Concentrations. *J Lipid Res,* 4**,** 461-9.

NEUFELD, K. M., KANG, N., BIENENSTOCK, J. & FOSTER, J. A. 2011. Reduced anxiety-like behavior and central neurochemical change in germ-free mice. *Neurogastroenterology & Motility,* 23**,** 255-e119.

NEUNLIST, M., DOBREVA, G. & SCHEMANN, M. 1999. Characteristics of mucosally projecting myenteric neurones in the guinea-pig proximal colon. *J Physiol,* 517 (Pt 2)**,** 533-46.

NGARMUKOS, C., CHAILURKIT, L. O., CHANPRASERTYOTHIN, S., HENGPRASITH, B., SRITARA, P. & ONGPHIPHADHANAKUL, B. 2012. A reduced serum level of total osteocalcin in men predicts the development of diabetes in a long-term follow-up cohort. *Clin Endocrinol (Oxf),* 77**,** 42-6.

NGUYEN, N. Q., DEBRECENI, T. L., BAMBRICK, J. E., CHIA, B., WISHART, J., DEANE, A. M., RAYNER, C. K., HOROWITZ, M. & YOUNG, R. L. 2015. Accelerated intestinal glucose absorption in morbidly obese humans: relationship to glucose transporters, incretin hormones, and glycemia. *J Clin Endocrinol Metab,* 100**,** 968-76.

NICHOLS, D. E. & NICHOLS, C. D. 2008. Serotonin receptors. *Chem Rev,* 108**,** 1614-41.

NIEUWDORP, M., GILIJAMSE, P. W., PAI, N. & KAPLAN, L. M. 2014. Role of the microbiome in energy regulation and metabolism. *Gastroenterology,* 146**,** 1525-33.

NIGHTINGALE, J. M., KAMM, M. A., VAN DER SIJP, J. R., MORRIS, G. P., WALKER, E. R., MATHER, S. J., BRITTON, K. E. & LENNARD-JONES, J. E. 1993. Disturbed gastric emptying in the short bowel syndrome. Evidence for a 'colonic brake'. *Gut,* 34**,** 1171-1176.

NILSSON, O., AHLMAN, H., GEFFARD, M., DAHLSTRÖM, A. & ERICSON, L. E. 1987. Bipolarity of duodenal enterochromaffin cells in the rat. *Cell and Tissue Research,* 248**,** 49-54.

NODA, M., HIGASHIDA, H., AOKI, S. & WADA, K. 2004. Multiple signal transduction pathways mediated by 5-HT receptors. *Mol Neurobiol,* 29**,** 31-9.

NOHR, M. K., PEDERSEN, M. H., GILLE, A., EGEROD, K. L., ENGELSTOFT, M. S., HUSTED, A. S., SICHLAU, R. M., GRUNDDAL, K. V., POULSEN, S. S., HAN, S., JONES, R. M., OFFERMANNS, S. & SCHWARTZ, T. W. 2013. GPR41/FFAR3 and GPR43/FFAR2 as cosensors for short-chain fatty acids in enteroendocrine cells vs FFAR3 in enteric neurons and FFAR2 in enteric leukocytes. *Endocrinology,* 154**,** 3552-64.

NOMURA, S., SHOUZU, A., OMOTO, S., NISHIKAWA, M. & IWASAKA, T. 2005. 5-HT2A receptor antagonist increases circulating adiponectin in patients with type 2 diabetes. *Blood Coagul Fibrinolysis,* 16**,** 423-8.

NOZAWA, K., KAWABATA-SHODA, E., DOIHARA, H., KOJIMA, R., OKADA, H., MOCHIZUKI, S., SANO, Y., INAMURA, K., MATSUSHIME, H., KOIZUMI, T., YOKOYAMA, T. & ITO, H. 2009. TRPA1 regulates gastrointestinal motility through serotonin release from enterochromaffin cells. *Proc Natl Acad Sci U S A,* 106**,** 3408-13.

NZAKIZWANAYO, J., DEDI, C., STANDEN, G., MACFARLANE, W. M., PATEL, B. A. & JONES, B. V. 2015. Escherichia coli Nissle 1917 enhances bioavailability of serotonin in gut tissues through modulation of synthesis and clearance. *Sci Rep,* 5**,** 17324.

OFFERMANNS, S. 2014. Free fatty acid (FFA) and hydroxy carboxylic acid (HCA) receptors. *Annu Rev Pharmacol Toxicol,* 54**,** 407-34.

OH, C. M., NAMKUNG, J., GO, Y., SHONG, K. E., KIM, K., KIM, H., PARK, B. Y., LEE, H. W., JEON, Y. H., SONG, J., SHONG, M., YADAV, V. K., KARSENTY, G., KAJIMURA, S., LEE, I. K., PARK, S. & KIM, H. 2015. Regulation of systemic energy homeostasis by serotonin in adipose tissues. *Nat Commun,* 6**,** 6794.

OHARA-IMAIZUMI, M., KIM, H., YOSHIDA, M., FUJIWARA, T., AOYAGI, K., TOYOFUKU, Y., NAKAMICHI, Y., NISHIWAKI, C., OKAMURA, T., UCHIDA, T., FUJITANI, Y., AKAGAWA, K., KAKEI, M., WATADA, H., GERMAN, M. S. & NAGAMATSU, S. 2013. Serotonin regulates glucose-stimulated insulin secretion from pancreatic beta cells during pregnancy. *Proc Natl Acad Sci U S A,* 110**,** 19420-5.

OHTA, Y., KOSAKA, Y., KISHIMOTO, N., WANG, J., SMITH, S. B., HONIG, G., KIM, H., GASA, R. M., NEUBAUER, N., LIOU, A., TECOTT, L. H., DENERIS, E. S. & GERMAN, M. S. 2011. Convergence of the insulin and serotonin programs in the pancreatic beta-cell. *Diabetes,* 60**,** 3208-16.

OLESKIN, A. V., EL'-REGISTAN, G. I. & SHENDEROV, B. A. 2016. Role of neuromediators in the functioning of the human microbiota: "Business talks" among microorganisms and the microbiota-host dialogue. *Microbiology,* 85**,** 1-22.

PAPPENHEIMER, J. R. 1993. On the coupling of membrane digestion with intestinal absorption of sugars and amino acids. *Am J Physiol,* 265**,** G409-17.

PARK, S., KIM, D. S., KWON, D. Y. & YANG, H. J. 2011. Long-term central infusion of adiponectin improves energy and glucose homeostasis by decreasing fat storage and suppressing hepatic gluconeogenesis without changing food intake. *J Neuroendocrinol,* 23**,** 687-98.

PATEL, B. 2014. Mucosal adenosine triphosphate mediates serotonin release from ileal but not colonic guinea pig enterochromaffin cells. *Neurogastroenterology and motility : the official journal of the European Gastrointestinal Motility Society,* 26**,** 237-246.

PAULMANN, N., GROHMANN, M., VOIGT, J. P., BERT, B., VOWINCKEL, J., BADER, M., SKELIN, M., JEVSEK, M., FINK, H., RUPNIK, M. & WALTHER, D. J. 2009. Intracellular serotonin modulates insulin secretion from pancreatic beta-cells by protein serotonylation. *PLoS Biol,* 7**,** e1000229.

PEIRIS, H., RAGHUPATHI, R., JESSUP, C. F., ZANIN, M. P., MOHANASUNDARAM, D., MACKENZIE, K. D., CHATAWAY, T., CLARKE, J. N., BREALEY, J., COATES, P. T., PRITCHARD, M. A. & KEATING, D. J. 2012. Increased expression of the glucose-responsive gene, RCAN1, causes hypoinsulinemia, beta-cell dysfunction, and diabetes. *Endocrinology,* 153**,** 5212-21.

PENKO, D., ROJAS-CANALES, D., MOHANASUNDARAM, D., PEIRIS, H. S., SUN, W. Y., DROGEMULLER, C. J., KEATING, D. J., COATES, P. T., BONDER, C. S. & JESSUP, C. F. 2015. Endothelial progenitor cells enhance islet engraftment, influence beta-cell function, and modulate islet connexin 36 expression. *Cell Transplant,* 24**,** 37-48.

PERRY, R. J., PENG, L., BARRY, N. A., CLINE, G. W., ZHANG, D., CARDONE, R. L., PETERSEN, K. F., KIBBEY, R. G., GOODMAN, A. L. & SHULMAN, G. I. 2016. Acetate mediates a microbiome–brain–β-cell axis to promote metabolic syndrome. *Nature,* 534**,** 213-217.

PINTON, P., GIORGI, C., SIVIERO, R., ZECCHINI, E. & RIZZUTO, R. 2008. Calcium and apoptosis: ER-mitochondria Ca2+ transfer in the control of apoptosis. *Oncogene,* 27**,** 6407-18.

PISSIOS, P. & MARATOS-FLIER, E. 2007. More than satiety: central serotonin signaling and glucose homeostasis. *Cell Metab,* 6**,** 345-7.

PLOVIER, H., EVERARD, A., DRUART, C., DEPOMMIER, C., VAN HUL, M., GEURTS, L., CHILLOUX, J., OTTMAN, N., DUPARC, T., LICHTENSTEIN, L., MYRIDAKIS, A., DELZENNE, N. M., KLIEVINK, J., BHATTACHARJEE, A., VAN DER ARK, K. C., AALVINK, S., MARTINEZ, L. O., DUMAS, M. E., MAITER, D., LOUMAYE, A., HERMANS, M. P., THISSEN, J. P., BELZER, C., DE VOS, W. M. & CANI, P. D. 2017. A purified membrane protein from Akkermansia muciniphila or the pasteurized bacterium improves metabolism in obese and diabetic mice. *Nat Med,* 23**,** 107-113.

RACKÉ, K., REIMANN, A., SCHWÖRER, H. & KILBINGER, H. 1995. Regulation of 5-HT release from enterochromaffin cells. *Behavioural Brain Research,* 73**,** 83-87.

RAGHUPATHI, R., DUFFIELD, M. D., ZELKAS, L., MEEDENIYA, A., BROOKES, S. J., SIA, T. C., WATTCHOW, D. A., SPENCER, N. J. & KEATING, D. J. 2013. Identification of unique release kinetics of serotonin from guinea-pig and human enterochromaffin cells. *J Physiol,* 591**,** 5959-75.

RAGHUPATHI, R., JESSUP, C. F., LUMSDEN, A. L. & KEATING, D. J. 2016. Fusion Pore Size Limits 5-HT Release From Single Enterochromaffin Cell Vesicles. *J Cell Physiol,* 231**,** 1593-600.

RAHMAN, M. K., NAGATSU, T. & KATO, T. 1981. Aromatic L-Amino-Acid Decarboxylase Activity in Central and Peripheral-Tissues and Serum of Rats with L-Dopa and L-5-Hydroxytryptophan as Substrates. *Biochemical Pharmacology,* 30**,** 645-649.

RAPKIN, A. J., EDELMUTH, E., CHANG, L. C., READING, A. E., MCGUIRE, M. T. & SU, T. P. 1987. Whole-blood serotonin in premenstrual syndrome. *Obstet Gynecol,* 70**,** 533-7.

RAVUSSIN, Y., KOREN, O., SPOR, A., LEDUC, C., GUTMAN, R., STOMBAUGH, J., KNIGHT, R., LEY, R. E. & LEIBEL, R. L. 2012. Responses of Gut Microbiota to Diet Composition and Weight Loss in Lean and Obese Mice. *Obesity (Silver Spring, Md.),* 20**,** 10.1038/oby.2011.111.

RAYBOULD, H. E. 1991. Capsaicin-sensitive vagal afferents and CCK in inhibition of gastric motor function induced by intestinal nutrients. *Peptides,* 12**,** 1279-83.

RAYBOULD, H. E., GLATZLE, J., ROBIN, C., MEYER, J. H., PHAN, T., WONG, H. & STERNINI, C. 2003. Expression of 5-HT3 receptors by extrinsic duodenal afferents contribute to intestinal inhibition of gastric emptying. *Am J Physiol Gastrointest Liver Physiol,* 284**,** G367-72.

RAYBOULD, H. E. & TACHE, Y. 1988. Cholecystokinin inhibits gastric motility and emptying via a capsaicin-sensitive vagal pathway in rats. *Am J Physiol,* 255**,** G242-6.

RAYBOULD, H. E. & ZITTEL, T. T. 1995. Inhibition of gastric motility induced by intestinal glucose in awake rats: role of Na(+)-glucose co-transporter. *Neurogastroenterol Motil,* 7**,** 9-14.

RAYNER, C. K., PARK, H. S., WISHART, J. M., KONG, M., DORAN, S. M. & HOROWITZ, M. 2000. Effects of intraduodenal glucose and fructose on antropyloric motility and appetite in healthy humans. *Am J Physiol Regul Integr Comp Physiol,* 278**,** R360-6.

REIGSTAD, C. S., SALMONSON, C. E., RAINEY, J. F., 3RD, SZURSZEWSKI, J. H., LINDEN, D. R., SONNENBURG, J. L., FARRUGIA, G. & KASHYAP, P. C. 2015. Gut microbes promote colonic serotonin production through an effect of short-chain fatty acids on enterochromaffin cells. *FASEB J,* 29**,** 1395-403.

REIJNDERS, D., GOOSSENS, G. H., HERMES, G. D., NEIS, E. P., VAN DER BEEK, C. M., MOST, J., HOLST, J. J., LENAERTS, K., KOOTTE, R. S., NIEUWDORP, M., GROEN, A. K., OLDE DAMINK, S. W., BOEKSCHOTEN, M. V., SMIDT, H., ZOETENDAL, E. G., DEJONG, C. H. & BLAAK, E. E. 2016. Effects of Gut Microbiota Manipulation by Antibiotics on Host Metabolism in Obese Humans: A Randomized Double-Blind Placebo-Controlled Trial. *Cell Metab,* 24**,** 341.

REYNAUD, Y., FAKHRY, J., FOTHERGILL, L., CALLAGHAN, B., RINGUET, M., HUNNE, B., BRAVO, D. M. & FURNESS, J. B. 2016. The chemical coding of 5-hydroxytryptamine containing enteroendocrine cells in the mouse gastrointestinal tract. *Cell Tissue Res,* 364**,** 489-97.

RICHARDS, J. B., PAPAIOANNOU, A., ADACHI, J. D., JOSEPH, L., WHITSON, H. E., PRIOR, J. C., GOLTZMAN, D. & CANADIAN MULTICENTRE OSTEOPOROSIS STUDY RESEARCH, G. 2007. Effect of selective serotonin reuptake inhibitors on the risk of fracture. *Arch Intern Med,* 167**,** 188-94.

RIDAURA, V. K., FAITH, J. J., REY, F. E., CHENG, J., DUNCAN, A. E., KAU, A. L., GRIFFIN, N. W., LOMBARD, V., HENRISSAT, B., BAIN, J. R., MUEHLBAUER, M. J., ILKAYEVA, O., SEMENKOVICH, C. F., FUNAI, K., HAYASHI, D. K., LYLE, B. J., MARTINI, M. C., URSELL, L. K., CLEMENTE, J. C., VAN TREUREN, W., WALTERS, W. A., KNIGHT, R., NEWGARD, C. B., HEATH, A. C. & GORDON, J. I. 2013. Gut microbiota from twins discordant for obesity modulate metabolism in mice. *Science,* 341**,** 1241214.

RIDLON, J. M., KANG, D. J. & HYLEMON, P. B. 2006. Bile salt biotransformations by human intestinal bacteria. *J Lipid Res,* 47**,** 241-59.

RIOS-COVIAN, D., SALAZAR, N., GUEIMONDE, M. & DE LOS REYES-GAVILAN, C. G. 2017. Shaping the Metabolism of Intestinal Bacteroides Population through Diet to Improve Human Health. *Front Microbiol,* 8**,** 376.

RIPKEN, D., VAN DER WIELEN, N., WORTELBOER, H. M., MEIJERINK, J., WITKAMP, R. F. & HENDRIKS, H. F. 2016. Nutrient-induced glucagon like peptide-1 release is modulated by serotonin. *J Nutr Biochem,* 32**,** 142-50.

RITZE, Y., HENGELHAUPT, C., BARDOS, G., ERNST, B., THURNHEER, M., D'HAESE, J. G., BISCHOFF, S. C. & SCHULTES, B. 2015. Altered intestinal neuroendocrine gene expression in humans with obesity. *Obesity (Silver Spring),* 23**,** 2278-85.

ROEDIGER, W. E. 1980. Role of anaerobic bacteria in the metabolic welfare of the colonic mucosa in man. *Gut,* 21**,** 793-8.

ROGERS, G. B., KEATING, D. J., YOUNG, R. L., WONG, M. L., LICINIO, J. & WESSELINGH, S. 2016. From gut dysbiosis to altered brain function and mental illness: mechanisms and pathways. *Mol Psychiatry,* 21**,** 738-48.

ROSARIO, L. M., BARBOSA, R. M., ANTUNES, C. M., BALDEIRAS, I. E., SILVA, A. M., TOME, A. R. & SANTOS, R. M. 2008. Regulation by glucose of oscillatory electrical activity and 5-HT/insulin release from single mouse pancreatic islets in absence of functional K(ATP) channels. *Endocr J,* 55**,** 639-50.

ROTH, K. A. & GORDON, J. I. 1990. Spatial differentiation of the intestinal epithelium: analysis of enteroendocrine cells containing immunoreactive serotonin, secretin, and substance P in normal and transgenic mice. *Proc Natl Acad Sci U S A,* 87**,** 6408-12.

RUI, L. 2014. Energy metabolism in the liver. *Compr Physiol,* 4**,** 177-97.

RUPPIN, H., BAR-MEIR, S., SOERGEL, K. H., WOOD, C. M. & SCHMITT, M. G., JR. 1980. Absorption of short-chain fatty acids by the colon. *Gastroenterology,* 78**,** 1500-7.

SALONEN, A., LAHTI, L., SALOJARVI, J., HOLTROP, G., KORPELA, K., DUNCAN, S. H., DATE, P., FARQUHARSON, F., JOHNSTONE, A. M., LOBLEY, G. E., LOUIS, P., FLINT, H. J. & DE VOS, W. M. 2014. Impact of diet and individual variation on intestinal microbiota composition and fermentation products in obese men. *ISME J,* 8**,** 2218-30.

SAVAGE, A. P., ADRIAN, T. E., CAROLAN, G., CHATTERJEE, V. K. & BLOOM, S. R. 1987. Effects of peptide YY (PYY) on mouth to caecum intestinal transit time and on the rate of gastric emptying in healthy volunteers. *Gut,* 28**,** 166-170.

SAVASTANO, D., CARELLE, M. & COVASA, M. 2005. Serotonin-type 3 receptors mediate intestinal Polycose- and glucose-induced suppression of intake. *American journal of physiology. Regulatory, integrative and comparative physiology,* 288**,** 508.

SCARPELLINI, E., IANIRO, G., ATTILI, F., BASSANELLI, C., DE SANTIS, A. & GASBARRINI, A. 2015. The human gut microbiota and virome: Potential therapeutic implications. *Dig Liver Dis,* 47**,** 1007-12.

SCHÄFERMEYER, A., GRATZL, M., RAD, R., DOSSUMBEKOVA, A., SACHS, G. & PRINZ, C. 2004. Isolation and receptor profiling of ileal enterochromaffin cells. *Acta Physiologica Scandinavica,* 182**,** 53-62.

SCHNEEBERGER, M., EVERARD, A., GÓMEZ-VALADÉS, A. G., MATAMOROS, S., RAMÍREZ, S., DELZENNE, N. M., GOMIS, R., CLARET, M. & CANI, P. D. 2015. Akkermansia muciniphila inversely correlates with the onset of inflammation, altered adipose tissue metabolism and metabolic disorders during obesity in mice. *Scientific Reports,* 5**,** 16643.

SCHRAENEN, A., LEMAIRE, K., DE FAUDEUR, G., HENDRICKX, N., GRANVIK, M., VAN LOMMEL, L., MALLET, J., VODJDANI, G., GILON, P., BINART, N., IN'T VELD, P. & SCHUIT, F. 2010. Placental lactogens induce serotonin biosynthesis in a subset of mouse beta cells during pregnancy. *Diabetologia,* 53**,** 2589-99.

SCHWORER, H., RACKE, K. & KILBINGER, H. 1989. GABA receptors are involved in the modulation of the release of 5-hydroxytryptamine from the vascularly perfused small intestine of the guinea-pig. *Eur J Pharmacol,* 165**,** 29-37.

SEELEY, R. J., CHAMBERS, A. P. & SANDOVAL, D. A. 2015. The role of gut adaptation in the potent effects of multiple bariatric surgeries on obesity and diabetes. *Cell Metab,* 21**,** 369-78.

SHAJIB, M. S. & KHAN, W. I. 2015. The role of serotonin and its receptors in activation of immune responses and inflammation. *Acta Physiol (Oxf),* 213**,** 561-74.

SHAJIB, M. S., WANG, H., KIM, J. J., SUNJIC, I., GHIA, J. E., DENOU, E., COLLINS, M., DENBURG, J. A. & KHAN, W. I. 2013. Interleukin 13 and serotonin: linking the immune and endocrine systems in murine models of intestinal inflammation. *PLoS One,* 8**,** e72774.

SHANBHOGUE, V. V., FINKELSTEIN, J. S., BOUXSEIN, M. L. & YU, E. W. 2016. Association between insulin resistance and bone structure in non-diabetic postmenopausal women. *J Clin Endocrinol Metab***,** jc20161726.

SHI, Z. C., DEVASAGAYARAJ, A., GU, K., JIN, H., MARINELLI, B., SAMALA, L., SCOTT, S., STOUCH, T., TUNOORI, A., WANG, Y., ZANG, Y., ZHANG, C., KIMBALL, S. D., MAIN, A. J., SUN, W., YANG, Q., NOURALDEEN, A., YU, X. Q., BUXTON, E., PATEL, S., NGUYEN, N., SWAFFIELD, J., POWELL, D. R., WILSON, A. & LIU, Q. 2008. Modulation of peripheral serotonin levels by novel tryptophan hydroxylase inhibitors for the potential treatment of functional gastrointestinal disorders. *J Med Chem,* 51**,** 3684-7.

SIMANSKY, K. J. 1996. Serotonergic control of the organization of feeding and satiety. *Behav Brain Res,* 73**,** 37-42.

SJOGREN, K., ENGDAHL, C., HENNING, P., LERNER, U. H., TREMAROLI, V., LAGERQUIST, M. K., BACKHED, F. & OHLSSON, C. 2012. The gut microbiota regulates bone mass in mice. *J Bone Miner Res,* 27**,** 1357-67.

SPEAKMAN, J. R. & KEIJER, J. 2012. Not so hot: Optimal housing temperatures for mice to mimic the thermal environment of humans. *Mol Metab,* 2**,** 5-9.

SPENCER, N. J. & KEATING, D. J. 2016. Is There a Role for Endogenous 5-HT in Gastrointestinal Motility? How Recent Studies Have Changed Our Understanding. *Adv Exp Med Biol,* 891**,** 113-22.

SPENCER, N. J., NICHOLAS, S. J., ROBINSON, L., KYLOH, M., FLACK, N., BROOKES, S. J., ZAGORODNYUK, V. P. & KEATING, D. J. 2011. Mechanisms underlying distension-evoked peristalsis in guinea pig distal colon: is there a role for enterochromaffin cells? *Am J Physiol Gastrointest Liver Physiol,* 301**,** G519-27.

SPENCER, N. J., SIA, T. C., BROOKES, S. J., COSTA, M. & KEATING, D. J. 2015. CrossTalk opposing view: 5-HT is not necessary for peristalsis. *J Physiol,* 593**,** 3229-31.

SPILLER, R. C., JENKINS, D., THORNLEY, J. P., HEBDEN, J. M., WRIGHT, T., SKINNER, M. & NEAL, K. R. 2000. Increased rectal mucosal enteroendocrine cells, T lymphocytes, and increased gut permeability following acute Campylobacter enteritis and in post-dysenteric irritable bowel syndrome. *Gut,* 47**,** 804-11.

SPILLER, R. C., TROTMAN, I. F., ADRIAN, T. E., BLOOM, S. R., MISIEWICZ, J. J. & SILK, D. B. 1988. Further characterisation of the 'ileal brake' reflex in man--effect of ileal infusion of partial digests of fat, protein, and starch on jejunal motility and release of neurotensin, enteroglucagon, and peptide YY. *Gut,* 29**,** 1042-1051.

STAAL, R. G., MOSHAROV, E. V. & SULZER, D. 2004. Dopamine neurons release transmitter via a flickering fusion pore. *Nat Neurosci,* 7**,** 341-6.

STEFKA, A. T., FEEHLEY, T., TRIPATHI, P., QIU, J., MCCOY, K., MAZMANIAN, S. K., TJOTA, M. Y., SEO, G. Y., CAO, S., THERIAULT, B. R., ANTONOPOULOS, D. A., ZHOU, L., CHANG, E. B., FU, Y. X. & NAGLER, C. R. 2014. Commensal bacteria protect against food allergen sensitization. *Proc Natl Acad Sci U S A,* 111**,** 13145-50.

STULL, M. A., PAI, V., VOMACHKA, A. J., MARSHALL, A. M., JACOB, G. A. & HORSEMAN, N. D. 2007. Mammary gland homeostasis employs serotonergic regulation of epithelial tight junctions. *Proc Natl Acad Sci U S A,* 104**,** 16708-13.

SUAREZ-ZAMORANO, N., FABBIANO, S., CHEVALIER, C., STOJANOVIC, O., COLIN, D. J., STEVANOVIC, A., VEYRAT-DUREBEX, C., TARALLO, V., RIGO, D., GERMAIN, S., ILIEVSKA, M., MONTET, X., SEIMBILLE, Y., HAPFELMEIER, S. & TRAJKOVSKI, M. 2015. Microbiota depletion promotes browning of white adipose tissue and reduces obesity. *Nat Med,* 21**,** 1497-501.

SUMARA, G., SUMARA, O., KIM, J. K. & KARSENTY, G. 2012. Gut-derived serotonin is a multifunctional determinant to fasting adaptation. *Cell Metab,* 16**,** 588-600.

SYMONDS, E. L., PEIRIS, M., PAGE, A. J., CHIA, B., DOGRA, H., MASDING, A., GALANAKIS, V., ATIBA, M., BULMER, D., YOUNG, R. L. & BLACKSHAW, L. A. 2015. Mechanisms of activation of mouse and human enteroendocrine cells by nutrients. *Gut,* 64**,** 618-26.

SZEBENYI, S. A., LASKOWSKI, A. I. & MEDLER, K. F. 2010. Sodium/calcium exchangers selectively regulate calcium signaling in mouse taste receptor cells. *J Neurophysiol,* 104**,** 529-38.

TACK, J., CAMILLERI, M., CHANG, L., CHEY, W. D., GALLIGAN, J. J., LACY, B. E., MÜLLER-LISSNER, S., QUIGLEY, E. M. M., SCHUURKES, J., MAEYER, J. H. & STANGHELLINI, V. 2012. Systematic review: cardiovascular safety profile of 5-HT(4) agonists developed for gastrointestinal disorders. *Alimentary Pharmacology & Therapeutics,* 35**,** 745-767.

TACK, J. & DELOOSE, E. 2014. Complications of bariatric surgery: dumping syndrome, reflux and vitamin deficiencies. *Best Pract Res Clin Gastroenterol,* 28**,** 741-9.

TAKAHASHI, T., YANO, M., MINAMI, J., HARAGUCHI, T., KOGA, N., HIGASHI, K. & KOBORI, S. 2002. Sarpogrelate hydrochloride, a serotonin2A receptor antagonist, reduces albuminuria in diabetic patients with early-stage diabetic nephropathy. *Diabetes Res Clin Pract,* 58**,** 123-9.

TANAKA, K., HIRAI, T., ISHIBASHI, Y., IZUMO, N. & TOGARI, A. 2015. Modulation of osteoblast differentiation and bone mass by 5-HT2A receptor signaling in mice. *Eur J Pharmacol,* 762**,** 150-7.

TCHOUKALOVA, Y. D., KOUTSARI, C., VOTRUBA, S. B., TCHKONIA, T., GIORGADZE, N., THOMOU, T., KIRKLAND, J. L. & JENSEN, M. D. 2010. Sex- and depot-dependent differences in adipogenesis in normal-weight humans. *Obesity (Silver Spring),* 18**,** 1875-80.

THAZHATH, S., WU, T., YOUNG, R., HOROWITZ, M. & RAYNER, C. 2014. Glucose absorption in small intestinal diseases. *Expert review of gastroenterology & hepatology,* 8**,** 301-312.

TOBE, T., KIMURA, C. & FUJIWARA, M. 1967. Role of 5-hydroxytryptamine in the dumping syndrome after gastrectomy: histochemical study. *Annals of Surgery,* 165**,** 382-387.

TOLESSA, T., GUTNIAK, M., HOLST, J. J., EFENDIC, S. & HELLSTROM, P. M. 1998. Glucagon-like Peptide-1 Retards Gastric Emptying and Small Bowel Transit in the Rat (Effect Mediated Through Central or Enteric Nervous Mechanisms). *Digestive Diseases and Sciences,* 43**,** 2284-2290.

TOPPING, D. L. & CLIFTON, P. M. 2001. Short-chain fatty acids and human colonic function: roles of resistant starch and nonstarch polysaccharides. *Physiol Rev,* 81**,** 1031-64.

TOUGH, I. R., FORBES, S., TOLHURST, R., ELLIS, M., HERZOG, H., BORNSTEIN, J. C. & COX, H. M. 2011. Endogenous peptide YY and neuropeptide Y inhibit colonic ion transport, contractility and transit differentially via Y(1) and Y(2) receptors. *Br J Pharmacol,* 164**,** 471-84.

TREMAROLI, V. & BACKHED, F. 2012. Functional interactions between the gut microbiota and host metabolism. *Nature,* 489**,** 242-9.

TSAVKELOVA, E. A., KLIMOVA, S. Y., CHERDYNTSEVA, T. A. & NETRUSOV, A. I. 2006. Hormones and hormone-like substances of microorganisms: A review. *Applied Biochemistry and Microbiology,* 42**,** 229-235.

TUBIO, R. I., PEREZ-MACEIRA, J. & ALDEGUNDE, M. 2010. Homeostasis of glucose in the rainbow trout (Oncorhynchus mykiss Walbaum): the role of serotonin. *J Exp Biol,* 213**,** 1813-21.

TUDHOPE, S. J., WANG, C. C., PETRIE, J. L., POTTS, L., MALCOMSON, F., KIESWICH, J., YAQOOB, M. M., ARDEN, C., HAMPSON, L. J. & AGIUS, L. 2012. A novel mechanism for regulating hepatic glycogen synthesis involving serotonin and cyclin-dependent kinase-5. *Diabetes,* 61**,** 49-60.

TUO, B. G. & ISENBERG, J. I. 2003. Effect of 5-hydroxytryptamine on duodenal mucosal bicarbonate secretion in mice. *Gastroenterology,* 125**,** 805-14.

TUO, B. G., SELLERS, Z., PAULUS, P., BARRETT, K. E. & ISENBERG, J. I. 2004. 5-HT induces duodenal mucosal bicarbonate secretion via cAMP- and Ca2+-dependent signaling pathways and 5-HT4 receptors in mice. *Am J Physiol Gastrointest Liver Physiol,* 286**,** G444-51.

TURNBAUGH, P. J., HAMADY, M., YATSUNENKO, T., CANTAREL, B. L., DUNCAN, A., LEY, R. E., SOGIN, M. L., JONES, W. J., ROE, B. A., AFFOURTIT, J. P., EGHOLM, M., HENRISSAT, B., HEATH, A. C.,

KNIGHT, R. & GORDON, J. I. 2009. A core gut microbiome in obese and lean twins. *Nature,* 457**,** 480-4.

TURNBAUGH, P. J., LEY, R. E., MAHOWALD, M. A., MAGRINI, V., MARDIS, E. R. & GORDON, J. I. 2006. An obesity-associated gut microbiome with increased capacity for energy harvest. *Nature,* 444**,** 1027-31.

UCHIDA-KITAJIMA, S., YAMAUCHI, T., TAKASHINA, Y., OKADA-IWABU, M., IWABU, M., UEKI, K. & KADOWAKI, T. 2008. 5-Hydroxytryptamine 2A receptor signaling cascade modulates adiponectin and plasminogen activator inhibitor 1 expression in adipose tissue. *FEBS Lett,* 582**,** 3037-44.

UHING, M. R. & KIMURA, R. E. 1995. The effect of surgical bowel manipulation and anesthesia on intestinal glucose absorption in rats. *J Clin Invest,* 95**,** 2790-8.

URB, M. & SHEPPARD, D. C. 2012. The role of mast cells in the defence against pathogens. *PLoS Pathog,* 8**,** e1002619.

URIBE, A., ALAM, M., JOHANSSON, O., MIDTVEDT, T. & THEODORSSON, E. 1994. Microflora modulates endocrine cells in the gastrointestinal mucosa of the rat. *Gastroenterology,* 107**,** 1259-69.

VAN LAERE, K. M. J., HARTEMINK, R., BOSVELD, M., SCHOLS, H. A. & VORAGEN, A. G. J. 2000. Fermentation of Plant Cell Wall Derived Polysaccharides and Their Corresponding Oligosaccharides by Intestinal Bacteria. *Journal of Agricultural and Food Chemistry,* 48**,** 1644-1652.

VARSAMIS, P., LARSEN, R. N., DUNSTAN, D. W., JENNINGS, G. L., OWEN, N. & KINGWELL, B. A. 2017. The sugar content of soft drinks in Australia, Europe and the United States. *Med J Aust,* 206**,** 454-455.

VEGEZZI, G., ANSELMI, L., HUYNH, J., BAROCELLI, E., ROZENGURT, E., RAYBOULD, H. & STERNINI, C. 2014. Diet-induced regulation of bitter taste receptor subtypes in the mouse gastrointestinal tract. *PLoS One,* 9**,** e107732.

VELAGAPUDI, V. R., HEZAVEH, R., REIGSTAD, C. S., GOPALACHARYULU, P., YETUKURI, L., ISLAM, S., FELIN, J., PERKINS, R., BOREN, J., ORESIC, M. & BACKHED, F. 2010. The gut microbiota modulates host energy and lipid metabolism in mice. *J Lipid Res,* 51**,** 1101-12.

VINCENT, K. M., SHARP, J. W. & RAYBOULD, H. E. 2011. Intestinal glucose-induced calcium-calmodulin kinase signaling in the gut-brain axis in awake rats. *Neurogastroenterol Motil,* 23**,** e282-93.

VRIEZE, A., OUT, C., FUENTES, S., JONKER, L., REULING, I., KOOTTE, R. S., VAN NOOD, E., HOLLEMAN, F., KNAAPEN, M., ROMIJN, J. A., SOETERS, M. R., BLAAK, E. E., DALLINGA-THIE, G. M., REIJNDERS, D., ACKERMANS, M. T., SERLIE, M. J., KNOP, F. K., HOLST, J. J., VAN DER LEY, C., KEMA, I. P., ZOETENDAL, E. G., DE VOS, W. M., HOEKSTRA, J. B., STROES, E. S., GROEN, A. K. & NIEUWDORP, M. 2014. Impact of oral vancomycin on gut microbiota, bile acid metabolism, and insulin sensitivity. *J Hepatol,* 60**,** 824-31.

VRIEZE, A., VAN NOOD, E., HOLLEMAN, F., SALOJARVI, J., KOOTTE, R. S., BARTELSMAN, J. F., DALLINGA-THIE, G. M., ACKERMANS, M. T., SERLIE, M. J., OOZEER, R., DERRIEN, M., DRUESNE, A., VAN HYLCKAMA VLIEG, J. E., BLOKS, V. W., GROEN, A. K., HEILIG, H. G., ZOETENDAL, E. G., STROES, E. S., DE VOS, W. M., HOEKSTRA, J. B. & NIEUWDORP, M. 2012. Transfer of intestinal microbiota from lean donors increases insulin sensitivity in individuals with metabolic syndrome. *Gastroenterology,* 143**,** 913-6 e7.

WALTHER, D. J., PETER, J. U., BASHAMMAKH, S., HORTNAGL, H., VOITS, M., FINK, H. & BADER, M. 2003a. Synthesis of serotonin by a second tryptophan hydroxylase isoform. *Science,* 299**,** 76.

WALTHER, D. J., PETER, J. U., WINTER, S., HOLTJE, M., PAULMANN, N., GROHMANN, M., VOWINCKEL, J., ALAMO-BETHENCOURT, V., WILHELM, C. S., AHNERT-HILGER, G. & BADER, M. 2003b. Serotonylation of small GTPases is a signal transduction pathway that triggers platelet alpha-granule release. *Cell,* 115**,** 851-62.

WANG, F., KNUTSON, K., ALCAINO, C., LINDEN, D. R., GIBBONS, S. J., KASHYAP, P., GROVER, M., OECKLER, R., GOTTLIEB, P. A., LI, H. J., LEITER, A. B., FARRUGIA, G. & BEYDER, A. 2016. Mechanosensitive ion channel Piezo2 is important for enterochromaffin cell response to mechanical forces. *J Physiol*.

WANG, J., TANG, H., ZHANG, C., ZHAO, Y., DERRIEN, M., ROCHER, E., VAN-HYLCKAMA VLIEG, J. E., STRISSEL, K., ZHAO, L., OBIN, M. & SHEN, J. 2015. Modulation of gut microbiota during probiotic-mediated attenuation of metabolic syndrome in high fat diet-fed mice. *ISME J,* 9**,** 1-15.

WARDEN, S. J., BLIZIOTES, M. M., WIREN, K. M., ESHLEMAN, A. J. & TURNER, C. H. 2005. Neural regulation of bone and the skeletal effects of serotonin (5-hydroxytryptamine). *Mol Cell Endocrinol,* 242**,** 1-9.

WATANABE, H., AKASAKA, D., OGASAWARA, H., SATO, K., MIYAKE, M., SAITO, K., TAKAHASHI, Y., KANAYA, T., TAKAKURA, I., HONDO, T., CHAO, G., ROSE, M. T., OHWADA, S., WATANABE, K., YAMAGUCHI, T. & ASO, H. 2010. Peripheral serotonin enhances lipid metabolism by accelerating bile acid turnover. *Endocrinology,* 151**,** 4776-86.

WATANABE, H., SAITO, R., NAKANO, T., TAKAHASHI, H., TAKAHASHI, Y., SUMIYOSHI, K., SATO, K., CHEN, X., OKADA, N., IWASAKI, S., HARJANTI, D. W., SEKIGUCHI, N., SANO, H., KITAZAWA, H., ROSE, M. T., OHWADA, S., WATANABE, K. & ASO, H. 2014. Effect of peripheral 5-HT on glucose and lipid metabolism in wether sheep. *PLoS One,* 9**,** e88058.

WATTS, S. W., MORRISON, S. F., DAVIS, R. P. & BARMAN, S. M. 2012. Serotonin and blood pressure regulation. *Pharmacol Rev,* 64**,** 359-88.

WEISSBACH, H., REDFIELD, B. G. & UDENFRIEND, S. 1957. Soluble monoamine oxidase; its properties and actions on serotonin. *J Biol Chem,* 229**,** 953-63.

WEYER, C., FUNAHASHI, T., TANAKA, S., HOTTA, K., MATSUZAWA, Y., PRATLEY, R. E. & TATARANNI, P. A. 2001. Hypoadiponectinemia in obesity and type 2 diabetes: close association with insulin resistance and hyperinsulinemia. *J Clin Endocrinol Metab,* 86**,** 1930-5.

WHEATCROFT, J., WAKELIN, D., SMITH, A., MAHONEY, C., MAWE, G. & SPILLER, R. 2005. Enterochromaffin cell hyperplasia and decreased serotonin transporter in a mouse model of postinfectious bowel dysfunction. *Neurogastroenterology and motility : the official journal of the European Gastrointestinal Motility Society,* 17**,** 863-870.

WHITWORTH, T. L., HERNDON, L. C. & QUICK, M. W. 2002. Psychostimulants differentially regulate serotonin transporter expression in thalamocortical neurons. *The Journal of neuroscience : the official journal of the Society for Neuroscience,* 22.

WICHMANN, A., ALLAHYAR, A., GREINER, T. U., PLOVIER, H., LUNDEN, G. O., LARSSON, T., DRUCKER, D. J., DELZENNE, N. M., CANI, P. D. & BACKHED, F. 2013. Microbial modulation of energy availability in the colon regulates intestinal transit. *Cell Host Microbe,* 14**,** 582-90.

WIKOFF, W. R., ANFORA, A. T., LIU, J., SCHULTZ, P. G., LESLEY, S. A., PETERS, E. C. & SIUZDAK, G. 2009. Metabolomics analysis reveals large effects of gut microflora on mammalian blood metabolites. *Proc Natl Acad Sci U S A,* 106**,** 3698-703.

WOJDEMANN, M., WETTERGREN, A., HARTMANN, B., HILSTED, L. & HOLST, J. J. 1999. Inhibition of sham feeding-stimulated human gastric acid secretion by glucagon-like peptide-2. *J Clin Endocrinol Metab,* 84**,** 2513-7.

WOJDEMANN, M., WETTERGREN, A., HARTMANN, B. & HOLST, J. J. 1998. Glucagon-like peptide-2 inhibits centrally induced antral motility in pigs. *Scand J Gastroenterol,* 33**,** 828-32.

WOLF, K., BRAUN, A., HAINING, E. J., TSENG, Y. L., KRAFT, P., SCHUHMANN, M. K., GOTRU, S. K., CHEN, W., HERMANNS, H. M., STOLL, G., LESCH, K. P. & NIESWANDT, B. 2016. Partially Defective Store Operated Calcium Entry and Hem(ITAM) Signaling in Platelets of Serotonin Transporter Deficient Mice. *PLoS One,* 11**,** e0147664.

WONG, J. M., DE SOUZA, R., KENDALL, C. W., EMAM, A. & JENKINS, D. J. 2006. Colonic health: fermentation and short chain fatty acids. *J Clin Gastroenterol,* 40**,** 235-43.

WOO, S. H., RANADE, S., WEYER, A. D., DUBIN, A. E., BABA, Y., QIU, Z., PETRUS, M., MIYAMOTO, T., REDDY, K., LUMPKIN, E. A., STUCKY, C. L. & PATAPOUTIAN, A. 2014. Piezo2 is required for Merkel-cell mechanotransduction. *Nature,* 509**,** 622-6.

WRIGGLESWORTH, S. J. 1983. Heterogeneity of 5-hydroxytryptamine receptors in the rat uterus and stomach strip. *Br J Pharmacol,* 80**,** 691-7.

WU, S., YUAN, P.-Q., LAI, J., WONG, K., CHEN, M., OHNING, G. & TACHÉ, Y. 2011. Activation of Type 1 CRH receptor isoforms induces serotonin release from human carcinoid BON-1N cells: an enterochromaffin cell model. *Endocrinology,* 152**,** 126-137.

XU, H., BARNES, G. T., YANG, Q., TAN, G., YANG, D., CHOU, C. J., SOLE, J., NICHOLS, A., ROSS, J. S., TARTAGLIA, L. A. & CHEN, H. 2003. Chronic inflammation in fat plays a crucial role in the development of obesity-related insulin resistance. *J Clin Invest,* 112**,** 1821-30.

YADAV, V. K., BALAJI, S., SURESH, P. S., LIU, X. S., LU, X., LI, Z., GUO, X. E., MANN, J. J., BALAPURE, A. K., GERSHON, M. D., MEDHAMURTHY, R., VIDAL, M., KARSENTY, G. & DUCY, P. 2010. Pharmacological inhibition of gut-derived serotonin synthesis is a potential bone anabolic treatment for osteoporosis. *Nat Med,* 16**,** 308-12.

YADAV, V. K., OURY, F., SUDA, N., LIU, Z. W., GAO, X. B., CONFAVREUX, C., KLEMENHAGEN, K. C., TANAKA, K. F., GINGRICH, J. A., GUO, X. E., TECOTT, L. H., MANN, J. J., HEN, R., HORVATH, T. L. & KARSENTY, G. 2009. A serotonin-dependent mechanism explains the leptin regulation of bone mass, appetite, and energy expenditure. *Cell,* 138**,** 976-89.

YADAV, V. K., RYU, J. H., SUDA, N., TANAKA, K. F., GINGRICH, J. A., SCHUTZ, G., GLORIEUX, F. H., CHIANG, C. Y., ZAJAC, J. D., INSOGNA, K. L., MANN, J. J., HEN, R., DUCY, P. & KARSENTY, G. 2008. Lrp5 controls bone formation by inhibiting serotonin synthesis in the duodenum. *Cell,* 135**,** 825-37.

YAJIMA, T. & SAKATA, T. 1992. Core and periphery concentrations of short-chain fatty acids in luminal contents of the rat colon. *Comp Biochem Physiol Comp Physiol,* 103**,** 353-5.

YAMAUCHI, T., KAMON, J., WAKI, H., TERAUCHI, Y., KUBOTA, N., HARA, K., MORI, Y., IDE, T., MURAKAMI, K., TSUBOYAMA-KASAOKA, N., EZAKI, O., AKANUMA, Y., GAVRILOVA, O., VINSON, C., REITMAN, M. L., KAGECHIKA, H., SHUDO, K., YODA, M., NAKANO, Y., TOBE, K., NAGAI, R., KIMURA, S., TOMITA, M., FROGUEL, P. & KADOWAKI, T. 2001. The fat-derived hormone adiponectin reverses insulin resistance associated with both lipoatrophy and obesity. *Nat Med,* 7**,** 941-6.

YANG, G.-B. & LACKNER, A. A. 2004. Proximity between 5-HT secreting enteroendocrine cells and lymphocytes in the gut mucosa of rhesus macaques (Macaca mulatta) is suggestive of a role for enterochromaffin cell 5-HT in mucosal immunity. *Journal of Neuroimmunology,* 146**,** 46-49.

YANG, M. G., MANOHARAN, K. & MICKELSEN, O. 1970. Nutritional contribution of volatile fatty acids from the cecum of rats. *J Nutr,* 100**,** 545-50.

YANO, J. M., YU, K., DONALDSON, G. P., SHASTRI, G. G., ANN, P., MA, L., NAGLER, C. R., ISMAGILOV, R. F., MAZMANIAN, S. K. & HSIAO, E. Y. 2015. Indigenous bacteria from the gut microbiota regulate host serotonin biosynthesis. *Cell,* 161**,** 264-76.

YOON, Y. S., RYU, D., LEE, M. W., HONG, S. & KOO, S. H. 2009. Adiponectin and thiazolidinedione targets CRTC2 to regulate hepatic gluconeogenesis. *Exp Mol Med,* 41**,** 577-83.

YOSHIKAWA, T., INOUE, R., MATSUMOTO, M., YAJIMA, T., USHIDA, K. & IWANAGA, T. 2011. Comparative expression of hexose transporters (SGLT1, GLUT1, GLUT2 and GLUT5) throughout the mouse gastrointestinal tract. *Histochem Cell Biol,* 135**,** 183-94.

YOUNG, R. L. 2011. Sensing via intestinal sweet taste pathways. *Front Neurosci,* 5**,** 23.

YOUNG, R. L., CHIA, B., ISAACS, N. J., MA, J., KHOO, J., WU, T., HOROWITZ, M. & RAYNER, C. K. 2013. Disordered control of intestinal sweet taste receptor expression and glucose absorption in type 2 diabetes. *Diabetes,* 62**,** 3532-41.

YOUNG, R. L., LUMSDEN, A. L. & KEATING, D. J. 2015. Gut Serotonin Is a Regulator of Obesity and Metabolism. *Gastroenterology,* 149**,** 253-5.

YOUNG, R. L., LUMSDEN, A. L., MARTIN, A. M., SCHOBER, G., PEZOS, N., THAZHATH, S. S., ISAACS, N. J., CVIJANOVIC, N., SUN, E. W. L., WU, T., RAYNER, C. K., NGUYEN, N. Q., FONTGALLAND, D., RABBITT, P., HOLLINGTON, P., SPOSATO, L., DUE, S. L., WATTCHOW, D. A., LIOU, A. P., JACKSON, V. M. & KEATING, D. J. 2018. Augmented capacity for peripheral serotonin release in human obesity. *Int J Obes (Lond)*.

YOUNG, R. L., SUTHERLAND, K., PEZOS, N., BRIERLEY, S. M., HOROWITZ, M., RAYNER, C. K. & BLACKSHAW, L. A. 2009. Expression of taste molecules in the upper gastrointestinal tract in humans with and without type 2 diabetes. *Gut,* 58**,** 337-46.

YUSHKEVICH, P. A., PIVEN, J., HAZLETT, H. C., SMITH, R. G., HO, S., GEE, J. C. & GERIG, G. 2006. User-guided 3D active contour segmentation of anatomical structures: significantly improved efficiency and reliability. *Neuroimage,* 31**,** 1116-28.

YUSTA, B., HUANG, L., MUNROE, D., WOLFF, G., FANTASKE, R., SHARMA, S., DEMCHYSHYN, L., ASA, S. L. & DRUCKER, D. J. 2000. Enteroendocrine localization of GLP-2 receptor expression in humans and rodents. *Gastroenterology,* 119**,** 744-55.

ZANDER, M., MADSBAD, S., MADSEN, J. L. & HOLST, J. J. 2002. Effect of 6-week course of glucagon-like peptide 1 on glycaemic control, insulin sensitivity, and beta-cell function in type 2 diabetes: a parallel-group study. *Lancet,* 359**,** 824-30.

ZANIN, M. P., PHILLIPS, L., MACKENZIE, K. D. & KEATING, D. J. 2011. Aging differentially affects multiple aspects of vesicle fusion kinetics. *PLoS One,* 6**,** e27820.

ZELKAS, L., RAGHUPATHI, R., LUMSDEN, A. L., MARTIN, A. M., SUN, E., SPENCER, N. J., YOUNG, R. L. & KEATING, D. J. 2015. Serotonin-secreting enteroendocrine cells respond via diverse mechanisms to acute and chronic changes in glucose availability. *Nutr Metab (Lond),* 12**,** 55.

ZHANG, X., ZHAO, Y., ZHANG, M., PANG, X., XU, J., KANG, C., LI, M., ZHANG, C., ZHANG, Z., ZHANG, Y., LI, X., NING, G. & ZHAO, L. 2012. Structural changes of gut microbiota during berberine-mediated prevention of obesity and insulin resistance in high-fat diet-fed rats. *PLoS One,* 7**,** e42529.

ZHANG, Z. & JACKSON, M. B. 2010. Membrane bending energy and fusion pore kinetics in Ca(2+)-triggered exocytosis. *Biophys J,* 98**,** 2524-34.

ZHAO, S., LIU, W., WANG, J., SHI, J., SUN, Y., WANG, W., NING, G., LIU, R. & HONG, J. 2017. Akkermansia muciniphila improves metabolic profiles by reducing inflammation in chow diet-fed mice. *Journal of Molecular Endocrinology,* 58**,** 1-14.

ZHU, J. X., ZHU, X. Y., OWYANG, C. & LI, Y. 2001. Intestinal serotonin acts as a paracrine substance to mediate vagal signal transmission evoked by luminal factors in the rat. *J Physiol,* 530**,** 431-42.

Appendices

Appendix: Chapter 2

Table 6.1 – Reverse transcription reaction mixture components for cDNA synthesis

Component	Volume / reaction	Final concentration
10 x Buffer RT	2 µl	1x
dNTP Mix (5mM each dNTP)	2 µl	0.5mM each dNTP
Oligo-dT primer (10µM) (Qiagen)	2 µl	1µM
RNase inhibitor (Ambion) (10 units/µl)	1 µl	10 units
Omniscript® Reverse Transcriptase (Qiagen)	1 µl	4 units
Template RNA	12 µl	Variable
Total Volume	**20 µl**	
Rnase-free water to achieve 5 ng/µl cDNA	Variable	

Table 6.2 – Quantitative real-time PCR reaction components

Components	Volume/reaction
SYBR® Green qPCR Master Mix (2X)	12.5 µl
Forward Primer (10 µM)	0.75 µl
Reverse Primer (10 µM)	0.75 µl
Nuclease-free water	9 µl
Total Master Mix volume	**23 µl**
Template cDNA / nuclease free water	2 µl
Total reaction volume	**25 µl**

Table 6.3 – PCR Primer details*

Primer	Accession No.	Primer information	Product (bp)	Reference
β-ACTIN	NM_007393	Forward 5'-3': GGGGCAAGAGAGGTATCCTGACC Reverse 5'-3': CCCTGGATGCTACGTACATGGC	237	(Peiris et al., 2012)
TPH1	NM_001136084	Forward 5'-3': CAAAGAGAACAAAGACCATTC Reverse 5'-3': CGCAGTCAACAAATATCTCA	185	
SGLT1	NM_019810	Forward 5'-3': CGGAAGAAGGCATCTGAGAA Reverse 5'-3': AATCAGCACGAGGATGAACA	63	(Yoshikawa et al., 2011)
SGLT3	NM_017391	Forward 5'-3': AGGTACATGTTGGCCTCACC Reverse 5'-3': ATTTTTAGGGCATTCGCCTT	104	
GLUT1	NM_011400	Forward 5'-3': ATGGATCCCAGCAGCAAG Reverse 5'-3': CCAGTGTTATAGCCGAACTGC	92	(Yoshikawa et al., 2011)
GLUT2	NM_031197	Forward 5'-3': TCTTCACGGCTGTCTCTGTG Reverse 5'-3': AATCATCCCGGTTAGGAACA	71	(Yoshikawa et al., 2011)
GLUT5	NM_019741	Forward 5'-3': AGAGCAACGATGGAGGAAAA Reverse 5'-3': CCAGAGCAAGGACCAATGTC	64	(Yoshikawa et al., 2011)
FFAR1 (GPR40)	NM_194057	Forward 5'-3': CCCAGCTTGGTCTACACTCTCCATC Reverse 5'-3': GATGGCTTGGTACCCGAAGGGGAAG	234	(Lan et al., 2008)
FFAR2 (GPR43)	NM_146187	Forward 5'-3': CTTGATCCTCACGGCCTACAT Reverse 5'-3': CCAGGGTCAGATTAAGCAGGAG	137	(Sykaras et al., 2012)
FFAR3 (GPR41)	NM_181748	Forward 5'-3': TTCATATGGGGTTACTCGGC Reverse 5'-3': GATTTCTCCTATGCGGTTGG	68	
FFAR4 (GPR120)	NM_181748	Forward 5'-3': TTCATATGGGGTTACTCGGC Reverse 5'-3': GATTTCTCCTATGCGGTTGG	135	(Brown et al., 2003)
GPR84	NM_030720	Forward 5'-3': AGGTGACCCGTATGTGCTTC Reverse 5'-3': GTTCATGGCTGCATAGAGCA	176	
GPR92	NM_001163268	Forward 5'-3': GAGGTCCCAAGAAGGTCTCC Reverse 5'-3': GCAAACATCATGTCCAGGTG	239	
GPR119	NM_181751	Forward 5'-3': AATCCTGTCCCATGAGAATCTGA Reverse 5'-3': GCCAACACCATCATTCTTGTAGA	191	
T1R3	NM_031872	Forward 5'-3': TCAGAGCTTGCCCTCATTACAG Reverse 5'-3': TGTGCGGAAGAAGGATGGA	120	
T1R2	NM_031873	Mm_Tas1r2_1_SG (QT00142639, Qiagen)	137	(Young et al., 2013)

*Primers which do not have an explicit reference were designed in the course of this work.

Table 6.4 – Quantitative real-time PCR thermocycling conditions

PCR Cycle	Condition	
Hold	95°C (15 minutes)	
Annealing	55°C (20 seconds)	45 cycles
Extension	72°C (25 seconds)	
Denaturation	94°C (15 seconds)	
Hold	72°C (4 minutes)	
Hold	60°C (15 seconds)	
Melt	60°C to 99°C	

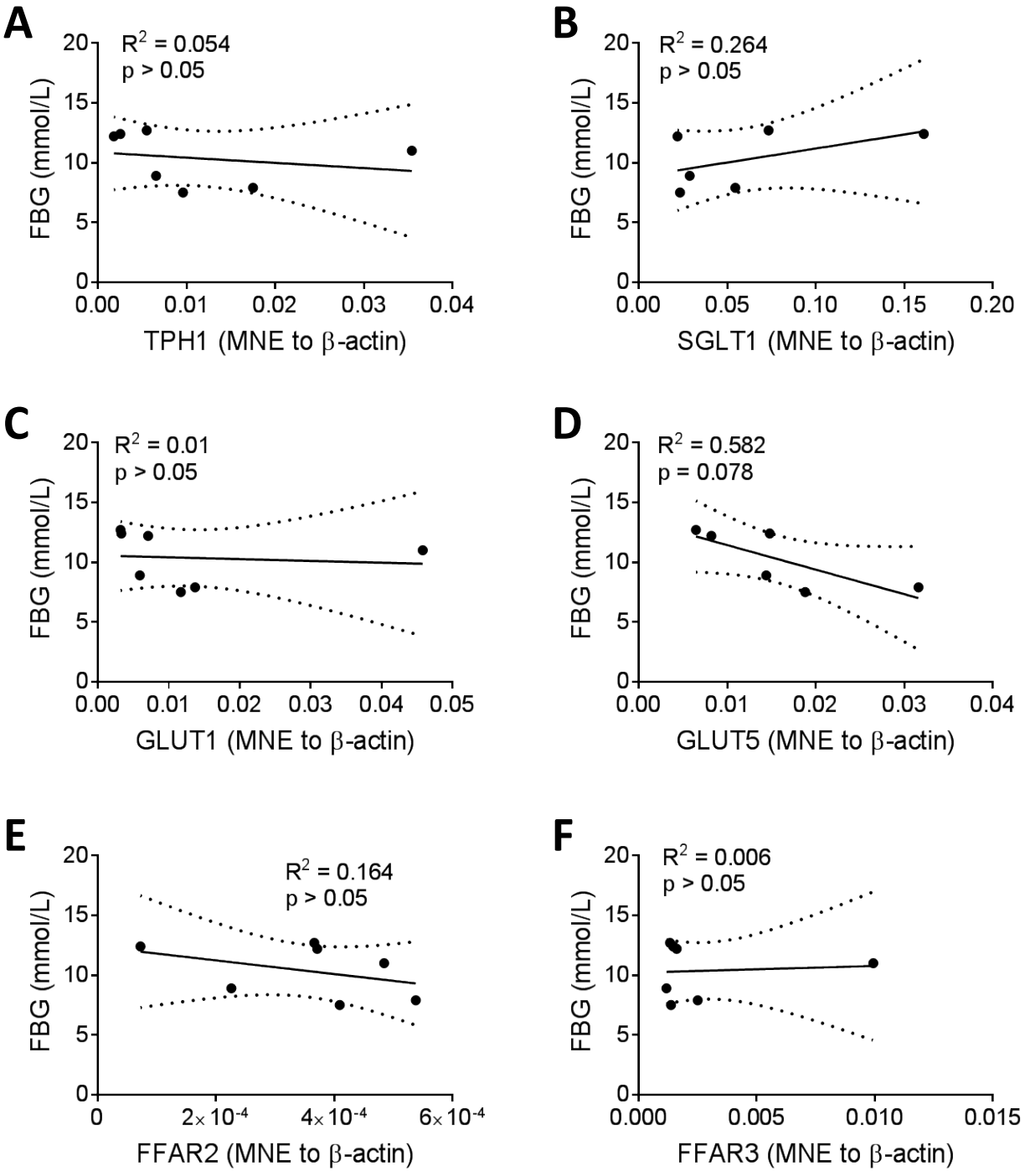

Figure 6.1 – Duodenal EC cell gene expression versus fasting blood glucose (FBG) in HFD-fed mice. Mean normalised expression (MNE) for (A) TPH1, (B) SGLT1, (C) GLUT1, (D) GLUT5, (E) FFAR2 and (F) FFAR3 in duodenal EC cells is not correlated with FBG in mice fed a HFD. Solid line represents linear regression ± 95% confidence interval.

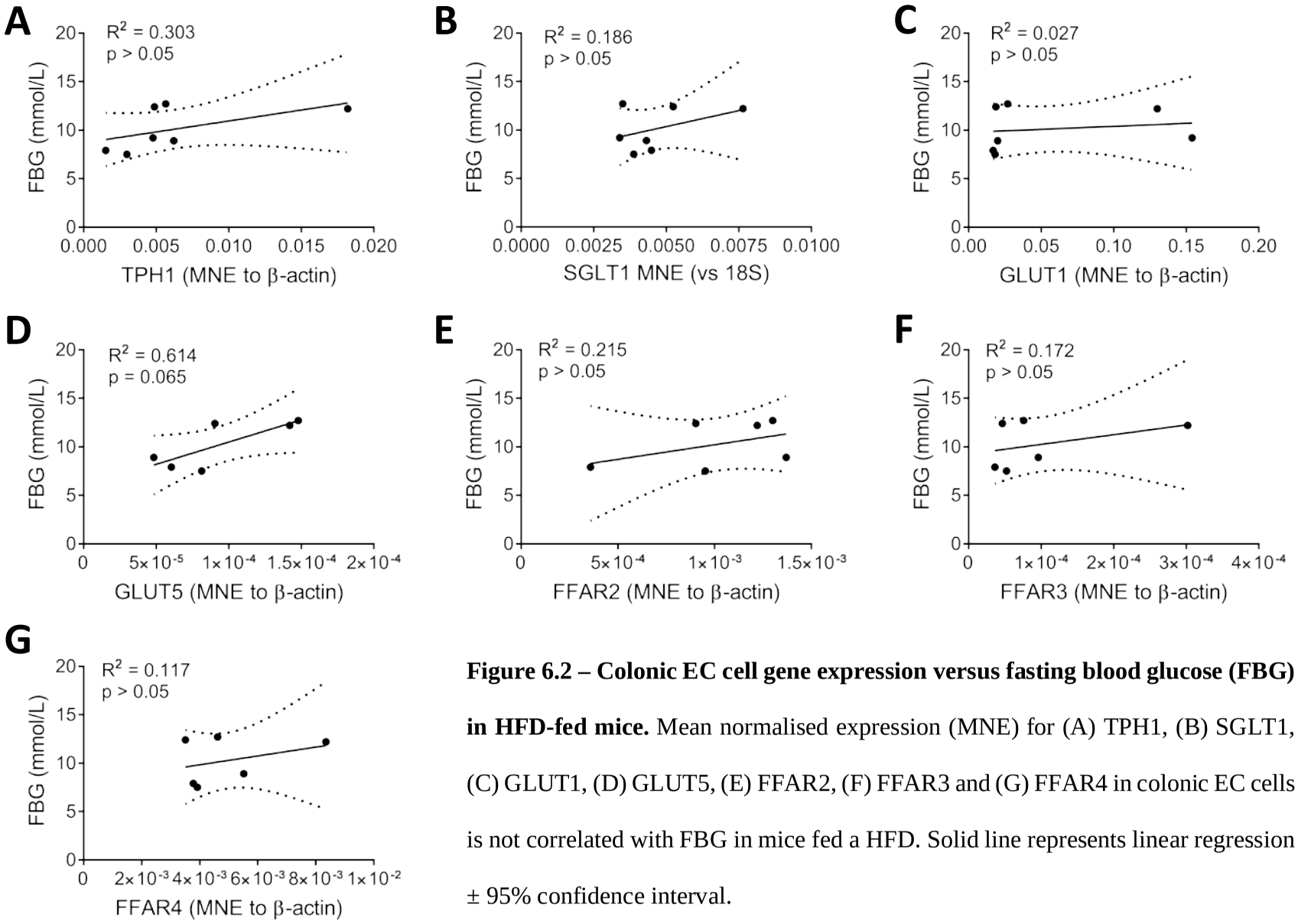

Figure 6.2 – Colonic EC cell gene expression versus fasting blood glucose (FBG) in HFD-fed mice. Mean normalised expression (MNE) for (A) TPH1, (B) SGLT1, (C) GLUT1, (D) GLUT5, (E) FFAR2, (F) FFAR3 and (G) FFAR4 in colonic EC cells is not correlated with FBG in mice fed a HFD. Solid line represents linear regression ± 95% confidence interval.

Appendix: Chapter 3

Table 6.5 – Calculated osmolarity for *in vitro* stimulants

Stimulant	Concentration	Osmolarity (osmol)
Glucose / Fructose	5 mM	0.12
	100 mM	2.4
	300 mM	7.2
	500 mM	12
Sucrose	5 mM	0.225
	100 mM	4.5
	300 mM	13.5
	500 mM	22.5
Acetate	1 mM	0.008
	10 mM	0.08
	100 mM	0.8
Propionate	1 mM	0.01
	15 mM	0.165
	30 mM	0.33
Butyrate	1 mM	0.014
	15 mM	0.21
	30 mM	0.42

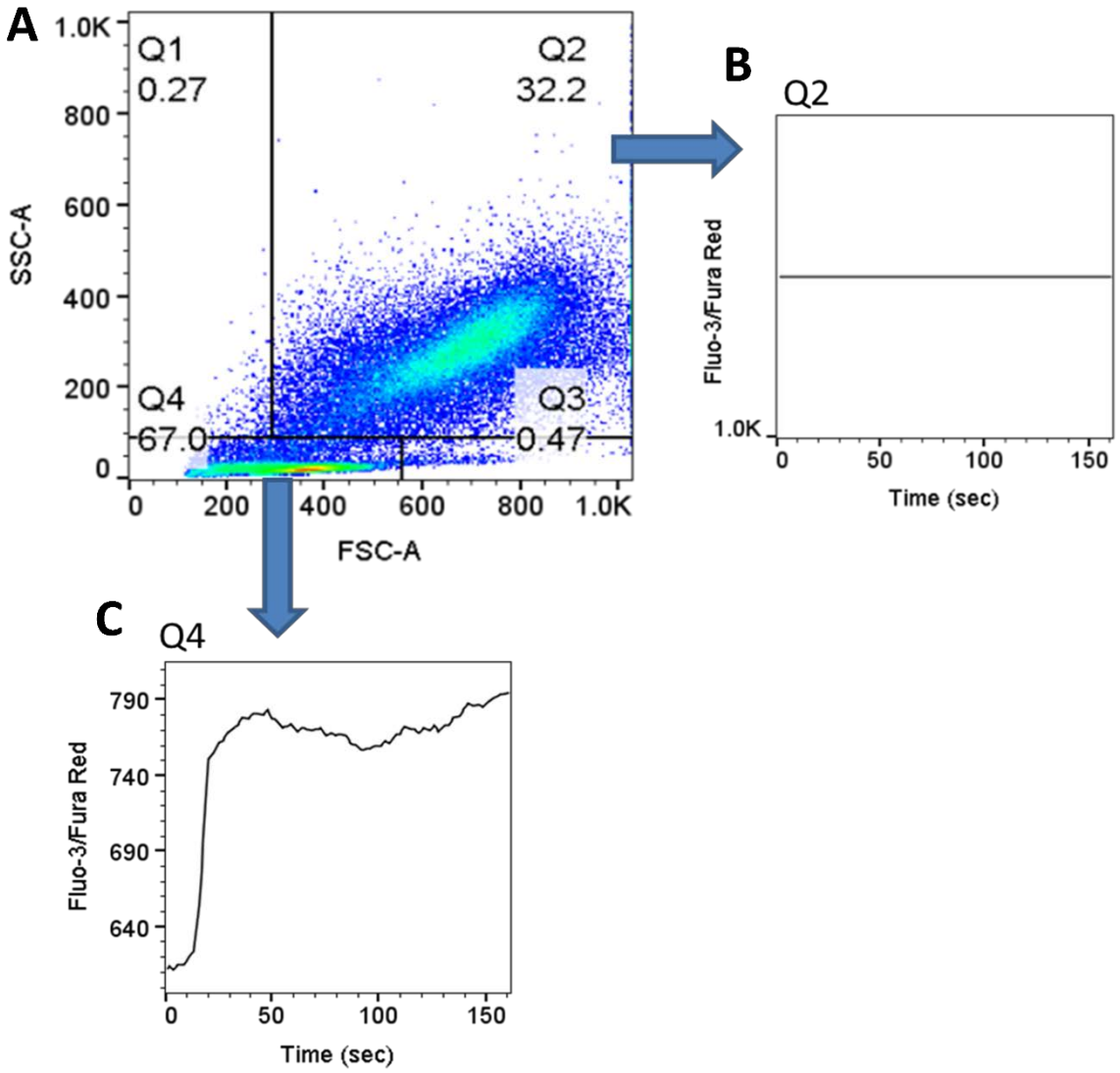

Figure 6.3 – Measurement of intracellular calcium in two gated populations of duodenal EC cells in response to thapsigargin (TG). (A) Isolated duodenal EC cell population costs of two subpopulations. (B) Larger cells gated within Q2, comprising around 30% of the total cell population, have a Fluo-3/Fura Red value consistent with cells that have already undergone calcium flux prior to flow cytometry. (C) Cell populations gated within Q4 show a typical increase in Fluo-3/Fura Red in response to TG stimulation.

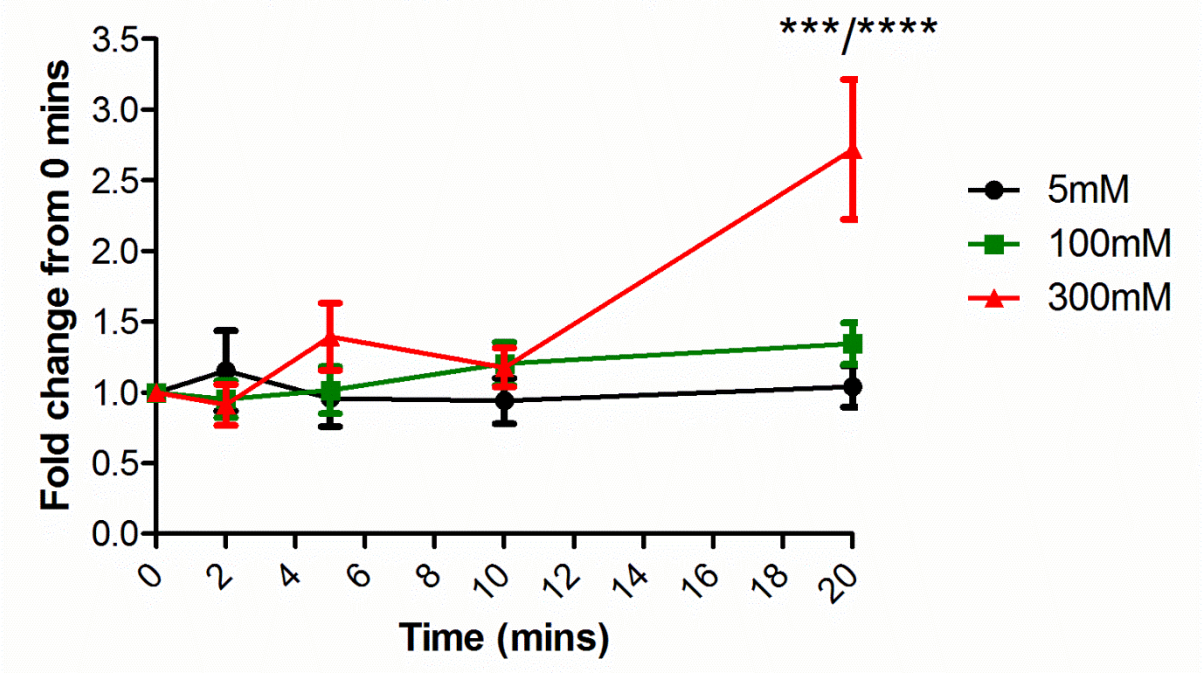

Figure 6.4 – Time course of 5-HT release from colonic EC cells exposed to increased concentrations of glucose in culture. (n = 3 mice, *** $p < 0.001$ *vs* 100 mM glucose, **** $p < 0.0001$ *vs* 5 mM glucose). Data are shown as mean ± SEM.

Appendix: Chapter 4

Table 6.6 – Quantitative real-time PCR reaction components for bacterial load analysis

Components	Volume/reaction
Platinum® SYBR® Green qPCR SuperMix-UDG with Rox	17.5 µL
Forward Primer (10 µM)	0.7 µL
Reverse Primer (10 µM)	0.7 µL
Nuclease-free water	15.1 µL
Total Master Mix volume	34 µL
Template cDNA /nuclease free water	1 µL
Total reaction volume	35 µL

Table 6.7 – Quantitative real-time PCR thermocycling conditions for bacterial load analysis

PCR Cycle	Condition	
Hold (UNG Incubation)	50°C (2 minutes)	
Hold	95°C (10 minutes)	
Denaturation	95°C (10 minutes)	40 cycles
Annealing/Extension	60°C (1 minute)	